Pathophysiological mechanisms in Parkinson`s Disease and Dystonia – converging aetiologies

A thesis submitted to the University College London

for the degree of Doctor of Philosophy

August 2020

by

Dr. Sebastian R. Schreglmann, FEBN

Declaration of Authorship

I, Sebastian Robert Schreglmann, confirm that the work presented in this thesis is my own. Where information has been derived from other sources, I confirm that this has been indicated in the thesis.

S. Schreglmann

Abstract

In this thesis I used a range of experimental approaches including genetics, enzyme activity measurements, histology and imaging to explore converging pathophysiological mechanisms of Parkinson`s disease and dystonia, two conditions with frequent clinical overlap.

First, based on a combined retro- and prospective cohort of patients, using a combination of lysosomal enzyme activity measurements in peripheral blood and brain samples, as well as a target gene approach, I provide first evidence of reduced levels of enzyme activity in Glucocerebrosidase and the presence of *GBA* mutations, indicating lysosomal abnormality, in a relevant proportion of patients with dystonia of previously unknown origin.

Second, based on a retrospective cohort of patients, I detail that a relevant proportion of genetically confirmed mitochondrial disease patients present with a movement disorder phenotype - predominantly dystonia and parkinsonism. Analysing volumetric MRI data, I describe a patterned cerebellar atrophy in these particular patients. This also includes the first cases of isolated dystonia due to mitochondrial disease, adding the latter as a potential aetiology for dystonia of unknown origin.

Third, I used a combination of post-GWAS population genetic approaches and tissue-based experiments to explore in how far the strong association between advancing age and Parkinson´s disease is mediated via telomere length. Although the initial finding of an association between genetically determined telomere length and PD risk did not replicate in independent cohorts, I provide evidence that telomere length in human putamen physiologically shortens with advancing age and

is regulated differently than in other brain regions. This is unique in the human brain, implying a particular age-related vulnerability of the striatum, part of the nigro-striatal network, crucially involved in PD pathophysiology.

I conclude by discussing the above findings in light of the current literature, expand on their relevance and possible direction of future experiments.

Impact Statement

The work described in this thesis summarizes part of my research activity during my time as a PhD student at the Institute of Neurology. It presents experimental evidence documenting a convergence between some of the pathophysiological aspects underlying Parkinson´s disease and dystonia. Utilizing enzyme activity measurements, genetic analyses, and quantitative imaging along careful clinical phenotyping, it provides evidence for lysosomal and mitochondrial dysfunction as an underlying abnormality in a proportion of dystonia cases of previously unknown origin.

In particular, the results on lysosomal dysfunction may indicate a so far unrecognized, novel disease mechanism in dystonia. Given the high frequency of sporadic, i.e. idiopathic dystonia, these findings provide a starting point to explore this mechanism further, and possibly establish novel therapeutic avenues in dystonia. Given the paucity of causative treatment options in this condition, the impact on our understanding of dystonia pathophysiology and patient well-being is potentially substantial. Further, the generated results offer relevant pilot data for future grant applications supporting larger-scale studies to replicate these initial results and further dissect their molecular basis, impact and potential treatment.

The results from the analysis of mitochondrial disease patients are equally fascinating, as they highlight cerebellar dysfunction as a common anatomical substrate for movement disorders in this patient group and imply that a proportion of (task-specific) dystonia might be caused by so far unrecognized mitochondrial disease.

Further, this work provides a potential link between advancing age and conditions anatomically linked to the striatum, such as PD and dystonia, by revealing an age-related telomere length attrition in the human putamen by qPCR and Southern blot quantification. Together with the identification of brain region-specific telomere length regulation and the fact that this has not been described in other regions of the human brain, indicates a process unique to the putamen. Although attempts to provide population genetic evidence for an association of genetic determined telomere length with PD via Mendelian Randomization failed to replicate, the presented results contribute to unravel this prominent and well-established, but poorly understood phenomenon.

My time at the Institute of Neurology and the resulting close interaction with brilliant, knowledgeable, experienced and dedicated teachers and colleagues was beneficial in many ways: As an academic clinician, working in one of the most varied and highly regarded movement disorder clinics gave me the opportunity to hone my clinical skills and establish a knowledge base for my patients` benefit that I will draw from for years to come. As a scientist, the exchange of ideas, the research education I received, the academic network, and the personal interactions with colleagues around the square and beyond had a lasting effect on my scientific reasoning and affirm my intention to pursue an academic career in movement disorder research. Having experienced the collaborative, dynamic and productive spirit at the Institute of Neurology has left a marked impression and influenced my way to approach ideas and projects. Finally, I leave this place with the invaluable gift of contacts for future collaboration and friends for life.

Table of contents:

Figures:

Tables:

Acknowledgements

My time at the Institute of Neurology at Queen Square was influenced by a large number of colleagues and friends, who made this one of the most exciting and gratifying experiences in my life so far, and I am deeply grateful for having met them.

First, I would like to express my gratitude to my primary supervisor Professor Kailash Bhatia for his support and mentorship and passionately teaching me the art of movement disorder diagnosis. To learn from his clinical experience has been a real gift and I am particularly grateful for the liberty he granted me to direct my research interests.

On a similar note, I am equally indebted to my secondary supervisor Professor Nicholas Wood for his constant guidance and support and - crucially - scientific scrutiny: "try to disprove your findings as good as you can" will stay with me forever!

It was a real pleasure to have shared the 6th floor fellow`s office and clinics with my dear colleagues and friends Anna Latorre, Stephanie Hirschbichler, Elisa Menozzi, Anna Sadnicka, Anne-Catherine Huys, Eoin Mulroy and Amit Batla and having met the many visiting clinical fellows – memories of fascinating clinics and long botox afternoons as well as the many memorable evenings at the Swan Pub will stay with me!

Ms Linda Taib, whom I frequently refer to as “the fellows` guardian angel”, needs special mentioning, as without her skills and knowledge of administrative intricacies of the Square, I would have been lost a number of times.

Working between different research groups was made possible by the effortless friendliness, genuine interest and generous spirit of members of the Neurogenetics Lab, in particular Dr Alan Pitman, David Murphy, Mark Gaskin, Hallgeir Jonvik, as well as Dr Boniface Mok and Dr Jana Vandrovcova. Many thanks also to Stephanie Efthymiou for patiently teaching me Sanger Sequencing. It was a particular pleasure to have shared bench space with my colleagues and friends Lea R`Bibo, Heather Ging, Gilbert Thomas Black and Hector Garcia-Moreno on the 9th floor.

I would also like to thank the people and colleagues I met through collaborations across the Square: Dr Zane Jaunmuktane and Karen Shaw at the Queen Square Brain Bank & Dr Julio Acosta-Cabronero and Dr John Thornton from the Functional Imaging Laboratory; Professor Simon Heales and Dr Derek Burke from the NHNN Neurometabolics unit; Dr Kevin Mills, Jenny Hallqvist and Ivan Doykov from Great Ormond Street`s Neurometabolics Centre, Professor John Rothwell and Dr. Lorenzo Rocchi from the Human Neurophysiology Lab, the enthusiastic Grossman lab team of Dr Robert Peach, Dr Eddy Rhodes and Junheng Li at Imperial College and Dr Sabato Santaniello and Xu Zhiang from the University of Connecticut. It has been a particularly rewarding experience to have worked with Dr Nir Grossman, whose meticulous scientific approach I greatly admire. The low-key attitude and incredible structured work spirit made collaborations with Professor Parashkev Natchev and Dr Ashwani Jha from the neighbouring 6th floor offices always extremely enjoyable.

My sincere thanks go to Dr Kazu Tomita and Tomas Goncalvez at UCL Cancer Institute`s O´Gorman Building, Demis Kia and Alastair Noyce, colleagues at the IPDGC and COURAGE-PD network and in particular Mie Rizig for her upbeat, collaborative spirit.

A special thanks goes to my dear friend Marian Galovic, with whom I shared the journey from our previous work in St. Gallen to the same corridor at the centre of neurological gravity at QS, and who in parallel endured the ups and downs of a neuroscience PhD – from Titanic to the Revenant…..!

Finally, my real gratitude belongs to my dear *Liebes*, Magdalena, who has been a constant support throughout this at times demanding endeavour, for her kind patience, understanding and endurance. Our journey would be impossible without your positive spirit and nature and I feel ever so grateful to have you by my side.

Publications:

Manuscripts on preprint servers/under review:

Non-invasive Amelioration of Essential Tremor via Phase-Locked Disruption of its Temporal Coherence
Schreglmann SR, Wang D, Peach R, Li J, Zhang X, Latorre A, Rhodes E, Panella E, Boyden ES, Barahona M, Santaniello S, Bhatia KP, Rothwell J, Grossman N.
with Nature Neuroscience

Lysosomal enzyme deficiency and GBA mutations in Dystonia
Schreglmann SR, Burke D, Batla A, Kresojevic N, Wood N, Heales S, Bhatia KP.

Accepted Manuscripts:

Penetrance of Parkinson's Disease in LRRK2 p.G2019S Carriers Is Modified by a Polygenic Risk Score.
Iwaki H, Blauwendraat C, Makarious MB, Bandrés-Ciga S, Leonard HL, Gibbs JR, Hernandez DG, Scholz SW, Faghri F; **International Parkinson's Disease Genomics Consortium (IPDGC),** Nalls MA, Singleton AB. Mov Disord. 2020 Jan 20. doi: 10.1002/mds.27974.

Genetic variability and potential effects on clinical trial outcomes: perspectives in Parkinson's disease.
Leonard H, Blauwendraat C, Krohn L, Faghri F, Iwaki H, Ferguson G, Day-Williams AG, Stone DJ, Singleton AB, Nalls MA, Gan-Or Z; **International Parkinson's Disease Genomic Consortium (IPDGC).**J Med Genet. 2019 Nov 29 doi: 10.1136/jmedgenet-2019-106283.

Identification of novel risk loci, causal insights, and heritable risk for Parkinson's disease: a meta-analysis of genome-wide association studies.

Nalls MA, Blauwendraat C, Vallerga CL, Heilbron K, Bandres-Ciga S, Chang D, Tan M, Kia DA, Noyce AJ, Xue A, Bras J, Young E, von Coelln R, Simón-Sánchez J, Schulte C, Sharma M, Krohn L, Pihlstrøm L, Siitonen A, Iwaki H, Leonard H, Faghri F, Gibbs JR, Hernandez DG, Scholz SW, Botia JA, Martinez M, Corvol JC, Lesage S, Jankovic J, Shulman LM, Sutherland M, Tienari P, Majamaa K, Toft M, Andreassen OA, Bangale T, Brice A, Yang J, Gan-Or Z, Gasser T, Heutink P, Shulman JM, Wood NW, Hinds DA, Hardy JA, Morris HR, Gratten J, Visscher PM, Graham RR, Singleton AB; 23andMe Research Team; System Genomics of Parkinson's Disease Consortium; **International Parkinson's Disease Genomics Consortium**. Lancet Neurol. 2019 Dec;18(12):1091-1102. doi: 10.1016/S1474-4422(19)30320-5.

The Genetic Architecture of Parkinson Disease in Spain: Characterizing Population-Specific Risk, Differential Haplotype Structures, and Providing Etiologic Insight. Bandres-Ciga S, Ahmed S, Sabir MS, Blauwendraat C, Adarmes-Gómez AD, Bernal-Bernal I, Bonilla-Toribio M, Buiza-Rueda D, Carrillo F, Carrión-Claro M, Gómez-Garre P, Jesús S, Labrador-Espinosa MA, Macias D, Méndez-Del-Barrio C, Periñán-Tocino T, Tejera-Parrado C, Vargas-González L, Diez-Fairen M, Alvarez I, Tartari JP, Buongiorno M, Aguilar M, Gorostidi A, Bergareche JA, Mondragon E, Vinagre-Aragon A, Croitoru I, Ruiz-Martínez J, Dols-Icardo O, Kulisevsky J, Marín-Lahoz J, Pagonabarraga J, Pascual-Sedano B, Ezquerra M, Cámara A, Compta Y, Fernández M, Fernández-Santiago R, Muñoz E, Tolosa E, Valldeoriola F, Gonzalez-Aramburu I, Sanchez Rodriguez A, Sierra M, Menéndez-González M, Blazquez M, Garcia C, Suarez-San Martin E, García-Ruiz P, Martínez-Castrillo JC, Vela-Desojo L, Ruz C, Barrero FJ, Escamilla-Sevilla F, Mínguez-Castellanos A, Cerdan D, Tabernero C, Gomez Heredia MJ, Perez Errazquin F, Romero-Acebal M, Feliz C, Lopez-Sendon JL, Mata M, Martínez Torres I, Kim JJ, Dalgard CL; American Genome Center, Brooks J, Saez-Atienzar S, Gibbs JR, Jorda R, Botia JA, Bonet-Ponce L, Morrison KE, Clarke C, Tan M, Morris H, Edsall C, Hernandez D, Simon-Sanchez J, Nalls MA, Scholz SW, Jimenez-Escrig A, Duarte J, Vives F, Duran R, Hoenicka J, Alvarez V, Infante J, Marti MJ, Clarimón J, López de Munain A, Pastor P, Mir P, Singleton A; **International Parkinson Disease Genomics Consortium**. Mov Disord. 2019 Dec;34(12):1851-1863. doi: 10.1002/mds.27864.

Syringomyelia-associated Dystonia: Case Series, Literature Review, and Novel Insights.
Mulroy E, Balint B, Latorre A, **Schreglmann S**, Menozzi E, Bhatia KP. Mov Disord Clin Pract. 2019 May 3;6(5):387-392. doi: 10.1002/mdc3.12772

The endocytic membrane trafficking pathway plays a major role in the risk of Parkinson's disease.
Bandres-Ciga S, Saez-Atienzar S, Bonet-Ponce L, Billingsley K, Vitale D, Blauwendraat C, Gibbs JR, Pihlstrøm L, Gan-Or Z; **International Parkinson's Disease Genomics Consortium (IPDGC)**, Cookson MR, Nalls MA, Singleton AB. Mov Disord. 2019 Apr;34(4):460-468. doi: 10.1002/mds.27614

LRP10 in alpha-synucleinopathies
Kia DA, Sabir MS, Ahmed S, Trinh J, Bandres-Ciga S; **International Parkinson's Disease Genomics Consortium**, Lancet Neurol. 2018 Dec;17(12):1032. doi: 10.1016/S1474-4422(18)30401-0.

Neuroimaging advances in Parkinson´s disease
Rispoli V & **Schreglmann SR**, Bhatia KP, Current Opinion Neurology, 2018 Aug;31(4):415-424. doi: 10.1097/WCO.0000000000000584.

Letter to the Editor on „Mohammed N, Patra D, Nanda A. A meta-analysis of outcomes and complications of magnetic resonance-guided focused ultrasound in the treatment of essential tremor"
Schreglmann SR, Bhatia KP, Hägele-Link S, Werner B, Martin E, Kägi G. Neurosurg Focus, 2018 Jul;45(1):E15. doi: 10.3171/2018.3.FOCUS1898.

Functional lesional neurosurgery for tremor: back to the future?
Schreglmann SR, Krauss JK, Chang JW, Martin E, Bauer R, Hägele-Link S, Bhatia KP, Kägi G. JNNP, 2018 Jul;89(7):727-735. doi: 10.1136/jnnp-2017-316301.

Functional lesional neurosurgery for tremor: a systematic review and meta-analysis
Schreglmann SR, Krauss JK, Chang JW, Bhatia KP, Kägi G. JNNP, 2018 Jul;89(7):717-726. doi: 10.1136/jnnp-2017-316302.

Fokussierter Ultraschall in der Behandlung von Tremor – Focussed ultrasound ablation as tremor treatment
Schreglmann SR, Hägele-Link S, Werner B, Martin E, Kägi G. Der Nervenarzt, 2018 Jun;89(6):674-681. doi: 10.1007/s00115-017-0470-4.

Oligomer-prone E57K-mutant alpha-synuclein exacerbates integration deficit of adult hippocampal newborn neurons in transgenic mice
Regensburger M, **Schreglmann SR**, Masliah E, J Winkler, B Winner. Brain Structure & Function, 2018 Apr;223(3):1357-1368. doi: 10.1007/s00429-017-1561-5.

Sodium oxybate for excessive daytime sleepiness and sleep disturbance in Parkinson's disease: A double-blind, placebo-controlled, crossover, phase 2a study
Büchele F, Hackius M, **Schreglmann SR**, Omlor W, Werth E, Maric A, Imbach LL, Hägele-Link S, Daniel Waldvogel S, Baumann CR. JAMA Neurology, 2018 Jan 1;75(1):114-118. doi: 10.1001/jamaneurol.2017.3171.

Increased sleep need and reduction of tuberomammillary histamine neurons after rodent traumatic brain injury
Noain D, Büchele F, **Schreglmann SR**, Valko PO, Gavrilov Y, Morawska MM, Imbach LL, Baumann CR. J Neurotrauma. 2018 Jan 1;35(1):85-93. doi: 10.1089/neu.2017.5067.

Movement disorders in genetically confirmed mitochondrial disease and the putative role of the cerebellum
Schreglmann SR & Riederer F, Galovic M, Ganos C, Kägi G, Waldvogel D, Jaunmuktane Z, Schaller A, Hidding U, Krasemann E, Michels L, Baumann CR, Bhatia KP, Jung HH. Movement Disorders, 2018 Jan;33(1):146-155. doi: 10.1002/mds.27174. Epub 2017 Sep 13.

Parkinson´s disease - Advances in the clinical and differential diagnosis

Schreglmann SR, Bhatia KP, Stamelou M. Int. Rev. Neurobiology, Editors KP Bhatia, RK Chaudhuri, M Stamelou. Int Rev Neurobiol. 2017;132:79-127. doi: 10.1016/bs.irn.2017.01.007.

Functional lesional neurosurgery for tremor - a protocol for a systematic review and meta-analysis
Schreglmann SR, Krauss JK, Chang JW, Bhatia KP, Kägi G. BMJ Open, 2017 May 9;7(5):e015409. doi: 10.1136/bmjopen-2016-015409.

Unilateral cerebellothalamic tract ablation in essential tremor by MRI-guided focused ultrasound
Schreglmann SR, Bauer R, Hägele-Link S, Bhatia KP, Natchev P, Wegener N, Lebeda A, Werner B, Martin E, Kägi G; Neurology, 2017 Apr 4;88(14):1329-1333. doi: 10.1212/WNL.0000000000003795.

VPS13C—Another Hint at Mitochondrial Dysfunction in Familial Parkinson's disease
Schreglmann SR, Houlden H. Movement Disorders – 2016 May 16th

Pyridostigmine bromide versus fludrocortisone in the treatment of orthostatic hypotension in Parkinson`s disease – a randomized controlled trial
Schreglmann SR & Büchele F, Sommerauer M, Epprecht L, Kägi G, Hägele-Link S, Götze O, Zimmerli L, Waldvogel D, Baumann CR. Eur J Neurology, 2017 Apr;24(4):545-551. doi: 10.1111/ene.13260.

Introduction

Recent advances in imaging, genetics and meticulous clinical phenotyping have led to a partial decomposition of certain classic neurological conditions into distinct entities - the number of conditions previously grouped under a singular term hence has grown considerably. The study of movement disorders and their underlying pathophysiology relies on the recognition and careful differentiation between an ever-growing number of defined aetiologies. For Parkinson´s disease (PD) and dystonia, the two movement disorder presentations at the centre of this work, this is particularly true. The following paragraphs, together with the more detailed tables in the appendix, provide a rough introduction to these two conditions and their differential diagnoses.

1.1 Parkinson`s disease

1.1.1 Idiopathic Parkinson´s disease

Parkinson`s disease (PD) is a progressive, hypokinetic-rigid syndrome, pathophysiologically defined by a preferential loss of midbrain dopaminergic neurons, manifesting with bradykinesia, rigidity and tremor as the defining motor symptoms and an increasing need for dopamine replacement (Lang and Lozano, 1998). In contrast to secondary, atypical or genetic forms of parkinsonism, which are introduced below, the by far most frequent, sporadic form of PD of unknown aetiology is referred to as idiopathic PD (iPD).

One of the hallmark features of iPD is the sustained and marked response of motor symptoms to dopaminergic medication, as stated in several versions of published

diagnostic criteria (Calne *et al.*, 1992; Gelb *et al.*, 1999; Gibb and Lees, 1989; Litvan *et al.*, 2003). Over decades, levodopa-responsiveness has been used as a feature to differentiate iPD from the atypical parkinsonian conditions multiple system atrophy (MSA), progressive supranuclear palsy (PSP) and cortico-basal degeneration (CBD), (Hughes *et al.*, 2002), while some levodopa response has been described for MSA (Albanese *et al.*, 1995; Constantinescu *et al.*, 2007; Wenning *et al.*, 2000), PSP (Collins *et al.*, 1995; Litvan *et al.*, 1996; Williams *et al.*, 2005) and occasionally even CBD (Frucht *et al.*, 2000; Kompoliti *et al.*, 1998; Wenning *et al.*, 1998). Unlike in MSA and iPD, there have been reports of motor symptom worsening with PSP (Constantinescu *et al.*, 2007).

Clinically, the presence of true bradykinesia with decrement, a good response to dopaminergic medication, presence of a re-emerging tremor and classical PD non-motor features are suggestive of iPD (Schwingenschuh *et al.*, 2010). Motor fluctuations and levodopa-induced dyskinesia have been described as the only reliable clinical features to predict PD pathology in tremulous patients (Selikhova *et al.*, 2013).

Phenotypical classification of iPD is so far based predominantly on motor phenotype, differentiating tremor-dominant, indeterminate and postural instability gait disorder (PIGD)/akinetic-rigid subtypes (Stebbins *et al.*, 2013), which has also been appreciated by different activation patterns in functional MRI (Prodoehl *et al.*, 2013) as well as cortical grey matter volume patterns (Rosenberg-Katz *et al.*, 2013). Data also suggests that certain motor phenotypes may be associated with different rates of progression, with the akinetic-rigid phenotype displaying faster progression and more cognitive symptoms (Baumann *et al.*, 2014) than the tremor-dominant type (Tremblay *et al.*, 2013).

Subtyping based on motor symptoms alone however most likely does not allow definitive conclusions, as with disease progression the predominant motor phenotype can change (Vu *et al.*, 2012). Over time, motor symptoms invariably progress and may include levodopa non-responsive motor symptoms such as speech and swallowing problems. Furthermore, cognitive and behavioural symptoms, such as dysexecutive symptoms, apathy and the spectrum of non-intrusive to frightening delusions, perceived presence to visual hallucinations and psychosis develop over time. Data from a meta-analysis suggest that patients with non-tremor predominant motor symptoms and depression have more and more severe cognitive symptoms (Tremblay *et al.*, 2013).

Recent years have seen the increasing recognition of non-motor symptoms not only in sporadic (Adler, 2005) but also monogenic PD (Kägi *et al.*, 2010). It is now accepted that a considerable disease burden in PD is caused by non-motor symptoms (Gallagher *et al.*, 2010), which also influenced the current diagnostic criteria (Berg *et al.*, 2014). Several lines of evidence indicate that a diagnosis of PD based on motor symptoms alone falls short to capture important aspects of this multisystem disorder: a) the fact that clinically defining motor symptoms only occur after around 60% of substantia nigra neurons have already disappeared, b) Braak's observation of a continuous spread of alpha-synuclein pathology which does not begin in the substantia nigra but in the peripheral autonomic nervous system, dorsal motor nucleus of the vagal nerve and olfactory bulb (Braak *et al.*, 2004; Del Tredici and Braak, 2016), c) the clinical observation that PD non-motor symptoms often predate motor symptoms (Mollenhauer *et al.*, 2013; Sauerbier *et al.*, 2016). This has led to the conceptualization of a premotor or prodromal phase of PD, encompassing clinical non-motor as well as motor symptoms (Mahlknecht *et al.*, 2015; Siderowf and Stern,

2008). The current evidence supports a particular usefulness of the following prodromal symptoms to detect future PD: REM-sleep behaviour disorder > hyposmia > constipation > depression and anxiety (Mahlknecht *et al.*, 2015).

Cognitive symptoms typically associated with PD are executive dysfunction in planning, inhibition, working memory and learning (A. E. Taylor *et al.*, 1986). A multicentre study with over 1300 PD patients reported a 25.8% prevalence of mild cognitive impairment (Aarsland *et al.*, 2010), rendering cognitive symptoms among a frequent non-motor manifestation of the disease. Dementia with Lewy bodies (DLB) and Parkinson´s disease dementia (PDD) are characterized by the combination of PD and cognitive symptoms. The arbitrary rule to differentiate between PDD and DLB based the sequence of cognitive/motor decline alone has recently been challenged to accommodate for the increasingly recognized similarity between PD, DLB and PDD (Postuma *et al.*, 2016).

In the light of the above and the absence of a universally available biomarker for iPD, clinical skills remain essential for its correct identification and diagnosis. It is a sobering fact that a meta-analysis of 13 clinico-pathological studies indicated that the diagnostic accuracy of PD constantly remained suboptimal over the previous 25 years, reaching 74% in an non-expert and around 84% in a specialist setting (Rizzo *et al.*, 2016). In comparison to expert clinical diagnosis, the UK Brain Bank diagnostic criteria were more sensitive (81.3 % vs. 90.8%), but less specific (83.5% vs. 34%), with tremor disorders, atypical parkinsonian conditions and secondary parkinsonism to be the most frequent misdiagnoses (Rizzo *et al.*, 2016).

1.1.2 Differential diagnosis

Tremor disorders

Tremor is one of the most obvious clinical features in PD but can cause considerable confusion as to its aetiological origin.

Classic Essential Tremor (ET) with young-onset, bilateral symmetric, postural or action tremor of the arm, a positive alcohol-response and a positive family history is rarely confused with PD. But cases with a slightly asymmetric picture, some rest component and later age at onset can be more challenging. Establishing and recognizing true bradykinesia and re-emerging tremor, among other signs remains key in the differentiation to PD.

The group of patients initially described with asymmetric rest tremor and normal DaTSCANs (Scans Without evidence of Dopaminergic Deficit, SWEDDs) mimic parkinsonian rest tremor and have been reported to account for up to 15% of patients clinically diagnosed as PD (Schwingenschuh *et al.*, 2010). Most likely, SWEDDs are an umbrella term for different aetiologies with dystonic tremor being one of the most frequent ones. This is supported by the fact that some of these patients have been shown to have electrophysiological features of dystonia (Schwingenschuh *et al.*, 2010) and the description of single SWEDDs cases carrying *TOR1A* (Cáceres-Redondo *et al.*, 2012; Stamelou *et al.*, 2013), *ANO3* (Stamelou *et al.*, 2014) or *SGCE* mutations (Cilia *et al.*, 2014), as well as the clinical description of subtle dystonic features in numerous SWEDD cases (Erro *et al.*, 2016). Other cases have subsequently been diagnosed as ET, Fragile X premutation carriers or tardive syndromes (Erro *et al.*, 2016). A small proportion of SWEDD cases however do convert on DaTSCAN follow-up, which is suggestive of a slow progression towards

PD in at least a subset of SWEDDs patients – conversion rates between 3% after 2.4 yrs. (Marshall *et al.*, 2006) and 12.5% after 7.5 yrs. (Batla *et al.*, 2014) have been reported.

Fragile-X, the most frequent heritable cause of mental retardation (1:3600 life births) is caused by a non-coding >200 CGG repeats expansion in the *FMR1* gene (see Table S4). Fragile-X tremor ataxia syndrome (FXTAS) due to 55-200 CGG repeats, affects around 40% of male and 8% of female premutation carriers. It is often misdiagnosed as one of the atypical parkinsonian disorders because of its age at onset above 55 years with prominent action > intention > rest tremor, cerebellar gait ataxia and frequent parkinsonism. Additional neuropathy, family history of a tremor disorder, cognitive impairment or primary ovarian insufficiency are additional suggestive features (Leehey and Hagerman, 2012).

Atypical Parkinsonism

In clinical routine practice the group of atypical parkinsonian disorders is the most frequent differential diagnosis to iPD due to similarities in clinical presentation and age at onset (see Table S1). Differentiation is frequently difficult in early disease stages, whereas phenotypical differences become clearer with time.

Multiple System Atrophy (MSA), previously called Shy Drager syndrome, olivopontocerebellar atrophy or striato-nigral degeneration, is a sporadic neurodegenerative disorder with the clinical hallmark features of progressive autonomic, parkinsonian, cerebellar and pyramidal features of variable intensity – subtypes are defined by the predominant symptom at onset and early stages of the disease (Wenning *et al.*, 2004). The prevalence in the general population has been

reported at around 3.4-4.9 per 100.000 and the mean incidence at 0.7 per 100.000 person years (Fanciulli and Wenning, 2015).

The definitive diagnosis of MSA requires post-mortem evidence of widespread glial alpha-synuclein accumulation with pontine and cerebellar atrophy or striatonigral degeneration. Current diagnostic criteria define MSA as a sporadic, adult-onset, progressive disorder with poorly levodopa-responsive parkinsonism or cerebellar syndrome with autonomic failure (Gilman *et al.*, 2008).

Progressive Supranuclear palsy (PSP) has been established as a disease entity in 1964 and was described as a characteristic combination of progressive parkinsonism with early falls, supranuclear vertical gaze palsy, pseudobulbar dysfunction, axial rigidity and mild cognitive impairment (Steele *et al.*, 1964), now called Richardson's syndrome. The prevalence is estimated to be 5-6/100.000. The classic neuropathological changes of PSP are tau aggregates in astrocytes (tufts), oligodendrocytes (coiled bodies) and neurons (neurofibrillary tangles), which are distinct from other tauopathies. PSP is a sporadic condition in the vast majority of cases, however a number of familial PSP cases have been reported from different groups: while mutations in the *MAPT* gene have been found in both sporadic and familial PSP cases, patients with a PSP phenotype have rarely been found in kindreds with *LRRK2* gene mutations and otherwise classical PD presentations (Im *et al.*, 2015).

Further PSP phenotypes with predominant parkinsonian, gait freezing, aphasia or other symptoms have been described (see Table S1) (Williams et al., 2005, Williamset al., 2009, Respondek et al., 2014). Clinical diagnostic criteria according to the National Institute of Neurological Disorders and Stroke (NINDS)-PSP have been

widely used and the combined use of postural instability and supranuclear gaze palsy is appreciated as very specific but not sensitive to differentiate PSP from sporadic PD (Lopez *et al.*, 2016; Williams and Lees, 2009). Cases of PSP pathology with phenotypes overlapping with primary lateral sclerosis (Josephs *et al.*, 2006), and pallido-nigro-luysian-atrophy are rare (Ahmed *et al.*, 2008). Although cerebellar involvement was initially an exclusion criterion for PSP diagnosis, patients with post-mortem confirmed PSP pathology but clinically predominant cerebellar involvement have been described in Japan (Kanazawa *et al.*, 2009; Koga *et al.*, 2015).

Corticobasal degeneration (CBD), first described as "cortico-dentato-nigral degeneration with neuronal achromasia" in 1967 (Rebeiz *et al.*, 1967), is a sporadic pathological entity characterized by astrocytic, oligodendrocytic and neuronal four-repeat (4R) tau accumulation in the basal ganglia and cortex.

There are no population-based epidemiological data available, while the incidence for CBS has been reported around 0.02 per 100`000 patient years (Winter *et al.*, 2010) and the prevalence around 9 per 100`000 (Osaki *et al.*, 2011). While CBD refers to the pathology, corticobasal Syndrome (CBS) describes the typical clinical presentation and acknowledges the fact that different pathologies can result in near same phenotype (Grijalvo-Perez and Litvan, 2014). This includes an asymmetric presentation with typically early onset, severe limb rigidity, unilateral ideomotor apraxia or other cortical signs such as alien limb phenomena and cortical sensory loss. Mixed action-/postural- and resting tremor, clearly deviating from typical PD rest tremor, is frequently present, while dystonia starting in an upper limb is one of the typical early motor features in CBS. Stimulus-sensitive, cortical myoclonus is a classic feature, although present in only one fourth of patients. A similar fraction of

patients displays eye movement abnormalities at disease onset, especially increase latency of horizontal saccades ipsilateral to the apraxic limb with preserved velocity (Grijalvo-Perez and Litvan, 2014). CBS/CBD is a sporadic disorder, while some familial cases due *MAPT* (Bugiani *et al.*, 1999; Spillantini *et al.*, 2000) and progranulin (*PGRN*) gene mutations have been described (Masellis *et al.*, 2006; Spina *et al.*, 2007). However, CBD pathology has been found in patients with Richardson`s syndrome and progressive non-fluent aphasia (Armstrong *et al.*, 2013). Conversely, CBS has repeatedly been described to be associated with AD, FTLD-TDP43 and mixed Lewy-body/AD pathology (Alexander *et al.*, 2014; Armstrong *et al.*, 2013). The most recent update on new clinical criteria attempted to increase the sensitivity of the diagnosis (Armstrong et al., 2013), but first evidence from pathology-confirmed cases indicates this might not have led to an improvement in diagnostic specificity (Alexander *et al.*, 2014). The large variability among CBD phenotype and CBS pathology, including FTLD-TDP43, AD and others) has been identified as most problematic (Stamelou and Bhatia, 2016).

Monogenic Parkinson´s Disease

Around 10% of PD cases are familial and their identification contributed to the notion that PD is most likely not a single disease but a multitude of entities with shared phenotypical characteristics (Ferreira and Massano, 2016).

Clinical features such as ethnic background, age at onset, characteristic signs and symptoms and family history are important clues to differentiate these genetic forms from iPD. For example, *SNCA* mutation carriers are more commonly of Greek or Italian ethnic background, have a variable disease onset, and usually a more aggressive course with cognitive and autonomic dysfunction earlier than expected

in sporadic PD (Papadimitriou *et al.*, 2016). In contrast, mutations in the leucine-rich repeat kinase 2 (*LRRK2*), which have been confirmed to be the most frequent autosomal dominant genetic cause of PD in the Caucasian population, are more common in North-Africa and Ashkenazi Jewish ancestry, and clinically are often indistinguishable from classic sporadic, levodopa-responsive PD (Wider *et al.*, 2010). The most common genetic risk factor - also considered a dominant form of PD with reduced penetrance - are heterozygous *GBA* mutations (odds ratio 5.8) with a strong preponderance among populations of Ashkenazy Jewish descent (Sidransky *et al.*, 2009).

The familial monogenic forms of PD due to *GBA, VPS35*, *parkin, PINK1*, *DJ-1* show drastic and sustained positive response to levodopa but also levodopa-induced dyskinesia very early on in their course. Most of the recessive PD mutations including *PLA2G6*, *ATP13A2* and *FBX07* have a clear levodopa-response and levodopa-induced dyskinesia early on in their course but a more variable response later (Ferreira and Massano, 2016; Schneider *et al.*, 2010; 2013). Among *LRRK2* PD patients, levodopa-response can be variable, while the great majority of them are responsive (Wider *et al.*, 2010). Cases of *DNAJC6* positive PD show either no response to levodopa if onset is juvenile, or good response if onset is in late adulthood (Köroğlu *et al.*, 2013; Olgiati *et al.*, 2016). *VPS31* (Sharma *et al.*, 2012) and *VPS13C* are rare causes of PD (Lesage *et al.*, 2016). A brief but more detailed overview is provided in Table S2.

NBIAs and Rare Symptomatic Parkinsonism

The syndromic combination of parkinsonism with predominant dystonic features,

cognitive impairment, variable additional signs and iron deposition in the basal ganglia with an autosomal-recessive family history is present in the group of neurodegeneration with brain iron accumulation (NBIAs). The anatomical distribution and pattern of suggestive MRI findings should be assessed on susceptibility- or T2 star-weighed sequences and helps in the differentiation (see Table S3).

In addition to the mentioned, most important and frequent differential diagnoses there is a continuously increasing list of heredo-degenerative disorders that result in parkinsonism (see Table S4): When chorea is an additional clinical feature, Huntington's disease (HD) (in particular juvenile) and HD-like syndromes are likely differentials. This includes dentate-rubro-pallidoluysian atrophy (DRPLA), neuroferritinopathy, neuroacanthocythosis (Schneider *et al.*, 2007) and McLeod syndrome (Jung *et al.*, 2011) – the latter two are characterized by acanthocytes, hepatomegaly and parkinsonism.

Orofacial dysmorphic features in the context of childhood onset cognitive impairment and early onset PD can be indicative of a 22q deletion syndrome (Mok *et al.*, 2016). External ophthalmoplegia in combination with parkinsonism and neuropathy is suggestive of mitochondrial disease, such as in *POLG* mutations (Dolhun *et al.*, 2013; Hudson *et al.*, 2007; Invernizzi *et al.*, 2008; Kazunori Sato *et al.*, 2011). Additional nocturnal central apnoea/hypoventilation, especially in the context of parkinsonism with prominent depression and apathy is indicative of autosomal-dominant Perry syndrome (Wider and Wszolek, 2008). Hepatosplenomegaly, anaemia and thrombocytopenia in a PD patient should prompt the differential of *GBA* mutation-related PD, as these are frequent features especially

in carriers of the p.N370S *GBA* mutation (Brockmann and Berg, 2014). Metabolic, toxic and structural causes of parkinsonism should always be excluded (see

Table S5).

Secondary Parkinsonism

Drug-induced parkinsonism has been suggested to occur in around 15% of patients on long-term neuroleptic treatment. In addition to a suggestive history (all neuroleptics apart from Clozapine and drugs derived from them, such as anti-emetics, are potential culprits), normal DaTSCAN imaging and olfactory testing can differentiate this entity from PD, although neuroleptic exposure has been reported to unmask pre-symptomatic PD (Wenning *et al.*, 2011).

Vascular parkinsonism is supposed to account conservatively for about 3-4% of cases of parkinsonism and is clinically characterized by lower body parkinsonism with early urinary incontinence and cognitive decline with often impaired postural reflexes and pyramidal signs in the lower limbs. Tremor is usually absent and DaTSCANs usually normal, unless lesions affect the striatum (Korczyn, 2015). The literature on levodopa-response is conflicting, although most authors deny any meaningful effect (Korczyn, 2015).

1.1.3 Risk factors

Although the exact mechanism causing iPD is unknown, decades of epidemiological research have consistently identified several established risk factors.

Age

Ever since the first description of the condition, the role of advancing age has been described as the most consistent risk factor for sporadic PD. The most current estimates document both incidence as well as prevalence rate of PD to increase with age - the annual incidence rate increases from 3.1 per 100 000 for the age of 40-49 years to 93.1 per 100 000 for the age of 70-79 years (Bower *et al.*, 1999; 2000). Similarly, a meta-analysis on all published door-to-door / population-based random sampling assessments reported prevalence rates to increase from 41 per 100`000 (40-49 years) to 1903 per 100`000 above 80 years of age (Pringsheim *et al.*, 2014). The relation between aging and PD therefore is intriguing and a number of molecular mechanisms linking the two, such as impaired lysosome/proteasome functioning, inflammation, oxidative stress and mitochondrial dysfunction have been suggested (Collier *et al.*, 2017; Reeve *et al.*, 2014), their exact interplay, as well as the role of genetic mechanisms influencing PD risk through ageing, remain unknown.

Environment

Several environmental factors, most consistently pesticide exposure and previous head trauma, are associated with and thought to contribute to increased risk for sporadic PD (Dick *et al.*, 2007; Poewe *et al.*, 2017). However, a recent umbrella review of meta-analyses on environmental risk factors provided Class 1 evidence for

physical activity (decreased risk), whereas the data on the effect of previous head injury, anxiety and depression, beta-blocker intake, smoking and serum uric acid were more heterogeneous (Bellou *et al.*, 2016). In assessing the evidence, the authors were however sceptical in how far various forms of information bias, residual confounding and reverse causation might explain some of these effects (Bellou *et al.*, 2016). For example, constipation, as well as anxiety and depression are now actually considered prodromal markers rather than risk factors by many in the field (Berg *et al.*, 2015), documenting the difficulties of standard epidemiological approaches in dissecting cause from consequence.

Genetics

It is now generally acknowledged that around 10% of cases of PD are of familial origin (de Lau and Breteler, 2006).

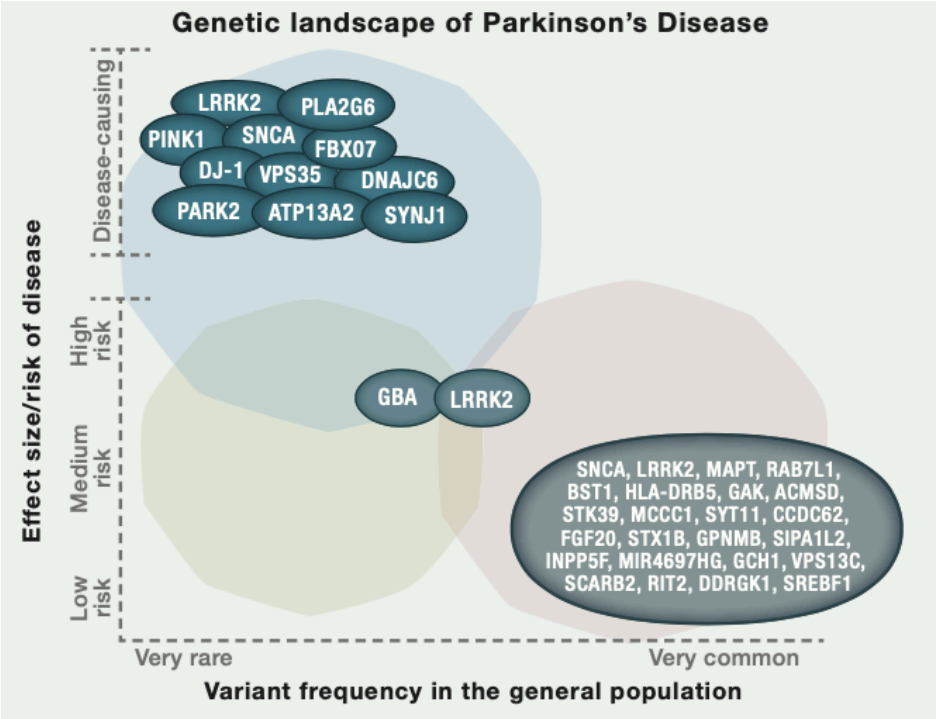

Figure 1.1: Genetic landscape of Parkinson´s Disease;
reproduced from (Bras et al.*, 2015)*

Given the progress to identify genetic forms of and risk alleles for PD in recent years, current estimates suggest between 26-36% of disease risk to be explained by genetic factors, depending on global prevalence (Nalls *et al.*, 2019). This leaves the majority of the disease risk and cases – i.e. sporadic PD - still to be explained. Alongside the identification of a number of monogenic causes of parkinsonian conditions (see Table S2), recent years were marked by large genome wide association studies (GWAS) and the recognition of genetic variants acting as susceptibility risk factors to develop the condition (International Parkinson Disease Genomics Consortium *et al.*, 2011; Nalls *et al.*, 2014; 2019). In the meantime the picture of the genetic landscape in PD has become clearer - in between rare, monogenic, disease-causing mutations (such as *PINK, PARKIN, DJ-1, PLA2G6, FBX07, ATP13A2, DNAJC6, SYNJ1, VPS13C, RAB39B* and *VPS31*), and very common variants with a very low individual effect size (for latest list of n=72, see (Nalls *et al.*, 2019)), *LRRK2* and *GBA* have been identified as high-risk variants for developing typical PD, as summarized in (Bras *et al.*, 2015).

1.1.4 Neuropathology

PD is caused by progressive neuronal accumulation of alpha-Synuclein in the brain, ultimately leading to a degenerative loss of particularly dopaminergic neurons in Substantia nigra pars compacta, but also cholinergic neurons of the basal nuclus of Meynert, Locus coeruleus and raphe, as well as ultimately diffuse cortical neuronal

loss (Lang and Lozano, 1998). This process propagates in stages in a rostro-cranial direction, starting at the dorsal motor nucleus of the glossopharyngeal and vagus nerve as well as anterior olfactory nucleus, ascending from the brain stem to finally also reach the cortex (Braak *et al.*, 2003). The formation of cytoplasmic inclusions called Lewy bodies, first described over a century ago (Lewy, 1920), and consisting of intracytoplasmic, fibrillary structures (Wakabayashi *et al.*, 2007), as well as Lewy neurites, inclusions within nerve fibres, are the pathological hallmark of the disease. Although characteristically based on alpha-Synuclein (Spillantini *et al.*, 1997), Lewy bodies consist of over 70 further molecules (Wakabayashi *et al.*, 2007). Within the substantia nigra, the ventrolateral tier of dopaminergic neurons is most vulnerable to the disease progress (Fearnley and Lees, 1991; Gibb and Lees, 1991), leading to a progressive loss of dopaminergic afferents to the striatum, which causes bradykinesia, the main motor symptom of the condition (Lees *et al.*, 2009).

1.1.5 Pathophysiological mechanisms

The knowledge on the genetic origins of PD has shed light on a number of processes involved in its pathophysiology (Singleton and Hardy, 2016):

Alpha-Synuclein proteostasis, aggregation and propagation

Seminal reports of *SNCA* point mutations (Polymeropoulos *et al.*, 1997; Zarranz *et al.*, 2004) and multiplications (Singleton *et al.*, 2003) and their clinical effects in affected kindreds, have established the central role of alpha-Synuclein in PD pathophysiology. Physiologically, alpha-Synuclein is expressed in the cytosol, exerting a function in synaptic vesicle dynamics, mitochondrial function and

intracellular trafficking (Vekrellis *et al.*, 2011). Alpha-Synuclein in its aggregate and particularly in its oligomeric form (Outeiro *et al.*, 2008) is neuro-toxic (Kramer and Schulz-Schaeffer, 2007). Therefore both overexpression (Singleton *et al.*, 2003), but also confirmation changes (Polymeropoulos *et al.*, 1997; Zarranz *et al.*, 2004) and errors in its degradation can lead to protein aggregation from soluble alpha-Synuclein monomers, to oligomers, small protofibrils and finally insoluble fibrils. Lewy bodies and Lewy neurites, although mainly consisting of alpha-synuclein fibrils, are considered not as a toxic protein aggregation but result of a cellular protein clearing mechanism (Kramer and Schulz-Schaeffer, 2007; McNaught *et al.*, 2002).

Although the exact mechanism of how alpha-synuclein pathology spreads throughout the (central) nervous system according to the Braak stages (Braak *et al.*, 2003) is still debated, observations from cell transplantation experiments formed the basis for the hypothesis that alpha-synuclein can propagate in a prion-like fashion (Angot *et al.*, 2010; Brundin *et al.*, 2008). On post-mortem analysis, fetal midbrain dopaminergic cell grafts were shown to develop both alpha-synuclein and ubiquitin positive Lewy-body like inclusions 11-16 years after transplantation into the striatum of PD patients (Kordower *et al.*, 2008; Li *et al.*, 2008). This seminal observation, although initially based on three cases only, indicated a cell-to-cell propagation of the causative pathology (Braak and Del Tredici, 2008) and has led to numerous studies confirming *in vitro* that a) alpha-synuclein can exist in its normal and a self-propagating conformation, b) resulting in alpha-synuclein aggregation and c) neuronal cell death, i.e. behaving in a prion-like manner (Brundin *et al.*, 2016).

Lysosomal dysfunction

Alpha-Synuclein is cleared from the cytosol through the ubiquitin-proteasome and lysosome-autophagy system and a reduction in the efficacy of these systems, as for example with advancing age (Kaushik and Cuervo, 2015) or GBA-related lysosomal dysfunction (Fernandes *et al.*, 2016), leads to increased levels of protein accumulation (Murphy *et al.*, 2014). Multiple lines of evidence have linked impaired functioning of the lysosome-autophagy system with the G2019S *LRRK2* gene mutation (Madureira *et al.*, 2020). In fact, there is now evidence to suggest a synergistic interplay between the activity of glucocerebrosidase (GCase), encoded by GBA, and LRRK2 kinase in the clearance of alpha-synuclein (Ysselstein *et al.*, 2019).

Furthermore, mutations in VPS35, a key retromer in transmembrane trafficking, have been identified to be associated with reduced activity in lysosomal functioning via lysosome-associated glycoprotein 2 (LAMP2), causing both neurodegeneration and developmental aberrations in dendritic and axonal differentiation (Tang *et al.*, 2020). Finally, ATP13A2 mutations cause early-onset PD via a toxic effect of defective lysosomal polyamine export (van Veen *et al.*, 2020).

Conversely, mutations in GBA, causing Gaucher`s disease, the most frequent lysosomal disorder, are established as the most common genetic risk factor for PD (Bras *et al.*, 2015; Sidransky *et al.*, 2009). Furthermore, replication-verified analyses based on whole-exome sequencing data documented a significant excess aggregate burden of rare lysosomal mutations in PD vs. controls by the sequence kernel association test – optimal (SKAT-O). Importantly, this association still remained after the removal of GBA variants already known to be a risk factor (Robak *et al.*, 2017).

Mitochondrial dysfunction and oxidative stress

Mitochondria are the main source of cellular energy supply via the electron transport chain and their malfunction particularly affects tissue with a high energy consumption, like neurons (DiMauro *et al.*, 2013). Several lines of evidence imply a relevant role of mitochondrial dysfunction in PD: a) toxic effects of MPTP (Ballard *et al.*, 1985) and rotenone (Betarbet *et al.*, 2000), both causing PD in humans and animal models, are effected by the inhibition of mitochondrial Complex I; b) on a cellular level there is reduced levels of nicotinamide adenine dinucleotide (NADH) ubiquinone (CoQ) reductase, i.e. Complex I deficiency (Schapira *et al.*, 1989), limited to the substantia nigra of PD patients (Mann *et al.*, 1992); c) the association of several genetic causes of familial PD with the physiological function of mitochondria, such as *parkin* and its interaction with *PINK1* (Pickrell and Youle, 2015), *DJ-1* (Ryan *et al.*, 2015), vacuolar protein sorting 13C (*VPS13C*) (Lesage *et al.*, 2016), but also mitochondrial polymerase gamma (POLG) (Davidzon *et al.*, 2006; Dolhun *et al.*, 2013; Invernizzi *et al.*, 2008). While parkin and PINK1 have been established to affect mitophagy, i.e. the process of removal of defective mitochondria, and mitochondrial trafficking, many monogenic causes of PD incl. LRRK2, VPS35, parkin and PINK1 have been associated with reduced energy supply via an affected oxidative stress response and dysfunctional electron transport chain gene on a molecular level – reviewed in (Park *et al.*, 2018).

Increasingly, mitochondrial dysfunction is similarly appreciated as a common mechanism in sporadic PD (Park *et al.*, 2018).

Oxidative stress is intricately linked with mitochondrial dysfunction, as >90% of reactive oxygen species (ROS) in neurons are generated through mitochondria and electron chain dysfunction.

Iron metabolism

Neuromelanin (NM) is a dark, insoluble pigment and a by-product of catecholamine-synthesis. Its production appears to be governed by the cytosolic content of dopamine or other catecholamines and is Fe^{3+}-mediated (Martin-Bastida *et al.*, 2017). NM is a pigment that can act in a neuroprotective or toxic role in neurons, depending on the cellular context: while its synthesis reduces toxic Iron-Dopa-complexes such as Aminochrome and its presence in the cell acts as an important chelator to metals such as iron, copper and zinc, its release into the extracellular space from dying neurons leads to neurodegeneration via the activation of microglia (Zucca *et al.*, 2015). NM content differs considerably between different neuronal populations and is particularly abundant in neurons of the Substantia nigra (SN) and Locus coeruleus (LC), but also to a lesser degree in putamen, premotor cortex and cerebellum (Acosta-Cabronero *et al.*, 2016).

Physiologically, NM decreases in an anatomy-dependent way with advancing age at a rate of 2.1%, 5.4% and 6.9% per decade respectively in the lateral, medial ventral and dorsal tier of the SN, which is greatly accelerated (45% loss/decade) in patients with PD (Fearnley and Lees, 1991). At the same time, iron accumulates within dopaminergic midbrain neurons, likely via effects of mitochondrial dysfunction and oxidative stress, and in turn leading to more ROS production (Muñoz *et al.*, 2016).

1.2 Dystonia

Dystonia is defined as sustained or intermittent muscle contractions causing abnormal, often repetitive, movements, postures, or both, affecting movement control in a focal, segmental or generalized distribution (Albanese *et al.*, 2013). In this, dystonia can refer to a clinical sign and a condition with dystonia being the main feature. The condition is currently classified according to two axes – clinical presentation and aetiology. Dystonia can present as focal, segmental, generalised or affecting a hemi-body. The age at onset can fall into infancy (0-2 years), childhood (3-12 years), adolescence (13-20 years), early (21-40 years) or late adulthood (>40 years). In the majority of cases, generalized dystonia is often characterized by childhood or juvenile onset, while adult-onset most often causes focal or segmental dystonia, often associated with considerable functional impairment in working-age adults. According to its presentation, it can manifest as an isolated or combined condition, the latter being defined as presenting as dystonia + chorea, parkinsonism, ataxia, myoclonus or tremor.

It is difficult to give exact prevalence rates for even the most common forms of dystonia (Asgeirsson *et al.*, 2006) with the most reliable numbers for cervical dystonia stating a clinic-based prevalence of 16:100`000 (Steeves *et al.*, 2012), respectively population-based prevalence of 732:100`000 (Müller *et al.*, 2002). For most acquired and genetic forms of dystonia, prevalence is unknown.

Given the multitude of phenotypes associated with dystonia, pattern recognition is key in order to identify the underlying aetiology. Dystonia can be idiopathic, inherited, or acquired in origin, and the following paragraphs introduce each aetiological background in more detail.

1.2.1 Idiopathic/Sporadic dystonia

Idiopathic dystonia, sometimes also referred to as sporadic, encompasses dystonic conditions without identifiable cause. All idiopathic dystonia presents isolated, i.e. without other neurological features. The different variants of idiopathic dystonia follow a typical pattern regarding age at onset and distribution. For example, focal limb dystonia, mainly consisting of musician`s dystonia and writer`s cramp, typically manifests in the 4th decade of life. Cervical dystonia, the most common form of focal dystonia, typically manifests around the same time (mean age at onset 41 years), while spasmodic dysphonia typically begins slightly later (mean age at onset 50 years) (Asgeirsson *et al.*, 2006) . The sixth/seventh decade of life is the typical age at onset for facial dystonia, including blepharospasm, oromandibular dystonia/Meige syndrome.

For the majority of adult-onset, focal dystonia, after exclusion of Wilson´s disease, structural abnormalities and potential iatrogenic causes, the underlying aetiology remains unknown, i.e. idiopathic. Although the above described patterns are typical, a minority of cases that follow these particular clinical patterns are acquired or genetic.

For cervical dystonia, the most frequent form of idiopathic dystonia, one study found 109 of 130 cases (84%) to be idiopathic, rendering 16% acquired or genetic (Strader *et al.*, 2011). The identification of alternative underlying disease mechanisms that might become a target for treatment options therefore is of paramount importance in a condition where treatment so far relies on symptomatic approaches only.

1.2.2 Genetic forms of dystonia

Since the identification of mutations in GCH1 as the underlying cause for dopa-responsive dystonia in 1994, a whole gamut of genes causing both isolated and combined dystonia have been identified. The first to describe a familial form of isolated generalized dystonia, however, was Oppenheim in 1911 coining the term `dystonia musculorum deformans`, subsequently called primary torsion dystonia, which was subsequently identified to be caused by a single GAG-deletion in the torsinA (TOR1A) gene (Ozelius *et al.*, 1997). By now, this mutation is the most frequent known genetic cause of early-onset generalized dystonia, with an estimated prevalence of 1:2,000-6,000 in the Ashkenazy Jewish population. The original description of mutations in the THAP domain containing 1 (THAP1) gene as another cause of autosomal-dominant isolated dystonia came from a large Mennonite family (Fuchs *et al.*, 2009). Since, over 100 distinct mutations in this gene have been described to cause familial, early-onset isolated dystonia (Blanchard *et al.*, 2011). Another relatively frequent genetic cause for isolated dystonia, often associated with dysmorphia, short stature and intellectual disability, are mutations in the histone methyltransferase gene KMT2B (Meyer *et al.*, 2016).

2012 brought the identification of monogenic familial forms of focal, isolated dystonia mainly affecting the cranio-cervical region due to mutations in the genes Guanine Nucleotide-Binding Protein G(Olf) Subunit Alpha (GNAL) (Fuchs *et al.*, 2013), Anoctamin 3 (ANO3) (Charlesworth *et al.*, 2012), and Cip1-interacting zinc finger protein 1 (CIZ1) (Xiao *et al.*, 2012). The prevalence of these mutations seems to differ between populations but overall accounts for <1% of cases of isolated,

adult-onset dystonia and has so far not lead to dedicated treatment options (Balint and Bhatia, 2014).

Dopamine-responsive dystonias (DRDs) are relatively static, hyperkinetic, combined dystonia syndromes with a sustained response to low doses of dopamine (Segawa *et al.*, 2003; Wijemanne and Jankovic, 2015). Typically, onset is in childhood or infancy, often beginning in the lower limbs with secondary generalization, often marked diurnal fluctuation and excellent and persistent response to levodopa treatment. As a group of conditions, they are particularly relevant, as simple dopamine replacement treatment can result in full reversal of symptoms. Previously, the mean time to correct diagnosis has been reported as 13.5years (Tadic *et al.*, 2012). The most common form of DRD is GTP Cyclohydrolase-1 *(GCH1)* deficiency, an autosomal-dominant disease, first described in 1976 (Segawa *et al.*, 1976), causing a dopamine deficiency by partial shortage of tetrahydrobiopterin (BH4). Although GCH1 deficiency is nearly eponymous to DRD, mutations in a number of genes encoding enzymes in the dopamine-synthesis pathway cause similar phenotypes. A much rarer, autosomal recessive form of DRD is Tyrosine hydroxylase *(TH)* deficiency (THD), similarly resulting in dopamine, but also adrenaline and noradrenaline deficiency. Clinically THD presents as an infantile onset hypokinetic-rigid syndrome (type A) starting with bradykinesia and generalizing dystonia with marked and sustained response to Levodopa, respectively a neonatal-onset complex encephalopathy with poor prognosis and much less predictable Levodopa response (type B) (Willemsen *et al.*, 2010). Mutations in 6-Pyruvoyl-tetrahydropterin Synthase (PTS) and Sepiapterin Reductase (SPR) deficiency similarly affect BH4 biosynthesis, whereas mutations in Carbinolamine-4a-dehydratase (PCD) or Dihydropteridine Reductase

(DHPR) interfere with the regeneration of BH4 (see Figure 1.2). Aromatic L-amino Acid Decarboxylase (AADC) deficiency yet affects not only dopamine but also serotonin synthesis with more pronounced effect on sleep (Brun *et al.*, 2010). More recently, mutations in the SLC6A3 gene, resulting in Dopamine Transporter (DaT) deficiency syndrome, and in the SLC18A2 gene, resulting in Vesicular Monoamine Transporter (VMAT) disease (Marecos *et al.*, 2014), have been described. Finally, there also have been singular cases reported, in which spinocerebellar ataxia (SCA) 3, hereditary spastic paraparesis (HSP)11 and ataxia telangiectasia presented as DRD (Wijemanne and Jankovic, 2015).

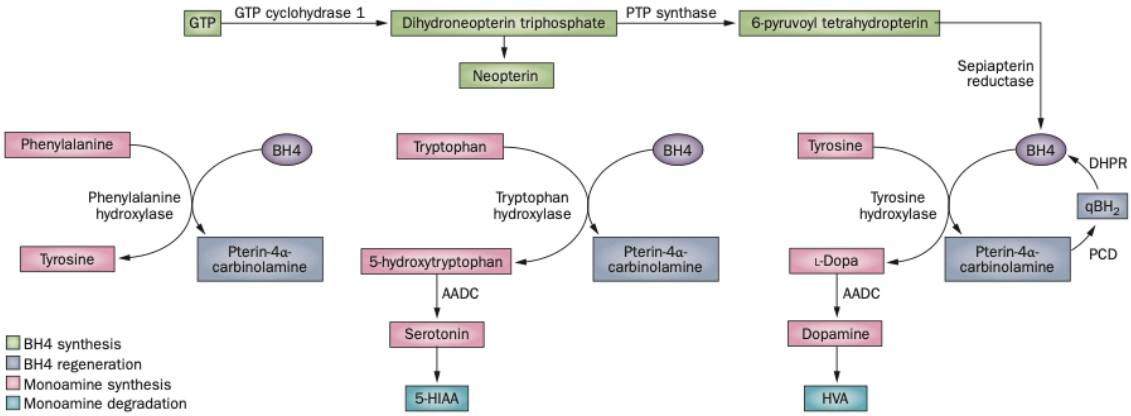

Figure 1.2: Dopamine Synthesis Pathway;
reproduced from (Wijemanne and Jankovic, 2015).

Myoclonus-dystonia is an entity classically affecting neck and upper limbs with ´lightning-fast`, shock-like myoclonus and a clear response to alcohol. Mutations in the Epsilon-Sarcogylcan (SCGE) gene (Zimprich *et al.*, 2001) appear to account for the majority of these cases with mutations in Potassium Channel Tetramerization Domain Containing 17 (KCTD17) (Mencacci *et al.*, 2015) trailing. In one kindred a

mutation in the Calcium Voltage-Gated Channel Subunit Alpha1 B (CACNA1B) gene resulted in a more leg-predominant form of myoclonus-dystonia causing instability while standing (Groen *et al.*, 2011). Individual cases with confirmed mutations in GCH1 (Leuzzi *et al.*, 2002) and TH (Stamelou *et al.*, 2012) and a myoclonus-dystonia phenotype have been reported as well.

A myoclonus-dystonia phenotype can also develop in the course of benign hereditary chorea, a condition with onset in infancy, often developing into a phenotype marked by either myoclonus-dystonia and concurrent thyroid and lung disease due to mutations in Thyroid Transcription Factor-1 (TITF1), episodic hyperkinesia/dystonia due to mutations in Adenylate Cyclase 5 (ADCY5) or - rarely - pure dystonia due to SLC16A2 mutations (Peall and Kurian, 2015).

The entity of Dystonia-Parkinsonism captures a range of conditions with predominant axial dystonia and parkinsonian features and is caused by mutations in three genes: Protein Kinase, Interferon-inducible Double-stranded RNA-dependent activator (PPKRA) (Camargos *et al.*, 2008), TATA-Box Binding Protein Associated Factor 1 (TAF1) especially in Filipino males from Panay, and Solute Carrier Family 6 Member 3 (SLC6A3). Cases with a particularly immediate onset of symptoms, often within days or hours after certain trigger events such as heat exposure, childbirth, psychological stress or alcohol consumption, are referred to as rapid-onset dystonia parkinsonism with mutations in the ATPase Na+/K+ Transporting Subunit Alpha 3 (ATP1A3) as an identified genetic cause (de Carvalho Aguiar *et al.*, 2004).

Paroxysmal dystonia are conditions with brief (seconds to hours) of involuntary posturing triggered by certain factors. These can be sudden movement in paroxysmal kinesiogenic dyskinesia/dystonia (PKD) due to mutations in Proline

Rich Transmembrane Protein 2 (PRRT2), Sodium Voltage-Gated Channel Alpha Subunit 8 (SCN8A) or Potassium Voltage-Gated Channel Subfamily Member A (KCNA1), physical activity such as in paroxysmal exercise-induced dyskinesia/dystonia (PED) due to Solute Carrier Family 2 Member 1 (SCL2A1) in GLUT-1 deficiency, or spontaneously as in non-kinesiogenic dystonia/dyskinesia due to Paroxysmal Nonkinesiogenic Dyskinesia Protein (PNKD), Calcium Voltage-Gated Channel Subunit Alpha1 A (CACNA1A) or Potassium Calcium-Activated Channel Subfamily M Alpha 1 (KCNMA1).

As a note of caution and probably also reflecting their prevalence, several of the above genes have not been confirmed independently so far, such as CIZ1 (Xiao *et al.*, 2012), HPCA (Charlesworth *et al.*, 2015), and VPS16 (Cai *et al.*, 2016).

Furthermore, genetic conditions affecting the accumulation of heavy metals, such as in manganese transportopathies caused by mutations in SLC30A10 or SLC39A14, or copper in Wilson disease due to ATP7B, cause a combined dystonia phenotype. Similarly, disorders of iron accumulation, such as neurodegeneration with brain iron accumulation (NBIAs), cause combined dystonia (see Table S3).

Finally, several rare metabolic conditions, like glutaric acidaemia type 1 caused by mutations in Glutaryl-CoA Dehydrogenase (GCDH) and GM1/GM2-gangliosidosis by Galactosidase beta 1 (GLB), Hexosaminidase Subunit Alpha/Beta (HEXA/HEXB) or GM2 Ganglioside Activator (GM2A) mutations result in an infancy-onset combined dystonic phenotype, often with cognitive decline (Sedel *et al.*, 2008).

1.2.3 Acquired forms of dystonia

The exposure of an individual to ischaemic, toxic, iatrogenic, infectious or autoimmune events can lead to an acquired dystonia. Brain ischaemia, may it be due

to global ischaemia, focal stroke or haemorrhage, can cause dystonia, particularly if it affects the putamen, and to a lesser degree the caudate nucleus, but less so the globus pallidus (Bhatia and Marsden, 1994; Janavs and Aminoff, 1998). Prime toxin culprits are carbon monoxide, methanol, disulfiram, cyanide, manganese and mercury. Although the insult is systemic, dystonia often presents with focal symptoms and also in combination with parkinsonism, tremor, chorea and ataxia but also neuropathy, visual loss and decreased vigilance (Janavs and Aminoff, 1998). Bacterial, viral (in particular Japanese B encephalitis) and fungal meningitis and encephalitis can cause usually transient dystonic +/- choreatic, ballistic movement abnormalities due to vasculitic ischaemia of the basal ganglia (Janavs and Aminoff, 1998).

There is characteristic time frames between the acute insult and development of symptoms, which most likely are due to age-dependent variability in neuroplasticity, myelination and metabolic response: dyskinesia classically begins within 14 days in "post-pump chorea" in infants and after thalamotomy in adults, whereas childhood injuries to the above-mentioned structures take much longer (up to 3 years) than in adults (within months) to come to effect.

Neuroleptic-induced dystonia classically presents as acute dystonic reactions affecting the orofacial and cranio-cervical region but also opisthotonus in young and in partiuclar male patients, whereas tardive dyskinesia, typically presenting with stereotypical, repetitive oro-facial movements, tongue protrusion and lip smacking in elderly and in particular female patients (Frei *et al.*, 2018).

Autoimmune-mediated causes of encephalitis, often associated with subtle but characteristic movement disorders, have increasingly become recognized as causes of dystonia, mainly due to Anti-N-Methyl-D-Aspartate receptor (anti-NMDAR)-

antibodies resulting in cranio-cervical, hemi-dystonia, dystonic seizures +/- opisthotonus (Dash and Pandey, 2019) and Voltage-gated Potassium Channel (VGKC)-complex/LGI1-antibodies, resulting in facio-brachial dystonic seizures (Irani *et al.*, 2011).

1.2.4 Neuropathology

So far, the search for a consistent pathology signature in dystonia has proven difficult, as no consistent, unifying pattern of pathological changes has emerged for primary dystonia. For the most frequent genetic form of isolated dystonia caused by mutations in *TOR1A* (DYT1) subtle changes of ubiquitin, torsinA, and lamin A/C-positive perinuclear inclusion bodies in cholinergic and other neurons in the pedunculopontine nucleus, cuneiform nucleus, and griseum centrale as well as tau/ubiquitin-positive signals in neuromelanin-positive neurons of the SN pars compacta and LC have been described (McNaught *et al.*, 2004), but failed to replicate (Paudel *et al.*, 2014). More recently, the so far largest neuropathology study investigating cervical dystonia, identified a significantly reduced density of cerebellar Purkinje cells by stereological quantification in patients with mutations in the *THAP1* gene (DYT6) irrespective whether they were symptomatic or not (Prudente *et al.*, 2013). The same study however could not replicate consistent changes in basal ganglia, cerebral cortex, or red nucleus as implied previously (Neychev *et al.*, 2011).

In summary, there does not seem to be a single unifying neuropathology finding consistently identifiable across all types of dystonia (Kaji *et al.*, 2018). However, more and more evidence is pointing at a network dysfunction involving cerebellum,

basal ganglia (esp. posterior putamen and globus pallidus) and cortex (supplementary motor area) as a common core in dystonia pathophysiology (Quartarone and Hallett, 2013).

1.2.5 Pathophysiological mechanisms

Replacing the long-held concept of dystonia as a psychiatric disorder, and guided by initial lesion-based clinical observation (Marsden *et al.*, 1985), for some time dystonia was viewed as a disorder primarily affecting the basal ganglia, as summarized in (Jinnah *et al.*, 2017). Experimental interventional evidence from lesional and deep brain stimulation studies (Vidailhet *et al.*, 2013), local field potential recordings and functional imaging (Karimi and Perlmutter, 2015) meanwhile confirmed a major causal role of basal ganglia circuits in dystonia pathophysiology (Peterson *et al.*, 2010).

In addition, electrophysiology has identified phenomena such as increased cortical plasticity (increased long-term potentiation (LTP) and decreased long-term depression (LTD), respectively) and loss of inhibition as cortical hallmark features of dystonia (Hallett, 2011; Quartarone and Hallett, 2013). Sensory tricks, such as the geste antagoniste, first described by Meige and Feindel at the end of the 19th century, have long been appreciated as dystonia-specific clinical phenomena (Poisson *et al.*, 2012), but only recently been quantified by electrophysiology and functional imaging (Nelson *et al.*, 2009). Several lines of evidence, including pathology, transcranial magnetic stimulation and eyeblink classical conditioning, meanwhile support the role of the cerebellum in dystonia (Filip *et al.*, 2013; Sadnicka *et al.*, 2012; Shakkottai *et al.*, 2016).

Additional insight into disease mechanisms have come from the growing number of monogenic dystonias: Foremost, dopa-responsive dystonia (GCH1, TH, SPR etc.) highlights the role of the dopaminergic system, as L-dopa completely and consistently reverses dystonic symptoms. Equally, iatrogenic dystonic reactions due to exposure to dopamine receptor blocking agents have long been appreciated (Schönecker, 1956). Studies in transgenic mouse models of DRD and patients with the clinically similar DYT3 Dystonia-Parkinsonism-syndrome showed a selective depletion of dopaminergic neurons in the striatal striosome compartment, regulating the efferent structures of the direct and indirect basal ganglia pathways (Goto *et al.*, 2005; 2013; Kenta Sato *et al.*, 2008). More recently, molecular insight into monogenic conditions complemented the above: GNAL, predominantly expressed in striatal medium spiny neurons, regulates dopaminergic D1 (direct pathway) and adenosine A2A (indirect pathway) receptor signalling (Hervé, 2011). Human and animal studies have also documented reduced dopaminergic D2 receptor expression in dystonia related to TOR1A and SGCE (Napolitano *et al.*, 2010; Zhang *et al.*, 2012).

Functionally, the striatum serves as the main afferent basal ganglia structure, where convergent cortical glutamatergic signals are integrated by medium spiny neurons (MSN) and are directed onwards to the basal ganglia output structures. Striatal plasticity is mainly located at the dendritic spines of MSNs, which constitute 95% of striatal neurons (Dupuis *et al.*, 2014). Both nigro-striatal dopaminergic afferents as well as GABAergic and cholinergic striatal interneurons physiologically modulate MSN activity (Peterson *et al.*, 2010).

On a cellular level, a reduced number of D2, and an increased number of D1 dopamine receptors in several dystonias supports the view of dopamine – in general

- acting through an imbalance between the direct and indirect basal ganglia pathways (Simonyan *et al.*, 2017). The well-appreciated clinical effect of anti-cholinergic medication on dystonia is based on suppressing the abnormal cholinergic overactivity within the striatum emerging from this imbalance (Eskow Jaunarajs *et al.*, 2015).

1.3 Overlap between Dystonia and Parkinson`s Disease

From the above overview it is evident that there are multiple clinical and aetiological overlaps between parkinsonism and dystonia. Starting with conditions with a predominantly parkinsonian phenotype, the most obvious clinical entity is Young-onset Parkinson´s disease (YOPD). Around 20% of YOPD patients may initially present with dystonia of variable degree, which might become even more prevalent with advancing disease (Wickremaratchi *et al.*, 2011). Mutations in the *parkin* gene, the most common cause of recessive PD, typically present as YOPD with an early-onset, slowly progressive parkinsonism with frequent and prominent (foot) dystonia, good levodopa-response but early occurrence of levodopa-induced dyskinesia (Ferreira and Massano, 2016; Kägi *et al.*, 2010). Mutations in *PINK1*, the second most frequent cause of early-onset autosomal recessive PD, presents with often prominent dystonia and cognitive impairment (Massano and Bhatia, 2012), whereas mutations in *DJ-1,* accounting for only 1% of early-onset PD cases, presents with frequent focal dystonia, including blepharospasm (Ferreira and Massano, 2016). Similarly, dystonia has been described as a prominent feature in cases with early-onset PD due to mutations in *SYNJ1* (oromandibular and limb dystonia) (Quadri *et al.*, 2013), *DNAJC6* (Köroğlu *et al.*, 2013) and VPS13C (Lesage *et al.*, 2016).

On the other hand, there are a number of dystonic conditions with co-existing parkinsonism of metabolic or genetic origin (see Table S5), such as Wilson disease, the manganese transportopathies, glutaric aciduria type 1, GM1/GM2 gangliosidosis, Rapid-onset Parkinsonism, dopamine transporter deficiency (Kurian *et al.*, 2009; Lohr *et al.*, 2016), early-onset dystonia-parkinsonism (Charlesworth *et*

al., 2013), Perry syndrome (Wider and Wszolek, 2008), Lubag (Rosales, 2010), vesicular monoamine transporter disease and, most importantly, the group of dopa-responsive dystonias (DRDs). Relating to the latter, the most obvious overlap comes from GCH-1, as - based on the initial clinical observations - mutations in *GCH1* have been found to be more frequent in PD cases than controls (OR 7.5, 95% CI 2.4 – 25.3). Hence, pathological *GCH1* mutations not only cause DRD but are also predisposing to nigrostriatal degeneration (Mencacci *et al.*, 2014).

Similarly, both movement disorder phenotypes show a considerable overlap regarding their underlying aetiology. Mitochondrial dysfunction is one of the most consistently reported underlying pathology in PD, identified from several lines of evidence: activity of mitochondrial complex I, a central part of the mitochondrial electron transport chain, is reduced in the substantia nigra and other types of tissue in patients with PD when compared to controls (Schapira, 2008); environmental toxins predominantly acting on mitochondria such as Rotenone and 1-Methyl-4-phenyl-1,2,3,6-tetrahydropyridin (MPTP) are known to cause Parkinsonism (M. T. Lin and Beal, 2006); mutations in the nuclear encoded mitochondrial polymerase gamma (POLG) frequently causes Parkinsonism (Davidzon *et al.*, 2006; Dolhun *et al.*, 2013; Invernizzi *et al.*, 2008) and several of the genes in which mutations have been identified to cause familial Parkinsonism have been found to have a physiological role related to mitochondrial function: *parkin* and its interaction with *PINK1* (Pickrell and Youle, 2015), *DJ-1* (Ryan *et al.*, 2015), but also less frequent genetic causes, such as vacuolar protein sorting 13C (*VPS13C*) (Lesage *et al.*, 2016).

At the same time, mitochondrial disease (MiD) - caused by a variety of mitochondrial mutations but most frequently documented in Leigh Syndrome - frequently presents with dystonia (Finsterer, 2008; Macaya *et al.*, 1993).

Lysosomal dysfunction has been equally implicated as a leading pathophysiological mechanism in PD, most prominently due to mutations in Glucocerebrosidase (*GBA*) (Neumann *et al.*, 2009; Sidransky *et al.*, 2009) and genes less frequently implied in lysosomal function (Robak *et al.*, 2017). Dystonia has been described in the context of lysosomal dysfunction due to GM1 gangliosidosis and Niemann-Pick type C (Sedel *et al.*, 2008).

1.4 Age – a disease-defining factor in Dystonia and Parkinson´s Disease

In PD, another peculiar, epidemiologically well-established connection is the increasing risk of PD with age. Ever since the first description of the condition, advancing age has been reported as the most consistent risk factor for PD (de Lau and Breteler, 2006). Both incidence (Bower *et al.*, 1999; 2000) and prevalence rate of PD (Pringsheim *et al.*, 2014) increase dramatically and consistently with advancing age but peculiarly capping off after the 8th decade of life - the reason for this remains so far unknown. The relationship between aging and PD is intriguing and a number of molecular mechanisms shared between the two, have been suggested as causal, such as impaired lysosome, proteasome and mitochondrial function, as well as increased inflammation and oxidative stress (Collier *et al.*, 2017; Reeve *et al.*, 2014)), although the exact mechanisms are still debated (Rodríguez *et al.*, 2015). The role of genetic mechanisms influencing the ageing process in PD risk remain, however, unknown.

The association with age is similarly present in dystonia in particular in cases with isolated, idiopathic dystonia. Mean age at onset is typically later in blepharospasm> cervical dystonia > task-specific dystonia. Further, typical clinical presentations for many of the combined dystonia syndromes similarly cluster around certain ages.

1.5 Aim of this thesis

Based on the above described clinical and aetiological similarities between PD and dystonia and individual clinical observations, I generated hypotheses as to pathophysiological links between the two conditions involving lysosomal and mitochondrial dysfunction and aging-related processes.

In chapter I, starting from the phenotype, I studied a pro- and a retrospective cohort of dystonia patients in order to explore episodic evidence on lysosomal deficiency in patients with so far idiopathic dystonia. To this end, I applied lysosomal enzyme activity measurements in both peripheral blood and post-mortem brain tissue samples as well as Sanger sequencing of *GBA*.

In chapter II, starting from the underlying aetiology, I studied a cohort of patients with genetically confirmed mitochondrial dysfunction in order to examine changes in brain morphometry specific for movement-disorder phenotypes.

In chapter III, I explored in how far genetically determined telomere length as well as the spatial and temporal dynamics of telomere length in the healthy human brain might explain why PD risk is closely associated with advancing age. For this, I applied a Mendelian randomization approach utilizing existing large case-control PD GWAS data sets and the quantification of telomere length from different brain regions and across age from post-mortem human brain samples.

2 Techniques relevant to this thesis

The following summarizes the principles of the experimental methods and techniques used in this thesis, while details of their specific application are to be found in the methods section of each chapter.

2.1 Genetic methods – strategies and techniques

2.1.1 Models of inheritance and strategies to unravel them

The underlying genetic mechanisms of disease can be summarised in three main models of inheritance.

a) Mendelian Disease model

This describes the occurrence of disease by very rare (minor allele frequency (MAF) below 0.1-0.01%) but highly penetrant variants, affecting multiple members within a family. Family studies examine the segregation of gene variants according to phenotype. Previously, the identification of these variants relied on linkage analysis or homozygosity mapping, while more recently this has been superseded by the combination of NGS and Sanger sequencing confirmation.

The correct interpretation of the mode of inheritance is paramount to choosing an ideal approach and correct interpretation of results, as in dominant cases, only shared heterozygous variants, and in recessive cases, homozygous or compound heterozygous variants can be pathogenic. Sporadic disease, on the other hand, follows either recessive inheritance or are caused by *de novo* mutations.

In general, studying family members as distantly related as possible generates the shortest genetic overlap, i.e. number of shared variants, helping identifying the

causative one. These shared variants are then filtered for plausible pathogenic variants and segregation confirmed by Sanger sequencing within the index family. Non-affected family members can help further to reduce the number of potential culprits via segregation analysis. However, incomplete penetrance and unaffected family members being too young to manifest the condition are important caveats in the interpretation of segregation analysis. Ideally, the pathogenicity of potential variants is validated in additional kindreds (e.g. www.genematch.org).

b) Common disease-common variant model

This describes the occurrence of disease by relatively common (MAF >5%) single genomic variants, such as single nucleotide polymorphisms (SNPs), or the combination of genomic variants, inferring a relative rise in disease risk. Assessing the entirety of SNPs in an organism is referred to as genotyping.

Genome-wide association studies (GWAS), and more recently post-GWAS approaches, utilizing genotyping information of tens of thousands of individuals, have been employed to explore these associations by dedicated biostatistical methods, often in the context of large consortia, such as the International Parkinson´s Disease Genetics Consortium (IPDGC).

c) Common-disease-rare variant model

Increasingly recognized, rare gene variants can also exert an effect on disease without following clear mendelian inheritance and avoiding detection by GWAS approaches. This may be due to low penetrance or the presence of multiple variants at the same locus. Often, this relationship results in an inferred disease-risk intermediate between variants following a mendelian or common-variant model.

The most prominent example of this type of inheritance in movement disorders is *GBA* mutations in PD (Rogaeva and Hardy, 2008) which in fact has been identified to be the most frequent genetic risk factor known so far for this condition (Sidransky *et al.*, 2009). Most effectively, this inheritance model is detected by a candidate gene approach in which gene variants plausibly involved in the disease process, are studied. The most prominent examples of common disease-rare variant associations importantly have been identified by astute clinical observation, supporting the role of the clinician in the age of genome-driven medicine (e.g. *GBA* mutations in PD or *TREM2* variants in Alzheimer`s disease).

2.1.2 Dideoxynucleotide Sequencing

Commonly referred to as Sanger Sequencing after its developer Frederick Sanger, dideoxynucleotide sequencing is the most widely used sequencing technique and continues to be widely used for validation of alternative sequencing methods (Sanger 1977, Pittman&Hardy 2013).

In principle, polymerase chain reaction (PCR, see 2.2.4) is used to amplify identical DNA template molecules representing the region of interest within a gene target, such as an exon or a combination of exons. Respective primers for the PCR reaction are designed to capture not only the exon itself but also exon-intron boundaries in order to compensate for a drop in sequencing quality at the ends of a PCR amplicon. Amplified template DNA strands are then incubated in a reaction mix containing deoxyribonucleotides (dNTPs) and DNA polymerase.

Sequencing itself relies on the principle of random DNA polymerase inhibition by the interruption of DNA elongation through dideoxynucleotides (ddNTPs) paired with fluorescent markers emitting at certain wavelengths, that are added at a small

concentration to the reaction mix. As ddNTPs lack a certain hydroxyl-group, no further dNTP can be added and the strand elongation ends after a ddNTP. As the DNA polymerase advances along the DNA template across all amplified DNA molecules, the inclusion of a ddNTP hence leads to the termination of copy strand elongation and copied DNA molecules of different lengths marked with a fluorescent marker depending on the last ddNTP added. Using a combination of capillary electrophoresis and the measurement of laser-excited fluorescent light emissions, the DNA sequence can then be assembled from the sequence – the intensity profile of the four different fluorophores along the copy strand can then be read and interpreted as a chromatogram.

2.1.3 Next-generation sequencing

The development of next-generation sequencing (NGS) has drastically advanced the possibility to identify relevant genetic variants due to a substantial increase in sequencing yield and subsequent drop in cost. NGS technology is used to generate whole genome sequencing (WGS), whole exome sequencing (WES) or targeted gene arrays. Standard *short-read* NGS comes with the limitation of a maximum read length of 300 base pairs (bp) per sequencing reaction and the need for correction by aligning multiple overlapping reads in order to generate a continuous, complete sequence (resulting in the read depth), which is not suitable in situations involving long repetitive genomic elements, copy number alterations and structural variations, such as identification of pseudogenes with high homology. It is hence still best practice to confirm NGS hits by targeted Sanger sequencing.

With the introduction of the Oxford NanoPore technology, *long-read* NGS was established in 2014. This overcomes the difficulties in sequencing resolution of

short-read techniques (Goodwin *et al.*, 2016), although specialised software algorithms should be employed (Leija-Salazar *et al.*, 2019).

The interpretation of NGS sequencing data is crucial, as on average an individual`s exome contains 20`000 – 24`000 variants (depending on ethnic origin), of which ~98% are known benign polymorphisms and a large proportion synonymous, i.e. not leading to any change in the amino acid sequence or protein structure. Finding the causative variants therefore relies on adequate filtering and the interpretation of the biological effect of the variant found.

2.1.4 Genotyping and genome-wide association studies

Via the development of gene arrays, consisting of sequencing chips containing tens of thousands of SNPs across the genome, NGS has paved the way for GWAS. This type of study, first successfully applied to myocardial infarction (Ozaki *et al.*, 2002), identifies genetic variants associated with a trait in a hypothesis-free way by comparing the frequency of variants between cohorts of people with and without the trait in question. Given the large number of genetic variants in each human being (to date GWAS use approximately 1Mio. SNPs), the currently used statistical cut-off for genome-wide significance is $p<10^{-8}$, and GWAS studies therefore rely on sufficiently sized cohorts. Accordingly, the latest PD GWAS was based on 38`000 patients and 1.4M controls (Nalls *et al.*, 2019).

2.1.5 Post-GWAS approaches & Mendelian Randomization

Epidemiological research aims to establish the effect and strength of an exposure, such as a biomarker, environmental factor or drug-treatment, on an outcome, such

as a trait, a condition, or mortality rate. Observational epidemiology uses cross-sectional, longitudinal, cohort and case-control studies for this. However, their results, even if accounted for confounding by multiple regression, are prone to residual confounding by factors either unknown, not measured or not measurable. Reverse causation is another potential difficulty, which is present when the association between exposure and outcome is not caused by the exposure leading to a change in the outcome but the outcome in retrospect seemingly influencing the exposure.

In population genetics, novel statistical tools try to overcome these shortcomings utilizing available GWAS datasets. Under the assumption that large populations allow for quasi-randomization of genetic information at birth, genetic randomization replaces active randomization in a near infinite number of individuals carrying an unchanged genotype through their lifespan. Mendelian Randomization (MR) uses gene variants associated with intermediate phenotypes or exposures as instrumental variables (IV) for exposure effect estimation on disease risk. It thereby circumvents the limitations of classical epidemiological research by being less susceptible to confounding and reverse causality than observational studies (Burgess *et al.*, 2013). In order to achieve this, MR is based on three fundamental conditions, which have to be fulfilled:

- the variant must associate with the exposure
- the variant must not associate with any confounder of the exposure-outcome association
- the variant does not affect the outcome through any means other than through the exposure association

IVs are SNPs which individually are associated with the outcome at a genome-wide significance level (i.e. p-value of $<5x10^{-8}$). An MR instrument normally consists of a number of IVs, which are combined into an IV instrument. For each allele, Wald ratios are calculated by dividing the per-allele log-OR for the outcome by the per-allele difference in mean exposure for each of the IVs of the combined IV instrument. Results are then compiled in a forest plot and 95% confidence intervals (95% CI) for each Wald ratio are calculated.

Linear regression analysis of the variant-outcome association divided by the variant-exposure association then examines the combined effect of all IVs on the outcome. For this, several different methods exist: inverse-variance weighing (IVW) represents the assumption that if the exposure has a value of zero the outcome has a value of zero, i.e. that all variants are valid IVs (without pleiotropic effects). In contrast, penalized weighted median, as well as MR-Egger regression allow to relax this assumption to certain degrees. Penalized weighted median method performs under the assumption that no more than 50% of the weight of the MR effect estimate are derived from invalid (pleiotropic) IVs (Bowden *et al.*, 2016).In MR-Egger, the IV assumption of no horizontal pleiotropy is replaced by the Instrument Strength independent of the direct effect (InSIDE) assumption: this posits that the genetic instrument-risk factor association is not correlated with any pleiotropic association from the SNPs to the outcome (Bowden *et al.*, 2015). In doing so, MR-Egger relaxes one of the MR assumptions and allows to assess for the possibility of an aggregate unbalanced horizontal pleiotropic effect (Bowden *et al.*, 2015).

MR enables to assess causality rather than observational associations and is a particularly powerful approach in case-control settings. MR has previously been

used in the PD field to confirm (Noyce *et al.*, 2017; Pichler *et al.*, 2013; Simon *et al.*, 2014) or refute (Larsson *et al.*, 2017) epidemiological evidence on the influence of environmental factors on disease risk.

2.2 Molecular biology methods

2.2.1 DNA extraction from blood

Genomic DNA was extracted from whole blood (taken in ethylenediaminetetraacetic acid (EDTA) blood collection containers) in the UCL Institute of Neurology`s Diagnostic Genetics Laboratory using the FlexiGene© kit (Qiagen), according to manufacturer instructions.

In brief, 300µl of whole blood was mixed with 750µl of lysis buffer FG1, followed by a centrifugation step (20sec at 10`000x), after which the supernatant was discarded. The resulting pellet was homogenized by adding buffer FG2 and vortexing. Subsequent centrifugation and 5min inactivation of the protease in a heating block followed. Separated by centrifugation steps (3min, 10`000x), DNA was precipitated sequentially by 100% Isopropanol, and 70% Ethanol, respectively, after which the pellet was air-dried. Finally, DNA was dissolved in buffer FG3.

2.2.2 DNA extraction from tissue

DNA was extracted in an automated manner by LGC Genomics using its sbeadex livestock kit (LGC genomics, no.44702). The use of superparamagnetic microparticles and a two-step binding mechanism for nucleic acid purification allows the effective removal of impurities and potential inhibitors of enzymatic reactions in the absence of organic solvents: after an initial lysis step, based on a protease preparation in respective buffer, a binding mix containing the sbeadex

particles is added to the solution and the DNA concentrated in a pellet by magnetic force. After repeated washing steps, a pellet is formed using a magnet and the final, purified DNA is eluted using elution buffer for one hour at 55°C to increase DNA yield. Finally, the sbeadex particles are concentrated at the bottom of the tube by magnetic force, and the DNA pipetted into the final sample tube.

2.2.3 DNA quantification

DNA sample transfers were always done using filter pipette tips and large quantities of samples predominantly processed during quiet hours in the lab to avoid contamination. For a relative estimate of genomic DNA concentration and quality, the NanoDrop Spectrophotometer with ND-1000 software package was used. A 260/280nm ratio between 1.6-2.0 and 260/230nm between 2.0-2.2 is reflective of DNA of adequate quality for sequencing purposes. After calibration with miliQ double deionized water, the NanoDrop spectrophotometer was loaded with 1.5µl of sample solution. DNA concentration was expressed in ng/µl.

2.2.4 Agarose gel electrophoresis

Gel electrophoresis was used to assess the quality and size of DNA fragments. For this, 1x TBE (tris-borate-EDTA solution) solution was prepared using 12.1.g Trizma base (Sigma), 6.2g Boric Acid (Sigma), 0.7g Ethylenediaminetetraacetic acid (EDTA) (Sigma), dissolved in 1000ml of distilled water. An Agarose gel of 1.5% concentration was prepared using Ultrapure Agarose (Invitrogen) and TBE 1x buffer and stained with gel red (Cambridge Bioscience). Each lane of the agarose gel was loaded with 2.5ul of loading dye (Thermo Scientific) mixed with 2.5ul of

respective DNA sample. Samples were run along a DNA ladder of respective size (Gel Pilot wide range (200-4`500 bp; no. 239125; GelPilot Mid Range (100-2`000 bp; no. 239135) Gel Pilot 1kb (1`000-10`000bp; no. 239085), Quiagen) at 120mV for 30-35min and DNA fragments visualized using UV light.

2.2.5 Polymerase chain reaction

Polymerase Chain Reaction (PCR) uses alternating thermal cycles of heating and cooling to permit temperature-dependent reactions in order to exponentially amplify a target DNA sequence across several orders of magnitude. The reaction takes place within a closed compartment, typically a 20ul Eppendorf cup. It relies on the presence of a double-stranded DNA template, containing the sequence to be amplified, two primers, i.e. short single stranded DNA sequences complementary to the 3` (three prime) end of each strand of the sequence to be amplified, dNTPs, a suitable buffer solution and a heat resistant DNA polymerase. During a singular *initialization* step, heating up the reaction compartment to around 95°C for 10-15min activates the DNA polymerase in the reaction chamber. This is followed by repeated cycles of heating to 94-98°C for *DNA denaturation*, cooling to 50-65°C for *annealing* of forward and reverse primers that bind to each end of the sequence to be amplified, followed by an *elongation* step allowing the DNA polymerase to synthesize a new strand of DNA complementary to the template strand. The reaction is terminated with a *final hold* phase, during which the reaction mix is cooled to around 4°C to end any active reaction and prepare the sample for storage. In theory, this cyclic sequence leads to a doubling of the number of target DNA sequences with each cycle, following an exponential (2^n, n = number of cycles) pattern.

When setting up novel PCR cycle, the activation temperature was chosen depending on the PCR kit (TAQ polymerase) used, while the annealing temperature was chosen depending on the primer melting temperature Tm. Elongation temperature was always set at 72°C and duration only changed in case if all other attempts to suppress excessive background sequencing signal were unsuccessful. If Tm differed >3°C between primers of a primer pair, a touch-down program (in 0.5°C steps; 10°C Tm touch-down is normal) was chosen with the number of PCR cycles depending on the length of the amplicon. For PCR reactions of GC-rich templates (>65%), 3% DMSO was added, in order to aid in the denaturing of the triple bonds in GC-rich DNA according to general PCR (https://www.neb.com/tools-and-resources/usage-guidelines/guidelines-for-pcr-optimization-with-taq-dna-polymerase).

2.2.6 Enzymatic PCR purification

If a PCR amplification product was used for subsequent sequencing, the following enzymatic PCR purification step was included: A mixture of Fast-Alkaline phosphatase, removing unused dNTPs, and Exonuclease I, removing unused ssDNA, called ExoSap was added to the PCR amplification product. The ExosAP mix containing 50µl Exonuclease I (Thermo Fisher no. EF0651), 200µl FastAP (Thermo Fisher no. EN0582) and 750µl deionised water was then mixed with the PCR product at a ratio of 2:5 and run under the following settings:

ExosAP Cycle			
Time (min)	30:00	15:00	Hold
Temperature (°C)	37.0	80.0	4.0

2.2.7 Sanger Sequencing reaction and sample filtering

For the sequencing PCR reaction, per well, 3µl ExosAP product was mixed with 3.5µl deionised water, 2.0µl Sequencing Buffer and 0.5µl BigDye Terminator v1.1 (both Applied Biosystems no. 4336699) and 1.0µl of primer and run on the PCR light cycler:

Sequencing 3730 cycle					
Time (min)	01:00	00:30	00:15	04:00	Hold
Temperature (°C)	94.0	94.0	50.0	60.0	4.0
n cycles	1	25			

For sequencing reaction clean-up and removal of unused ddNTPs, a hydrated solution of Sephadex was prepared using 2.9 grams of Sephadex G-50 powder (Sigma-Aldrich, ref: 9004-54-0) and 40ml of autoclaved water. The solution was mixed well and allowed to hydrate for at least 30 minutes at 4°C. 350µl of this solution was pipetted into each well of a Corning FiltrEX 96-well, 0.66 mm glass fibre filter plate, which was then placed on top of an empty collection plate. A first centrifugation step (3 minutes at 700xg) generated the Sephadex columns, upon which the sequencing PCR product was carefully pipetted. Another centrifugation

step (5 minutes at 910xg) resulted in the final sequencing solution, which was then placed on the sequence reader.

2.2.8 TL measurements in human tissue

The ideal methodology to measure TL depends on the tissue available and clinical question asked, as summarized in Table 2.1. Telomere repeat fragment (TRF) assay refers to telomere Southern blot, which is the gold standard of absolute telomere length measurement. Other factors to consider are feasibility to process the needed number of samples and technical limitations. Finally, the precision and accuracy of an experimental method, expressed as the ratio of standard deviation to the mean, called coefficient of variation (CoV), is relevant. Overall CoV ranges of 1.25-12% (TRF) and 2.2-28% (Q-PCR) have been reported in the literature (Montpetit *et al.*, 2014). Comparative studies for TRF and Q-PCR reported CoVs of 1.74% vs. 6.45% (n=50) (Aviv *et al.*, 2011), respectively of 1.5% vs. 5.8% (n=681) (Elbers *et al.*, 2014). For MMQ-PCR, a method that reduces the potential of pipetting errors by multiplexing the measurement of the telomere and single copy gene in a single compartment, CoV has been reported as 3.13% (n=95) (Cawthon, 2009).

2.2.8.1 Telomere restriction fragment (TRF) analysis

Two µg of genomic DNA was digested with *Rsa*I and *Hin*fII at final volume 30 µl in accompanying Smart Cut buffer (NEB) at 37˚C overnight. Digested genomic DNA was separated in 30-cm long 0.8% agarose gels and transferred to a nylon membrane (Hybond N-, GE Healthcare) via capillary action after treating the gel with 1 N sodi-

Table 2.1: Comparison of telomere length measurement techniques

Technique	Requirements	Advantages	Disadvantages
Terminal restriction fragment (TRF) – Southern blot			
	• Substantial amount of DNA (10^5 cells, >1μg)	• Established gold standard • Most commonly used • Used to calibrate other methods • Small errors	• Dependency on restriction enzyme chosen (sub-telomeric region error) & blot analysis • Requires substantial amounts of DNA • Insensitive to very short telomeres • Resolution 1kb
Single Telomere Length Analysis (STELA) – single molecule PCR			
	• Very little DNA (<100pg) • Significant experience in single-molecule PCR	• Quantification of TL from single chromosome • No sub-telomeric region error • Resolution 0.1kb	• Usually restricted to well-characterized telomeric regions (XpYp, 2p, 11p, etc.) • Technically challenging • Labour intensive • Cannot measure mean TL across different chromosomes • Inaccurate in TL >20kb • Only feasible in small sample size (5-10)
Quantitative fluorescence in-situ hybridization (Q-FISH)			
	• Small sample, >20 metaphase chromosomes • Live cells	• Measures individual chromosomes • Resolution 0.3kb	• Not feasible in post-mitotic cells without metaphase chromosomes • Only feasible in small sample size (5-10)

Flow FISH			
	• Individual cells in suspension • Live cells	• Only method validated for clinical use • High-throughput • Semi-automated • Resolution 0.2-0.3kb	• Limited to fresh/ non-fixed blood • Multiple wash steps • Meticulous calibrations and controls
Quantitative or monochrome-multiplex PCR (Q-PCR, MMQ-PCR)			
	• To be measured in triplicate to reduce potential error • nanograms of DNA	• Short timeline and cost • MMQ-PCR reduces error rate due to pipetting	• Variability within and between measurements • Susceptible to copy number variations of single copy gene used as standard to calculate T/S ratio

um chloride and alkaline solution (sodium hydroxide). DNA on the membrane was crosslinked by UV and hybridised with the ^{32}P-labelled human telomere DNA fragment (from an *Eco*RI-digested pKazu-hTelo plasmid (55xTTAGGG repeats, cloned into pCR4 TOPO-blunt vector). A DNA ladder (Hyperladder™ 1kb) was probed with a *Schizosaccharomyces pombe* telomere DNA delivered from *Eco*RI & *Bam*HI-digested p1742 plasmid. Hybridized probe was detected using Storm Phosphorimager.

2.2.8.2 Monochrome multiplex quantitative-PCR (MMQ-PCR)

Real time PCR (rtPCR) amplification allows the constant measurement of the amplification product during amplification cycles, as fluorescent dyes are activated with each amplification cycle. The fluorescence intensity is proportional to the DNA concentration in the reaction compartment. The analysis of the resulting amplification plot utilizes an arbitrary fluorescence threshold and the threshold cycle, termed C*t,* constituting the PCR cycle at which the fluorescent threshold is reached per sample.

Quantitative PCR (qPCR) refers to relative quantification, which generates the ratio of the copy number of a target gene to the copy number of a house-keeping or so-called single copy gene.

Using qPCR, telomere length can be measured by establishing the factor by which a sample differs from a reference DNA sample - Genomic DNA from HEK293K cell line (ATCC® CRL-3216™) was used as a reference and standard for all experiments in this work - in its ratio of telomere repeat copy number to single copy gene copy number (Cawthon, 2002). Monochrome multiplex q-PCR (MMQ-PCR) is based on

the principle of multiplexing the reaction to measure both telomere (T) and single copy gene (S) copy numbers in the same reaction container, halving the need for reagents and minimizing the possibility of pipetting errors, as both reactions utilize the very same DNA contents (Cawthon, 2009). This is achieved by using a single fluorescent DNA-intercalating dye, as telomere and single copy gene (e.g. Albumin) amplification differs dramatically in their absolute copy number and onset/PCR cycle of signal emittance. Furthermore, single copy gene signals can be collected at a temperature at which the telomere product is melted, eliminating potential interfering signals.

T/S ratio was then calculated with T (the number of nanograms of the standard DNA that matches the experimental sample for copy number of the telomere template) divided by S (the number of nanograms of the standard DNA that matches the experimental sample for copy number of albumin). Telomere copy number is presented as fold-enrichment against the reference HEK293T standard in the same reaction plate. If T/S >1.0, the sample has an average telomere length greater than that of the reference HEK293T cells. Normalisation of T/S by commercially available immortalised cell line minimises day-to-day variation of qPCR. MM-qPCR was repeated at least three times per sample.

2.3 Biocomputational methods

2.3.1 Primer design

Primers were designed using the Primer3plus online tool (http://www.bioinformatics.nl/cgi-bin/primer3plus/primer3plus.cgi). DNA sequences were identified from online repositories (http://genome.ucsc.edu /index.html or http://ensembl.org), according to gene or exome position (hg19/GRCh37.p13 or GRCh38.p12, according to reference used). A primer base sequence was chosen to result in an amplicon of ideally <1000bp in length (for Sanger sequencing, <100bp for qPCR), including about 100bp of intronic caps either end and an ideal primer pair chosen according to the following princples of primer design: a) ideal melting (50-55°C, max 65°C) and annealing temperature to avoid secondary annealing and less than 5°C difference between pairs), b) ideal GC content (ideally 50-55%, extremes 40-60%), c) low self-complementarity (describing the propensity to form primer-dimers), d) avoidance of repeats (single or dinucleotide repeats or runs of single bases) and e) adequate primer variant specificity (to avoid cross homology to other genes) assessed by Primer-BLAST (https://www.ncbi.nlm.nih.gov/tools/primer-blast/) and UCSC`s In-silico PCR tool (https://genome.ucsc.edu/cgi-bin/hgPcr?wp_target=&db=hg19&org=Human&wp_f=&wp_r=&wp_size=4000&wp_perfect=15&wp_good=15&wp_showPage=true&hgsid=705440349_4w0xXYH0x7FR4kxIer46obBRAaf7). Primers were ordered from SigmaAldrich at a concentration of 0.025 µmole, as desalted product in tris(hydroxymethyl)amino-methane (TRIS) - Ethylenediaminetetraacetic acid (EDTA) buffer solution at 100µMol concentration, if not specified otherwise.

For reverse-complementing nucleotide sequences, an automatic, online-based tool was used in order to minimize errors (https://www.bioinformatics.org/sms/rev_comp.html).

2.3.2 Sanger Sequencing Analysis

Each Sanger sequencing sample was sequenced on a 3730 DNA Analyser (Applied Biosystems, Foster City, CA, USA) and chromatograms visualized using Codon Code Aligner software for Mac (CodonCode Corporation, Version 7.0.1). Reference sequences of the gene in question were generated from https://www.ensembl.org/index.html and chromatogram reads from both forward and reverse strand compared to the reference in order to detect variants. Practice guidelines for the correct analysis and interpretation of sequence changes were followed (Ellard *et al.*, 2016).

Sequencing quality is most commonly denoted by the probability of error for each base call. The prototype QC algorithm called Phred, assessing this by peak mobility and shape analysis, expresses this as 10x the log of likelihood of error, called the phred score (Ewing and Green, 1998). A phred score of 20 hence translates into a 1/100 chance (99% confidence), a score of 30 into a 1/1000 chance (99.9% confidence) and score of 40 into a 1/10`000 chance (99.99% confidence) of erroneously calling a certain base. Along confirmation of sequence variants by repeat analysis, generally a phred score cut-off of 20 was used to judge the reliability of sequencing results.

2.4 Human Post-mortem Tissue Analysis

2.4.1 Sample Sources and Tissue Handling

For human tissue samples, consent for post-mortem examination and research has been obtained in accordance with routine local procedures of the sampling site (Queen Square Brain Bank (QSBB), Edinburgh Brain bank), and the study was approved by the respective Local Research Ethics Committee. At QSBB, individuals had been approached on the basis of their clinical presentation or diagnosis during lifetime and consented to donating their brain after death. At Edinburgh Sudden Death Brain and Tissue Bank (https://gtr.ukri.org/projects?ref=G0600969) tissue samples had been collected from healthy individuals, who died suddenly and unexpectedly – the latter being a unique source of healthy control tissue samples for biomedical research.

At all sites, brain tissue was sampled fresh at post mortem. Similarly, all cases had detailed neuropathological review for diagnostic purposes and to exclude signs of alternative diagnoses.

At QSBB, brains were partitioned and the right hemisphere prepared for snap freezing: brain stem and cerebellum (approximately 5mm slices), cortex (10mm slices) and basal ganglia, thalamus, hippocampus and anterior frontal cortex (en bloc) were cut and snap frozen in -80°C liquid nitrogen vapour. The left hemisphere was fixed in 10% buffered formalin for 3 weeks and subsequently sliced according to brain region. Tissue blocks were selected for processing, dehydrated in graded alcohol preparations and xylene penetrated before paraffin wax embedding according to local standard pathology procedures.

At the Edinburgh Sudden Death Brain and Tissue Bank, brains were then partitioned and the left hemisphere cut into 1cm^3 tissue blocks and snap frozen in -80°C liquid nitrogen vapour. The remainder of the left and the complete right hemisphere was then cut in 10mm slices in the coronal plane and fixed in 10% buffered formalin for a minimum of 48 hours. After several graded alcohol dehydration steps and complete xylene penetration, tissue blocks were paraffin wax embedded according to local standard pathology procedures.

2.4.2 Histopathology

Paraffin-embedded tissue blocks were identified as per anatomy and, after identification of tissue orientation, sections were cut on a sliding microtome and mounted on double-subbed glass slides. All human tissue samples were stained routinely in heamatoxylin and eosin for anatomical orientation.

Immunohistochemistry staining was performed according to a standard avidin-biotin complex protocol. Antibody binding sites were visualized using the chromogen diaminobenzidine, and sections were counterstained using Mayer's haematoxylin.

2.4.3 Enzyme Activity Measurements

Activity of lysosomal enzymes in white blood cells and post mortem brain tissue was measured according to methods established in the laboratory of the National Hospital of Neurology and Neurosurgery Neurometabolic Unit. They follow the sequence of homogenization, measurement of protein concentration and enzyme

activity measurement. Throughout the following, all preparation steps were performed on wet ice, in order to preserve enzyme activity.

2.4.3.1 Tissue Homogenisation

Independent of origin (leucocytes, cultured cells or tissue), tissue needs to be disrupted in order to expose the enzyme and measure its´ activity. Depending on the mechanical and biochemical characteristics of the tissue of origin, the preferred methods for disruption are freezing and thawing, homogenization or sonication. For brain tissue samples, hand homogenisation was performed using a ground glass homogeniser.

2.4.3.2 Measurement of Protein Concentration

For the majority of enzyme assays, except those done on plasma or erythrocytes, the enzyme activity is related to the protein concentration. The Bicinchoninic acid (BCA) Protein Assay is a highly sensitive method for the spectrophotometric determination of protein concentration. This reagent system is based on the Biuret reaction of protein with Cu^{2+} in an alkaline medium yielding Cu^{1+}. BCA, in the form of its water-soluble sodium salt, is a highly sensitive, stable and highly specific reagent for the cuprous ion (Cu^{1+}). Macromolecular structure and four peptides (cysteine, cystine, tryptophan, and tyrosine) have been reported to be responsible for the colour formation in protein samples when assayed with BCA. The purple reaction product, formed by the interaction of two molecules of BCA with the one cuprous ion (Cu^{1+}), is water-soluble and exhibits a strong absorbance at 562 nm. This allows the spectrophotometric quantitation of protein in aqueous solutions.

Additional advantages include compatibility with ionic and non-ionic detergents, a stable working reagent, less protein-to-protein variation than with other methods, broad linear working ranges with excellent sensitivity and the ability to change the protocol, which provides flexibility (P. K. Smith *et al.*, 1985).

2.4.3.3 Measurement of Enzyme Activity

For the protein assay a method described by Wenger et al. was used, which is based on differentiating activities of β–glucosidase in different cell compartments, i.e. the cytosol and lysosome. Taurocholate inhibits cytosolic enzyme and activates lysosomal β–glucosidase, while Triton also activates lysosomal β–glucosidase. Hence a mixture of Triton X–100 and pure taurocholate was used to obtain the activity of lysosomal β–glucosidase activity only (Wenger *et al.*, 1978). At acid pH β–glucosidase hydrolyses the substrate 4–methylumbelliferyl–β–D–glucopyranoside to 4–methylumbelliferone and glucose. Adding alkaline buffer stops the enzyme reaction and causes 4–methylumbelliferone to fluoresce at a different wavelength from unhydrolysed substrate, thereby permitting its measurement in the presence of a vast excess of unhydrolysed substrate (Wenger *et al.*, 1978).

2.5 Magnetic Resonance Imaging

2.5.1 MRI raw Data Acquisition, Anonymisation and Imaging File Conversion

Study participants were screened for potential contraindications to MR imaging according to the local neuroradiology departments SOPs before entering the MRI suite and imaging data acquisition according to the imaging protocol. All MRI sequences were taken in head first supine orientation. Raw imaging data acquired was then stored in standard DICOM format and stored on a PACS system. Files were anonymised using DICOM Cleaner (https://www.dclunie.com/pixelmed/software/webstart/DicomCleanerUsage.html) in accordance to local SOPs of the respective neuroradiology department and applicable data protection law before transfer to computers for analysis.

Statistical parametric mapping (SPM), a suite of Matlab (https://uk.mathworks.com) functions and routines was used for conversion, processing and subsequent analysis of imaging data (https://www.fil.ion.ucl.ac.uk/spm/software/). For qualitative and quantitative analysis, imaging files were converted from DICOM into NIfTI format using either dcm2nii (https://www.nitrc.org/plugins/mwiki/index.php/dcm2nii:MainPage) or the in-house, bespoke DicomToNifti tool on SPM. For image viewing and co-registration, FSLeyes (https://zenodo.org/record/1887737#.XEEB_qf35TY), an image viewer application based on FSL, a comprehensive library of MRI analysis tools, was used (S. M. Smith *et al.*, 2004).

2.5.2 Voxel-based Morphometry

Voxel-based morphometry (VBM) is a frequently applied, automated post-processing imaging tool in neuroscience. It entails a voxel-wise comparison of the localisation of grey matter voxels between different groups of subjects, allowing an un-biased, comprehensive assessment of volumetric anatomical differences across the whole brain (Ashburner and Friston, 2000). The pre-processing of imaging data for analysis involves segmentation, i.e. tissue classification (1), normalisation, i.e. transferring of high-resolution images of all participants to a common stereotactic space allowing co-registration (2), and grey-matter smoothing (3).

Segmentation

After removal of tissue information relating to non-brain parts (skull, etc.), intensity non-uniformities caused by magnetic field inhomogeneities are corrected using a bias correction algorithm. Tissue can then be segmented into grey / white matter and cerebrospinal fluid for further analysis.

Normalisation

During spatial normalisation, all subjects` data is transformed to the same stereotactic space, in order to allow voxel-wise comparison across subjects. Mathematically, this is achieved by minimizing the residual sum of square differences between them during the registration of each image to the same template image. In SPM, this is done in two steps, involving the estimation of the optimum affine transformation as well as accounting for global nonlinear shape differences, as present along the normal distribution of head and brain shapes and sizes (Ashburner and Friston, 2000). Iterations of these steps result in an accurate

mean template and deformations fields. These deformation fields, describing where and how exactly images were adjusted to match the mean template, are then used to warp the initial images into a common stereotactic space. During analysis, the information on deformation fields is again used to correct for volume changes due to normalisation, allowing for unbiased volumetric comparison even after normalisation to standard space.

The output of the high-dimensional Diffeomorphic Anatomical Registration using Exponentiated Lie algebra (DARTEL) method used in SPM to create a study-specific normalisation atlas is in Montreal Neurological Institute (MNI) space. The MNI space had been derived originally from 305 healthy control individuals` brain MRI scans.

Spatial smoothing

In order to ensure a) a Gaussian distribution of random errors in the data, rendering the data more normally distributed, hence increasing the validity of parametric testing results and b) compensation for inexact spatial normalization, normalised tissue data is convolved with an isotropic (i.e. all sides of tissue voxels have the same side length) Gaussian function. This process is called smoothing. As far as possible, the size of the smoothing kernel should be chosen similar to the size of the expected differences between groups of brains (Ashburner and Friston, 2000), resulting in a kernel size of 4-12mm full width at half maximum.

The analysis using parametric statistical testing employs general linear model statistics in a mass-univariate approach, applying the same test to each voxel simultaneously. Using Gaussian random field theory as the underlying principle, this ultimately identifies regions of grey matter changes significantly associated with clinical or alternative outcome parameters (Ashburner and Friston, 2000).

3 Chapter I: The role of GBA in dystonia

3.1 Statement of contribution

I developed the study design, collected samples, clinical and imaging information from all subjects, performed all Sanger sequencing experiments and brain sample preparations, analysed and interpreted the data. Derek Burke from the Enzyme Unit at Great Ormond Street Hospital and the Neurometabolics Unit performed all enzyme activity measurements.

3.2 Abstract

Objective: To explore the possible role of lysosomal dysfunction in clinical (n=130) and post mortem (n=10) cohorts of patients with dystonia.

Background: Glucocerebrosidase (GCase) deficiency due to mutations of the glucosidase acid beta (GBA) gene causes autosomal-recessive Gaucher`s disease. GBA mutations are associated with an increased risk to develop Parkinson`s Disease, while an association with dystonia has not been reported so far. Some lysosomal storage disorders nevertheless present with a dystonic phenotype.

Methods: A prospective (n=51) and retrospective (n=79) cohort of patients with combined and isolated dystonia were screened for white cell lysosomal enzyme activity using a fluorescence-based essay. Sanger Sequencing of GBA exons 1-11 was performed using an established protocol in all n=97 cases with available DNA. In cases with suspicious clinical examination or a positive family history, nigro-striatal degeneration was excluded by DaT scan. Further, lysosomal enzyme activity was measured in different brain regions of age-, sex- and post-mortem delay-matched

cases with dystonia of unknown origin (n=10) and healthy controls (n=10) from the Queen Square brain bank.

Results: After exclusion of possible alternative aetiologies in n=14 cases on follow-up, decreased GCase activity was measured in a range typical for homozygous (n=2; 1.7%) or heterozygous (n=23; 19.8%) GBA mutation carriers. The frequency of *GBA* mutations (5/80 = 6.25%) was significantly higher than in controls (3/257=1.17%) of a historical control group from the same ethnic background (P=0.02; odds ratio=5.64, 95% confidence interval = 1.44 – 21.58) – known pathogenic mutations E326K, T369M and N370S were found. We also identified lower Glucocerebrosidase activity in the cerebellar dentate nucleus (P=0.048) in dystonia than healthy control brains. Nigro-sitratal degeneration was excluded in n=19 (17.2%) cases with dystonia of unknown origin where there was suspicion based on clinical examination or family history.

Conclusion: This study provides evidence for peripheral and central lysosomal dysfunction in a significant proportion and across the clinical spectrum of dystonia. As in Parkinson´s disease, this was found irrespective of *GBA* mutation status, indicating a possible role of lysosomal dysfunction as a more general disease mechanism in dystonia.

3.3 Background

3.3.1 Lysosomal function in health and disease

Lysosomes, first described in 1955 by later Nobel laureate Christian de Duve (De Duve *et al.*, 1955), are membrane-bound acidic (pH 4-5) cell organelles found in all eukaryotic cells, harbouring an array of over 60 acid hydrolases. These enzymes are capable of digesting nucleic acids, lipids, proteins, polysaccharides, cell organelles and bacteria. In addition to degradation of intracellular macromolecules, lysosomes are further involved in autophagy, receptor recycling and cell death (Appelqvist *et al.*, 2013). Initially considered to be the "cell`s waste bin", lysosomes are by now considered to fulfil a more complex role within the endosomal-lysosomal system, playing a key part in the regulation of cellular metabolic homeostasis (Coutinho and Alves, 2015).

Lysosomal storage disorders (LSDs) are a heterogeneous group of conditions caused by dysfunction of the lysosomal pathway by either a defect or deficiency in enzyme activity, trafficking, lysosomal membrane proteins or soluble non-enzymatic lysosomal proteins. While many of the most common of these conditions were recognized in the late 19th and early 20th century (Fabry, 1898; Gaucher, 1882; Niemann, 1914; Pick, 1926; Pompe, 1932; Sachs, 1887; Tay, 1881), it took until 1963 for them to be grouped together (Hers, 1963). The common patho-aetiology of lysosomal storage disorders is the incomplete processing and subsequent accumulation of the substrate within the lysosome, causing progressive functional impairment within the organelle, cell and ultimately organ. Although individually each of the over 50 genetically distinct disorders grouped as LSDs is very rare, as a group their incidence has been reported as 1 in 5000.

Gaucher`s disease (GD) is the most frequent lysosomal storage disorder (LSD), characterized by decreased GCase enzyme activity. GD is an autosomal recessive disorder affecting the mononuclear phagocytic system. The decrease in GCase activity causes an accumulation of the primary GCase substrate glucocerebroside in cells of the monocyte-macrophage system, manifesting viscerally as fatty deposition predominantly in spleen and bone marrow, leading to anaemia and thrombocytopaenia (Grabowski, 2008). The pathophysiology behind the near pathognomonic macrophage activation in GD is not entirely understood and both the obvious excess glucocerebroside accumulation, as well as an abnormal folding of mutant protein have been argued to trigger the inflammatory response, ultimately leading to macrophage activation (Grabowski, 2008).

Clinically, presentation is variable and GD is generally classified by the presence and aggressiveness of neuronal symptoms: the most common, Type I, is the classically so called non-neuronopathic form, presenting with a high level of phenotypic heterogeneity including hepatosplenomegaly and thrombocytopaenia from infancy to late adulthood and is particularly frequent among the Ashkenazy Jewish population (one in 800 livebirths). The concept of Type I to have no neurological involvement at all has however been challenged recently (Chérin *et al.*, 2010). Type II is the infantile onset, acute neuronopathic form presenting with oculomotor apraxia, strabism and generalized dystonia often leading to aspiration pneumonia and death, while type III is the juvenile, subacute onset neuronopathic form, presenting with horizontal supranuclear gaze palsy, ataxia, myoclonus epilepsy, dementia and spasticity leading to death before adulthood (Hruska *et al.*, 2008; Siebert *et al.*, 2014). More recently, however, it has been appreciated that these

classic subtypes are part of a spectrum within this condition (Mullin *et al.*, 2019; Sidransky and Lopez, 2012).

The identification of low GCase activity as the cause of the condition has led to the successful establishment of enzyme replacement therapy with mannose-terminated GCase (Weinreb *et al.*, 2002) and substrate avoidance therapy (Bennett and Mohan, 2013). While visceral manifestations of the disease are susceptible to this form of therapy, lung, lymph nodes and CNS tissue remain inaccessible.

3.3.2 GBA - gene and physiological function

The 7604 base pair (bp) *GBA* gene (MIM# 606463) is located on chromosome 1q21, comprises of 11 exons and 10 introns (Horowitz *et al.*, 1989) and codes for the 497 amino acid protein GCase (Li *et al.*, 2015). A non-translated 5769 bp pseudo-gene (*GBAP*), containing large deletions of *Arthrobacter luteus* sequences flanked by direct repeats in the introns, sharing 96% exonic sequence homology (Horowitz *et al.*, 1989), is located approximately 16kb downstream of the functional *GBA* gene. Together with the presence of another six genes at the locus, this explains frequent chromosomal rearrangements and misalignments in this region (Tayebi *et al.*, 2003; Winfield *et al.*, 1997).

Currently there are over 300 different mutations described for *GBA* (Beutler *et al.*, 2005; Koprivica *et al.*, 2000; Winfield *et al.*, 1997)(for an updated list, see: http://www.hgmd.cf.ac.uk/ac/all.php).

GBA mRNA has two methionine start codons located in Exon 1 and Exon 2, which, after cleavage of a 39-amino acid, respectively 19-amino acid signal peptide, results in functional acid β glucosidase, respectively GCase protein. GCase, ubiquitously

expressed across all cell types, catalyses the hydrolysis of glycolipid glucocerebrosidase to ceramide and glucose. It is transported from the site of its synthesis in the endoplasmic reticulum to the lysosomes via lysosomal membrane protein 2 (LIMP2) with its optimal operational range at pH 4.7-5.9 (Migdalska-Richards and Schapira, 2016).

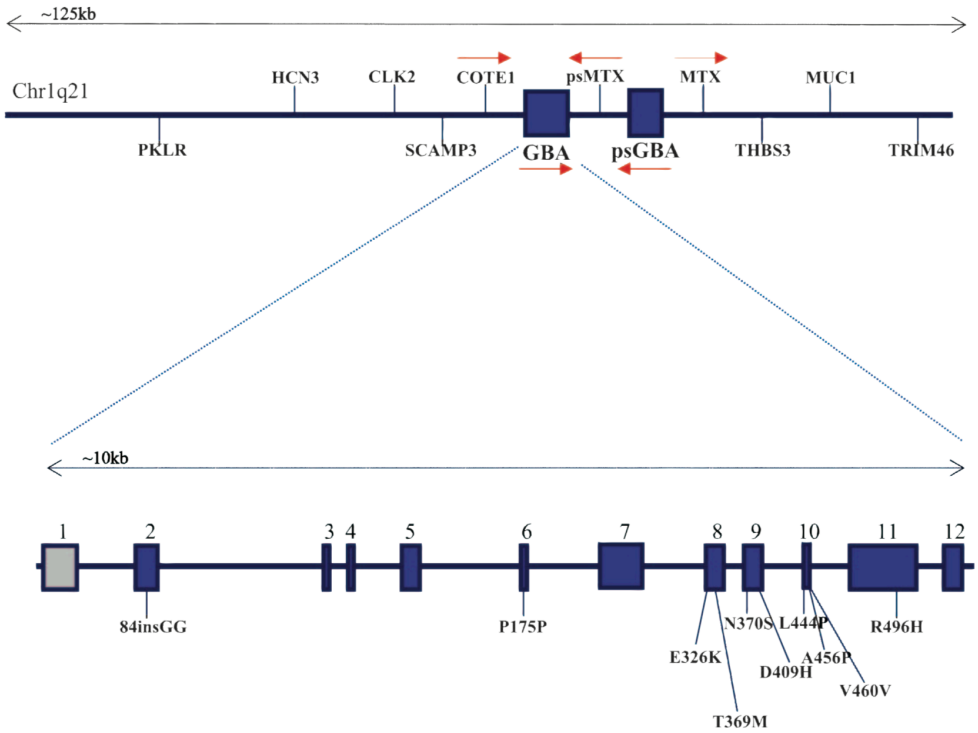

Figure 3.1: Structure of the GBA gene locus and neighbouring GBAP; reproduced from (Clark et al.*, 2007)*

3.3.3 GBA in Parkinson´s Disease and other synucleinopathies

Over the past two decades, an association between *GBA* mutations and PD increasingly became apparent and is now widely accepted (Brockmann and Berg, 2014; Neumann *et al.*, 2009; Sidransky *et al.*, 2009). Initial reports were based on

the meticulous clinical observation that some GD patients developed PD: first mentioned in a mother and daughter with confirmed GD, psychosis, depression and dementia (Neil *et al.*, 1979), one of the early reports already described a young age at onset (mean 48.8 years) in six cases, five of which were of Ashkenazy Jewish extraction (Neudorfer *et al.*, 1996). Additional cases confirmed, that clinical presentation is often indistinguishable from sporadic PD, including asymmetric motor onset, development of wearing-off and dyskinesia but younger age at onset (Bembi *et al.*, 2003). The first case series examining the frequency of the most frequent *GBA* mutations (N370S, L444P, 84GG, IVS+1, V349L, R496H) in 99 PD patients, 74 Alzheimer`s disease patients and 1543 healthy control Ashkenazy Jews confirmed the younger age at onset in mutation carriers (Aharon-Peretz *et al.*, 2004). *GBA* mutations were subsequently reported from pathologically confirmed cases (Eblan *et al.*, 2005). Soon it became apparent that sequencing only the most frequent *GBA* mutations would underestimate the mutation load by as much as 30 - 43% (Bras *et al.*, 2009; Lesage *et al.*, 2010).

A combined genetics/brain histology study reported the frequency of GBA mutations among PD patients of non-Jewish descent to be 4.18% (33 patients/790 controls) (Neumann *et al.*, 2009). In the largest study from 16 international centres (5691 patients/4898 controls), the frequency of GBA mutations in non-Jewish PD patients was found to be 7% (Sidransky *et al.*, 2009). Overall, the OR for carrying a GBA mutation in patients with PD has been calculated as 5.43 (95%CI 3.89 – 7.57) (Sidransky *et al.*, 2009).

Clinically, PD patients with *GBA* mutations have a slightly earlier age at onset and less asymmetric presentation, less tremor and bradykinesia, but more cognitive

symptoms than idiopathic cases (Brockmann *et al.*, 2011; McNeill *et al.*, 2012; Neumann *et al.*, 2009; Sidransky *et al.*, 2009).

GBA-related PD has been mostly described in the presence of heterozygous (Sidransky and Lopez, 2012), and rarely in homozygous or compound heterozygous mutation state (Clark *et al.*, 2007; Lesage *et al.*, 2010) – the latter so far involving variants N370S or L444P. Similar to GD, there is a clear preponderance of certain variants that occur more frequently with disease. Out of 13 studies that based their results on GBA whole exon analysis (including n=4966 patients from China, Portugal, Greece, Japan, Britain, North-Africa, French-Canada, Europe and Korea), eight reported L444G and six N370S as the most frequent variants detected (Sidransky and Lopez, 2012). In the studies including Caucasian samples, N370S accounted for 36% in a Portuguese sample (Bras *et al.*, 2009), 47% in a French Caucasian sample (Lesage *et al.*, 2010) and 24% in a British sample (Neumann *et al.*, 2009), while L444P was present in 22% of the French-Caucasian (Lesage *et al.*, 2010) and 33% of the British sample (Neumann *et al.*, 2009). Interestingly, N370S is rarely found in Asian populations (Mitsui *et al.*, 2009), while L444P is found irrespective of ethnic background (Sidransky and Lopez, 2012).

Several observations indicate that mild and severe GBA mutations differentially affect the risk for PD, with severe mutations leading to a younger age at onset and higher odds ratio (Gan-Or *et al.*, 2009; 2015).

Although known to cause GD, these mutations can also be found in clinically unaffected individuals in a population-dependent manner: in studies that examined the full *GBA* sequence, this frequency has been reported in 7.1% of Ashkenazy Jews (Clark *et al.*, 2007), respectively in 0.5% of a Spanish (Setó-Salvia *et al.*, 2012), 0.7% of a Portuguese (Bras *et al.*, 2009), 1.0% of a French (Lesage *et al.*, 2010), 1.17% of

a British (Neumann *et al.*, 2009) and 2.1% of a US-American Caucasian sample (Clark *et al.*, 2007). Even when examining only the most frequent GBA variants, the carrier frequency among healthy individuals of Ashkenazy origin is 6.2% (Aharon-Peretz *et al.*, 2004), respectively 6.35% (Gan-Or *et al.*, 2008). In a British sample, 1.2% of healthy controls of non-Jewish origin were GBA mutation carriers (Neumann *et al.*, 2009). A random screening of 2000 cord blood samples in Portugal estimated the carrier frequency of the N370S variant to be 0.0043 (Lacerda *et al.*, 1994). The only population-based study, done in a predominant white Caucasian/European-ancestry population in Australia, reported a general frequency of GD-causing *GBA* variants in one in 57´000 livebirths (Meikle *et al.*, 1999).

In terms of neuropathology, a combined genetics/histology study reported widespread α-Synuclein accumulation with more pronounced neocortical deposition amongst mutation carriers (Neumann *et al.*, 2009). This is in line with the clinical observation of more pronounced cognitive involvement in GBA carriers vs idiopathic PD patients (Brockmann *et al.*, 2011; McNeill *et al.*, 2012; Neumann *et al.*, 2009; Sidransky *et al.*, 2009). Neuropathological examination in a limited number of cases has also shown that GCase was present in a mean 75% (32-90%) of Lewy bodies of patients with PD harbouring a *GBA* mutation, whereas sporadic PD negative for *GBA* mutations showed on average GCase in 4% of Lewy bodies (Goker-Alpan *et al.*, 2010). A fascinating post-mortem brain study reported reduced GCase protein expression and catalytic activity not only in samples from PD patients known to carry *GBA* mutations, but also in the SN and cerebellum of sporadic PD cases, implying a more general role of lysosomal dysfunction in PD pathophysiology (Gegg *et al.*, 2012).

GBA mutations are associated with synucleinopathies more in general, as demonstrated in Lewy body dementia: first described in a small prospective case series (Goker-Alpan *et al.*, 2008), this observation has now been corroborated in larger cohort studies (Clark *et al.*, 2009), candidate gene approach studies (Michael A Nalls *et al.*, 2013) and most recently also in a GWAS study (Guerreiro *et al.*, 2018). Interestingly, the latter in fact provided evidence that *GBA* mutations might result in higher odds ratio for Lewy body dementia risk (OR 2.5, 95%CI: 1.88-3.46) than apolipoprotein-E (APOE; OR 2.4) or α-synuclein (SNCA; OR 0.73).

3.3.4 Aim and Hypotheses

Cervical and task-specific dystonia are adult-onset conditions characterized by involuntary excessive muscle activity associated with considerable pain and work impairment. For the majority of focal dystonias, after exclusion of Wilson´s disease, structural abnormalities and potential iatrogenic causes, the large majority of cases are rendered "idiopathic" (Evatt *et al.*, 2011) – for cervical dystonia, one study found 109 of 130 cases (84%) to be idiopathic (Strader *et al.*, 2011). Without better understanding of the underlying disease mechanism, these cases can only be treated symptomatically.

So far, dystonia has been associated with lysosomal dysfunction as part of the clinical presentation in lysosomal storage disorders, such as in chronic forms of GM1 gangliosidosis (Arash-Kaps *et al.*, 2019), GM2 gangliosidosis (Meek *et al.*, 1984), and less frequently in Niemann Pick type C and Kuf`s disease (Ebrahimi-Fakhari *et al.*, 2018; Sedel *et al.*, 2008).

To back up incidental clinical observations from a small number of cases, the aim of this work was to investigate in how far lysosomal dysfunction is detectable in patients with dystonia. Hence, experiments were designed in particular to prove the hypotheses that in patients with dystonia there is:

a) lower activity of lysosomal enzymes in blood and brain
b) higher frequency of GBA gene mutations

than in suitable controls.

3.4 Methods

3.4.1 Participants

Dystonia patients were recruited from the movement disorder outpatient clinic at the National Hospital of Neurology, Queen Square, London. Patients with an unknown cause of dystonia without parkinsonism and a clinical presentation deviating from recognized idiopathic dystonic syndromes (Fung *et al.*, 2013) (e.g. late onset leg predominant dystonia, isolated foot dystonia in adults, young onset generalised dystonia negative for DYT1 mutations, rapid progressive dystonia and additional myoclonus or chorea) were screened for structural, acquired and degenerative causes of dystonia. This included a retrospective, detailed review of clinical records, neuroimaging, blood tests including routine blood count, blood film, blood chemistry for liver and renal parameters, serum copper, caeruloplasmin, genetic analysis according to clinical suspicion, organic acids, amino acids and blood white cell enzyme activity as part of their clinical diagnostic work-up. In case of clinical suspicion or a positive family history suggestive of PD, the integrity of the nigrostriatal system was assessed via dopamine-transporter (DaT) scan imaging. Medical records were reviewed for additional demographic and clinical information, in particular pertaining to signs, time course of symptom development and family history. Furthermore, samples from consecutive patients with sporadic cervical dystonia and normal routine diagnostic tests (Fung *et al.*, 2013) were prospectively assessed for white blood cell (wbc) enzyme activity measurements.

3.4.2 Brain samples

Fresh frozen brain tissue samples from individuals with dystonia and controls without neurological symptoms were identified from the QSBB (see Table S7). Written informed consent for post-mortem examination and research had been obtained in accordance with routine local procedures and was approved by the local research ethics committee. At post mortem, brains were partitioned and the right hemisphere prepared for snap freezing in -80°C liquid nitrogen vapour. Tissue microdissection was performed by an experienced dissector at the Brain Bank according to standardized procedures.

The brain regions studied in this work were chosen based on their presumed role in dystonia pathophysiology due to cerebellar (Kaji *et al.*, 2018; Shakkottai *et al.*, 2016), tectal (Holmes *et al.*, 2012; Mc Govern *et al.*, 2017) or basal ganglia (Goto *et al.*, 2005; 2013; Hanssen *et al.*, 2018; Neychev *et al.*, 2011) dysfunction, and tissue availability from pallidum (PALL), cerebellar dentate nucleus (CDN), cerebellar cortex (CRB), and superior colliculus (SCoL).

3.4.3 Protein assay sample preparation

Lysosomal enzyme activity measurements were performed in blood (Burke *et al.*, 2013) and brain homogenate samples (Gegg *et al.*, 2012) as reported, using a clinical routine, fluorescence-based essay, performed at the United Kingdom Accreditation service (UKAS)-accredited laboratory of the Enzyme Unit at Great Ormond Street Children`s Hospital, London.

Brain homogenisations were performed according to internal laboratory protocol: Fresh frozen brain samples were kept frozen on dry ice throughout processing and

cut into pieces weighing 5-10mg, transferred into cooled ground glass homogenisers (Jencons 361-045 or (mini) 361 - 046) and triple-distilled water (18.2 MΩ purity grade) added to reach 5% weigh/volume. Half of the volume was added before homogenisation, the other half to rinse the glass mortar. Samples were carefully hand homogenised to uniform consistency, avoiding frothing, and immediately fast frozen in liquid nitrogen and stored at -80°C until processing. In order to maintain protein integrity and quality, samples as well as homogenisation utensils were kept on dry (sample container, surface for cutting, tweezers, pre-labelled Eppendorf cups), respectively wet ice (mortar and pestel, double-distilled water, scalpel) throughout.

For protein concentration measurements, Bovine Serum Albumin (BSA) (1 mg/ml in 0.15M NaCl and 0.05% sodium azide; Sigma P 0914) was used for standard curve calculation. Each sample was prepared in two concentrations (2.5µl sample + 47.5µl distilled H_20; 5µl sample + 45 µl distilled H_20) and the higher of both measurements used as the final protein concentration. After the addition of 1ml bicinchoninic acid (BCA) (Sigma B9643), each sample was incubated at 37°C for 10 minutes. After addition of 20µl of 4% Copper sulphate solution (Cupric sulphate, ($CuSO_4.5H_2O$) VWR 100913P), and 20min incubation at 37°C, absorbance was read at 562nm (Cecil 2040 Spectrophotometer).

The mean protein concentration in enzyme preparation was calculated from the standard curve (mg/ml). Duplicate protein concentrations outside a margin of error of 20% were repeated.

3.4.4 Lysosomal enzyme activity measurements

For protein assay, fast frozen samples were diluted to a concentration of 2mg/ml. Eppendorf cups containing 80µl Na taurocholate solution (Na taurocholate pure (Calbiochem; no. 580218); 20mg/ml H2O, 37.2mmol/L) and 20µl enzyme solution containing 10-60µg protein per sample (20 µl water for blank samples) were prepared and 100µl substrate solution (4–methylumbelliferyl–β–D–glucopyranoside (MWt. 338) Melford M1097; 1.69 mg substrate/ml McIlvaine citrate–phosphate pH 5.4 buffer (5 mmol/L), dissolved by warming to 80°C) added at timed intervals and incubated at 37°C for 60minutes. At timed intervals 1.0ml stopping reagent (0.25 M glycine buffer pH 10.4) was added. Fluorescence was read on a Fluorimeter (Perkin Elmer LS 55) with the excitation set at 365nm at an emission wavelength of 450nm.

The enzyme activity was calculated in nmol/hour/mg protein. Wbc enzyme activities were compared to internal lab reference ranges established according to UKAS criteria. Based on measurements from patients with confirmed *GBA* mutation status, GCase activity ranges were categorised as typical for homozygous (<2.4µmol/l/h) or heterozygous *GBA* mutation carriers (2.5-5.4µmol/l/h), heterozygous carriers/unaffected overlap (5.4-8.9µmol/l/h) or unaffected individuals (>8.9µmol/l/h). As there is no commercially available internal or external quality control material available, each batch of samples contained a sample from an unaffected individual from a previous batch as carryover quality control.

As there are no validated reference ranges for brain sample enzyme activity, activity levels were directly compared between groups.

In addition to GCase, at least beta-Galactosidase (b-GAL; reference range: 130-303µmol/l/h) and/or Chitotriosidase (CHIT; reference range 0-150µmol/l/h) activity was measured in all patient samples.

3.4.5 Genetic analyses

3.4.5.1 GBA primer design

In order to provide an overview of the mutation burden in the *GBA* gene, all available samples were sequenced for all Exons 1-11. Primers used to amplify all exonic and some intronic regions of the *GBA* gene were used as described initially by (Koprivica *et al.*, 2000) and subsequently by (Chahine *et al.*, 2013; Mitsui *et al.*, 2009; Neumann *et al.*, 2009; Oeda *et al.*, 2015; Stone *et al.*, 2000; Tsuang *et al.*, 2012). As established, *GBA* exons were amplified in a first step in fragments, spanning Exon1-5, Exon5-7 and Exon8-11, before sequencing each individual exon. This GBA-specific step is necessary to confidently be able to discern between GBA and GBAP amplification, as the individual exonic primers cannot differentiate between the real/pseudogene. Amplicon length and primer binding locations were confirmed against the GBA reference sequence (transcript ID: ENST00000368373.8; GBA-202; GRCH38.p12 built; www.ensemble.org).

Next page:

Table 3.1: summary of primers used for GBA sequencing including their 5'-to-3' nucleotide sequence and resulting amplicon length.

Exon	Forward Primer	Reverse Primer	Amplicon length
1-5	5′-cctaaagttgtcaccatac-3′	5′- agcagacctaccctacagttt-3′	2972 bp
5-7	5′-gacctcaaatgatatacctg-3′	5′- agtttgggagccagtcattt-3′	2105 bp
8-11	5′- tgtgtgcaaggtccaggatcag-3′	5′-accacctagaggggaaagtg-3′	1682 bp
1	5’-ctgtgtcatgtgacgctcct-3’	5’-cagtgccaggattccagaag-3’	274 bp
2	5’-cctgcccaggagagtagttg-3’	5’-ctctgtgctacctccccact-3’	193 bp
3	5’-caaggggtgaggaattttga-3’	5’-tatcagtacccagcgggaaa-3’	395 bp
4	5’-ttcccgctgggtactgatac-3’	5’-gacagaatgggcagagtgaga-3’	298 bp
5	5’-caggagcccaagttccc-3’	5’-tgtctgtacaagcagacctaccc-3’	338 bp
6	5’-gctgaaccggatgcactg-3’	5’-gctaaatgggaggccagtc-3’	298 bp
7	5’-acacccagctggtctggtc-3’	5’-tggatgctggatttgaaggt-3’	349 bp
8	5’-agttccagaagcctgtgtgc-3’	5’-cttctgtcagtctttggtgaaa-3’	337 bp
9	5’-cccacatgtgacccttacct-3’	5’-tgtaggagatgataggcctggt-3’	296 bp
10 + 11	5’-gggtccgtgggtgggt-3’	5’-tgctgtgccctctttagtca-3’	494 bp

For quality control purposes a) the sequence length of amplification PCR fragments was compared against fragments of the pseudogene *GBAP* (transcript-ID ENST00000486869.5, GBAP-207: Exon 1-5 1704bp; Exon 5-7 990bp; Exon 8-11 1220bp) as calculated from Ensemble. Gel electrophoresis blots of respective PCR fragments were checked against DNA ladders for matching fragment size; b) primer sequences were checked using the PrimerBlast tool (https://www.ncbi.nlm.nih.gov/tools/primer-blast/index.cgi): whereas individual Exons did map to both *GBA* and *GBAP*, primers for GBA fragments importantly did map only to GBA (PrimerBlast settings: PCR product size 70-4000bp, “nr (non redundant)”, “homo sapiens”); c) sequencing results for each Exon were aligned in CodonCode Aligner against standard Exon sequences derived from the Ensembl transcript and checked for homology.

3.4.5.2 GBA Sanger sequencing

For the amplification PCR the following reagents were used in a total reaction volume of 15µl: 7.5µl fast start PCR master mix (Roche no.10368820), 0.5µl of 10µM forward primer, 0.5µl of 10µM reverse primer, 5µl deionised water and 1.5µl genomic DNA template (at a concentration of 40-80ng/µl). The PCR light cycler was programmed as follows for the amplification of *GBA* fragments:

Amplification PCR GBA Exon1-5						
Time (min)	15:00	00:45	00:45	03:00	07:00	Hold
Temperature (°C)	94.0	94.0	58.0	72.0	72.0	4.0
n cycles	1	37			1	

Amplification PCR GBA Exon5-7						
Time (min)	15:00	00:45	00:45	03:00	07:00	Hold
Temperature (°C)	94.0	94.0	61.0	72.0	72.0	4.0
n cycles	1	37			1	

Amplification PCR GBA Exon8-11						
Time (min)	15:00	00:45	01:30	03:00	07:00	Hold
Temperature (°C)	94.0	94.0	64.0	72.0	72.0	4.0
n cycles	1	37			1	

All PCR products were run on a 1.5% Agarose gel with gel red (see 2.2.4) and GelPilot Wide Range DNA ladder (Quiagen, no.239125) to rule out amplification of *GBAP*, followed by enzymatic PCR purification using ExosAP (see 2.2.6) and sequencing reaction (see 2.2.7).

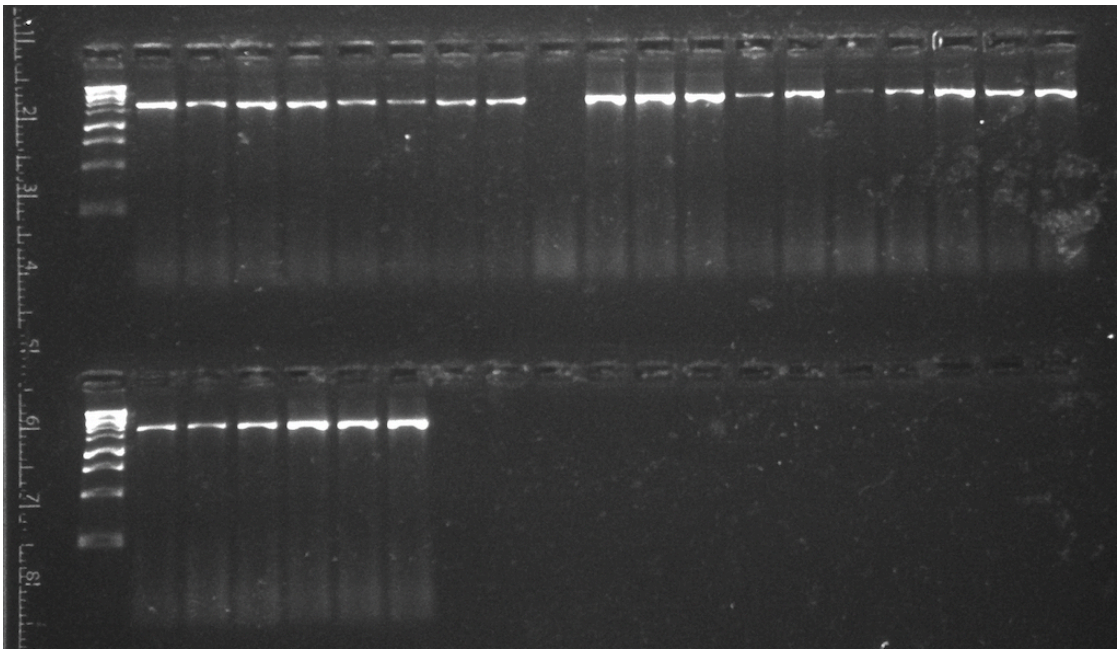

Figure 3.2: Gel electrophoresis blot to check the correct amplicon length of GBA PCR fragments

Fragments of Exon 8-11 of a number of DNA samples are compared against a respective DNA ladder, confirming correct amplification to 1682 bp length. Note that the signal intensity indicates that sample no. 59116 (10th column from left, top row) and no. 64662 (16th column from left, top row) was not/not sufficiently amplified in this run.

Sequencing was performed on a 3730 DNA Analyzer (Thermo Fisher, no. 3730S). Chromatograms were read using CodonCodeAligner, v7.0.1 software for Mac (CodonCode Corporation, Centerville, MA, USA). Analysis of sequencing reads in

forward and reverse direction was performed in clean, complete reads only and all mutations confirmed by re-amplification of the individual patient DNA. Allele names follow the common nomenclature, excluding the first 39 amino acids of the leader sequence.

3.4.6 Statistical analysis

After testing for normal distribution (Shapiro-Wilk test), patient demographics and enzyme activity measurements were compared using independent samples t test and analysis of covariance (ANOVA) with Tukey`s post-hoc test for parametric, respectively Mann-Whitney-U and Kruskall-Wallis test with Dunn`s post-hoc test for non-parametric data – dependence of enzyme activity with age was assessed using linear regression. Frequencies of genotype were compared using a one-sided, family history and sex using a two-sided Fisher`s exact test. The degree of variation between brain enzyme activity measurements between patients and controls was compared using two sample testing of the coefficient of variation (CoV), defined as the ratio of the standard deviation to the mean. All tests were considered statistically significant in case of a P-value < 0.05 (two-tailed), which was adjusted in case of multiple comparison. Prism 8.0 (GraphPad Inc., San Diego, CA, USA) was used for statistical analyses.

3.5 Results

3.5.1 Clinical cohort

Overall, white cell enzyme activity was measured in n=130 patients with dystonia (see Table 3.2). Of these, cases with an unknown cause of dystonia and a clinical presentation deviating from recognized dystonia syndromes had been collected retrospectively (n=79), while cases with isolated, cervical dystonia had been collected prospectively (n=51). After the identification of n=14 cases with a confirmed alternative aetiology causing dystonia (genetic, structural or alternative diagnosis) on clinical follow-up (see Table 3.5), n=116 cases with *dystonia of unknown origin* remained. Among retrospectively collected cases (n=67), the affected body region at the onset of the condition was cervical (n=14), oro-facial / laryngeal (n=11), leg (n=14), arm/hand (n=14), generalized (n=5), or segmental (n=9). Based on clinical features, there was clinical suspicion of an underlying functional origin in n=7 cases. In comparison to prospectively collected cervical dystonia cases (n=49), retrospectively collected cases were younger (P<0.0001), had a younger age at onset (P=0.001), shorter disease duration (P=0.01) and more frequently had undergone DAT scan imaging (P=0.007; see Table 3.2). There was no difference in sex distribution or frequency of positive family history between cohorts.

Of the n=97 cases of *dystonia of unknown origin* for which DNA samples were available for complete Sanger sequencing of *GBA* Exons 1-11, retrospectively collected cases (n=51) were younger (P<0.0001), had a younger age at onset (P<0.0001) and more frequently had undergone DAT scan imaging (P<0.001) than prospectively collected cases (n=46). There was no difference in sex distribution,

frequency of positive family history and frequency of *GBA* mutation carriers between cohorts (see Table 3.2).

The genetic background of the above described cohorts was predominantly Caucasian with other ethnicities representing around one fifth of cases (see Figure 3.3).

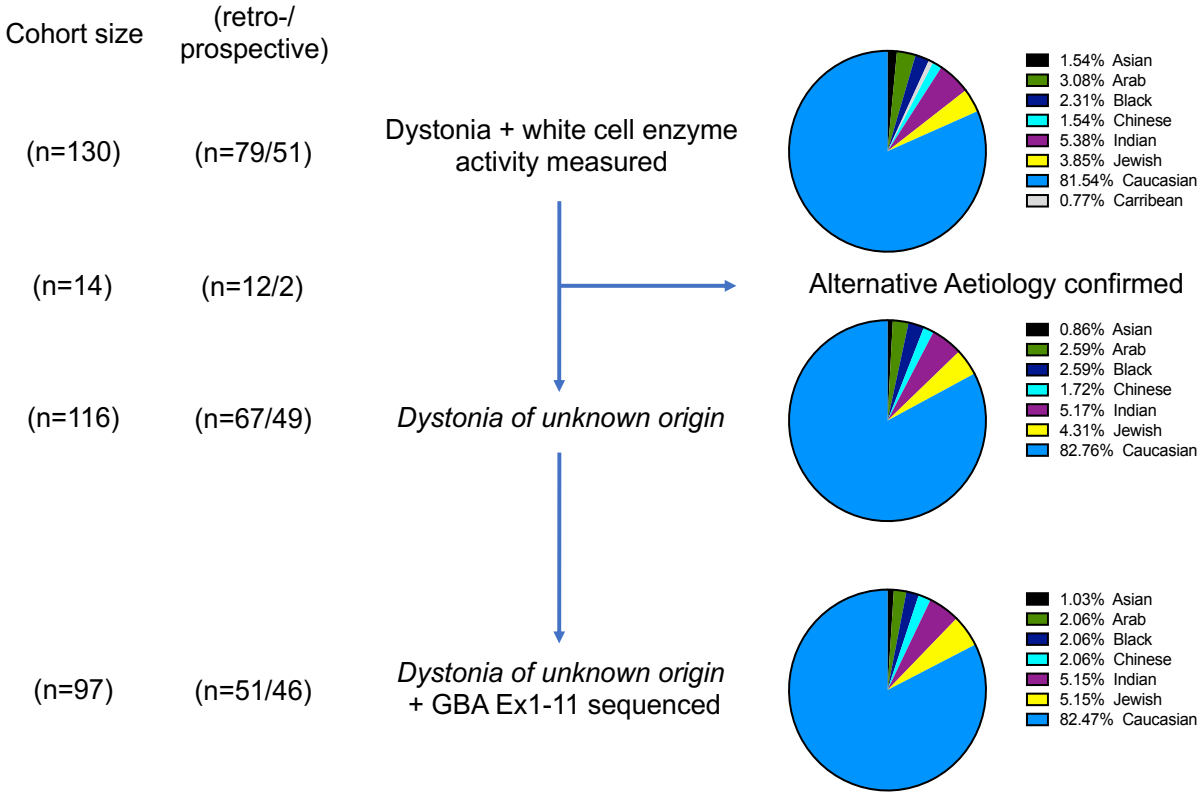

Figure 3.3: Description of the clinical cohort.

White blood cell lysosomal enzyme activity measurements were done in the complete cohort of n=130 dystonia patients. An alternative aetiology of dystonia was confirmed on follow-up in n=14 (see Table 4). Of the remaining n=116 patients with dystonia of unknown origin, *DNA for complete sequencing of Exons 1-11 of the* GBA *gene was available in n=97 cases. The proportion of cases with an unknown cause of dystonia and a clinical presentation deviating from recognized dystonia syndromes (collected retrospectively) and cervical dystonia cases (collected prospectively), as well as the ethnicity distribution of respective sub-cohorts, are displayed. The proportion of patients of Caucasian ancestry did not differ between sub-cohorts.*

Table 3.2: Summary clinical and demographic details.

Test statistics for comparison between sub-cohorts as well as details of post-hoc tests are given (retrospective vs prospective; # retrospective vs. alt. aetiology; $ prospective vs alt aetiology)*

	Complete cohort	**Sub-cohorts**			**Sub-Cohort Comparison**	**d**
		Dystonia of unknown origin		Alternative Aetiology	(test statistic; exact p-level)	post-hoc test
		Retrospective cohort	Prospective cohort			
Dystonia + white cell enzymes measured	n=130	n=67	n=49	n=14		
age	50.4 ± 17	44.2 ± 15.2	61.8 ± 12.0	43.0 ± 20.8	$F_{2, 125} = 21.9$; P<0.0001	* P<0.0001, # P=0.95, $ P=0.001
sex (% female)	54.6%	49.3%	59.2%	64.3%	Chi-square$_2$ = 2.69, P=0.26	n.a.
age at symptom onset	32.5 ± 17.6	27.9 ± 18	40.2 ± 12.8	30.3 ± 21.3	H=13.96, n=67, 49, 13, P<0.0009	* P=0.001, # P=0.99, $ P=0.07
disease duration (years)	18.3 ± 14.6	15.82 ± 14.67	21.2 ± 12.39	12.7 ± 9.11	H=10.23, n=66, 45, 14, P=0.006	* P=0.01, # P>0.99, $ P=0.065
GCase wbc enzyme activity	7.72 ± 2.76	6.95 ± 2.53	8.55 ± 2.62	8.03 ± 3.47	H=10.40, n=67, 49, 14, P=0.0055	* P=0.0039, # P=0.87, $ P=0.99
b-GAL wbc enzyme activity	190.5 ± 51.75	189.23 ± 57.29	195.20 ± 42.62	176.93 ± 54.73	H=1.704, n=67, 49, 13, P=0.43	n.a.
CHIT wbc enzyme activity	41.51 ± 39.21	37.56 ± 34.28	47.73 ± 38.48	38.0 ± 60.54	H=6.257, n=64, 48, 13, P=0.043	* P=0.24, # P=0.62, $ P=0.06
DAT Scans (n, %)	29 (22.3%)	17 (25.4%)	3 (6.1%)	9 (64.3%)	Chi-square$_2$ = 22.0, P<0.001	* P=0.007, # P=0.009, $ P<0.001
positive fam hx for PD	20 (15.4%)	7 (10.4%)	10 (20.4%)	1 (7.1%)	Chi-square$_2$ = 2.94, P=0.23	n.a.
positive fam hx for Dyst	20 (15.4%)	7 (10.4%)	8 (16.3%)	4 (28.6%)	Chi-square$_2$ = 3.23, P=0.20	n.a.

Dystonia of unknown origin + GBA ex1-11 sequenced	n=97	n=51	n=46		
age	51.6 ± 16.0	43.7 ± 15.2	61.1 ± 11.1	T_{93} = 6.468, P<0.0001	n.a.
sex (% female)	53.6%	47.1%	60.9%	P=0.22	n.a.
age at symptom onset	32.8 ± 16.6	25.4 ± 16.1	41.5 ± 12.6	T_{91} = 4.984, P<0.0001	n.a.
disease duration (years)	18.14 ± 12.5	17.66 ± 14.08	19.67 ± 9.87	U=845.5, n=50, 42, P=0.11	n.a.
GCase wbc enzyme activity	7.62 ± 2.87	6.63 ± 2.53	8.72 ± 2.65	T_{95} = 3.988, P=0.0001	n.a.
b-GAL wbc enzyme activity	187.55 ± 48.79	179.25 ± 53.87	196.40 ± 41.49	T_{91} = 1.712, p=0.09	n.a.
CHIT wbc enzyme activity	43.68 ± 38.72	37.88 ± 38.27	49.86 ± 38.66	U=782.5, n=48, 45, P=0.02	n.a.
DAT Scans (n, %)	18 (18.6%)	16 (31.4%)	2 (3.9%)	P<0.001	n.a.
GBA mutation carriers	5 (5.2%)	4 (7.8%)	1 (1.9%)	P=0.37	n.a.
positive fam hx for PD	17 (17.5%)	6 (7.6%)	11 (21.6%)	P=0.18	n.a.
positive fam hx for Dyst	15 (15.5%)	6 (7.6%)	9 (17.6%)	P=0.40	n.a.

post-hoc test: * retrospective vs prospective; # retrospective vs. Alt. Aetiology; $ prospcetive vs alt aetiology

3.5.2 Lysosomal enzyme activity in blood

The activity of wbc lysosomal enzymes (in µmol/l/h) GCase, b-GAL and CHIT was compared to established, lab internal reference ranges in all n=130 cases of the combined cohort - activity of GCase was assessed as the main determinant of lysosomal activity.

Among the n=116 cases of *dystonia of unknown origin*, wbc GCase activity was measured in the homozygous (n=2; 1.7%), heterozygous (n=23; 19.8%), heterozygous/overlap (n=61; 52.6%) and unaffected (n=30; 25.8%) range (Figure 3.4). Mean wbc GCase activity was lower in the retrospectively vs. prospectively collected cases (P=0.0039; see Table 3.2). Activity of b-GAL, a marker of general lysosomal activity, did not differ between sub-cohorts, and was found below reference range in 12 cases (retrospective n=9; prospective n=3), all of which had GCase activity within the heterozygous (n=10) or heterozygous/overlap (n=2) range. Activity in CHIT, a marker of macrophage activation, similarly did not differ between sub-cohorts, and was found above mildly elevated in 3 cases (retrospective n=2; prospective n=1), all of which had GCase activity within the heterozygous/unaffected overlap range.

Similarly, in the n=97 cases of *dystonia of unknown origin* in which GBA exons 1-11 were sequenced, wbc GCase (P=0.0001) and CHIT (P=0.02), but not b-GAL activity was different between the retrospective and prospective cohort (not shown).

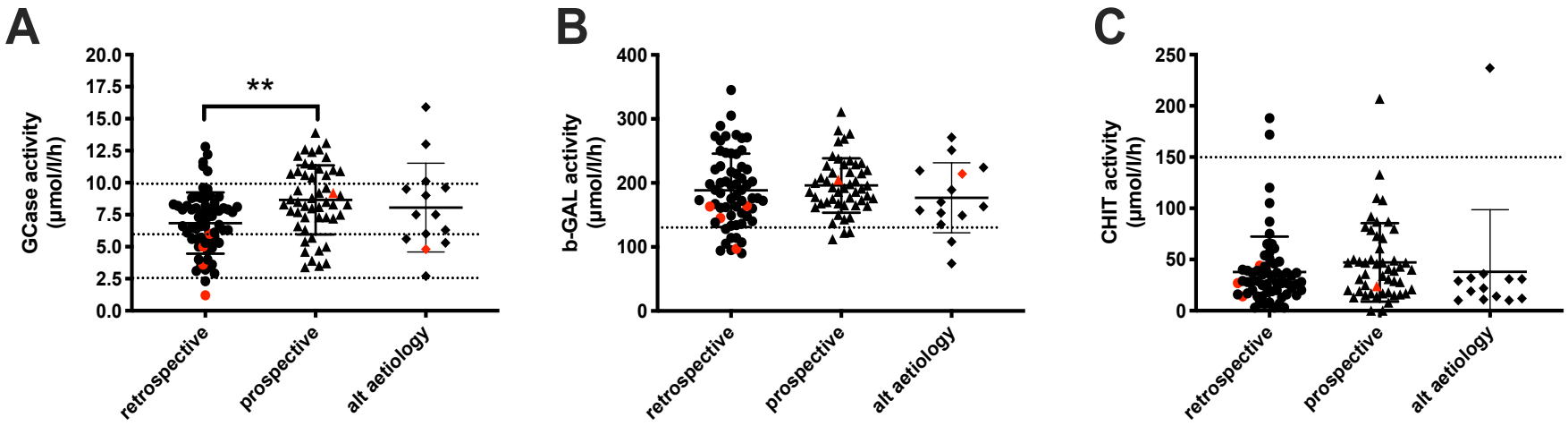

Figure 3.4: White blood cell lysosomal enzyme activity in dystonia patients.

Enzyme activity (in µmol/l/h) is displayed for n=116 cases of dystonia of unknown origin *(n=67 retrospective; n=49 prospective cases) and n=14 cases with a confirmed alternative aetiology for Glucocerebrosidase (GCase; A), beta-galactoisdase (b-GAL; B) and chitotriosidase (CHIT; C) – mean GCase activity was lower in retrospective than prospective cases (P=0.001). Dotted lines indicate internal enzyme activity reference ranges – GCase: typical for homozygous* GBA *mutations (<2.4µmol/l/h), heterozygous* GBA *mutations (2.5-5.4µmol/l/h), heterozygous / unaffected overlap (5.4-8.9µmol/l/h) or unaffected (>8.9µmol/l/h); beta-Galactosidase (b-GAL; B) normal (130-303µmol/l/h); Chitotriosidase (CHIT; C): normal (0-150µmol/l/h). Red symbols indicate cases with confirmed pathogenic* GBA *mutations.*

Among cases with *dystonia of unknown origin*, neither GCase (P=0.25) nor b-GAL (P=0.97), but CHIT activity showed a trend to correlate with age ($F_{1,108}$=3.726; r^2=0.033; P=0.056 see Figure 3.5 A-C), in keeping with the literature (Guo *et al.*, 1995; Ramanathan *et al.*, 2013).

There was a robust positive correlation between GCase and b-GAL activity ($F_{1,110}$=28.02; r^2=0.20; m=8.58; P<0.0001), which was not observed between GCase and CHIT (P=0.45), respectively b-GAL and CHIT (P=0.57; see Figure 3.5 D-F).

Only mean wbc CHIT activity (male: 34.96 ± 28.24 nmol/hr/mg protein; female: 47.53 ± 41.09; Mann-Whitney U test; U=1172; P=0.026), but neither GCase activity (male: 8.01 ± 2.73; female: 7.28 ± 2.6; independent sample t test; P=0.14) nor b-GAL activity (male: 199.0 ± 45.97; female: 185.7 ± 55.16; P=0.17) differed between the sexes (see Figure 3.5 G-I).

Following page:

Figure 3.5: Correlation analysis of white blood cell lysosomal enzyme activity.

While there was no detectable correlation between GCase and b-GAL with age (A-B), CHIT activity showed a trend for higher activity levels with advanced age (P=0.056; C). Among enzyme activity measurements, there was a robust positive correlation between GCase and b-GAL (P<0.0001; D) which was not present between GCase and CHIT (P=0.45; E) nor b-GAL and CHIT (P=0.57; F). Comparing between the sexes, there was a higher activity only for CHIT in females (G), while neither GCase nor b-GAL differed between male and female (H-I). Dotted lines indicate internal enzyme activity reference ranges – GCase: typical for homozygous GBA *mutations (<2.4µmol/l/h), heterozygous* GBA *mutations (2.5-5.4µmol/l/h), heterozygous / unaffected overlap (5.4-8.9µmol/l/h) or unaffected (>8.9µmol/l/h); b-GAL: normal (130-303µmol/l/h); CHIT: normal (0-150µmol/l/h); . * indicates p < 0.05, ** indicates p<0.005, *** indicates p<0.0005 across the figure; all measurements in µmol/l/h;*

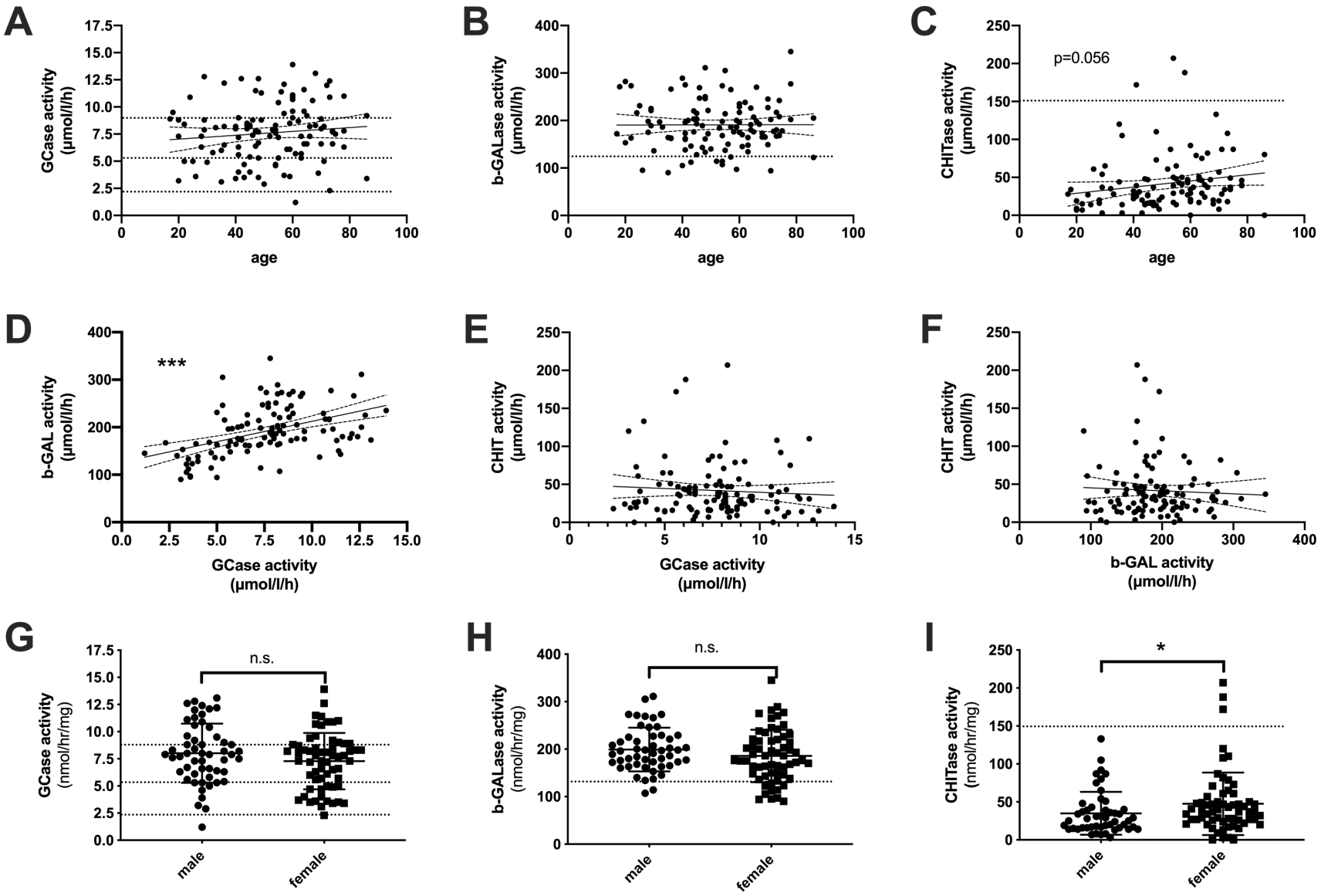
A
GCase activity (µmol/l/h)
age
B
b-GALase activity (µmol/l/h)
age
C
CHITase activity (µmol/l/h)
p=0.056
age
D
b-GAL activity (µmol/l/h)
***
GCase activity (µmol/l/h)
E
CHIT activity (µmol/l/h)
GCase activity (µmol/l/h)
F
CHIT activity (µmol/l/h)
b-GAL activity (µmol/l/h)
G
GCase activity (nmol/hr/mg)
n.s.
male
female
H
b-GALase activity (nmol/hr/mg)
n.s.
male
female
I
CHITase activity (nmol/hr/mg)
*
male
female

In the n=14 cases with a confirmed alternative aetiology, wbc GCase activity was measured in the heterozygous (n=4; 28.6%), heterozygous/overlap (n=7; 50%) and unaffected (n=3; 21.4%) range (see Table 3.5). Neither mean activity levels for GCase, nor b-GAL or CHIT were different from cases with *dystonia of unknown origin* (see Table 3.2). GCase activity was decreased in several cases of genetically (activity level in heterozygote/unaffected overlap range in four of five cases, mean 7.2 ± 3.44µmol/l/h) and structurally confirmed alternative aetiologies (all three cases in heterozygous/unaffected overlap range, mean 6.0 ± 0.29µmol/l/h), while there was only one PD case with low GCase activity, who also was found to carry a heterozygous *GBA* E326K mutation (heterozygous range; see Table 3.5).

3.5.3 Mutations in GBA

DNA of n=97 cases of *dystonia of unknown origin* of mixed genetic background was available for sequencing. Of these, known pathogenic *GBA* mutations were found in five cases (5.15%; see Table 3.3). In comparison with a historic series of n=257 controls of Caucasian ancestry from the same area and sequenced according to the same sequencing protocol, which had identified three *GBA* mutation carriers (1.17%) (Neumann *et al.*, 2009), known pathogenic *GBA* mutations were significantly more frequent among patients with *dystonia of unknown origin* (one-sided Fisher´s exact test, p=0.04; OR=4.6; 95% CI=1.18-17.57). After matching for ethnicity (five out of 80 Caucasian cases of *dystonia of unknown origin*), the frequency of *GBA* mutations in this population was 6.25% (p=0.02; OR=5.64; 95% CI=1.44-21.58).

Three of the dystonic mutation carriers (and one case eventually diagnosed as YOPD) were found to be heterozygous for E326K (carrier frequency 3%), one was heterozygous for T369M (1%), and the one with the lowest overall GCase activity carried both a heterozygous T369M and N370S mutation (1%), although it could not be determined if in cis or trans compound heterozygous state as neither continuous amplicons of sufficient quality across both exons, nor samples from the patients parents were available for analysis.

A

B

C

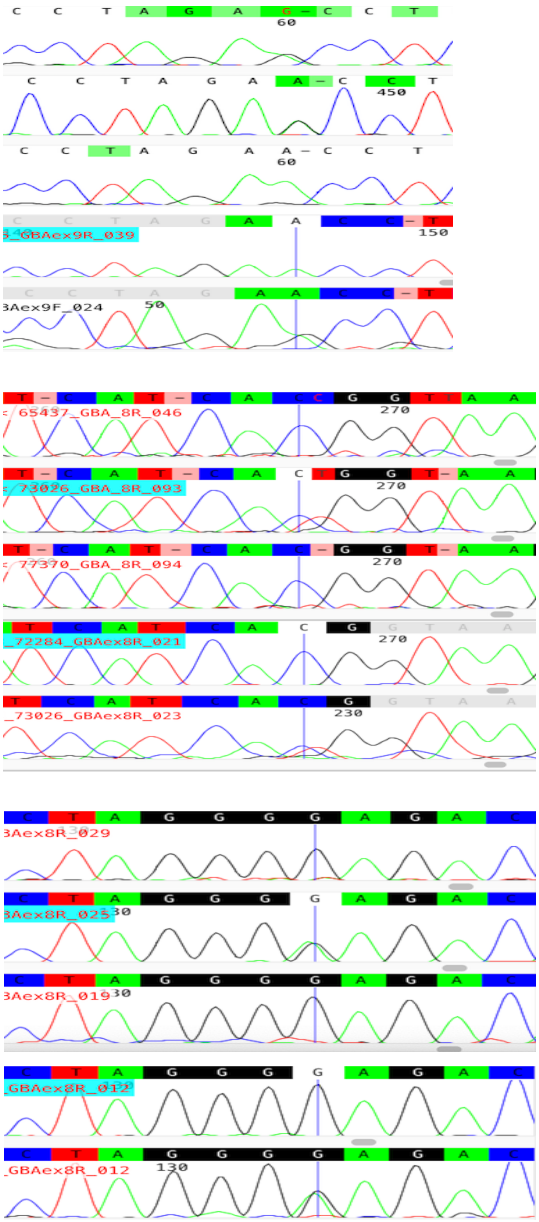

Figure 3.6: Example raw Sanger sequencing chromatograms

Visualization on Codon code aligner software: Sequencing reads showing a heterozygous N370S mutation on both forward (first row) and reverse strand (second row) and replication sequence of the same patient (fifth row) in comparison to healthy controls (third - forth row; A).

Sequencing reads showing a heterozygous T369M mutation on forward strand (second row) and replication forward strand sequence of the same patient (fifth row) in comparison to healthy controls (first, third -forth row; B).

Sequencing reads showing a heterozygous E326K mutation on the forward strand of two patients (second & fifth row) in comparison to healthy controls (first, third -forth row; C).

3.5.4 Cases with dystonia and GBA mutations

Four of the five cases with a pathogenic *GBA* mutation belonged to the retrospectively collected group of patients with a clinical presentation deviating from recognized dystonia syndromes: e.g. Case no.1 presented with congenital cataract and isolated foot dystonia from the age of 47 and repeatedly negative DaT scans over a 14 year follow-up, Case no.12 presented writer`s cramp from the age of 45 developing into profound craniocervical and laryngeal dystonia, Case no.24 with dystonic posturing of both hands from the age of 15, progressive tongue biting and cervical dystonia on a background of non-REM parasomnias, Case no. 37 with the combination of upper limb dystonic posturing from the age of 13 and slowly progressive leg spasticity. There was however also a prospectively sampled case (no.99) with cervical dystonia without additional features and an inconspicuous age at onset of 44 years.

Mean age at onset among these cases was 32.4 ± 16.9 years and clinical follow-up since symptom onset was 16.6 ± 5.6 years. Wbc GCase enzyme activity was measured in the homozygous (n=1; 20%), heterozygous (n=2; 40%), heterozygous/overlap (n=1; 20%) and unaffected (n=1; 20%) range, while b-GAL was below the normal range in one case only (case no. 12).

Table 3.3: Known pathogenic GBA *mutations identified in patients with dystonia*

Allele name[a]	***GBA* cDNA**	**Protein**[b]	**Exon**	**Dystonia Cases**		**Controls**	
				n	Carrier frequency	n	Carrier frequency
E326K	c.1093G>A	p.Glu365Lys	8	3	3%	0	0%
T369M *	c.2023C>T	p.Thr408Met	8	2	2%	0	0%
N370S *	c.1226A>G	p.Asn409Ser	9	1	1%	1	0.39%
R257Q	c.887G>A	p.Arg296Gln	7	0	0%	1	0.39%
V458L	c.1489G>T	p.Val497Leu	10	0	0%	1	0.39%
					5.15%		1.17%

a Allele names follow the common nomenclature and apply to the processed protein, not including the 39-residue signal peptide.

b Protein names are based on the primary translation product and include the 39-residue signal peptide.

c Carrier frequency for each GBA mutation in regard to the total number of dystonia patients (total n=97).

d Carrier frequency for each GBA mutation in regard to the total number of historic controls from the same ethnicity and center (total n=257).

* case 1 (see Table GBA mutations carriers), carried both a heterozygous T369M and heterozygous N370S variant - it was not possible to determine if in compound or combined heterozygous state (c.1226A>G(;)c.2023C>T, p.Asn409Ser(;)p.Thr408Met)

One more GBA mutation (het. E326K) was identified in one patient in the alternative aetiology cohort, which had clinically converted to PD (see Table 3.5)

Table 3.4: Descriptive details of dystonia patients with known pathogenic GBA *mutations.*

All patients are of Caucasian ancestry. Lysosomal enzyme activity reference ranges: b-Glucocerebrosidase (GCase) activity (homozygous: <2.4; heterozygous: 2.5-5.4; heterozygous/unaffected overlap: 5.4 - 8.9; unaffected range:8.9-16.8 µmol/hr/mg), b-Galactosidase (b-GAL) activity (131-303 µmol/hr/mg), Chitotriosidase (CHIT) activity (0-150 µmol/hr/mg); polysomnography (PSG), deep brain stimulation (DBS), globus pallidus internus (GPi);

case no.	Sex	AAO	AGE	Phenotype	GCase	b-GAL	CHIT	Genetics	Family history	Brain MRI	DaT SCAN
1	m	47	61	Isolated foot dystonia, insidious onset, very slowly progressive; congenital cataract	1,2	145	n.d.	GBA het. N370S + T369M	none	non-significant white matter changes	repeatedly normal
12	f	45	59	Onset with writer`s cramp, progressive worsening and craniocervical and laryngeal involvemend, treated with bilat. GPi DBS	3,6	97	27	GBA het E326K; Negative for DYT1 deletion	Familial hypercho les-terolemia	focal area of nonspecific signal change in supratentorial white matter	n.d.

24	m	15	25	non-REM parasomnias throughout childhood into adulthood (PSG proven), from age 15 dystonic posturing of hands, from age 19 tongue biting and cervical dystonia	5,0	163	14	GBA het. E326K; negative for DYT1, DYT6, DRPLA, PANK2, HD, Friedreich`s	none	normal	n.d.
37	f	13	35	dystonic posture in upper limbs, from 20ies slowly progressive leg spasticity	6,0	164	44	GBA het T369M; GCH-1, BSCL2, Spastin, Atlastin neg.	daughter similarly affected	normal	n.d.
99	f	42	65	cervical dystonia	9,2	205	24	GBA het E326K	none	normal	n.d.

3.5.5 Cases with alternative aetiology

During clinical follow-up since initial presentation, a definitive diagnosis could be established in 14 out of 130 cases (retrospective n=12; prospective n=2; Table 3.5). The aetiology of dystonia was identified by either genetic testing (one each for mutations in MAPT, SCA12, SCA17, SEPN1, KMT2B n=5), additional information about previous, especially paediatric investigations (supporting pallidal necrosis, striatal lesion or ADEM during infancy; n=8) or the development of PD by fulfilling clinical diagnostic criteria and showing an abnormal DaT scan (n=6).

Among these six PD cases, three (cases no. 20 (carrying a heterozygous E326K *GBA* mutation), 96 & 102), developed parkinsonian symptoms within 2.3 ± 0.5 years (mean ± std.) of symptom onset and were diagnosed at 41.7 ± 6.8 years of age as young-onset PD (YOPD). Interestingly, the other three cases (no. 105, 106 & 130) initially were diagnosed with CD and developed parkinsonian symptoms with much more latency (14.0 ± 6.5 years) and were diagnosed at 66.3 ± 8.3 years of age as PD. There were no peculiar clinical features noted in both their dystonic or parkinsonian presentation, apart from the unusually late onset of CD symptoms in case no. 105 at 72 years of age. Only the E326K heterozygous carrier had wbc GCase activity in the heterozygous range, while in all other PD cases GCase was normal.

Table 3.5: Descriptive details of patients with dystonia and confirmed alternative aetiology;

abbreviations: heterozygous (het.), negative (neg.), # no consent for research sequencing, $ incomplete sequencing due to insufficient amount/quality of DNA sample available;

case no	AGE, SEX	AAO	Phenotype (age in years)	GCase	b-GAL	CHIT	Genetics	Family history	Brain MRI	DaT SCAN
Alternative genetic cause for dystonia										
3	56, f #	55	right hand dystonic tremor, gait slowing, frontal cognitive dysfunction (55), frontotemporal dementia	2,7	108	31	het MAPT positive, C9orf72, SCA17, JPH3, HD negative	mother Alzheimer`s disease at advanced age	no obvious changes/atrophy	bilaterally abnormal
25	38, f	32	aggressive dementia & segmental dystonia (32) dyspraxia (34)	5,3	157	36	SCA17 positive; HD, prion protein gene, GBA negative	one of two monozygous twins, other twin apparently unaffected	cerebellar and posterior atrophy	not done
59	34, f	13	axial (13) & cervical dystonia (18)	7,5	189	11	SEPN1 positive; DYT1, GBA negative	none	normal	not done

60	39, f	30	alcohol-responisve myoclonic dystonia of the hands (30), then progress to cranio-cervical region (34)	7,5	271	19	SCA12 positive, DYT11, GBA negative	father affected similarly	mild generalized volume loss	normal
127	24, m	6	microcephalus, cerebellar symptoms (6), generalised dystonia with predominant oromandibular & tongue involvement	**13,0**	149	29	KMT2B positive; common mitochondrial mutations, SCA 1, 2, 3, PKAN, GBA negative	none	normal	not done
Alternative structural cause for dystonia										
30	23, m	4	diarrhoea, drop in consciousness, meningo-encephalitis / ADEM with wide-spread CT abnormalities, pyramidal signs (4), generalized dystonia since then, predominantly neck, arms, upper body, anarthria	5,6	163	14	DYT 1 negative	none	normal (prior to DBS), previously wide-spread CT abnormalities in keeping with ADEM	not done
36	20, f $	0	developmental delay, generalized dystonia with leg onset (1), speech and cerebellar involvement (2) amblyopia (7)	6,0	219	10	PANK2 negative	sister with same condotion	bilateral pallidal atrophy & necrosis and cerebellar atrophy	normal

40	17, m	12	premature birth (32 weeks of gestation), delayed early motor milestones, right foot dystonia (12)	6,3	135	12	DYT1, GBA negative	none	left lentiform nucleus mature damage & caudate nucleus atrophy	not done
Alternative diagnosis of Parkinson´s disease										
20	46, m	44	YOPD: tension in groin and foot turning in (44), shoulder, neck, speech, generalized dystonia, parkinsonism (46)	4,8	214		GBA het E326K positive, DYT1, Parkin, LRRK2 negative	none	normal on repeat MRIs	bilaterally abnormal
96	47, f $	45	YOPD: foot + jaw dystonia (45), REM-sleep behaviour disorder (46), parkinsonism (47)	9,0	74	31	None	unknown	normal	asymmetrically abnormal
102	37. f $	26	YOPD: retrocollis (26), arm tremor (29), leg stiffnes & Parkinsonism (32), anxiety & depression; L-dopa induced dyskinesia	9,5	170	10	Parkin, LRRK2, DYT1, mt m3243, POLG, mt rearrangements negative	paternal granddad "Lewy body disorder", grandmother dementia	normal	asymmetrically abnormal
105	90, f	72	CD (72), then PD (78)	9,6	153	237	GBA neg.	none	mild generalized atrophy, small vessel disease, foci of mature cerebellar damage, signal change superior cerebellar peduncle	bilaterally abnormal

106	72, m $	40	CD (40), then hand tremor with abnormal DAT/PD (62)	10,1	251	22	FMR, SCA 1,2,3,6,7,12, 17, GBA negative	daughter and son cervical dystonia	supratentorial white matter changes, moderate small vessel disease	abnormal
130	59, f	45	CD + blepharospasm (45), then PD (59)	15,9	224	32	GBA neg.	niece cervical dystonia and depression	normal	abnormal

3.5.6 DaT scan imaging data

In addition to six cases that developed PD on follow-up (see Table 3.5), DaT scan imaging data had been acquired from n=20 (17.2%) of n=116 cases with *dystonia of unknown origin,* with the majority (n=17) stemming from the retrospective cohort. Case no.1 (heterozygous N370S + T369M carrier) had serial negative scans (see Figure 3.7), while case no.47 was judged to have a pathological DaT scan most likely as a consequence of various lesional basal ganglia interventions decades earlier and was excluded from further analysis.

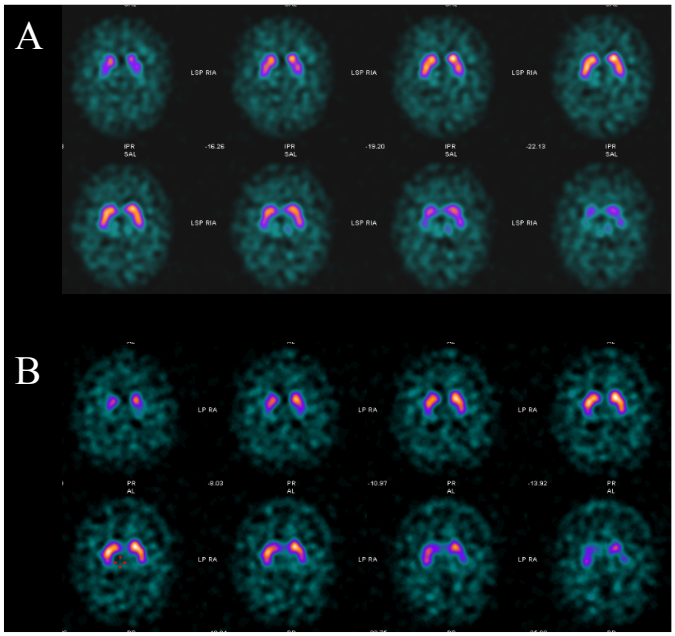

Figure 3.7: Example negative DaT Scans in dystonia patients

Serial negative DaT scans of case no.1 with identified GBA *heterozygous N370S + T369M genotype taken 10 (A) and 13 years (B) after dystonia onset.*

In the remaining n=19 (16.4%) dystonia cases with normal DaT scan imaging, mean age at onset was 34.8 ± 16.5 years (range: 4 – 68 years), mean disease duration to DaT scan was 14.6 ± 11.8 years (range: 1-45 years) and wbc GCase activity was measured in the homozygous (n=2; 10%), heterozygous (n=6; 30%), heterozygous/overlap (n=8; 45%) and unaffected (n=3; 15%) range. In absolute measures, mean wbc activity (in µmol/hr/mg) was 6.6 ± 3.4 for GCase, 189.6 ± 53.2 for b-GAL and 20.9 ± 12.5 for CHIT.

Table 3.6: Descriptive details of patients with dystonia of unknown origin *and available DaT scans.*

*Case no.47 (marked with #) was excluded from statistical evaluation, as imaging changes were interpreted as related to pallidotomies decades earlier. retrospective cases: 1, 2, 4, 10, 16, 26, 42, 47, 53, 58, 62, 70, 90, 91, 116, 122, 129; prospective cases: 8, 19,46; b-Glucosidase wbc activity (reference range: homozygous: <2.4; heterozygous: 2.5-5.4; heterozygous/unaffected overlap: 5.4 - 8.9; unaffected:8.9-16.8 nmol/hr/mg); b-Galactosidase wbc activity (normal range 131-303 nmol/hr/mg); Chitotriosidase wbc activity (normal range 0-150 nmol/hr/mg); * image not available*

Case	Ethnicity	Sex	AAO	AGE	disease duration to DaT	Phenotype	GCase	Genetics	Family history	Brain imaging (MRI)	DaT SCAN
1	wb	m	47	62	15	isolated foot dystonia, congenital cataract	1,2	GBA het. N370S + T369M	none	non-significant changes	repeatedly normal
2	i	f	68	73	5	late-onset isolated foot dystonia left>right	2,3	GBA neg.	one of 8 healthy siblings, dementia (mother)	bilateral putaminal gliosis, without abnormal mineralisation, modest small vessel disease	normal

4	wb	m	29	50	21	focal hand-dystonia, initially task-specific, later also at rest and other tasks, professional pianist & conductor	2,9	GBA neg.	none	non-significant changes	normal *
8	wb	f	35	86	45	CD, ? slowing on finger tapping aged 70	3,4	none	none	normal	normal
10	wb	F	22	45	23	dystonic hand tremor, myoclonus, later segmental dystonia	3,5	DYT1 & GBA neg.	PD (maternal grandmother), MS (mother), remote family members muscular dystrophy	normal	normal
16	wb	F	38	45	5	left hemi-dystonia with torticollis, axonal peripheral neuropathy	4,0	DYT1, DYT5, common mitochondrial mutations & GBA neg.	PD (two aunts)	normal	normal *

19	wb	f	48	54	6	CD	4,7	SCGE & GBA neg.	PD (paternal uncle), hand tremor (father), restless legs (daughter)	cCT normal, no MRI	repeatedly normal
26	ch	m	34	49	15	generalized left sided dystonia with oromandibular involvement, cerebellar signs, very slow progression	5,3	DYT1, Parkin, GCH-1, SCA 1, 2, 3, 6, 7, 12, 17 & GBA neg.	none	non-significant changes	repeatedly normal
42	wb	m	41	42	1	onset left arm stiffness, rapid progressive tremor, cervical dystonia, writing difficulty, rest tremor, rigidity, some cerebellar signs	6,3	none	PD (grandfather)	slight asymmetric cerebral hemisphere atrophy	normal
47 #	wb	F	32	64	32	torticollis with retrocollis (32), partial thalamotomy with right leg dystonia as complication, developed left sided leg dystonia later, bilat. pallidotomies,	6,6	mtDNA, PD gene panel & GBA neg.	none	cCT normal, no MRI	bilaterally abnormal, ? due to pallidal inter-ventions *

						walking difficulties (62)					
49	ch	m	47	70	23	CD, ? asymmetric slowing on finger tapping aged 70	6,6	DYT1 & GBA neg.	none	mild cerebral atrophy, left anterior lobe hyperintensity	normal
53	w	M	12	28	16	dystonic tremor, most likely not linked to chronic hydrocephalus	7,3	DYT1 & GBA neg.	none	stable hydrocephalus	normal
58	wb	M	4	46	42	leg stiffening while walking, progression of dystonia (46), chorea, postural reflexes affected	7,4	GCH-1 & GBA neg.; genome wide array no signs of copy number variations;	rest tremor (father)	normal	normal
62	wb	M	43	54	11	asymmetric dystonic tremor	7,6	FMR1, SCA 1, 2, 3, 6, 7, 12 & GBA neg.	PD (mother), tremor (three brothers), strong family history for cystic fibrosis	Vascular leucencephalopathy, including subcortical white matter, bilateral striata and thalami.	normal

70	wb	M	51	54	3	musician´s dystonia: shoulder elevation (proximal muscle) on holding cello bow	7,9	DYT1 & GBA neg.	PD (mother)	normal	normal
90	w	F	5	20	13	delayed development, seizures, upper limb dystonia, no stereotypies	8,8	GBA neg.	unknown	not done	normal *
91	wb	M	19	29	5	dystonia, obsessive slowness	8,8	HD & GBA neg.	unknown	normal	normal *
116	wb	M	35	49	14	right foot dystonia, Marathon runner	11,3	GCH-1, DYT1 & GBA neg.	none	normal	normal
122	a	M	30	37	7	painful left upper segmental dystonia	12,2	DYT1, dystonia-parkinsonism panels & GBA neg.	consanguinity (parents 2nd degree cousins), cousin and brother with epilepsy	normal	normal
129	wb	f	54	62	8	left foot toe dystonia	13,9	GBA neg.	unilateral leg weakness (mother)	not done	normal *

3.5.7 Brain homogenate enzyme activity measurements

Enzyme activity (in nmol/hr/mg protein) for GCase and b-GAL were measured in brain tissue homogenates of healthy controls (Ctrl, n=10) and dystonia patients (Dystonia; n=10), matched for sex (Fisher`s exact test, p>0.99), age (two-tailed unpaired t test; t_{18}=1.93; P=0.07) and post-mortem delay (t_{17}=0.25; P=0.80). Due to the scarcity of dystonia donor brains, not only samples from patients with focal, segmental and generalized dystonia (n=5) but also with blepharospasm (n=5) were included (see Table S7).

Among Ctrl tissue samples, age at death had a significant influence on enzyme activity levels for GCase in CDN ($F_{1,9}$=9.056; r^2=0.501; m=-0.20; P=0.014) and PALL ($F_{1,7}$=9.807; r^2=0.584; m=0.411; P=0.016) but neither CRB (P=0.88) and SCoL (P=0.30), nor b-GAL activity in any of the regions studied (CDN, P=0.63; CRB, P=0.97; PALL, P=0.75; SCoL, P=0.35). Post mortem delay had a significant influence on enzyme activity levels for GCase in PALL ($F_{1,7}$=11.4; r^2=0.619; m=-0.17; P=0.011), but neither for GCase (CDN, P=0.10; CRB, P=0.83; SCoL, P=0.35) nor b-GAL (CDN, P=0.09; CRB, P=0.83; PALL, P=0.52; SCoL, P=0.81) in any of the other regions studied. There was no difference between sexes in enzyme activity across brain regions. Between brain regions, GCase activity was highest in SCoL and lowest in PALL (one-way ANOVA; $F_{3,38}$=4.336; P<0.01), whereas b-GAL activity was highest in CDN > CRB > CRB/PALL ($F_{3,38}$=24.36; P<0.0001; see Figure 3.8 A - B).

This region-specific pattern was lost in dystonia tissue samples for GCase (P=0.72) and attenuated for b-GAL ($F_{3,39}$=6.52; P=0.001; see Figure 3.8 C - D). Mean activity levels for GCase were lower in dystonia vs. Ctrl tissue samples in CDN (independent sample t test; t_{18}=2.12; P=0.048) and b-GAL in SCoL (t_{18}=2.23; P=0.038) but did not

reach statistical significance in other brain regions (see Figure 3.8 E - F). Describing the degree of dispersion of measurements per group, the CoV was significantly larger among dystonia samples for GCase activity in CDN (P=0.0008) and CRB (P=0.03) with a trend in SCol (P=0.056), as well as for b-GAL in CDN (P=0.0023) and SCoL (P=0.03; see Figure 3.8 G - H).

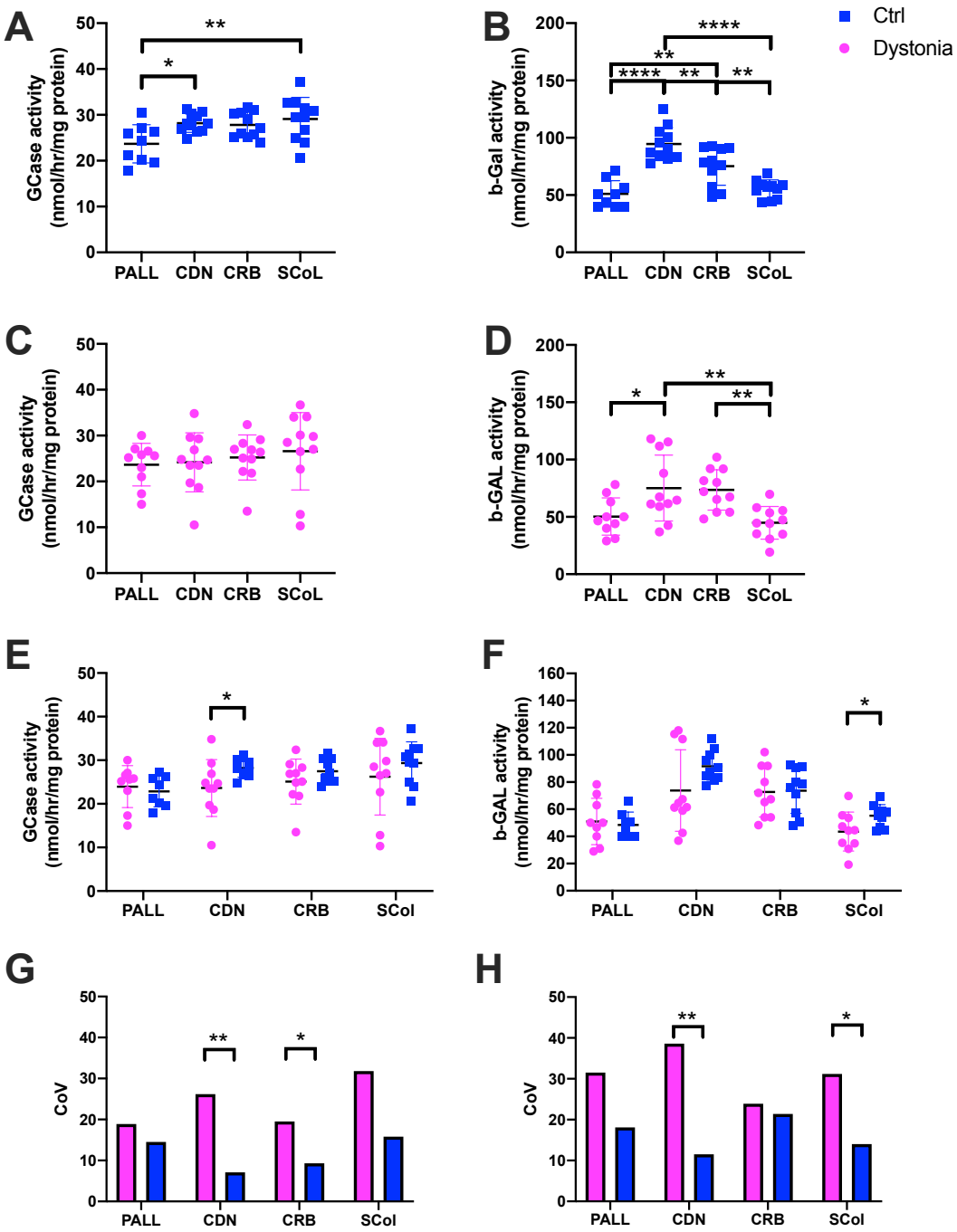

Figure 3.8: Brain homogenate lysosomal enzyme activity

Measurements in nmol/hr/mg protein in patients with dystonia (n=10, magenta) and controls (n=10, blue). Absolute enzyme activities (A-F) and coefficient of variation (G-H) are displayed per group and brain region. Pallidum (PALL), Cerebellar dentate nucleus (CDN), cerebellar cortex (CRB), superior colliculus (SCol);

3.6 Discussion

This work provides first evidence of decreased lysosomal enzyme activity in both combined and isolated dystonia. Using a comprehensive approach of enzyme activity quantification in wbc and brain tissue, as well as full sequencing of the *GBA* gene in a retrospective and a prospective cohort of dystonia patients, these results imply lysosomal dysfunction in a significant minority of dystonia cases.

3.6.1 Lysosomal dysfunction as a novel disease mechanism in dystonia

This argument is based on first) on the largest evaluation of peripheral lysosomal enzyme activity from dystonia patients. This shows a reduced wbc GCase activity within the range typically measured in homozygous or heterozygous *GBA* mutation carriers in a strikingly high 21.5% of cases of *dystonia of unknown origin*. The two cohorts studied represent two distinct parts - if not extreme ends - of the phenotypical spectrum within dystonia, spanning from frequent, relatively homogenous CD to much rarer cases not fitting idiopathic dystonic syndromes. Although the proportion of cases with decreased wbc GCase activity (homozygous or heterozygous *GBA* mutation carrier range) was higher in the retrospective (26.8%) than the prospective (16.3%) cohort, the finding of a similar metabolic pattern in both cohorts indicates that decreased peripheral lysosomal activity might be a common abnormality in different forms of dystonia.

Apart from GD, abnormal GCase activity so far has only been described in PD (Alcalay *et al.*, 2015; 2018; Atashrazm *et al.*, 2018). In parallel to GCase activity, reduced b-GAL activity was found in the CSF and patient-derived neurons of PD

patients, whereas in GD b-GAL activity in fibroblasts and leukocytes has been found increased (Schöndorf *et al.*, 2014), implying that the pattern of lysosomal activity differs between GD and PD. The positive correlation between peripheral GCase and b-GAL activity in our dystonia cohort hence shows similarity to the metabolic pattern in PD and points at a more general lysosomal dysfunction in dystonia. Similarly, normal CHIT activity in the large majority of samples argues against a macrophage activation pattern in dystonia, as present in GD. The higher mean CHIT activity among female vs. male patients with *dystonia of unknown origin* (P=0.026) has not been reported in healthy controls (Guo *et al.*, 1995; Ramanathan *et al.*, 2013), GD or PD patients (Alcalay *et al.*, 2015).

As wbc enzyme activity was only measured consistently for GCase, b-GAL and CHIT in this study, the full pattern of lysosomal dysfunction in dystonia remains to be established.

The finding of decreased lysosomal enzyme activities in cases with an alternative genetic cause for dystonia remains inconclusive, as lysosomal activity has not been reported in carriers of *MAPT* mutations and SCA17 so far. The observation of reduced LAMP-1 staining in fronto-temporal dementia due to *MAPT* however points to possible lysosomal deficiency in this condition (Bain *et al.*, 2019). Alternatively to being caused by genotype, GCase activity might be influenced by the dystonia disease process itself, i.e. an endophenotype like in Parkinson´s disease (Gegg *et al.*, 2012). Further studies will need to clarify this.

Second) this study identified a significantly higher rate of pathogenic *GBA* mutations among dystonia cases (6.25%) than healthy controls of the same ancestry (1.17%; p=0.02). In this cohort, heterozygous mutations E326K and T369M, as well as

T369M/N370S (compound or combined heterozygous state) were detected, with E326K being the most frequent. *GBA*-related PD has been mostly described in the presence of heterozygous (Sidransky and Lopez, 2012), and only rarely in homozygous or compound heterozygous mutation state (Clark *et al.*, 2007; Lesage *et al.*, 2010). Alleles E326K and T369M are established risk factors for PD (OR 1.71, 95% CI 1.55–1.89, respectively OR 1.74, 95%CI 1.19-2.55) (Zhang *et al.*, 2018) but not GD (Horowitz *et al.*, 2011; Mallett *et al.*, 2016; Pankratz *et al.*, 2012), while N370S is a risk factor for PD (OR 3.08, 95% CI 2.32–4.09) (Pankratz *et al.*, 2012) and the most frequent cause of GD across most populations (Alfonso *et al.*, 2007; Lacerda *et al.*, 1994).

Similar to GD, certain *GBA* variants have been reported to occur more frequently with PD than others. Of 13 studies that based their results on *GBA* whole exon analysis (including n=4966 patients from China, Portugal, Greece, Japan, Britain, North-Africa, French-Canada, Europe and Korea), eight reported L444G and six N370S as the most frequent variants detected (Sidransky and Lopez, 2012). Regarding individuals of Caucasian background, N370S accounted for 36% of carriers in a Portuguese study (Bras *et al.*, 2009), 47% in a French study (Lesage *et al.*, 2010) and 24% in a British study (Neumann *et al.*, 2009), while L444P was present in 33% of carriers in a British (Neumann *et al.*, 2009) and 22% in a French study (Lesage *et al.*, 2010). Interestingly, N370S is rarely found in Asian populations (Mitsui *et al.*, 2009), while L444P is found irrespective of ethnic background (Sidransky and Lopez, 2012).

Meanwhile, *GBA* is accepted as the most frequent genetic risk factor for PD (Bras *et al.*, 2015) with an OR of 5.43 (95% CI=3.89–7.57) (Sidransky *et al.*, 2009) and our data suggest a possibly similar OR of 5.64 (95% CI=1.44-21.58) in dystonia, although

of course based on a much smaller sample size. This makes it even more puzzling as to why the association between *GBA* and dystonia - like PD - has evaded multiple large-scale attempts from epidemiologists and geneticists before. It has been argued that for PD this might be due to a) epidemiologically, GD being much rarer than PD in the general population, b) genetic linkage studies not being able to detect this association as the *GBA* mutations are too rare in most but high-risk populations, such as Ashkenazy Jews, and c) genome wide association studies correcting for multiple-testing being too strict for this association to be detected, and also relying on the assumption that there is a single disease-associated allele per locus, which is not true for *GBA* with its multiple mutations (Rogaeva and Hardy, 2008).

It appears possible that in addition to less large-scale genetic studies undertaken in dystonia than PD, similar factors might have prevented the detection of *GBA* as a genetic risk factor in dystonia so far.

While the results presented in this work establish an association between lysosomal dysfunction and dystonia, they cannot prove a direct causal effect. Our genetic analyses are compatible with mutations in *GBA* to act as a modifier and risk factor and not in a mendelian fashion. Replication of our findings in other cohorts and more mechanistic studies including rescue experiments will be necessary to establish GBA mutations as a cause for dystonia. Given the relatively small sample size, genotype-phenotype correlations are currently not warranted.

Third) the finding of a region-specific decrease in lysosomal function in human brain tissue in dystonia. So far, human post-mortem brain tissue has been assessed for lysosomal enzyme activity mainly in the context of PD (Chiasserini *et al.*, 2015; Gegg *et al.*, 2012; Moors *et al.*, 2019; Rocha *et al.*, 2015). Apart from one study (Rocha *et*

al., 2015), GCase activity has been consistently reported as decreased in the SN in PD (Chiasserini *et al.*, 2015; Gegg *et al.*, 2012; Moors *et al.*, 2019), while there is less agreement on decreased activity in cerebellum (Gegg *et al.*, 2012; Rocha *et al.*, 2015), putamen (Gegg *et al.*, 2012), caudate (Chiasserini *et al.*, 2015) or hippocampus (Rocha *et al.*, 2015). Physiologically, GCase activity decreases with advancing age in substantia nigra and putamen (Rocha *et al.*, 2015). Mutations in *GBA* are known to lead to reduced GCase activity, which has been semi-quantified in blood for L444P (<5% residual wild type GCase activity) (Grabowski, 2008), and N370K (17.7%) as well as E326K (38.7%) in heterologous expression systems (Horowitz *et al.*, 2011). There is so far only rudimentary understanding however, why enzyme activities vary even between cases with the same *GBA* mutation, although genetic modifiers, such as scavenger receptor class B member 2 (SCARB2) - encoding lysosomal integral membrane protein type 2 (LIMP-2), the receptor involved in the trafficking of GCase within the cell - or transcription factor EB (TFEB), regulating expression of a wider lysosomal gene expression network, respectively GCase activators, such as Saposin C, have been shown to modulate GCase activity (Siebert *et al.*, 2014).

The brain regions studied here were chosen based on their presumed role in dystonia pathophysiology due to cerebellar (Kaji *et al.*, 2018; Shakkottai *et al.*, 2016), tectal (Holmes *et al.*, 2012; Mc Govern *et al.*, 2017) or basal ganglia (Goto *et al.*, 2005; 2013; Hanssen *et al.*, 2018; Neychev *et al.*, 2011) dysfunction, and tissue availability. In line with previous reports (Chiasserini *et al.*, 2015), our healthy control data indicate enzyme- and brain region-specific activity levels for GCase as well as for b-GAL. Even with this relatively small sample, we observed an attenuation of this pattern in dystonia with an increase in the inter-individual variability of activity levels mainly in cerebellar structures. Using GCase activity as

the main read-out and b-GAL as a control enzyme, our data point at primarily cerebellar changes in this patient population. The detection of decreased GCase activity in cerebellar dentate nucleus adds significantly to the abnormal enzyme activity finding in peripheral blood, as it implies a systemic deficiency associated with dystonia. It is also in keeping with mounting evidence for a pathophysiological role of the cerebellum in this condition (Filip *et al.*, 2017; Neychev *et al.*, 2011; Sadnicka *et al.*, 2012; Shakkottai *et al.*, 2016). Even further, it appears to point at a specific functional abnormality in the dentate nucleus, the main cerebellar efferent structure.

The above observations of decreased enzyme activity in central and peripheral tissue and genetics lend support to the hypothesis of lysosomal dysfunction in dystonia. Interestingly in PD, decreased GCase activity has consistently been reported both in blood and brain (SN) of patients with (PD+GBA) (Alcalay *et al.*, 2015; Atashrazm *et al.*, 2018) and without *GBA* mutations (PD-GBA) (Gegg *et al.*, 2012; Rocha *et al.*, 2015). Similarly, mitochondrial Complex 1 deficiency (Mizuno *et al.*, 1989; Schapira *et al.*, 1989) has been found in the SN of PD patients with (Morais *et al.*, 2014) and without mitochondrial mutations (Flønes *et al.*, 2018). Lysosomal dysfunction and Complex 1 deficiency, although anatomically not correlated with α-synuclein accumulation and neurodegeneration (Flønes *et al.*, 2018), are acknowledged as a key pathophysiological mechanism in PD (Poewe *et al.*, 2017). Lysosomal and mitochondrial dysfunction in PD are accepted as general disease mechanisms and not limited to mutation carriers.

The finding of decreased lysosomal enzyme activity irrespective of *GBA* mutation status in this work hence possibly points at a wider pathophysiological role of lysosomal dysfunction in dystonia.

3.6.2 Pathophysiological considerations

The pathophysiology of dystonia as a syndrome is believed to primarily involve cerebral cortex, basal ganglia and cerebellum (Hanssen *et al.*, 2018; Kaji *et al.*, 2018; Neychev *et al.*, 2011). So far, dystonia has been associated with lysosomal dysfunction as part of the clinical presentation in lysosomal storage disorders, such as in chronic forms of GM1 gangliosidosis (Arash-Kaps *et al.*, 2019), GM2 gangliosidosis (Meek *et al.*, 1984), and less frequently in Niemann Pick type C and Kuf`s disease (Ebrahimi-Fakhari *et al.*, 2018; Sedel *et al.*, 2008).

Human post-mortem neuropathology of the above disorders is scarce, but neuronal loss and gliosis primarily affecting striatum and pallidum has been reported in juvenile-onset, chronic GM1 gangliosidosis with dystonia (Suzuki, 1991), while selective neurodegeneration of cerebellar Purkinje cells has been reported in Niemann Pick type C (Walkley and Suzuki, 2004). Extensive brainstem and striatal gliosis as well as selective neuronal vulnerability in hippocampal fields CA2-4 and cerebral cortex layer 3 and 5 have been reported as unique pathology features in GD (Wong *et al.*, 2004). In GBA+PD, neurodegeneration is indiscernible from sporadic cases (Neumann *et al.*, 2009), while in PD-GBA lysosomal GCase protein levels and activity are selectively reduced in regions with pronounced alpha-Synuclein accumulation, implying a reciprocal relation between the two proteins (Murphy *et al.*, 2014). Interestingly, GCase expression and enzyme activity is decreased in both PD+GBA and PD-GBA not only in SN but also cerebellum, a structure not primarily involved in PD pathogenesis (Wu and Hallett, 2013). The fact that GCase activity in this work was primarily affected in the cerebellum adds a metabolic dimension to

the role of the cerebellum in dystonia pathophysiology, potentially shared by PD and dystonia.

3.6.3 Dystonia – Parkinson´s disease: a continuum?

Given the above described recurrent overlaps and similarities between dystonia and PD regarding frequency and type of GBA mutations, peripheral and cerebellar enzyme activity pattern, it is important to carefully evaluate possible alternative interpretations of the above results. In patients presenting with dystonia in adulthood, particularly if symptoms start in the limbs, young-onset PD (YOPD) is an obvious differential diagnosis. Around 20% of YOPD patients may initially present with dystonia of variable degree, which might become even more prevalent with advancing disease (Wickremaratchi *et al.*, 2011). The fact that, on careful clinical follow-up, we identified three YOPD cases (see Table 3.5) is in keeping with this. The exclusion of nigro-striatal degeneration in all clinically suspicious dystonia cases (16.4%) supports the interpretation that these cases are unlikely to develop nigro-striatal degeneration. DaT scans had been ordered based on clinical context, i.e. suspicion of bradykinesia, or because of a suggestive family history, and although the evaluation of nigrostriatal degeneration hence was not done systematically in all participants, it was done systematically on clinical suspicion. Furthermore, the time course between symptom onset and DaT scan argues against PD underlying a dystonic presentation, as on average, time to diagnosis in YOPD – in keeping with the literature (Rana *et al.*, 2012) - was 2.3 ± 0.5 years, while the mean disease duration to DaT scan in dystonia was 14.6 ± 11.8 years, making a (late) conversion highly unlikely.

For the large majority of cases in this series we are confident to have excluded an alternative underlying aetiology by exhausting differential diagnostic testing. However, the three cases that developed PD with a latency of 14.0 ± 6.5 years after an initial diagnosis of CD – two of which had a positive family history for CD - warrant attention, as they raise the possibility that there might be a (rare) continuum between dystonia and PD beyond YOPD. In this context, interestingly, olfactory dysfunction, a well-known and prevalent non-motor symptom in PD, has recently been described as a potential novel endophenotype in CD (Marek *et al.*, 2018).

Peculiarly, dystonia has only rarely been described as part of the clinical spectrum in GD so far (Machaczka *et al.*, 2018), which might be in part due to the scarcity of GD itself and the clinical difficulty to detect subtle dystonic features, leading to underreporting (Ebrahimi-Fakhari *et al.*, 2018). Alternatively, dystonia due to lysosomal dysfunction might be distinct from clinical GD. The findings of lysosomal activity pattern in dystonia aligning more closely with the pattern in PD, the fact that no obvious hepatosplenomegaly has been reported in any of the patients in this series, as well as the neuropathology pattern in GD not affecting any of the brain structures classically involved in dystonia (Wong *et al.*, 2004), argues for this.

The late conversion of cervical dystonia to PD has not been reported so far and opens the possibility of a rare continuum between the two conditions. Further studies will have to establish a causal link, in particularly in showing in how far this occurs at a rate above the background, population and age-corrected incidence for Parkinson´s disease.

3.6.4 Limitations and Conclusion

Limitations to this work predominantly apply to the heterogeneous, retrospectively collected cohort of combined dystonia cases: recruitment was performed at a tertiary referral centre`s movement disorder department, most certainly introducing selection bias. Retrospective data collection and the fact that genetic evaluations were not done by standardized means, i.e. a certain sequencing technique or gene panel, and that metabolic tests beyond lysosomal enzyme activities were done on a case-by-case basis, are inherent to such case series, but introduce additional heterogeneity and bias. Similarly, structural (CT, MRI) and functional (DaT Scan) imaging was ordered on the basis of pre-existing documentation and individual presentation. On the other hand, the heterogeneous nature of cases included in this cohort in clinical practice precludes a "one-size-fits-it-all" diagnostic approach due to financial constraints applying to the multitude of theoretically possible aetiologies. The carefully chosen additional diagnostic tests hence reflect the individual clinical presentation. With this in mind, we can confidently exclude most common aetiologies, but possibly cannot exclude additional cases with a rare alternative aetiology of dystonia. Importantly however, this does not impinge on the argument for lysosomal dysfunction in dystonia.

Generally, isolated CD constitutes a different clinical entity from combined dystonia and we want to avoid the impression that we would lump the two together. Nevertheless, the high proportion of *dystonia of unknown origin* among CD and the identification of a similar metabolic pattern and *GBA* mutations in both groups argues for a possible pattern of lysosomal dysfunction in dystonia as an overarching mechanism. As the identification of the disease mechanism has led to the successful

establishment of enzyme replacement (Weinreb *et al.*, 2002) and substrate avoidance therapy in GD (Bennett and Mohan, 2013), the identification of lysosomal dysfunction in dystonia might similarly pave the way for causative therapeutic options in the future.

In summary, through comprehensive clinical, peripheral and central enzyme activity measurements and genetic analysis, this work provides first evidence for a role of lysosomal dysfunction in dystonia pathophysiology. Additional studies are needed to examine co-factors determining GCase activity beyond *GBA* genotype. Although the pattern of decreased lysosomal activity in the brain points at a possible role of the cerebellar dentate nucleus, the mechanism by which lysosomal dysfunction leads to a dystonic phenotype, remains to be established.

4 Chapter II: The role of mitochondrial disease in movement disorders and dystonia

4.1 Statement of Contribution

I developed the project idea, performed the clinical characterization of all involved participants, performed the statistical analysis and interpreted the data. The voxel-based morphometry analysis was done together with Dr. Franz Riederer, who contributed the normative volumetric MRI data.

4.2 Abstract

Background: Mitochondrial disease can present with movement disorders. Data on this entity`s epidemiology, genetics and underlying pathophysiology however is scarce.

Objective: To describe clinical, genetic and volumetric imaging data of patients with mitochondrial disease presenting with movement disorders.

Methods: In this retrospective analysis of all genetically confirmed mitochondrial disease cases from three centres (n=50), the prevalence and clinical presentation of video-documented movement disorders was assessed. Voxel-based morphometry from high-resolution MRI was employed to compare cerebral and cerebellar grey matter volume between mitochondrial disease patients with and without movement disorders and healthy controls.

Results: 15/50 (30%) patients with genetically confirmed mitochondrial disease presented with hypokinesia (parkinsonism 3/15), hyperkinesia (dystonia 5/15, myoclonus 3/15, chorea 2/15) and ataxia (3/15) as movement disorders

presentation. In three cases, mitochondrial disease presented as adult-onset isolated dystonia. In comparison to healthy controls and mitochondrial disease patients without movement disorders, patients with hypo- and hyperkinetic movement disorders had significantly more cerebellar atrophy and an atrophy pattern predominantly involving cerebellar lobule VI and VII.

Conclusion: This series provides clinical, genetic, volumetric imaging and histology data pointing at a major involvement of the cerebellum in mitochondrial disease presenting with hyper- and hypokinetic movement disorders. As a working hypothesis addressing the particular vulnerability of the cerebellum to energy deficiency, this adds substantially to the pathophysiological understanding of movement disorders in mitochondrial disease. Furthermore, it provides evidence that mitochondrial disease can present as adult-onset isolated dystonia.

4.3 Background

4.3.1 Mitochondrial function in health and disease

Mitochondria are highly specialized cell organelles containing complexes I-V of the electron transporter chain, the main source of cellular energy supply. Their function relies on the integrity of both mitochondrial (mtDNA), i.e. extra-nuclear, and nuclear DNA (nDNA) (Alston *et al.*, 2017; Niyazov *et al.*, 2016). Mitochondrial disease (MiD) comprises a variety of multisystem disorders of impaired cellular energy production due to inherited changes in mtDNA and nDNA, or acquired mtDNA damage (Niyazov *et al.*, 2016).

Human mtDNA is generally inherited maternally, and normally contains the same sequence across mitochondria within a given cell, termed homoplasmy. The oxidative environment within the mitochondrion and errors in mtDNA repair mechanisms can lead, however, to different levels of mutant mtDNA, termed heteroplasmy. In general, for mtDNA point mutations heteroplasmy levels of 80-90% (lower levels for deletions) are considered sufficient to cause a relevant deficiency of oxidative phosphorylation, causing cell dysfunction (Chinnery and Hudson, 2013). The prevalence of mtDNA-related disease affecting any organ in the working-age population has been reported around 9 per 100´000 in parts of England (Schaefer *et al.*, 2008).

Ranging from mild to severe and sometimes fluctuating over time in severity, MiD can affect in principle any organ system, although brain and muscle have a particularly high energy demand and hence are frequently/preferentially affected (Muraresku *et al.*, 2018). Clinical presentation in MiD is notoriously heterogeneous (Liang *et al.*, 2014) and neurologically, these conditions can present with the full

gamut of symptoms affecting the central (CNS) and/or peripheral nervous system (PNS) (DiMauro *et al.*, 2013). Although classic neurological phenotypes have been described such as myoclonus epilepsy, ataxia and myopathy with ragged-red fibers (MERFF), mitochondrial encephalomyopathy, lactic acidosis and stroke-like episodes (MELAS), chronic progressive external ophthalmoparesis (CPEO) and others, the diversity of symptoms often impedes early recognition even by skilled clinicians (R. W. Taylor and Turnbull, 2005).

In clinical reality, therefore, the diagnostic process in MiD is rarely straight forward, relying on the interpretation of screening markers (Rodenburg *et al.*, 2013; Suomalainen *et al.*, 2011), metabolic tests (Milone and Wong, 2013; Wong *et al.*, 2010), muscle biopsy and genetic testing (Finsterer *et al.*, 2009). Technological advances in genetic analysis and increasing understanding of the intricate nature of mitochondrial genetics nowadays facilitates the diagnosis of MD, once a clinical suspicion has been established (Alston *et al.*, 2017; R. W. Taylor and Turnbull, 2005; R. W. Taylor *et al.*, 2014). These advances are reflected in a recent consensus statement (Parikh *et al.*, 2015), although not in universally accepted clinical diagnostic criteria (Niyazov *et al.*, 2016), rendering diagnosis relying by and large on previous mitochondrial disease criteria (Bernier *et al.*, 2002; Walker *et al.*, 1996).

Although treatment of MiD still mainly relies on the avoidance of mitochondria-toxic substances, i.e. during general anaesthesia, there are some aetiologies, such as stroke-like episodes in MELAS, during which i.v. L-Arginine can lead to rapid improvement (Muraresku *et al.*, 2018; Nightingale *et al.*, 2016). More recently, hypoxia has been suggested as a treatment option (Jain *et al.*, 2016), although the effect on humans is still under exploration.

4.3.2 Mitochondria in movement disorders

Mitochondrial dysfunction in PD is evident through the effect of mitochondria-toxic substances causing parkinsonism (Betarbet *et al.*, 2000; Langston and Ballard, 1983), Complex I deficiency limited to the SN (Mann *et al.*, 1992; Schapira *et al.*, 1989) and the fact that it has been documented in several familial (Pickrell and Youle, 2015) (Davidzon *et al.*, 2006; Dolhun *et al.*, 2013; Invernizzi *et al.*, 2008; Lesage *et al.*, 2016; Ryan *et al.*, 2015; Schreglmann and Houlden, 2016) but also sporadic PD (Park *et al.*, 2018). Mitochondrial dysfunction hence has a relevant role in PD pathophysiology (also see 1.1.5).

In MiD patients, movement disorders have been described as part of the neurological presentation with a prevalence of 11% in biopsy-confirmed cases (Truong *et al.*, 1990), and 6.2% in genetically or biochemically confirmed cases (Martikainen *et al.*, 2016). Parkinsonism (Baloh *et al.*, 2007; Horvath *et al.*, 2007; Luoma *et al.*, 2004), dystonia (Macaya *et al.*, 1993; Sudarsky *et al.*, 1999), myoclonus (Hanna and Bhatia, 1997; Truong *et al.*, 1990) and less frequently chorea (Caer *et al.*, 2005; Truong *et al.*, 1990) have been described in MiD patients. So far, unspecific white matter and basal ganglia abnormalities have been associated with movement disorders in MiD (Barragán-Campos *et al.*, 2005; Valanne *et al.*, 1998). Repeatedly, ataxia has been reported as one of the most frequent symptoms of MiD - its precise prevalence is however unknown (Zeviani *et al.*, 2012). So far it has been acknowledged that MiD can be the origin of combined dystonia (Truong *et al.*, 1990), whereas MiD has not been reported as the cause for isolated dystonia.

4.3.3 Aim and Hypotheses

MiD as a multi-system disorder can affect different tissue through energy supply failure. Although various movement disorder phenotypes have been described in MiD, their frequency, genetic features and exact clinical characteristics are unknown. Similarly, the anatomical substrate of movement disorders in this patient population has not been well established.

Although dystonia is a relatively frequent presentation in MiD, it is also unclear if it can present as isolated dystonia. Since a large proportion of isolated dystonia cases remain of unknown aetiology even after extensive investigation (Strader *et al.*, 2011), this would open the possibility that mitochondrial dysfunction is a more frequent cause in this patient population.

The aim of this work was hence to explore genetic and clinical characteristics including a cerebral volumetric quantification of genetically confirmed MiD patients with movement disorders to prove the hypotheses that:

a) there is a structural substrate for movement disorders among MiD patients
b) MiD can present as isolated dystonia

4.4 Materials and Methods

Local ethics committees of the participating centres approved this retrospective analysis and all patients provided written informed consent for participation. All patients with genetically confirmed MiD from academic neurology centres in Zurich and St. Gallen / Switzerland and Hamburg / Germany were identified and included. Criteria for MiD confirmation (Bernier *et al.*, 2002) were a) presence of a known disease-causing mtDNA or nuclear mutation, b) deletion of mtDNA with >50% heteroplasmy in muscle tissue or presence of the deletion in blood. Muscle biopsy criteria were a) presence of (if <30 yrs) or >2% ragged red fibres, b) >2% COX-negative fibres, or c) succinate dehydrogenase (SDH) positive/ragged blue fibre staining.

All tissue samples were sampled as part of the routine clinical diagnostic work-up. Open muscle biopsy tissue from a clinically affected muscle (or by default: quadriceps femoris, vastus lateralis) was prepared for histochemistry and snap-frozen according to standard procedures of the participating centre. DNA was extracted from muscle or blood and the mitochondrial genome screened for structural changes by long-range PCR and/or Southern Blot and mutations by single strand confirmation polymorphism (SSCP), restriction fragment length polymorphism (RFLP) and direct Sanger-sequencing or by complete mtDNA sequencing using NGS. In cases of multiple mtDNA deletions, nuclear genes *POLG*, *POLG2*, *c10orf2* and *SLC25A4* were screened. Cases with potential confounding factors inducing secondary mtDNA changes (e.g. necrotizing myopathy, HIV, symptoms compatible with ALS on follow-up, etc., n=7) were excluded from analysis.

For one patient each, post-mortem brain tissue, respectively brain PET imaging collected on clinical grounds was available for analysis.

4.4.1 Estimation of total and cerebellar grey matter volume

Healthy control imaging data comprised of high-resolution 3-dimensional T1-weighted sequences acquired at 3 Tesla from a healthy control (ctrl) population (n=110). MRI data were analysed with Statistical Parametric Mapping (SPM8, http://www.fil.ion.ucl.ac.uk/spm/software/spm8/) running on MATLAB R2008b (Mathworks). High resolution MRI images were segmented into grey matter, white matter and cerebrospinal fluid compartments, using the VBM8 toolbox (http://dbm.neuro.uni-jena.de/vbm/). This includes normalization to MNI space with high-dimensional warping, and smoothing with a 6 mm Gaussian kernel. Grey matter volume was compared between subjects with MiD and the control population using an ANCOVA model with age, gender and total intracranial volume as nuisance variables within SPM to investigate grey matter atrophy patterns. We defined t-contrasts to investigate grey matter decreases and increases in MiD + move vs. ctrl. and MiD - move vs. controls, using a threshold of $p<0.05$ corrected for multiple comparisons with family-wise error at voxel level. Significant clusters were labelled automatically, based on probabilistic cytoarchitectonic maps, using the Anatomy toolbox (Eickhoff *et al.*, 2005) http://www.fz-juelich.de/inm/inm-1/DE/Forschung/_docs/SPMAnatomy Toolbox/SPMAnatomyToolbox_node.html.

In addition, cerebellar grey matter volume was extracted from the normalized grey matter segments using the MarsBaR toolbox (http://marsbar.sourceforge.net/). After scaling for total intracranial volume, cerebral and cerebellar grey matter

volumes were compared between groups using an ANCOVA correcting for age and gender.

4.4.2 Ancillary analyses and statistical analysis

Mounted sections of post-mortem brain tissue available from one patient (no.16) was qualitatively compared to an age-matched control using standard histology staining methods (haematoxylin and eosin & Bielschowsky technique).

Brain FDG-PET imaging data, collected on clinical grounds from one patient (no.7), was qualitatively assessed for changes in regional glucose metabolism.

Comparison of clinical details was done employing two-sided Student`s t-test and χ^2 test where appropriate. Statistical analysis was performed using IBM SPSS 22.0.

4.5 Results

4.5.1 Demographic and clinical details

50 patients with a genetically confirmed diagnosis of MiD (40 from muscle, 9 from blood, 1 from muscle and blood) were identified. Genetic testing revealed single (n=22) and multiple (n=8) large scale mtDNA deletions and point mutations (n=17) (m.3243A>G n=7; m.8344A>G n=4; m.13513G>A, m.1399G>A, m.8993T>G, m.3310C>T, m.3271T>C, m.8356T>C; n=1 each) as well as nDNA mutations (*POLG* n=3, SDHA, SURF1, n=1 each) – two cases had *POLG* mutations and multiple mtDNA deletions, while in the third *POLG* mutation case only nDNA but not mtDNA results were available. For one additional patient with post-mortem brain tissue available for analysis (no.16, no genetics attempted) diagnosis was confirmed by muscle biopsy only. 32 of 50 cases (64%) showed CNS involvement (cognitive, affective, migraine, epilepsy, retinal, vestibular, movement control and sleep abnormalities), while 31 (62%) had PNS involvement (peripheral neuropathy or myopathy).

15 of these 50 patients (30%) had hyper-/hypokinesia or ataxia either as a presenting complaint (n=6, 40%) or during the course of the disease (see Table 4.1). Phenotypes were dystonia (n=5, corresponding to 10% of MiD cases), parkinsonism (n=3, 6%), myoclonus (n=2, 4%), chorea (n=2, 4%) and ataxia (n=3, 6%). Among MiD patients with CNS involvement (n=32), patients with hypo-/hyperkinetic movement disorders more frequently presented cerebellar features (10 of 13, 77%), than patients without (3 of 19, 16%; χ^2 = 11.9, p<0.001). There were no significant differences in demographics (age at onset, sex), other clinical symptoms, or rate of confirmatory muscle biopsy results or laboratory parameters (serum creatine kinase / lactate, CSF lactate and protein) between groups (not shown).

Table 4.1: Clinical, morphological, biochemical and genetic features of mitochondrial disease patients with movement disorders

No	Age (yrs), sex	Movement disorder (age at onset)	Age & initial symptoms	Additional neurological symptoms	Therapy-response	Biopsy finding	Genetic testing	Family history	Imaging
Genetically confirmed MiD									
1	67, m	right-sided Parkinsonism (50yrs)	50yrs, progressive stiffness in right leg	Supranuclear gaze palsy, inattention, positive pyramidal signs, insomnia, panic attacks, restless legs, neurogenic urge incontinence, colour blind for blue (tritanopia)	partial L-dopa response (UPDRS OFF 76, ON 66)	no ragged-red/blue fibres, singular Cox-negative fibres	muscle: 7-9 kB deletion in m.2471.04 (82%)	1 sister mt-genome deletions & POLG1-mutations (p.Y831C, p.E1143G); 2 brothers died aged 30 diagnosed with MS, 1 sister right-sided walking difficulties; many affected family members with restless-legs; mother diabetes mellitus;	MRI: infratentorial atrophy;
2	78, m	axial & symmetrical Parkinsonism, head drop (68yrs)	63yrs, ptosis, ophthalmoplegia;	CPEO, swallowing difficulties	worsening of symptoms on CoenzymeQ 10; positive	ragged-red & ragged-blue fibres, mitochondrial paracristalline inclusions	muscle: 5kB-deletion in m.2203.1 (>95%); POLG1/2,	none	MRI: vascular periventricular leukencephalopathy,

					effect of L-Dopa and dopamine agonists but dyskinesia		ANT1, Twinkle negative		supra- & infratentorial atrophy;
3	73, f	atypical parkisonism, early backward falls (68yrs)	61yrs, stroke-like episodes	partial epileptic seizures, bilateral vestibulo-cochlear dysfunction, retinopathy, symmetrical distal polyneuropathy, psychotic episodes (MELAS)	L-Dopa not tried because of psychotic episodes; Risperdal for psychotic episodes since age 70; seizures: Levetiracetam	not done	blood: m.3243A>G mutation in tRNALeu gene	maternal grandmother blind, mother and siblings diabetes mellitus	MRI: periventricular, microangiopathic changes
4	48, m	chorea (39yrs)	34yrs, CPEO	CPEO, severe sensori-motor polyneuropathy, bilateral vestibulopathy, myopathy with tetraparesis, ataxia, autoskopic hallicinations;	no treatment wanted	ragged-red fibres, paracristallinic mitochondrial inclusions on electron microscopy	muscle: multiple 7-8kb mtDNA deletions (30-50%)	mother coeliac disease, no further family history	MRI: infratentorial atrophy, pontine/medullary hyperintense lesions;
5	69, f	chorea (60yrs)	childhood, limb weakness	polyneuropathy, cerebellar dysarthria, ataxia, saccadic intrusions, night blindness, slowly progressive tetraparesis	-	Cox-negative fibres, mitochondrial accumulation & paracristallinic	muscle: 7-13 kbp deletion in m.2492.01 (62%)	mother and maternal aunt "slow runners", many cases of night blindness in family	MRI: T2-hypointense alterations in SN & Ncl. Ruber; fronto-parietal &

						mitochondrial inclusions			cerebellar/pontine atrophy;
6	56, m	segmental dystonia	41yrs, impaired vision	retinitis pigmentosa, bilateral vestibulo-cochlear dysfunction, shoulder girdle muscle atrophy (NARP)	no treatment for cervical dystonia wanted	pectoralis muscle: normal histology	muscle: mtDNA ATPase6 gene m.8993T>G mutation (75%)	1 brother with delayed developmental milestones, "movement difficulties" and retinitis pigmentosa	MRI: symmetrical cerebellar atrophy;
7	43, m	task-specific dystonic tremor (32yrs)	dystonic tremor, temporary limb rigidity (32 yrs)	Subclinical polyneuropathy, hypometric saccades, waxing and waning of rigidity over time	no improvement with oral anticholinergics	reduced COX-complex enzyme activity in skin biopsy	compound heterozygote deletion (m.845delCT) and missense mutation (m.202D>H) SURF1 gene	daughter died in infancy due to Leigh syndrome, 1 healthy daughter, 1 daughter with delayed developmental milestones and raised serum lactate	brain PET: reduced striatal and cerebellar glucose metabolism;
8	55, w	Writer´s cramp (32yrs; isolated for 17yrs)	32yrs, writer´s cramp	migraine, pancerebellar syndrome with dysmetric saccades, cerebellar dysarthria, axial ataxia, negative myoclonus, segmental dystonia	Botolinumtoxin for writer`s cramp; beneficial effect of clonazepam for myoclonus	not done	blood: m.8344A>G mutation MTTK gene	Son & brother (confirmed MTTK mutation), mother writer´s cramp	not done

				right arm, writer´s cramp (MERRF)					
9	27, m	Writer´s cramp (27yrs)	26yrs, unsteady gait	hypometric saccades, cerebellar dysarthria, positive and negative myoclonus, segmental dystonia with writer`s cramp, limb and axial ataxia	no medication	not done	blood: m.8344A>G mutation MTTK gene	mother & maternal uncle confirmed MTTK mutation, maternal grandmother writer´s cramp	not done
10	59, m	Writer`s cramp (16yrs; isolated for 39yrs)	16yrs, writer`s cramp	sensorineural hearing-impairment, cerebellar dysarthria, discrete limb ataxia, writer`s cramp with motor overflow	no medication	not done	blood: m.8344A>G mutation MTTK gene	sister & nephew confirmed MTTK mutation, mother writer´s cramp	not done
11	19, m	myoclonus (16yrs)	1yr, delayed developmental milestones	stroke-like episodes, psychomotor slowing, dysdiadochokinesia, appendicular ataxia, stimulus-insensitive myoclonus, atactic gait, MELAS	stable with oral L-Arginin	not done	blood: m.3243A>G mutation	one sibling stillbirth at 32 weeks gestation, one maternal greatuncle with epilepsy & mental retardation	MRI: severe cerebellar atrophy, pattern of DWI/ADC-hyperintensity during stroke-like attacks
12	48, m	myoclonus (teenage)	6yrs, writing difficulties	hypometric saccades, proximal muscle atrophy, dysarthrophonia,	not known	paracristallinic inclusions on electron microscopy	blood: m.8356T>C mutation	1 healthy sister	MRI: confluent infra- & supratentori

				positive & negative myocloni, axial & appendicular ataxia, symmetric limb tremor, abasia					al signal alterations
13	51, m	gait ataxia (24 yrs)	24 yrs, gait ataxia	CPEO, cerebellar syndrome with gait ataxia and dysarthria, neuropathy, encephalopathy	worsening of symptoms on Coenzyme Q10	normal	muscle: mtDNA 8900kb deletion (>90%)	father diagnosed with Parkinson`s disease aged 70, first sister diagnosed with Friedreich`s ataxia died aged 27 of epileptic status, second sister died of unknown cause, third sister deaf	not done
14	36, m	limb and gait ataxia (28 yrs)	26 yrs, stroke-like episode	mild limb and gait ataxia, cerebellar speech, complex-partial epileptic seizures, myopathy, amblyopia, vestibulo-cochlear dysfunction, stroke-like episodes, psychomotor slowing, MELAS	stable on regular aerobic exercise and Coenzyme Q10	not done	muscle: m.3243A> G mutation	mother and maternal uncle with type 2 diabetes, deafness & small stature, sister genetically confirmed mtA3243G mutation without symptoms	MRI: multiple temporal and parietal cortical T2- and FLAIR-hyperintensi ties, generalized atrophy
15	19, m	limb ataxia (12 yrs)	8 yrs, Wolf-Parkinson-White syndrome	mitochondrial encephalomyopathy with peripheral wastening, stroke-like episodes,	stable on regular aerobic exercise, L-Arginin, L-	normal	muscle: m.3243A> G mutation	none	not done

				komplex-partial seizures, psychomotor slowing, mild limb ataxia, MELAS	Carnitin, Levetirace-tam, Carba-mazepine				
Biopsy confirmed MiD									
16	65, f	myoclonus (48yrs)	41yrs, gait ataxia	CPEO, sensori-neural hearing loss, cerebellar syndrome, encephalopathy with generalized tonic-clonic seizures, positive pyramidal tract signs, axonal polyneuropathy, myopathy, MERRF	benefit from clonazepam for myoclonus	ragged-red fibres	no genetics attempted	brother died aged 20 of epileptic status and neurological disorder of unknown origin	MRI: microvascul ar changes Caudate nucleus, generalized atrophy

Table 4.2: Demographic and clinical features of subjects with high-resolution MRI included in voxel-based morphometry analysis (# referring to original case number on

Table 4.2).

Case #	age (yrs), sex	age & initial symptoms	neurological symptoms	muscle biopsy	Tissue, genetic result (heteroplasmy in %)	family history	laboratory / imaging results
MiD patients *with* movement disorders							
1	67, m	50yrs, progressive stiffness in right leg	Parkinsonism, right-sided, supranuclear gaze palsy, inattention, positive pyramidal signs, insomnia, panic attacks, restless legs, neurogenic urge incontinence, colour	normal, no ragged-re/blue fibres, singular Cox-negative fibre	muscle: 7-9 kB deletion in m.2471.04 (82%)	1 sister mt-genome deletions & POLG1-mutations (p.831Y>C, p.1143E>G); 2 brothers died aged 30 diagnosed with MS, 1 sister right-sided walking	MRI: infratentorial atrophy;

			blind for blue (tritanopia)			difficulties; many affected family members with restless-legs; mother diabetes mellitus;	
2	78, m	63yrs, ptosis, ophthalmoplegia;	axial & symmetrical Parkinsonism, head drop, CPEO, swallowing difficulties	ragged-red & ragged-blue fibres, mitochondrial paracristallinie inclusions	muscle: 5kB-deletion in m.2203.1 (>95%); POLG1/2, ANT1, Twinkle negative	none	MRI: vascular periventricular leukencephalopathy, supra- & infratentorial atrophy;
3	73, f	61yrs, stroke-like episodes	Parkinsonism, atypical, early backward falls, partial epileptic seizures, bilateral vestibulo-cochlear dysfunction, retinopathy, symmetrical distal polyneuropathy, psychotic episodes (MELAS)	not done	blood: m.3243A>G mutation in tRNALeu gene	maternal grandmother blind, mother and siblings diabetes mellitus	MRI: periventricular, microangiopathic changes
5	69, f	childhood, limb weakness	Chorea, polyneuropathy, cerebellar dysarthria, ataxia, saccadic intrusions, night blindness, slowly progressive tetraparesis	Cox-negative fibres, mitochondrial accumulation & paracristallinic mitochondrial inclusions	muscle: 7-13 kbp deletion in m.2492.01 (62%)	mother and maternal aunt "slow runners", many cases of night blindness in family	MRI: T2-hypointense alterations in Substantia nigra & Ncl. Ruber; fronto-parietal & cerebellar/pontine atrophy;

11	19, m	1yr, delayed milestones	Myoclonus, stimulus-insensitive, stroke-like episodes, psychomotor slowing, dysdiadochokinesia, appendicular ataxia, atactic gait	Not done	blood: m.3243A>G mutation	one sibling stillbirth at 32 weeks gestation, one maternal greatuncle with epilepsy & mental retardation	MRI: severe cerebellar atrophy, pattern of DWI/ADC-hyperintensity during stroke-like attacks
MiD patients *without* movement disorders							
	23, f	15 yrs, migraine	migraine with aura, epilepsy with generalized and focal seizures, visual hallucinations, sensorineural hearing loss, myalgia	not done	muscle: POLG1 n.1399G>A mutation	none	MRI: bilateral posterior diffusion restriction
	45, f	4 yrs, sensorineural hearing loss	progressive encephalopathy with cognitive impairment, sensorineural hearing loss, urge incontinence, polyneuropathy with sensory ataxia, proximal myopathy	COX-negative, ragged red & blue fibres	muscle: m.8344A>G (24-40%)	mother head tremor, maternal uncle generalized muscle wastening	MRI: brain stem atrophy
	71, m	64 yrs, paraesthesia	demyelinating sensory-motor polyneuropathy, myopathy	normal, no ragged-re/blue fibres	muscle: 12kbp deletion (95%)	1 brother depression and suicide	MRI brain: normal

18, m	10 yrs, CPEO	CPEO, myopathy	not done	muscle: homozygote POLG n.467A>T mutation	none	MRI brain: diffuse mild white matter hyperintensities
51, m	43 yrs, ptosis	CPEO, migraine, mild encephalopathy	ragged-red fibres, COX-negative fibres	blood: m.3243A>G mutation	none	raised CK, MRI brain: mild hypertrophy of extra-ocular muscles; normal brain parenchyma
64, m	59 yrs, exercise intolerance	myopathy, mixed sensori-motor axonal polyneuropathy, sensorineural hearing loss, learning difficulties	COX-negative fibres	muscle: multiple 7-16kbp deletions (60%)	none	raised CK, HbA1c 6.1%; brain MRI: mild vascular lesions
64, f	60 yrs, myopathy	proximal myopathy, dysexecutive cognitive impairment	COX-negative fibres, paracristallinic inclusions on electron microscopy	muscle: homoplastic, 3-13kbp deletions (>95%)	son spinal muscular atrophy, daughter coeliac disease, mother died of multiple myeloma	mildly raised serum lactate, brain MRI normal
86, f	68 yrs, myopathy	migraine without aura, frontal behaviour, retinopathy, proximal myopathy	ragged red fibres, COX-negative fibres	muscle: 4,5-10kbp deletions (81-88%)	daughter similarly affected	brain MRI: mild white matter hyperintensities

4.5.2 Grey matter quantification

All identified MiD patients with available high resolution structural T1-weighted MRI scans were included for blinded analysis (n=13, MiD with movement disorders (MiD + move) n=5, MiD without movement disorders (MiD – move) n=8). MiD + move vs. MiD – move patients did not differ in age and sex, as well as clinically as to PNS (χ^2 = 0.33, *ns*) or CNS involvement (χ^2 = 0.68, *ns*).

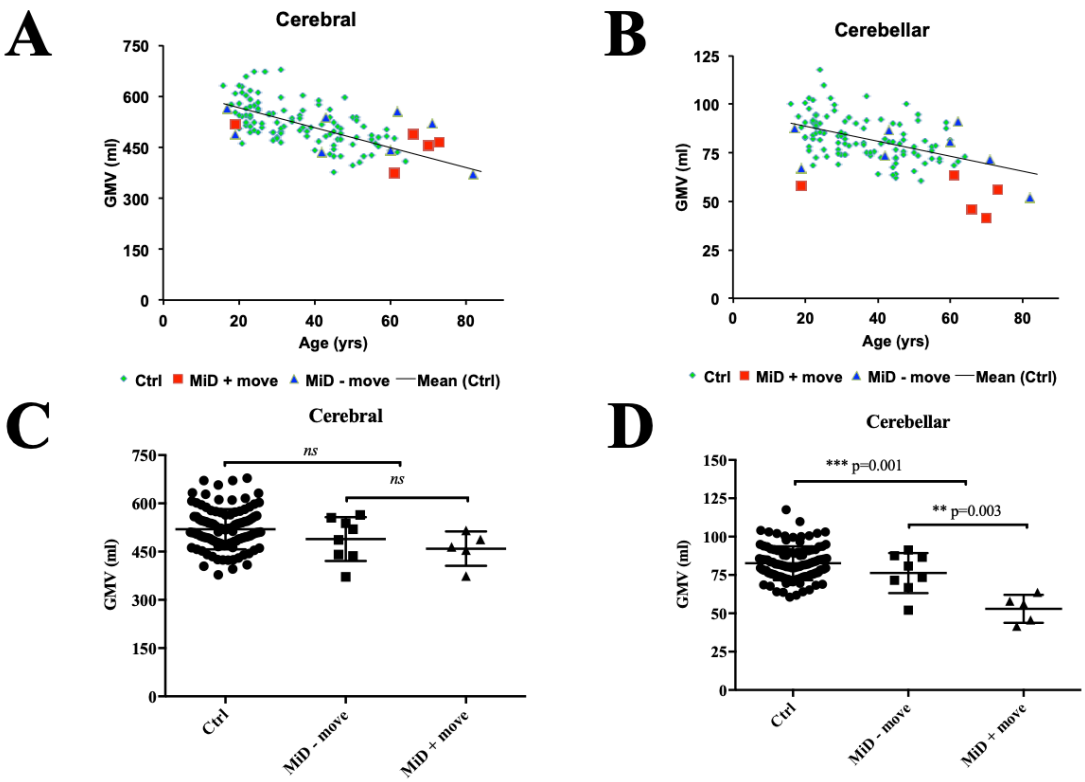

Figure 4.1: Volumetric quantification of supra- and infratentorial atrophy in mitochondrial disease patients with movement disorders:

Cerebral (A, B) and cerebellar (C, D) grey matter volume (GMV) in healthy controls (Ctrl, green rhomb, n=110) and subjects with mitochondrial disease with (MiD + move, red rectangle, n=5) and without movement disorders (MiD – move, blue triangle, n=8). Grey matter volume was scaled to total intracranial volume. Scatter plots (A, B) of GMV against age in years include a regression line of control subjects. P values in the scatter-box plots (C, D) represent results from an ANCOVA after correction for age and gender.

After correction for age and sex via multiple linear regression, there was no relationship between cerebral GMV and the presence of MiD (P=0.63). Similarly, after correction for age and sex there was no association of cerebral GMV with the presence of movement disorders among subjects with MiD (P=0.84) (see Figure 4.1 A, C).

Conversely, after correcting for age and sex, cerebellar GMV significantly correlated with the presence of MiD ($F_{(1,119)}$=11.74; P=0.001) and the presence of movement disorders ($F_{(1,9)}$=16.69; P=0.003; see Figure 4.1 B, D).

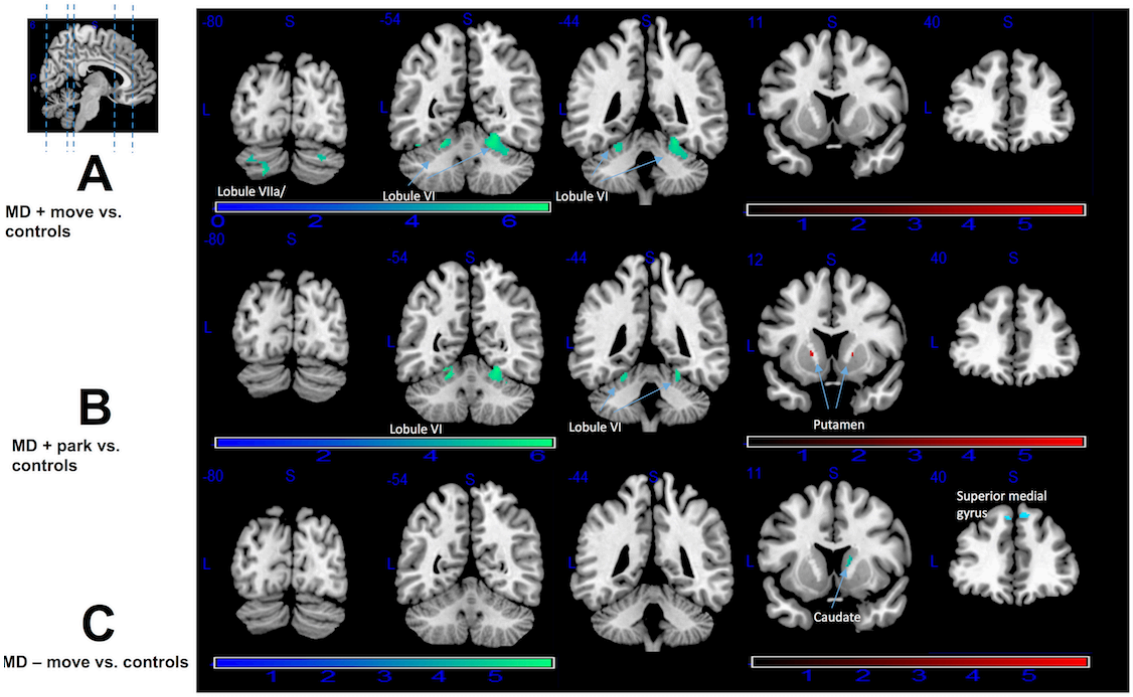

Figure 4.2: Whole brain GMV analysis in mitochondrial disease patients with movement disorders:

Voxel-based morphometry revealed significant clusters of atrophy predominantly in cerebellar lobules VI and VII in mitochondrial disease patients with movement disorders (A, n=5). A similar pattern of cerebellar atrophy was also found in the subgroup of mitochondrial patients with a parkinsonian phenotype (B, n=3), which in addition show significant volume

increase in the putamen. In contrast, patients with mitochondrial disease without movement disorders (C, n=8) showed no cerebellar atrophy but reduced grey matter in the superior medial gyrus and caudate when comparing to controls. All results are significant at p<0.05 corrected for multiple testing. Colour bars indicate T-scores for clusters of reduced (cold colours) or increased (hot colours) grey matter in patients with mitochondrial disease compared to controls, superimposed on the MRI of a healthy subject. The blue number on the left upper side of coronal section indicates the level of section (Montreal Neurological Institute coordinate y), L indicates left, S indicates superior.

Whole brain voxel-wise analysis revealed a cerebellar atrophy pattern in MiD + move (n=5; Figure 2.1.1A), but not MD - move (n=8; see Figure 4.2 A) when compared to controls (all p<0.05, corrected for multiple testing). This pattern affected mainly lobule VI bilaterally and lobule VIIa/Crus II on the left (see Table 4.3). A similar cerebellar atrophy pattern was seen in a subset of MiD patients with parkinsonism (n=3; see Figure 4.2 B), who also showed a grey matter increase in the putamen bilaterally. In comparison to controls, the MiD – move group showed atrophy in the right and left superior medial gyrus, as well as in the right caudate (see Figure 4.2 C).

Table 4.3: Significant areas of grey matter volume changes assessed by voxel-based morphometry analysis:

Results are presented by group comparison and cluster size. Cluster size refers to the number of contiguous voxels in which a significant p value was achieved. Voxel T value refers to the maximal T score within each cluster. Abbreviations x, y, z refer to Montreal Neurological Institute (MNI) spatial coordinates.

Controls > MiD + move						
Region	cluster	p	T	x	y	z
R cerebellum, lobule VI	1477	0.000	6.76	24	-53	-15
		0.002	5.73	32	-57	-27
		0.002	5.63	32	-48	-26
L cerebellum, lobule VIIa, Crus II	207	0.000	6.47	-32	-75	-44
L cerebellum, loble VIIa Crus I		0.003	5.52	-27	-78	-36
L cerebellum, lobule VIIa Crus I		0.010	5.24	-36	-77	-35
L cerebellum, lobule VI	56	0.000	6.21	-23	-65	-15
		0.038	4.89	-21	-75	-17
L cerebellum, lobule VI	310	0.000	6.14	-21	-54	-20
		0.001	5.77	-24	-45	-21
L fusiform gyrus	30	0.001	5.76	-42	-56	-21
R cerebellum, lobule VIIIa (hem)	53	0.002	5.72	24	-65	-51
L middle temporal gyrus	35	0.003	5.58	-62	-18	-8
R cerebellum, lobule VIIa Crus I	61	0.004	5.46	27	-81	-32
Controls < MiD + move						
	none					
Controls > mito - move						
Region	Cluster	p	T	x	y	z
L superior medial	133	0.000	7.29	-6	50	41
L superior medial		0.000	6.39	-6	42	47
L superior medial		0.001	5.82	-6	56	30
R superior medial	188	0.000	6.69	9	44	47
R superior medial		0.000	6.46	9	54	35
R superior medial		0.006	5.38	9	59	26
R caudate	68	0.000	6.06	12	8	14
Controls < MiD - move						
	none					
Controls > MiD + park						
Region	Cluster	p	T	x	y	z
R cerebellum, lobule IV	731	0.000	6.23	24	-54	-15

R cerebellum, lobule V		0.002	5.64	24	-44	-17
R cerebellum, lobules I-IV		0.009	5.30	27	-32	-23
L cerebelllum, lobule VI	242	0.001	5.99	-20	-53	-18
L cerebellum, lobule VI		0.006	5.39	-23	-63	-15
		0.008	5.32	-24	-44	-20
Controls < MiD + Park						
L putamen	39	0.001	5.88	-15	9	2
R putamen	18	0.003	5.55	17	11	2
L putamen	35	0.004	5.50	-32	-12	-3

4.5.3 Histology and PET imaging data

Analysis of the metabolic activity pattern by brain FDG-PET imaging in case no.7 with task-specific dystonia revealed decreased brain glucose metabolism in the cerebellar cortex as well as striatum (see Figure 4.3).

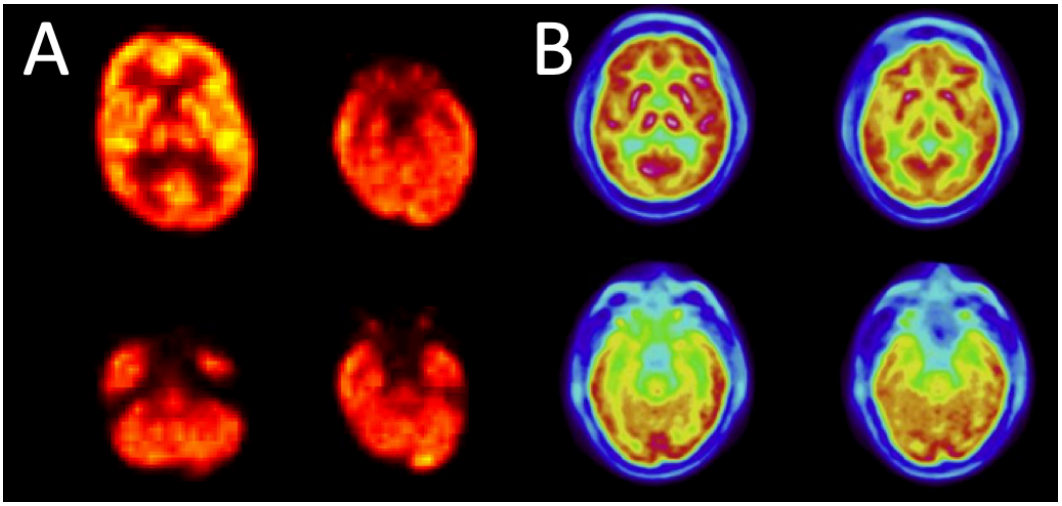

Figure 4.3: Decreased glucose metabolism in striatum and cerebellar cortex in dystonia due to mitochondrial disease:

Routine clinical brain FDG-PET scan from case no.7 presenting with a task specific, isolated dystonia, showing decreased glucose metabolism in striatum and cerebellar cortex (A) in comparison to a healthy control (B). Note that colour settings for image A ("lava") and B ("rainbow") differ, but nontheless illustrate different binding intensities.

Histological analysis of the formalin-fixed brain (1169g) of case no.16 with myoclonus revealed pronounced neuronal loss in the cerebellar dentate nucleus (see Figure 4.4) and to a lesser extent in substantia nigra pars compacta, as well as in the oculomotor and inferior olive nucleus (not shown). Otherwise, qualitative analysis of basal ganglia, cortical structures, locus coeruleus and cerebellar Purkinje, molecular and granular cell layers revealed no abnormalities.

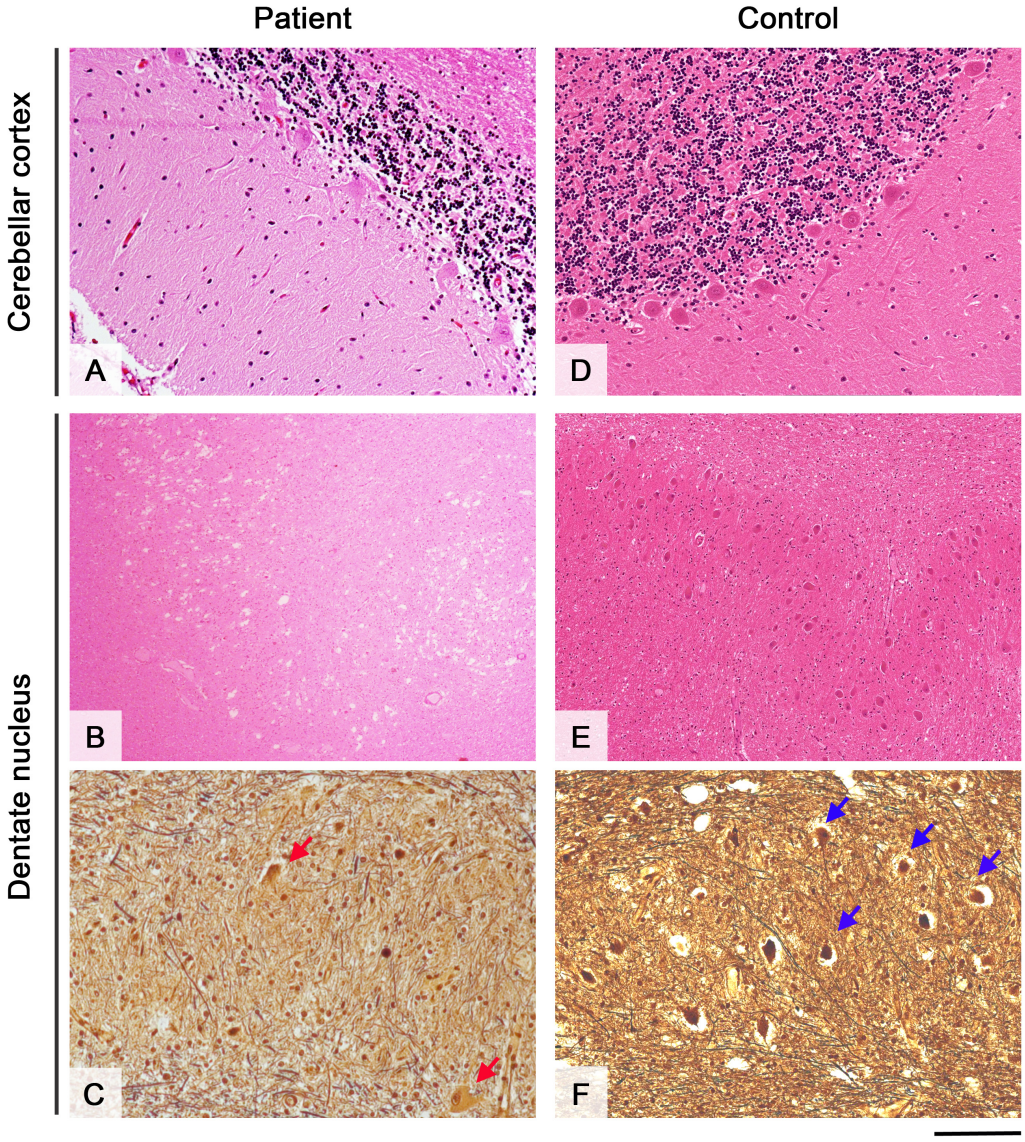

Figure 4.4: Pronounced cell loss in cerebellar dentate nucleus with relatively preserved cortical architecture:

Post mortem histology in case no. 13 (A, B and C) in comparison with age-matched control (D, E and F). The cerebellar cortical cytoarchitecture is relatively well preserved (A), while the cerebellar dentate nucleus in contrast shows marked neuronal loss and spongiosis (B) – this is accentuated in the high-power view (red arrows highlight some of the remaining neurons, C). In the control tissue neurons are frequent (blue arrows highlight some of the neurons) without apparent gliosis (F). The images A, B, D and E are stained with routine haematoxylin and eosin. The images C and F are stained with Bielschowsky technique. Scale bar: 200μm in A and D, 270μm in B and E, 100μm in C and F.

4.6 Discussion

4.6.1 Prevalence of movement disorders in mitochondrial disease

This large series of genetically confirmed, video-documented MiD cases with detailed clinical information shows that movement disorders are frequent clinical presentations of this disorder. While the 30% prevalence rate is higher than previously reported (Martikainen *et al.*, 2016; Truong *et al.*, 1990), no study reports population-based cross-sectional data and sampling and referral bias most likely explain this difference. In addition, the higher prevalence in the present study is due to the novel observation that MiD can present as isolated dystonia as well as the inclusion of ataxia as a form of movement disorder. The relative prevalence of movement disorders among MiD patients has been reported to be most frequent for dystonia, with parkinsonism, myoclonus and chorea following (Caer *et al.*, 2005; Hanna and Bhatia, 1997; Horvath *et al.*, 2007; Sudarsky *et al.*, 1999; Truong *et al.*, 1990). Our results are in keeping with that and suggest that dystonia in its´ isolated or combined form is present in up to 10% of adult MiD patients.

4.6.2 Characteristic clinical features

Dystonia is a well-established presentation in MiD (Hanna and Bhatia, 1997; Truong *et al.*, 1990). It is the most common movement disorder presentation in childhood onset Leigh`s syndrome (Finsterer, 2008; Macaya *et al.*, 1993) and has been described as a feature in Leber`s hereditary optic neuropathy (LHON) (Hanna and Bhatia, 1997). In our cohort, the majority of dystonia cases were task-specific (cases no.7-10). Cases no.8-10 with a familial m.8244A>G mutation did not present as MERRF but as a pan-cerebellar syndrome with writer's cramp. Importantly, cases

no.8 and 10 initially presented as isolated writer's cramp for up to 39 years duration before developing additional symptoms aiding testing towards a mitochondrial cause. Even more strikingly, case no.7 never developed clinically relevant additional features and was only tested and identified positive for MiD because of a suggestive family history. These three cases (no.7, 8 & 10) present first evidence to suggest that MiD can present as isolated dystonia. In analogy, 9% of patients with ataxia due to MiD have recently been found to present with isolated ataxia (Bargiela *et al.*, 2015). Of clinical relevance, this observation opens the possibility that MD might be the cause of isolated dystonia cases so far labeled as sporadic or idiopathic.

Parkinsonism in MD has been described with mutations in nuclear genes *POLG* (Brandon *et al.*, 2013; Hudson *et al.*, 2007; Luoma *et al.*, 2004; Mukai *et al.*, 2013), *OPA1, MPV17* and *TWINKLE* (Tranchant and Anheim, 2016). Less frequently it has been associated with (multiple) mtDNA deletions (Casali *et al.*, 2001; Horvath *et al.*, 2007; Mancuso *et al.*, 2008), as in cases no.1 & 2. Case no.3 is the first patient with an m.3243A>G mutation and parkinsonism reported. Clinically, however, parkinsonism in this series often included atypical features, such as marked rigidity, positive pyramidal signs, marked neuropsychiatric involvement, CPEO or stroke-like episodes 5-7 years before the onset of bradykinesia. In case no.3, vertical saccades were preserved years after postural control had been lost, deviating from e.g. a classic presentation of progressive supranuclear palsy. As in case no.2, parkinsonism due to MiD might respond moderately to dopaminergic medication and may develop motor fluctuations in due course (Martikainen *et al.*, 2016).

Chorea has been reported in Leigh`s syndrome in children but only very rarely described as a feature of adult onset MiD. It is of note that both chorea cases in this series had marked polyneuropathy, as three of the six previously described chorea

MiD cases with detailed clinical description (Caer *et al.*, 2005; Jackson *et al.*, 1995; Nakagaki *et al.*, 2005; Nelson *et al.*, 1995; Truong *et al.*, 1990), pointing to a potential pseudoathetotic rather than a choreatic aetiology *sensu strictu*. Clinically, proximal choreatic movements (e.g. of the tongue) are however suggestive of true chorea.

Myoclonus classically has been reported in the context of MERRF (Hanna and Bhatia, 1997; Truong *et al.*, 1990), as in case no.13. Case no.11 is the first description of myoclonus caused by the common mt.3243A>G mutation.

Ataxia is known to be amongst the most frequent symptoms in MiD, associated with many different genetic mutations causing central, i.e. cerebellar, sensory or combined ataxia (Zeviani *et al.*, 2012).

Fluctuations in symptom severity might help to differentiate movement disorders due to MiD from a neurodegenerative etiology, such as with rigidity in case no.8. Although this has been described before in Leigh`s syndrome (Debray *et al.*, 2007) putative mechanisms for this *waxing and waning* such as changes in heteroplasmy levels over time are speculative and so far elusive.

4.6.3 Cerebellar involvement in mitochondrial disease and associated movement disorders

The present volumetric quantification substantiates the notion that cerebellar atrophy is among the most frequent MRI abnormalities in MiD (Barragán-Campos *et al.*, 2005; Scaglia *et al.*, 2005) and associates this for the first time with the presence of movement disorders. In this MiD cohort, hypo-/hyperkinetic movement disorders were associated with significantly more cerebellar symptoms while no other clinical pattern could be identified. The single post-mortem histology

demonstrating dentate nucleus cell loss with otherwise preserved anatomy, including cerebellar Purkinje and granular cell layer (see Figure 4.4), lends further support to the above observation, but deviates from the notion that cortical myoclonus is primarily associated with Purkinje cell loss (Ganos *et al.*, 2014). Similarly, the single brain FDG-PET is further circumstantial functional imaging evidence of decreased glucose metabolism in cerebellar cortex and striatum in MiD patients with MD (see Figure 4.3).

Although our results suggest a predominant involvement of cerebellar lobules VI and VII, we do not propose that our limited number of cases is sufficient to establish this as a definitive pattern. Nevertheless, it is an intriguing observation, as cerebellar lobule VI has been found to be involved not only in human sensorimotor integration and movement control in functional imaging (Stoodley and Schmahmann, 2009) but also direct cortical stimulation studies (Mottolese *et al.*, 2013). Beyond that, atrophy of lobule VI, respectively lobule VIIa has been reported in PD (Planetta *et al.*, 2014) and early manifest Huntington`s disease (Wolf *et al.*, 2015), while fMRI hypo-metabolism in lobule VI has been reported in both dystonia (Filip *et al.*, 2017) and the parkinsonian variant of multiple system atrophy (Planetta *et al.*, 2014) as well as in a motor timing trial in PD (Husárová *et al.*, 2014). The putaminal volume increase in the small subgroup of MiD parkinsonism cases confirms additional basal ganglia involvement in this group and is in line with findings in PD (Jia *et al.*, 2015; Reetz *et al.*, 2009). The etiology of this volume increase remains to be clarified but has been interpreted as a potential compensatory mechanism (Jia *et al.*, 2015). While the current understanding of movement disorder pathophysiology in MiD hinges in large parts on the basal ganglia (Martikainen *et al.*, 2016; Truong *et al.*, 1990), the present report establishes an association of movement disorders in MiD

with cerebellar dysfunction and atrophy. This significantly adds to the known neuroimaging changes in MiD with movement disorders, which predominantly described frequent but unspecific white matter and basal ganglia changes (Barragán-Campos *et al.*, 2005; Martikainen *et al.*, 2016; Valanne *et al.*, 1998).

As individual cases also showed variable degrees of supratentorial (no.2, 12, 14) or pontine (no. 5) brain atrophy, we cannot exclude additional, less consistent patterns of cortical or subcortical atrophy in MiD patients with or without movement disorders. The limited number of data points in this study however discourages from drawing additional conclusions.

4.6.4 Pathophysiological considerations

The role of the cerebellum in movement disorders and its` connection to the basal ganglia is a field of continuing development (Sadnicka *et al.*, 2012). Anatomically, a topographical, di-synaptic, reciprocal connection from the subthalamic nucleus to the cerebellar cortex and cerebellar dentate nucleus to the striatum links both structures (Bostan *et al.*, 2010). Evidence for a functional role of the cerebellum has been collected most consistently for dystonia - data from expression levels of genes involved in monogenic forms of dystonia, mechanisms in animal models of the disease, human electrophysiology and structural and functional imaging point at a cerebellar involvement in addition to changes in the basal ganglia and motor cortex (Filip *et al.*, 2013; Sadnicka *et al.*, 2012; Shakkottai *et al.*, 2016). Similarly, myoclonus has been associated with cerebellar dysfunction in a number of conditions (Ganos *et al.*, 2014). A loss of inhibitory cerebellar control over the cortex has been proposed for both etiologies (Ganos *et al.*, 2014; Shakkottai *et al.*, 2016). In both

Huntington´s disease (Feigin *et al.*, 2007) and PD functional imaging data suggests cerebellar hyper-metabolism (Wu and Hallett, 2013), which has been interpreted as a compensatory mechanism to balance basal ganglia dysfunction (Rees *et al.*, 2014; Wu and Hallett, 2013).

Metabolic changes due to MiD mainly affect energy-intensive tissue and among neuronal tissue the cerebellum with its large Purkinje cells is particularly prone to associated vulnerability (Zeviani *et al.*, 2012). Thus, cerebellar hypo-metabolism and dysfunction - ultimately leading to cerebellar atrophy – might be viewed as a putative unifying pathophysiological mechanism of different movement disorders in MiD.

4.6.5 Changes in mitochondrial disease without movement disorders

Whereas our analysis found no significant cerebellar changes in the group of MiD patients without movement disorders, atrophy in the bilateral superior medial gyrus and right caudate nucleus were present. Both structures have been implicated in working memory (Jia *et al.*, 2015) and other cognitive domains (Bauer *et al.*, 2015) but detailed neuropsychometry data to substantiate this possible relationship was unfortunately not available in our cases.

4.6.6 Limitations and Conclusion

MiD is a rare disorder in clinical neurology practice, while the estimated prevalence of clinically manifest mtDNA disease across medical specialties among adults of working age has been reported at 9.2 per 100´000 in the North East of England (Schaefer *et al.*, 2008). The referral basis of participating centres does not allow

excluding potential selection bias in this work. We also acknowledge that the retrospective nature of our analysis as well as the limited number of subjects from each pheno- and genotype hamper the generalizability of our findings and warrant prospective verification. In the future one would like to combine structural and functional imaging data from a larger, multicentre data set of MiD patients with movement disorders to further delineate the role of basal ganglia and cerebellar structures. Furthermore, our data do not allow drawing conclusions on the functionality of the nigro-striatal system in parkinsonian patients described in this report as DAT-SPECT imaging was not available.

Another limitation was the lack of high-resolution imaging data from healthy control subjects above the age of 62, while 5 of the MiD subjects included in the VBM analysis were in this age range. Extrapolation of results beyond the margins of control data is generally susceptible to error. Given the clear difference between cerebral and cerebellar volume according to control/patient cohort on the VBM plots over age, the effect however was judged consistent and substantial enough to draw the above conclusions.

Nevertheless, this report is one of the largest series of genetically confirmed MiD patients with movement disorders and the detailed clinical, as well as genetic and imaging data presented provide interesting pilot data to guide future studies. It establishes MiD as a potential cause of isolated dystonia so far classified as idiopathic, and strengthens the link between cerebellar involvement and movement disorders in MiD.

5 Chapter III: Parkinson´s Disease and the Role of genetic determinants of Ageing

5.1 Statement of Contribution

I contributed project idea, performed all MMQ-PCR and Southern blots in the laboratory of Dr Kazu Tomita, at the Cancer Institute, O´Gorman Building, UCL, London, performed all analyses and wrote the manuscript.

Demis Kia performed the Mendelian Randomization analyses on the IPDGC, and Sandeep Grover on the COURAGE-PD data sets.

5.2 Abstract

Background: Age is the most consistently described risk factor for PD. Shortening of telomere length with advancing age, arguably a measure of 'biological' age, is a known phenomenon and epidemiologically correlated with age-related disease.

Objective: To explore a possible association between the genetic predisposition for telomere length, brain telomere length, advancing age and PD risk.

Methods: A Mendelian Randomisation analysis was applied to PD GWAS summary statistics of an exploratory (IPDGC 2014: 13,708 cases, 195,282 ctrl) and two independent confirmation case-control datasets (IPDGC 2019: 37.688 cases, 1.474.079 ctrl; COURAGE-PD: 12,576 cases, 9,565 crtrl). Telomere length was measured by telomere Southern blot for distribution (n=6) and Monochrome Multiplex-qPCR for mean telomere length in post-mortem putamen and spleen (n=98 donors: 81% male; age 20 to 79 years; mean: 52.0 ± 13.4 years), "region matched" brain regions (n=10; 100% male, mean: 55.3 ± 1.95 years) and "SN vs.

CRBL" brain regions (n=10; 100% male, mean: 52.9 ± 4.15 years) from corresponding donors.

Results: The increased odds ratio to develop PD of 1.29 (95% CI: 1.05-1.58) per standard deviation increase in leucocyte telomere length discovered in the exploratory dataset did not replicate in either confirmation datasets. There was a highly significant negative correlation between telomere length and age in both spleen and putamen, indicating age-related telomere attrition in the human striatum. Telomere length was also found to be brain region-specific due to differences in the expression levels of genes involved in telomere length regulation.

Conclusion: This work found no convincing evidence for a causal association between PD risk and genetically determined telomere length, a cellular marker of ageing. The telomere length quantification results, however, indicate that telomere length in the putamen physiologically shortens with advancing age and is regulated differently to other brain regions. Telomere length attrition with age is a so far unique observation in the human brain, pointing at a selective age-related vulnerability of the nigro-striatal network, possibly explaining age-related conditions with a strong pathophysiological connection to the striatum, such as PD.

5.3 Background

5.3.1 Parkinson´s disease and Aging – Epidemiology

Ever since the first description of the condition (Parkinson, 1817), the role of advancing age has been described as the most consistent factor contributing to an individual´s risk of developing sporadic PD (Pringsheim *et al.*, 2014). Sporadic PD is very rarely diagnosed before the age of 50 (Van Den Eeden *et al.*, 2003). More detailed, its annual incidence in both sexes has been reported to increase from 3.1 per 100 000 in the fourth decade of life to 17.4 per 100 000 (5th decade), 52.5 per 100 000 (6th decade) and 93.1 per 100 000 (7th decade) in a large, community-based cohort (Bower *et al.*, 1999; 2000). Regarding the absolute incidence rate this might even be an underestimation, as door-to-door prevalence studies have been reporting consistently 39-53% higher incidence rates than record-based studies (Benito-León *et al.*, 2004; de Lau *et al.*, 2004). Similarly, a meta-analysis on all published door-to-door / population-based random sampling assessments reported prevalence rates to increase from 41 per 100`000 (4$^{th}$ decade), 107 per 100`000 (5th decade), 428 per 100`000 (6$^{th}$ decade), 1078 per 100`000 (7th decade) to 1903 per 100`000 above 80 years of age (Pringsheim *et al.*, 2014). The association with age even entered clinical jargon, as patients presenting with suggestive symptoms and signs before 20 or 45 years of age are commonly labelled as "juvenile PD" and "early/young-onset" (YOPD) respectively (Muthane *et al.*, 1994; Schrag and Schott, 2006; Wickremaratchi *et al.*, 2009).

Of clinical relevance, younger age at onset of PD has been described to not only show higher rates of dystonic symptoms at onset, a potentially slower disease progression but also influence the response to medication, reflected in a higher rate of dyskinesia

on dopaminergic treatment (Wickremaratchi *et al.*, 2009). Similarly, the pattern of dopaminergic terminal loss throughout putamen and caudate nucleus seem to be different, with YOPD patients displaying less denervation of the caudate nucleus in relation to the putamen (Liu *et al.*, 2015).

The relationship between aging and PD therefore is well established and intriguing, while the causative links remains unknown.

5.3.2 Parkinson´s disease and Ageing - Pathophysiology

Brain volume, weight and cell number are considered greatest in early teenage years, followed by only minor loss over the following 5 decades of life and a 2-3% loss of brain weight per decade between the ages of 50-90 (Stark and Pakkenberg, 2004). The CA1 and subiculum subdivisions of the human hippocampus have been shown to exhibit a significant neuronal loss with ageing, estimated at 67% (CA1) and 32% (subiculum) between the ages of 16 and 99 years (Simić *et al.*, 1997). In comparison, a stereology study estimated the degree of neuronal loss in the neocortex at approximately 10% between 20 and 90 years of age, only (Pakkenberg and Gundersen, 1997). In the subtantia nigra pars compacta, the anatomical structure of salient pathophysiological changes in PD, a relevant proportion (around 30%) of healthy aged individuals show mild to severe loss of dopaminergic neurons without clinical signs of parkinsonism, as reported in a large histopathology series of 750 elderly individuals (Buchman *et al.*, 2012). Stereological histology work in humans does support the notion that continuous cell loss with age happens at a substantially higher rate (5-10% per decade) to pigmented, dopaminergic neurons than to other neuronal populations (Fearnley and Lees, 1991; Stark and Pakkenberg, 2004).

However, the pattern of midbrain dopaminergic cell loss appears to differ between normal ageing, affecting preferentially dorsal tier neurons, and PD, affecting preferentially ventral tier neurons (Fearnley and Lees, 1991; Gibb and Lees, 1991). Based on additional observations of decreasing cell counts in dopaminergic cell populations in the ventral tegmental or retro-rubral area with age, it has been argued that dopaminergic cells might be particularly prone to age-related damage in general (Reeve *et al.*, 2014). Hence, SNpc neurons have received most attention when trying to explain the role of ageing in PD (reviewed in (Collier *et al.*, 2017; Reeve *et al.*, 2014)).

On a cell-level, certain characteristics of the dopaminergic midbrain neuron have been argued to be responsible for this particular vulnerability: In contrast to most other neuronal populations, dopaminergic midbrain neurons display continuous endogenous 2-4Hz pace-making activity relying on L-type Cav1.3 subunit Ca^{2+}-channels (Surmeier, 2007). Activity of these channels is thought to contribute to dopamine metabolism and the cells` reliance on it increases with age - it has been shown that blocking them by e.g. Isradipine protects dopaminergic neurons from cell loss by reverting back to a juvenile pacing mechanism (Chan *et al.*, 2007).

Dopamine metabolism is similarly a detrimental factor, as monoamine oxidase creates a number of oxidative species during dopamine synthesis, contributing to mitochondrial damage (reviewed in (Sulzer, 2007)).

Iron-metabolism is another contributing factor, as iron and neuromelanin are particularly abundant in the SN and the Locus coeruleus (LC) (Acosta-Cabronero *et al.*, 2016). Brain tissue physiologically contains iron, >90% of which is stored in the form of ferritin, and the basal ganglia are particularly rich in iron. Imaging studies have shown that ferritin accumulates throughout the basal ganglia in a linear

fashion as a function of age (Bartzokis *et al.*, 2007), with higher inter-individual variability from the age of 50 onwards (Acosta-Cabronero *et al.*, 2016). Neuromelanin (NM) is a by-product of catecholamine-synthesis and its production governed by cytosolic content of dopamine or other catecholamines (Martin-Bastida *et al.*, 2017). NM is a pigment that can act in a neuroprotective or toxic manner in neurons: while its synthesis reduces toxic Iron-Dopa-complexes and its presence in the cell acts as an important chelator to metals such as iron, copper and zinc, its release into the extracellular space from dying neurons leads to neurodegeneration via the activation of microglia (Zucca *et al.*, 2015). The accumulation of iron and neuromelanin are hence age-dependent processes.

Finally, midbrain dopaminergic neurons exhibit a much larger axon terminal field than any other neuron type known: the most comprehensive histology data stem from rats and indicate that the number of synapses given rise by a single SNpc neuron (102`000-245`000) exceeds the number of synapses given rise by e.g. striatal medium spiny neurons (300-500), or striatal GABAergic interneurons (5000) by at least two orders of magnitude (Bolam and Pissadaki, 2012). The fact that this complex axonal arbour is un-myelinated and can reach an estimated length of up to 4.5m per cell in humans (Bolam and Pissadaki, 2012), places these cells under tremendous metabolic demand (Surmeier, 2007).

On top, there are several mechanisms that have been identified to interfere with cell function in PD, in particular relating to energy metabolism and protein degradation: The observation of SN cell loss and subsequent development of parkinsonism after exposure to MPPT+, resulting in the inhibition of complex I of the electron transport chain (Langston and Ballard, 1983), started a thread of discoveries into the role of mitochondrial dysfunction in PD: reduced complex I activity and protein expression

in the SN of sporadic PD patients (Schapira *et al.*, 1989), increasing levels of somatic mutations in mitochondrial genes with age (Corral-Debrinski *et al.*, 1992) and anatomic location relevant to the condition (Soong *et al.*, 1992), induction of SNpc neuronal cell loss and parkinsonism in a murine model by experimental induction of multiple mitochondrial gene deletions (Pickrell *et al.*, 2011) and the identification of familial forms of PD related to genes involved in mitochondrial function and clearance, such as *Parkin*, *Pink1* and *DJ-1* (Pickrell and Youle, 2015), to name a few (Schapira, 2008).

On the other hand, the degradation of protein content in health is channelled through either the ubiquitin-proteasome or the lysosomal autophagy system. The efficiency of the autophagy system decreases with age. Both mechanisms, mitochondrial dysfunction and protein clearance dysfunction, show age-related changes and have thus been referred to as potential mechanisms linking ageing and PD risk. Similarly, data on non-human primate midbrain dopaminergic neurons supports the view that ageing is associated with a progressive, region-specific reduced lysosomal and impaired proteasomal function, increased oxidative stress and exaggerated glial activation/neuroinflammation, representing a pre-parkinsonian state (Collier *et al.*, 2017).

In summary, there is data to suggest that normal ageing and a pre-parkinsonian state may represent a continuum. Nevertheless, the mechanism linking cellular aging and PD risk remain largely elusive. The aim of the work in this chapter was to elucidate this relationship further.

5.3.3 Ageing, Telomeres and Neurodegenerative Disease

Around 25% of human lifespan variability can be explained by genetic factors (Herskind *et al.*, 1996), exerting merely any effect before the age of 60 (Hjelmborg *et al.*, 2006). Telomere biology represents one of the fundamental biological mechanism related to ageing. In the majority of species with linear chromosomes, chromosome ends are covered by repetitive hexanucleotide complex $(TTAGGG)_n$ repeats with a single stranded overhang of 50 to 300 nucleotides in length called telomeres in order to protect DNA from degradation (Moyzis *et al.*, 1988; Shay and Wright, 2019). They play an essential part in genomic stability by preventing DNA damage response mechanisms leading to apoptosis (Aubert and Lansdorp, 2008; Klapper *et al.*, 2001). At the telomere tip the protein complex Shelterin, consisting of proteins TERF1, TERF2, TINF2, TERF2IP, ACD and POT1, together with the DNA helicase RTEL1 binds to the single-stranded overhang and folds it back to the double-stranded telomeric DNA to form a T-loop. This prevents the recognition and misinterpretation of telomeric DNA as damaged by DNA damage repair mechanisms and subsequent degradation (Palm and de Lange, 2008). In particular, Shelterin prevents the kinases ATM and ATR to bind to DNA, signalling DNA double-strand breaks inducing cell-cycle arrest. It similarly prevents the non-homologous end joining pathway, which ultimately leads to chromosome end fusion (Maciejowski and de Lange, 2017).

Telomere length (TL) in humans ranges in size between 0.15 to 15 kilobases (kb) and depends on age (Aubert and Lansdorp, 2008; Lindsey *et al.*, 1991; Müezzinler *et al.*, 2013; Slagboom *et al.*, 1994), sex (Gardner *et al.*, 2014), race (Sanders and Newman, 2013), chromosome length (Mayer *et al.*, 2006; Wise *et al.*, 2009), as well as cell type and mitotic activity (Aubert and Lansdorp, 2008). It shows considerable

inter-individual variability while a positive correlation of TL between different tissues of the same donor has been shown for some tissue types (Takubo *et al.*, 2002). TL decreases with each cell cycle (Aubert and Lansdorp, 2008) due the "end-replication problem" of lagging-strand synthesis, describing the inability of the polymerase to replicate to the very end of the template DNA strand during DNA replication (Watson, 1972).

Advancing chronological age hence causes progressive telomere length (TL) shortening (Lindsey *et al.*, 1991; Slagboom *et al.*, 1994), best documented in leucocyte TL (LTL): the annual TL attrition in humans from this has been estimated at around 20-40 base pairs (bp) per year in peripheral blood as confirmed by a meta-analysis of 124 cross-sectional and five longitudinal studies (Müezzinler *et al.*, 2013). LTL heritability has been estimated between 30-75% (Jeanclos *et al.*, 2000, Njajou *et al.*, 2007, Slagboom *et al.*, 1994) and is modified by paternal age at conception. The continued shortening of TL is the biological reason behind the *Hayflick limit*, describing the limited proliferative lifespan of cultured primary human cells. If telomeres shorten below a minimal length, either replicative senescence or telomere crisis, a state of widespread genomic instability, occurs (Maciejowski and de Lange, 2017).

Telomere elongation is a fundamental cell function counteracting the effect of TL attrition with mitosis. In the majority of tissue, telomerase acts as a telomere elongating ribonuclein (Schmidt and Cech, 2015), consisting mainly of the RNA template TERC (MIM:602322) and the reverse transcriptase TERT (MIM:187270). Dysfunctional telomerase activity leading to shortened LTL is the mechanism of several, rare monogenic conditions, such as dyskeratosis congenita, idiopathic

pulmonary fibrosis or Hutchinson-Gilford progeria, documenting the connection between short TL and premature ageing (Klapper *et al.*, 2001, Aubert *et al.*, 2008).

LTL is highly heritable (Broer *et al.*, 2013; Jeanclos *et al.*, 2000; Njajou *et al.*, 2007; Slagboom *et al.*, 1994) and genome wide association studies (GWAS) have identified several single nucleotide polymorphisms (SNPs), genetically determining LTL (Codd *et al.*, 2013; Levy *et al.*, 2010; Li *et al.*, 2020). Several epidemiological studies have investigated the correlation between LTL and chronic diseases, including atherosclerosis, cardiovascular and degenerative diseases and many types of cancers (Samani *et al.*, 2001; Aviv, 2012; Wang *et al.*, 2014; Dapos;Mello *et al.*, 2015; Hou *et al.*, 2015; Helby *et al.*, 2017; Kalson *et al.*, 2018). Similarly, there is evidence to suggest LTL as an index of cognitive function (Hägg *et al.*, 2017) and cellular ageing in the human central nervous system, reflected by an inverse correlation with the risk of dementia and mortality (Honig *et al.*, 2012; Kume *et al.*, 2012; Martin-Ruiz *et al.*, 2006), as well as brain atrophy patterns (Jacobs *et al.*, 2014; King *et al.*, 2014).

LTL has been studied in neurodegenerative disease, most prominently Alzheimer`s disease (AD), where shorter LTL has been found to be associated with increased disease risk (Thomas *et al.*, 2008; Zhan *et al.*, 2015). LTL and its association with disease risk has similarly, repeatedly been studied in PD with variable and conflicting results - a meta-analysis summarizing 956 cases and 1284 controls provided inconclusive results (standardized mean difference 0.36 (95%CI 0.25 - 0.96; p=0.25), mainly due to substantial heterogeneity (I^2=97%) (Forero *et al.*, 2016). Conceptually, these previous PD studies were hampered by the application of different methodological approaches and the fact that it is impossible to retrospectively stratify for environmental exposures known to influence telomere

length (Mirabello *et al.*, 2009), as well as residual confounding and reverse causality, inherently plaguing classical epidemiological research.

5.3.4 Aim and Hypotheses

The main mechanism of telomere shortening in mitotic cells is cell division, rendering post-mitotic cell telomere length presumably stable. Neurons in the human cortex are considered post-mitotic throughout adult life, and cross-sectional studies on cortical samples found no age-related TL attrition in the human brain (Allsopp *et al.*, 1995; Nakamura *et al.*, 2007; Takubo *et al.*, 2002; Tomita *et al.*, 2018). Longitudinal measurement of human brain telomer length is not feasible and cross-sectional cortical brain samples so far indicated no attrition with age. The dynamics of TL in subcortical nuclei, like the striatum, however, have not been studied so far, and knowledge on TL between different brain regions is scarce (Mamdani *et al.*, 2015).

To establish a link between telomere biology, ageing and PD, this study was designed to confirm/refute the hypotheses that there is:

a) a causal relationship between genetically determined LTL and PD risk
b) a change in TL in the striatum with advancing age
c) altered TL regulation in brain regions connected to PD pathophysiology (basal ganglia) in comparison to other brain regions

5.4 Methods

5.4.1 Population genetics

5.4.1.1 PD GWAS data

PD GWA study summary statistics originated from several independent sources: the initial MR analysis was performed on data collated from 15 independent GWAS datasets of European descent, undertaken by the International Parkinson´s Disease Genetics Consortium (IPDGC) (Nalls *et al.*, 2014).

The replication attempts were based on PD GWA study summary statistics from two independent, well-characterized PD case-control cohorts: the exploratory MR analysis was performed on data from participants of European descent only collated for the so far largest PD GWAS study, undertaken by the International Parkinson´s Disease Genetics Consortium (IPDGC) (Nalls *et al.*, 2019). The confirmatory MR analysis was performed on separate data from participants of European and Asian descent, collated by the COmprehensive Unbiased Risk factor Assessment for Genetics and Environment in Parkinson's Disease (COURAGE-PD) consortium. This is an international consortium comprising of genetic data on susceptibility to Parkinson's disease (PD) with Caucasian ethnicity representing a major proportion of the study participants and a total sample size of 12,576 cases and 9,565 controls, collected from 27 participating sites spread across four continents.

Both data sources have undergone appropriated institutional review board (IRB) and ethical review, there was no separate IRB/ethical review required for this work.

5.4.1.2 Mendelian Randomization: instrument and calculations

For the initial MR analysis, we selected 11 SNPs as instrumental variables for LTL estimation, representing 10 independent genomic regions (see Table 5.1). All SNPs chosen had been established previously to be associated with leucocyte telomere length at a genome-wide significance level (i.e. p-value of $<5x10^{-8}$) (Codd *et al.*, 2013; Mangino *et al.*, 2012; Pooley *et al.*, 2013): seven SNPs representing six independent genomic regions, identified by (Codd *et al.*, 2013) were supplemented in this process by four more additional, independent SNPs (Mangino *et al.*, 2012; Pooley *et al.*, 2013). Calculations indicate that in combination these IVs explain 2% to 3% of the LTL variance in man (Telomeres Mendelian Randomization Collaboration *et al.*, 2017).

For the replication analysis we used an updated list of 15 SNPs as instrumental variables for LTL based on additionally published GWAS results (Li *et al.*, 2020) (see Table 5.2).

Wald ratios calculated by dividing the per-allele log-OR for PD by the per-allele difference in mean LTL for each of the IVs from the combined IV instrument. 95% confidence intervals (95% CI) were calculated from the standard error (SE) of each Wald ratio and results compiled in a forest plot. Linear regression analysis of the variant-outcome association divided by the variant-exposure association was performed using inverse-variance weighting (IVW; assumption of no pleiotropic effect), penalized weighted median (assumption that no more than 50% of the weight of the MR effect estimate are derived from invalid (pleiotropic) IVs), as well as MR-Egger regression (based on the Instrument Strength independent of the direct effect (InSIDE) assumption) (Bowden *et al.*, 2016). MR statistical analyses were performed on R (Project for Statistical

Computing). MR statistics were calculated and displayed for each IV and data set individually with the significance level set at a p-level of <0.05.

Table 5.1: List of instrumental variables (IV) in the exploratory analysis

IVs were used for calculation of Wald ratios denoting SNP position on chromosome (Chr), single nucleotide polymorphism (SNP)/marker name, nearest gene to marker, effect allele (EA), other allele (OA), effect allele frequency (EAF), beta, standard error and physiological function of the respective gene. IVs chosen were first described by (Codd et al.*, 2013) (denoted by *), (Pooley* et al.*, 2013) (denoted by #) and (Mangino* et al.*, 2012) (denoted by ‡).*

Chr	SNP	Nearest Gene	EA	OA	EAF	Beta	SE	Physiological Function
2	rs11125529	ACYP2 *	A	C	0.16	0.065	0.012	Muscle ion transporter
3	rs6772228	PXK #	T	A	0.87	0.041	0.014	Synaptic transmission
3	rs10936599	TERC *	C	T	0.76	0.1	0.011	Telomerase
4	rs7675998	NAF1 *	G	A	0.8	0.048	0.012	Ribosome
5	rs2736100	TERT *	C	A	0.52	0.085	0.013	Telomerase
10	rs9420907	OBFC1 *	C	A	0.14	0.142	0.014	*unknown*
17	rs3027234	CTC1 ‡	C	T	0.83	0.103	0.012	Telomere maintenance
19	rs412658	ZNF676 ‡	T	C	0.35	0.086	0.01	Transcript regulation
19	s8105767	ZNF208 *	G	A	0.25	0.064	0.011	*unknown*
20	rs755017	ZBTB46/RTEL1 *	G	A	0.17	0.019	0.012	Telomere elongation helicase
20	rs6028466	DHX35 ‡	A	G	0.17	0.058	0.013	Translation

Table 5.2: List of instrumental variables (IV) in the confirmation analysis

IVs used for calculation of Wald ratios denoting SNP position on chromosome (Chr), single nucleotide polymorphism (SNP)/marker name, nearest gene to marker, effect allele (EA), other allele (OA), effect allele frequency (EAF), beta, standard error and physiological function of the respective gene. Abbreviations: spinocerebellar ataxia (SCA).

Chr	SNP	Nearest Gene	EA	EAF	Beta	SE	Physiological Function
1	rs3219104	*PARP1*	C	0.83	0.042	0.006	Chromatin associated enzyme
3	rs10936600	*TERC*	T	0.24	−0.086	0.006	RNA component of Telomerase
4	rs13137667	*MOB1B*	C	0.96	0.077	0.014	Mitotic checkpoint
4	rs4691895	*NAF1*	C	0.78	0.058	0.006	Telomerase-associated protein
5	rs7705526	*TERT*	A	0.33	0.082	0.006	Telomerase
6	rs2736176	*PRRC2A*	C	0.31	0.035	0.006	Unknown, associated with SCA36
7	rs59294613	*POT1*	A	0.29	−0.041	0.006	Part of shelterin protein-complex
10	rs9419958	*STN1 (OBFC1)*	C	0.86	−0.064	0.007	Part of shelterin protein-complex
11	rs228595	*ATM*	A	0.42	−0.029	0.005	Cell cycle checkpoint kinase,
14	rs2302588	*DCAF4*	C	0.10	0.048	0.008	*Unknown*
16	rs3785074	*TERF2*	G	0.26	0.035	0.006	Part of shelterin protein-complex,
16	rs7194734	*MPHOSPH6*	T	0.78	−0.037	0.006	*unknown*
16	rs62053580	*RFWD3*	G	0.17	−0.039	0.007	DNA damage repair
19	rs8105767	*ZNF208*	G	0.30	0.039	0.005	Gene transcript regulation
20	rs75691080	*RTEL1 / STMN3*	T	0.09	−0.067	0.009	DNA helicase, shelterin interaction

5.4.2 Molecular biology

5.4.2.1 Human tissue samples

Attempts to identify sufficient quantities of corresponding pairs of brain and peripheral blood from healthy control human donors failed, as blood is not normally been collected at all tissue brain banks contacted throughout the MRC tissue bank network. Instead, corresponding pairs of spleen (as proxy for blood) and brain tissue were identified at the MRC Sudden Death Brain and Tissue Bank, Edinburgh.

Across populations, measurement methods and statistical models, telomere length in human tissue has been reported to be consistently influenced by age, sex and race in descending order (Sanders and Newman, 2013). Tissue pH has been reported once to influence TL measurements in SN, but not other brain regions (Mamdani *et al.*, 2015). Additional factors such as smoking, alcohol consumption, physical activity, socio-economic status and education, body mass index, lipid levels and glucose metabolism have been described to influence LTL, but only inconsistently so and generally with only a weak correlation coefficient <0.2 (Sanders and Newman, 2013). As the MRC Sudden Death Brain and Tissue Bank does not hold information on donor race, Tissue samples from control subjects without history or neuropathological features of neurodegenerative disease were identified and matched according to age, gender and brain pH in descending order, according to availability.

All tissue handling was done according to local standardized procedures and after ethical approval, samples were transferred individually in 7ml Bijou containers on dry ice and stored in -80°C freezers upon arrival.

Overall n=98 donors across the adult age spectrum with available brain and corresponding spleen samples were identified. For comparison between different brain regions, two subgroups of n=10 male donors were closely matched for age, brain tissue pH and post-mortem delay, according to tissue availability (see Table 5.5).

5.4.2.2 Tissue Dissection

In order to prevent DNA/RNA degradation, frozen tissue samples were kept at -80°C throughout the dissection process. Samples, respective containers and all tools touching the samples were kept on dry ice and utmost care was applied to prevent thawing throughout the dissection process. Samples were transferred from their original containers to sterile 10cm petri dishes for dissection, and then to pre-labelled RNAse/DNAse-free, sterile Eppendorf 2ml cups for storage. Involved stainless-steel bone-cutters and tweezers were cleaned in successive steps of 70% EtOH, double distilled H_2O, RNAse Zap and again double distilled H_2O between samples.

5.4.2.3 DNA extraction

DNA was extracted from all n=237 tissue samples in an automated manner by LGC Genomics using its sbeadex livestock kit (LGC genomics, no.44702). Quality and quantity of genomic DNA were assessed by Ethidium bromide staining followed by electrophoresis and Qubit fluorometer (Invitrogen) measurements.

5.4.2.4 Telomere restriction fragment (TRF) analysis

Two µg of genomic DNA was digested with *Rsa*I and *Hin*fII at a final volume 30 µl in Smart Cut buffer (NEB) at 37˚C overnight. Digested genomic DNA was separated in a 30-cm long 0.8% agarose gel and transferred to a nylon membrane (Hybond N-, GE Healthcare) via capillary action after treating the gel with 1 N sodium chloride and alkaline solution (sodium hydroxide). DNA on the membrane was crosslinked by UV and hybridised with the ^{32}P-labelled human telomere DNA fragment (from an *Eco*RI-digested pKazu-hTelo plasmid (55xTTAGGG repeats, cloned into pCR4 TOPO-blunt vector)). A DNA ladder (Hyperladder™ 1kb) was probed with *Schizosaccharomyces pombe* telomere DNA delivered from the *Eco*RI & *Bam*HI-digested p1742 plasmid. The hybridized probe was detected using a Storm Phosphorimager.

5.4.2.5 MMQ-PCR

For all MMQ-PCR experiments the Power SYBR Green reagents (Thermo Fisher, ref:4367659) were used for the master mix. Genomic DNA samples were normalised to the concentration of 5 ng/µl using diethylpyrocarbonate (DEPC) treated ultrapure water (Thermo Fisher, ref: R0601). Genomic DNA from HEK293K cell line (ATCC® CRL-3216™) was used as a reference at the same concentration (5ng/ul), as well as standard serial dilutions (150ng/ul; 50ng/ul; 16.6ng/ul; 5.5ng/ul; 1.8ng/ul).

Table 5.3: MMQ-PCR master mix contents

Reagents	50 reaction premix (µl)	Volumes per well (µl)	Final concentration/DNA amount per well (20µl)
Power SYBR Green master mix	375	7.5	0.75x
Primer hTeloG (100 µM)	90	1.8	900nm
Primer hTeloC (100 µM)	90	1.8	900nm
Primer ref.-Albumin F (100 µM)	90	1.8	900nm
Primer ref.-Albumin R (100 µM)	90	1.8	900nm
H_20	65	1.3	-
Premix	800 (16x50)	16	
DNA (5 ng/µl DNA)		4	20 ng
Total		20	

As telomeres have a repetitive hexanucleotide structure, amplification needs to ensure that only single copy amplicons are produced in order to avoid the possibility of long telomere amplicons melting at a temperature high enough to interfere with single copy gene detection in the multiplex essay. For telomere amplification, primers designed to generate a short, fixed-length amplification product were used (Cawthon, 2009):

TelG: ACACTAAGGTTTGGGTTTGGGTTTGGGTTTGGGTTAGTGT

TelC: TGTTAGGTATCCCTATCCCTATCCCTATCCCTATCCCTAACA

Primers for the single copy gene Albumin were designed to generate a 98bp product:

albu: CGGCGGCGGGCGGCGCGGGCTGGGCGGaaatgctgcacagaatccttg

albd: GCCCGGCCCGCCGCG CCCGTCCCGCCGgaaaagcatggtcgcctgtt.

Pipetted in triplicate in a 96-well plate, 25 actual samples and 7 control samples (5-step standard dilution, one standard positive control and one plain water sample) were processed per run on a Quant Studio 5 real-time PCR machine (Fisher Scientific). The plain water sample was used to control for contamination in the essay by verifying no amplification in the single copy gene amplification reaction, whereas amplification in the telomere amplification reaction is possible due to primer dimer formation. Runs were at least triplicated per sample. Standard serial dilutions measured on each plate were used to plot a standard curve for both the telomere and single copy gene amplification.

MMQ-PCR T/S									
Time (min)	15:00	00:15	00:15	00:15	00:10	00:15	00:10	00:15	Hold
Temperature (°C)	95.0	94.0	49.0	94.0	62.0	74.0 *	84.0	88.0 *	4.0
n cycles	1x	2x		32x					1x

Table 5.4: MMQ-PCR T/S thermal cycle

*The 74°C reads provided the Ct values for the amplification of the telomere template (in early cycles when the scg signal is still at baseline); the 88°C reads provided the Ct values for the amplification of the scg template (at this temperature there is no signal from the telomere PCR product, because it is fully melted) (Cawthon, 2009). * signal acquisition.*

The regression coefficient R^2 (ideally =1, meaning that the Ct measurement accuracy of the serial dilutions in the standard curve is absolute) and the efficiency of the PCR reaction (calculated as the natural logarithm of the inverted negative slope of the regression of 5-step standard samples Ct

measures, ideally = 2, meaning that per cycle the PCR product is doubled) were used to monitor experiment quality.

The T/S ratio was calculated per well and averaged per triplicate to minimize pipetting error. After normalization of T/S ratios against the mean of all standard positive control samples, results for each sample were averaged between runs and used for statistical comparison.

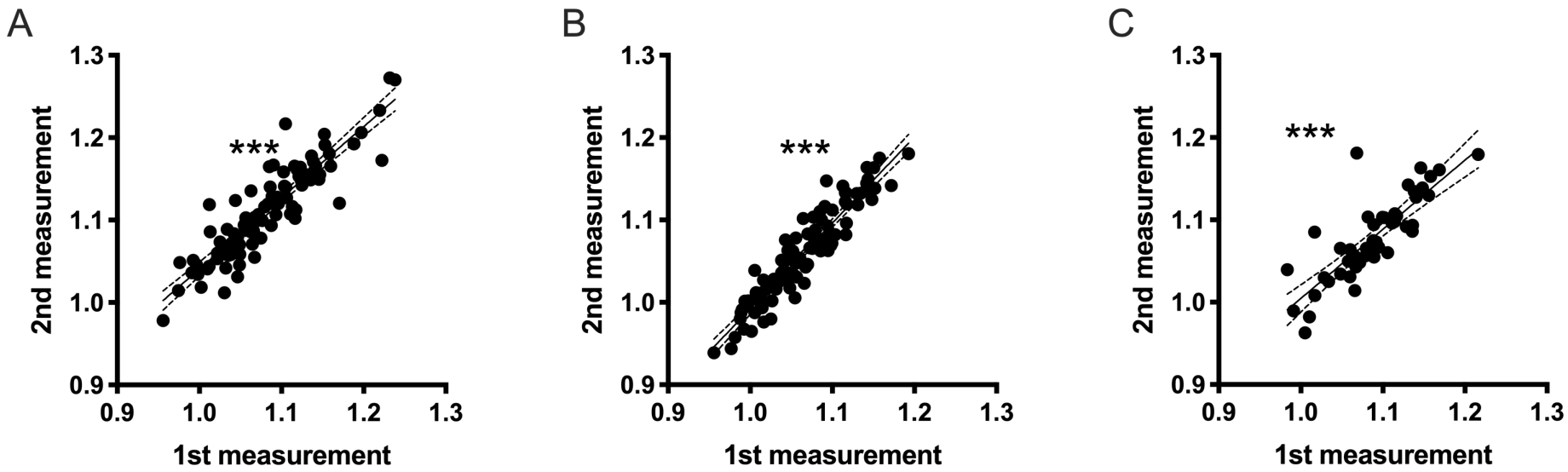

Figure 5.1: Repeat TL measurement correlations

*Plots depicting very good correlations for spleen (A), putamen (B) and brain region samples (C). *** indicating p<0.0005 on Pearson´s R test for correlation;*

5.4.3 Gene expression analysis

Data on gene expression of preselected genes, known to be involved in TL regulation were extracted from the Genotype-Tissue Expression (GTex) portal: https://www.gtexportal.org/home/multiGeneQueryPage

5.4.4 Wet Lab Statistical analysis

Statistical analysis (correlation analysis; un-paired, two-tailed t test; one-way ANOVA with Tukey`s multiple-comparisons) were done using GraphPad Prism v8.0.

5.5 Results

5.5.1 Mendelian Randomization – exploration

For the exploration MR analysis, PD GWAS summary statistics relating to 7,893,274 genetic variants (after imputation) to PD were available for 13,708 patients and 195,282 controls from the 2014 IPDGC dataset (Nalls *et al.*, 2014).

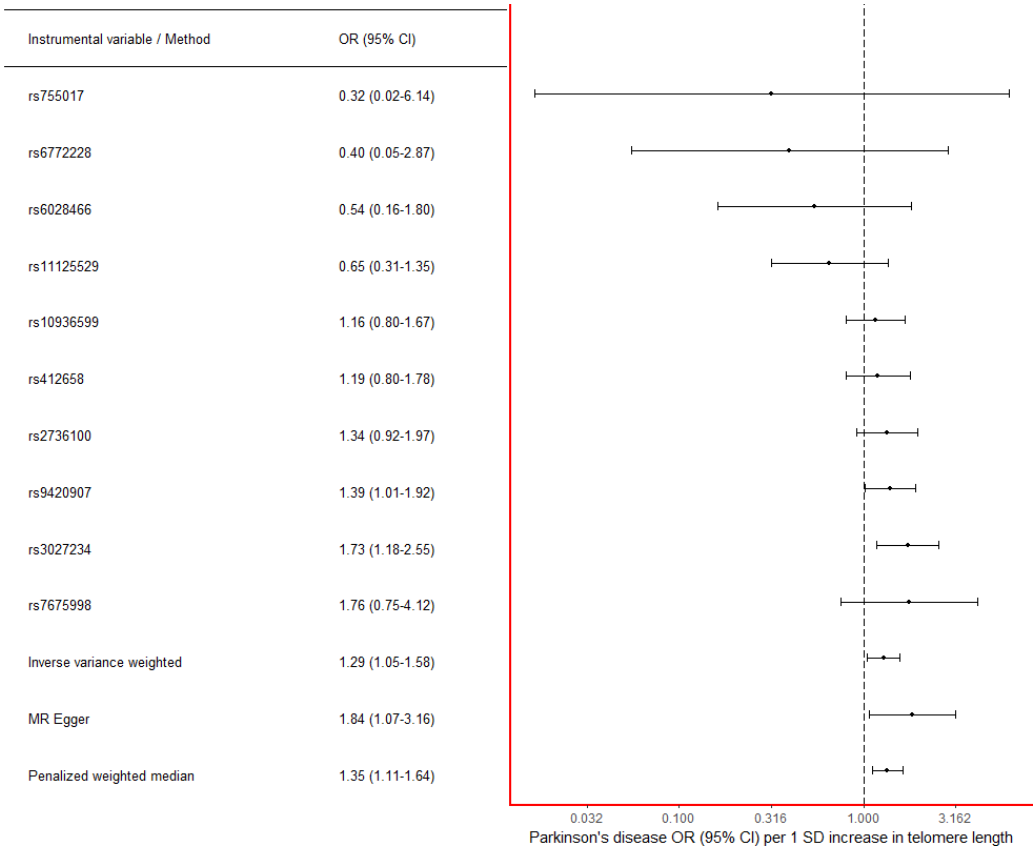

Figure 5.2: Forest plot of the exploratory IV analysis.

Wald ratios generated from SNPs associated with leucocyte telomere length (LTL) and risk for PD: Wald ratios including 95% CIs are listed per allele according to effect size in the instrumental variable analysis. Pooled effects using inverse-variance weighted (IVW) & MR-Egger regression are plotted below. Dots represent the point estimate, bars represent the 95% confidence interval. The Wald ratios of each IV are displayed over an x-axis showing the odds ratio for Parkinson´s disease per 1 standard deviation increase in telomere length.

Using the IVW method to pool the results from individual SNPs, the OR of PD per standard deviation telomere length increase was 1.29 (95% CI: 1.05-1.58; P=0.01). Likewise, MR-Egger (OR 1.84, 95% CI: 1.07–3.16; P=0.04) and penalized weighted median (OR 1.35; 95% CI: 1.11-1.64; P=0.03) showed a consistently significant result, surprisingly inferring an increased risk for PD with longer genetically determined TL. MR-Egger regression effect estimation showed an intercept at -0.04 ± 0.01 (P=0.08), suggesting potential directional bias in the IV estimates towards an underestimation of the true effect size (Figure 5.3).

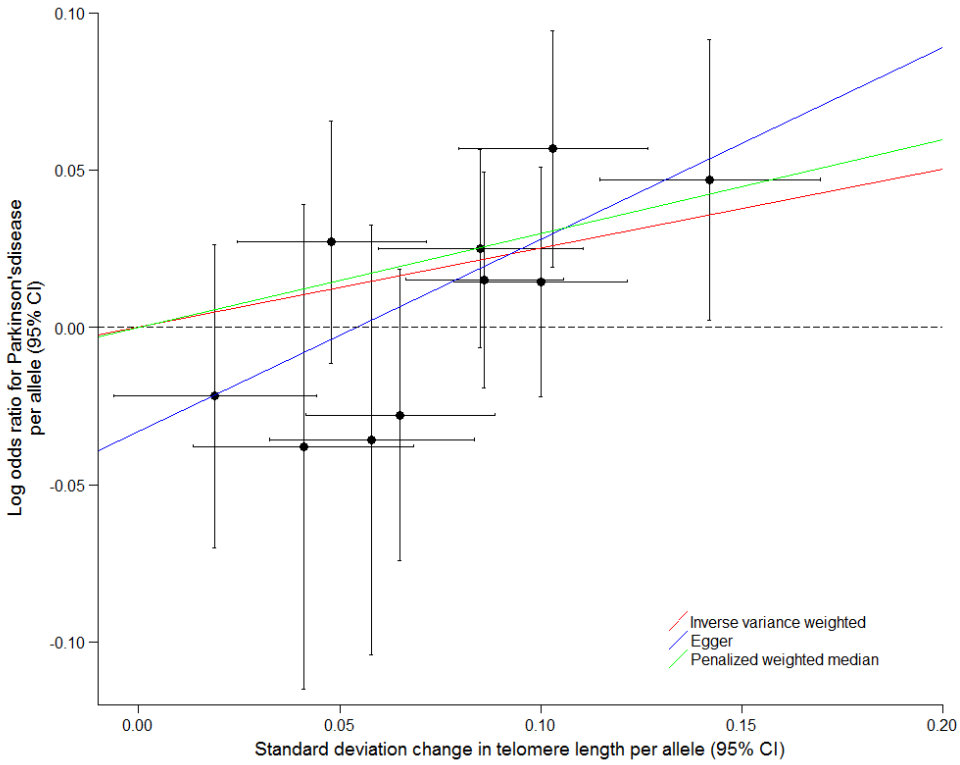

Figure 5.3: Scatter plot displaying the MR regression of the exploratory MR analysis

Whilst inverse-variance weighted and penalized weighted median regression work very similarly by forcing the regression line through the origin, MR-Egger does allow for the intercept on the y-axis to deviate from zero, giving additional information whether an observed effect might be over- or underestimated.

5.5.2 Tissue samples

Adult tissue samples from the MRC Sudden Death Brain and Tissue Bank (Millar *et al.*, 2007) were included according to tissue availability and demographic distribution - none of the included samples showed neuropathological evidence to suggest the presence of neurodegeneration (see Table S11). Cause of sudden death was cardiac (n=70 ischaemic; n=4 structural), significant psychiatric comorbidity (n=6 suicide; n=1 intoxication), ruptured aortic aneurysm (n=4), pulmonary embolism (n=4), unascertained (n=4), cerebral haemorrhage, asthma, diabetic coma, road traffic accident and peritonitis (n=1 each).

Table 5.5: Demographic details of the three human tissue sample collections used for TL quantification.

Abbreviations: cerebral white matter (CWM), cerebellum (CRBL), frontal cortex (FCTX), occipital cortex (OCTX), midbrain (MB), putamen (PUTM), spleen (SPL), substantia nigra (SN) and post-mortem interval (PMI)

	"Correlation"	**"CRBL+supratentorial"**	**"infra-tentorial"**
Origin/sample size	SPL, PUTM n=98 each	CWM, CRBL, FCTX, OCTX, PUTM n=10 each	SN, MB, CRBL, SPL n=10 each
Age (mean ± SD; yrs)	52.0 ± 13.4	55.3 ± 1.95	52.9 ± 4.15
Age range	20 - 79	53 - 58	49 - 58
Sex (% male)	81%	100%	100%
pH	6.28 ± 0.24	6.36 ± 0.11	6.27 ± 0.1
PMI	58.7 ± 22.1	51.3 ± 11.0	84.5 ± 24.8

Putamen and spleen samples were analysed from all n=98 donors ("correlation" data set), while matched groups of donors were selected for comparison between regions ("region matched" and "SN vs. CRBL"), according to tissue availability.

Sample groups were matched for age (Welch test; p=0.06) and pH (p=0.14), while PMI was significantly longer in "SN vs. CRBL" samples (one-way ANOVA; F=7.365; p=0.001).

5.5.3 MMQ-PCR essay quality control

Across all 25 MMQ-PCR runs included in the final analysis, indices of measurement quality were good: mean R^2 of telomere and albumin measurements were 0.9968, respectively 0.9970, the mean efficacy of telomere and albumin PCR amplification were 2.0183 and 1.9781.

The coefficient of variation, calculated for repeat (at least triplicate) telomere length measurements across all tissue samples using MM-qPCR, was 2.12% (n=238), comparing well with previous studies (Cawthon 2009). There was good correlation between repeat TL measurements in SPL (R^2=0.81, F=414.8, p<0.0001; m=0.86), PUTM (R^2=0.87, F=668.1, p<0.0001; m=1.04), as well as all region matched brain samples (R^2=0.68, F=102.6, p<0.001; m=0.84; see Figure 5.1).

5.5.4 Age-related attrition of Telomere Length in the human Putamen

TL from corresponding spleen, rich in blood cells, was used as a reference of individual 'biological' age. Starting with quantitative analysis, TRF/Southern blot comparison of extreme ages from "correlation" sample set showed significantly longer TL in young (mean ± SD; 21.3 ± 0.9 yrs.) vs. aged (73.7 ± 0.5) donors in n=6

corresponding SPL (10.8 ± 0.5 vs. 6.4 ± 0.6 kb; p=0.001) and PUTM (12.1 ± 0.7 vs. 7.4 ± 0.8; p=0.002) samples (Figure 5.4).

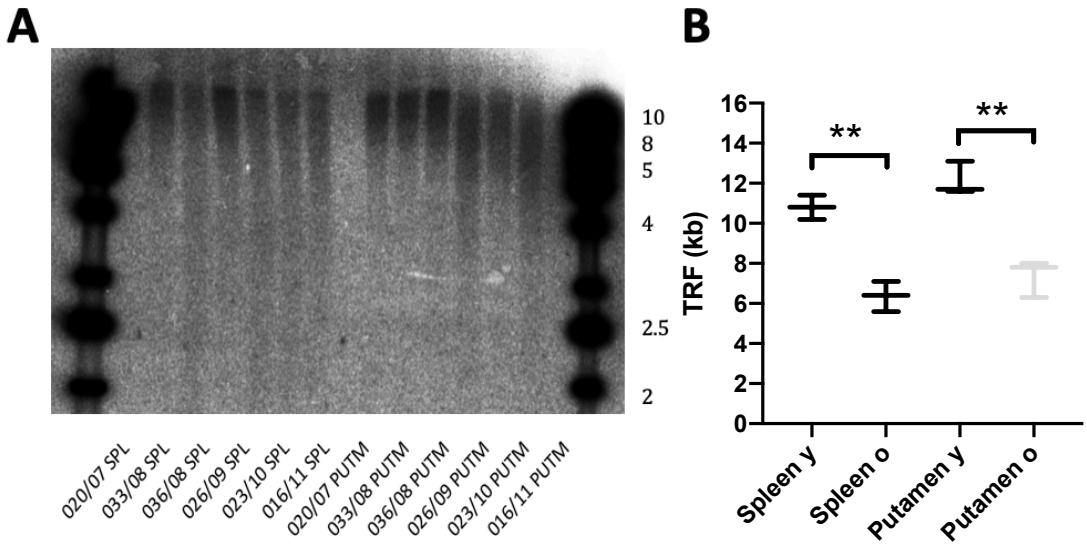

Figure 5.4: Temporal dynamic of human spleen (SPL) and putamen (PUTM) telomere length via Southern blot quantification.

*Telomere Restriction Fragment (TRF) analysis/Southern blot raw image (A) and mean length quantification (B), depicting n=6 corresponding sample pair of spleen (SPL) and putamen (PUTM) samples from young (y) vs. old (o) tissue donors, showing significantly longer TL in young vs. aged spleen (p=0.001) and putamen (p=0.002) samples; unpaired two-tailed t-test. TRF ladder in kilobases (kb). Shown values in boxes indicate mean and s.d. with whiskers indicating minimum and maximum. * indicates p < 0.05, ** indicates p<0.005, *** indicates p<0.0005 across the figure;*

Expanding this observation with n=98 corresponding sample sets from across normal adult age range, there was a significant positive correlation between SPL and PUTM TL on MMQ-PCR analysis (R^2=0.36, p<0.0001). As expected, there was a negative correlation of SPL TL with advancing age (F=16.17, p=0.0001; m=-0.0016). Surprisingly, this was also found for PUTM TL (F=28.78, p<0.0001; m=-0.0019; Figure 5.5).

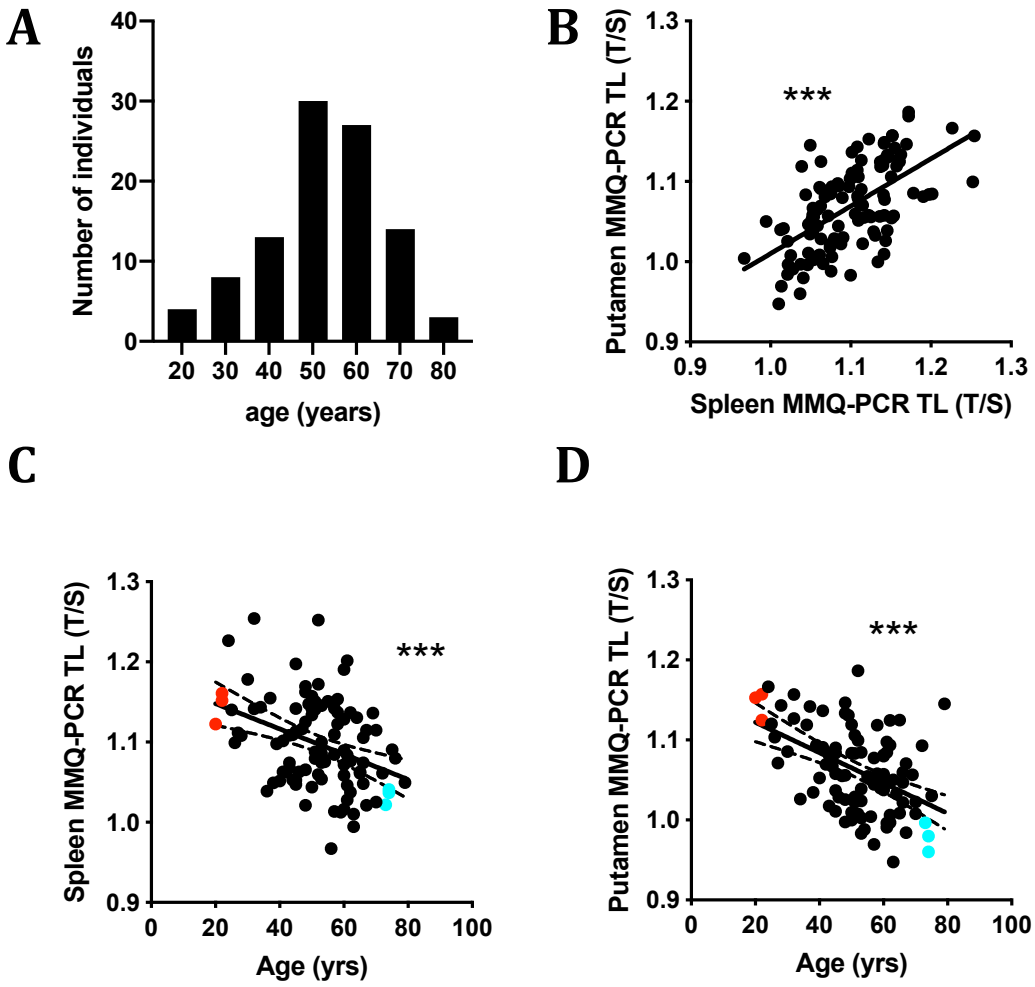

Figure 5.5: Temporal dynamic of human spleen (SPL) and putamen (PUTM) telomere length via MMQ-PCR quantification.

Age distribution of donors in the `correlation` dataset (A). Relative TL differences as assessed by MMQ-PCR (T/S) showed a significant positive correlation (n=98; Pearson correlation R^2=0.36; p<0.0001; slope m=0.59; F=63.23; p<0.0001) between peripheral blood/spleen and putamen samples (B). There was also a negative correlation between age and relative TL in spleen (R^2=0.14; p=0.0001; m=-0.0016; F=16.17; p=0.0001; C) and putamen (R^2=0.23; p<0.0001; m=-0.0019; F=28.78; p<0.0001; D) – coloured dots correspond to spleen and putamen samples of young (red), respectively aged (green) donors in the TRF analysis (

*Figure 5.4). * indicates p < 0.05, ** indicates p<0.005, *** indicates p<0.0005 across the figure;*

Whereas in SPL the negative correlation of TL with advancing age was independent of sex (male: n=80, F=9.13, p=0.0034; female: n=18, F=6.0, p=0.025), in PUTM this did not reach significance in females (male: F=27.97, p<0.0001; female: F=3.09, p=0.09; not shown).

As major depression has been reported to influence glial TL (Szebeni *et al.*, 2014), the exclusion of n=7 cases with significant psychiatric comorbidities did not change the correlations between SPL and PUTM TL (R^2=0.31, p<0.0001; not shown), as well as age-dependent TL attrition in SPL (F=10.21, p=0.0019; m=-0.0014; not shown) and PUTM (F=15.77, p=0.0001; m=-0.0016; not shown).

5.5.5 Telomere length in human brain is region-specific

To explore region-specific TL dynamics, we next compared samples from corresponding brain regions. Based on previous reports (Mamdani *et al.*, 2015), we first focused on cerebellar and brain stem (infra-tentorial regions): both absolute (TRF; n=4; ANOVA F=5.65; p=0.02; Figure 5.6A-B), as well as relative TL normalised to corresponding spleen TL (MMQ-PCR; n=10; ANOVA F=8.29; p=0.002; Figure 5.6C), showed longer TL in CRBL than in SN or MB.

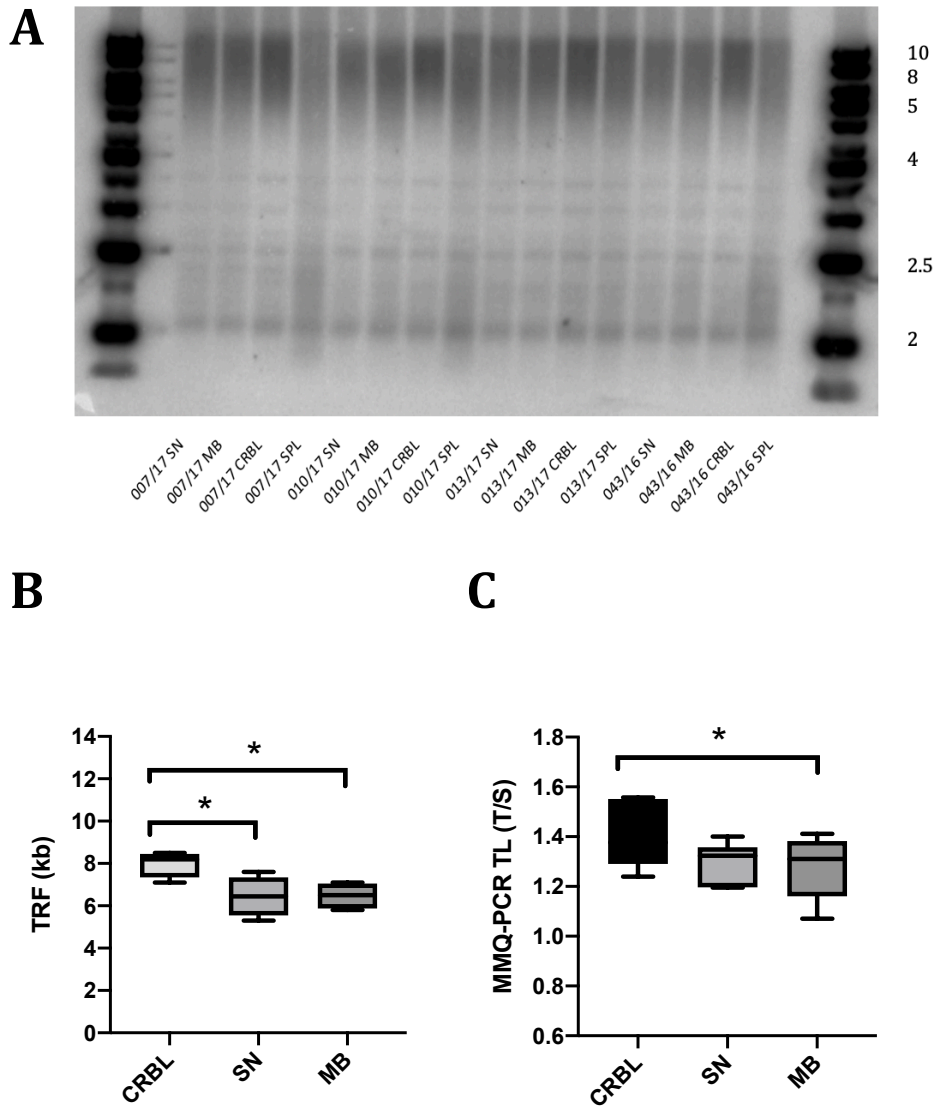

Figure 5.6: Region-specific human brain telomere length in infratentorial samples.

*Both absolute TL measurement using TRF/Southern blot (n=4; A-B) as well as relative TL measurement using MMQ-PCR (n=10; C) showed region-specific differences in TL. Cerebellar cortex (CRBL) TL was longer than substantia nigra (SN) and/or midbrain (MB) TL on absolute and relative assessment (A-C). TRF ladder in kilobases (kb). * indicates $p < 0.05$ across the figure; ANOVA post-hoc test results correctes for multiple comparison;*

According to tissue availability, we also assessed TL between CRBL and cortical (supratentorial) regions (MMQ-PCR; n=10; ANOVA F=3.23; p=0.02), indicating TL to be longest in CRBL and shortest in PUTM (Figure 5.7A).

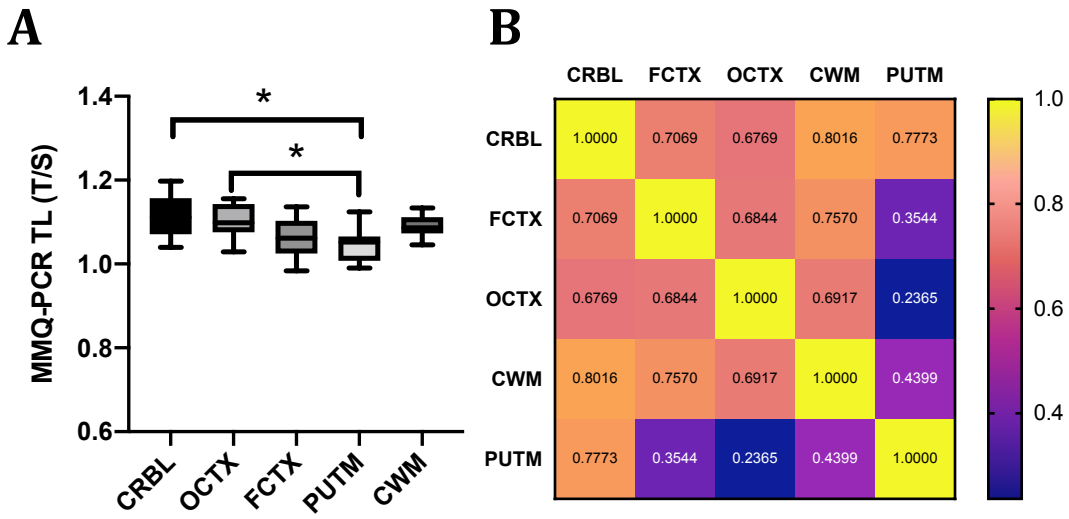

Figure 5.7: Region-specific human brain telomere length in "CRBL+supratentorial" samples:

*PUTM TL was significantly shorter than both CRBL and OCTX TL (A). Correlation matrix displaying the degree of TL inter-regional correlation within `CRBL + supratentorial` samples, indicating different TL dynamics in the PUTM. Heatmap displaying R^2 of sample pair correlations based on `CRBL+supratentorial` samples (n=10 each; B). Shown values in boxes indicate mean and s.d. with whiskers indicating minimum and maximum. ANOVA post hoc test results are displayed with p-values corrected for multiple comparison. * indicates $p < 0.05$ across the figure*

Correlation analysis in general revealed a high degree of positive correlation between TL of different brain regions (Figure 5.7B). Interestingly, PUTM TL showed much lower correlation with cortical grey (OCTX, FCTX) as well as white matter (CWM) TL than other regions. Together with the overall shortest TL measured in the PUTM this indicates that the dynamics of TL regulation differ between PUTM and the other brain regions studied.

5.5.6 Mendelian Randomization - replication

For the replication MR analysis, PD GWAS summary statistics relating to 7.784.415 genetic variants (after imputation) to PD were available for 37.688 patients and 1.474.079 controls from the 2019 IPDGC dataset (Nalls *et al.*, 2019).

Using the initial IV instrument, the effect size of PD per standard deviation telomere length increase across all IVs was 0.35 (95% CI: -0.25 – 0.78; P=0.64) for MR Egger and 0.09 (95% CI: -0.17 – 0.38; P=0.72) for IVW regression (Figure 5.8).

Using the updated IV instrument, the effect size of PD per standard deviation telomere length increase across all IVs was 0.88 (95% CI: 0.15 – 1.57; P=0.04) for MR Egger and 0.15 (95% CI: -0.22 – 0.46; P=0.34) for IVW regression (Figure 5.9). However, as the 95% CI of the IVW estimate crossed zero, this analysis did not detect a consistently significant association of PD risk with genetically determined LTL.

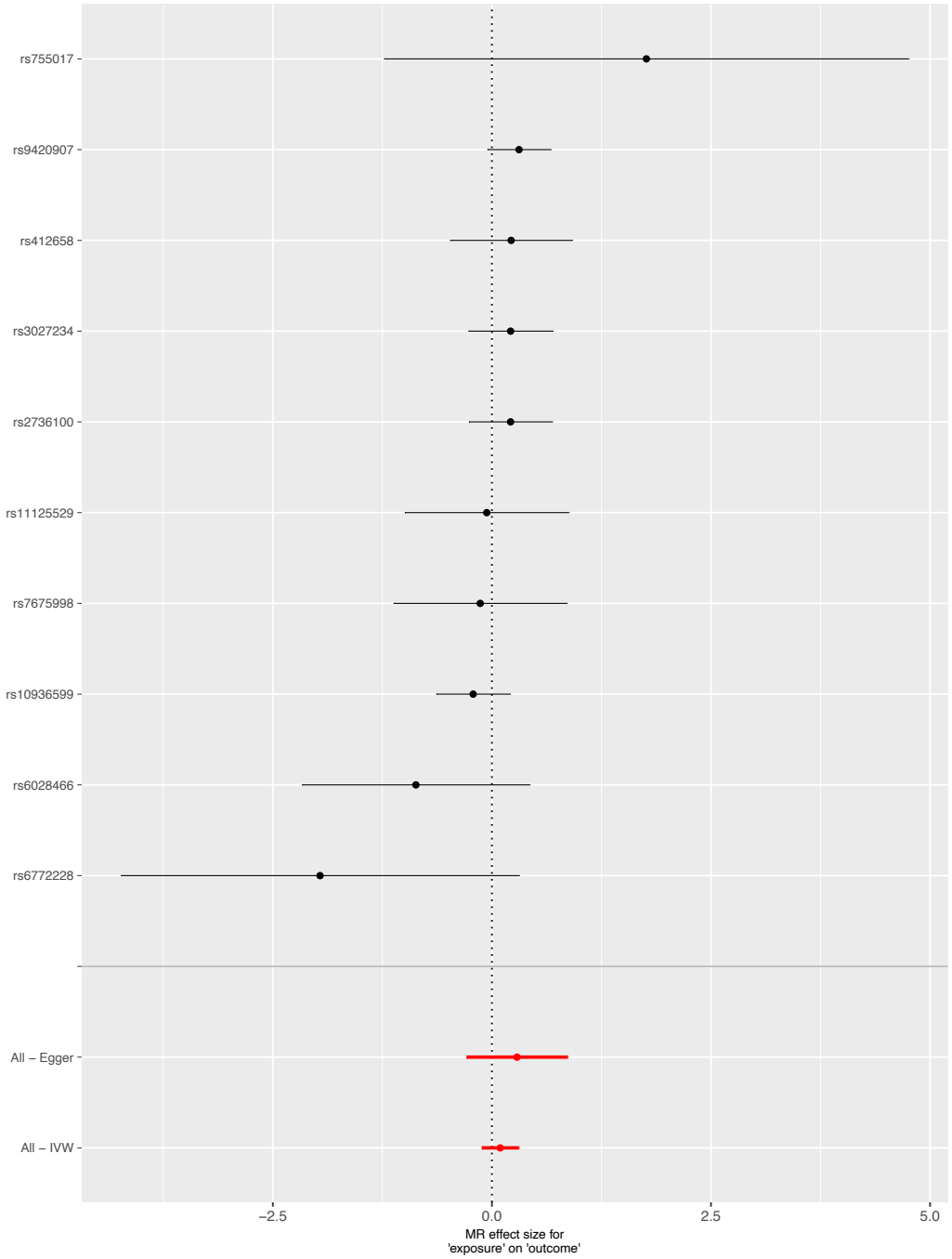

Figure 5.8: Forest plot of the confirmatory MR analysis using the initial IV instrument

Wald ratios generated from SNPs associated with leucocyte telomere length (LTL) and risk for PD: Wald ratios including 95% CIs are listed per allele according to effect size in the instrumental variable analysis. Pooled effects using inverse-variance weighted (IVW) & MR-Egger regression are plotted. Dots represent the point estimate, bars represent the 95% confidence interval. The wald ratios of each IV are displayed over an x-axis showing the non-significant effect size for Parkinson´s disease per 1 standard deviation increase in telomere length.

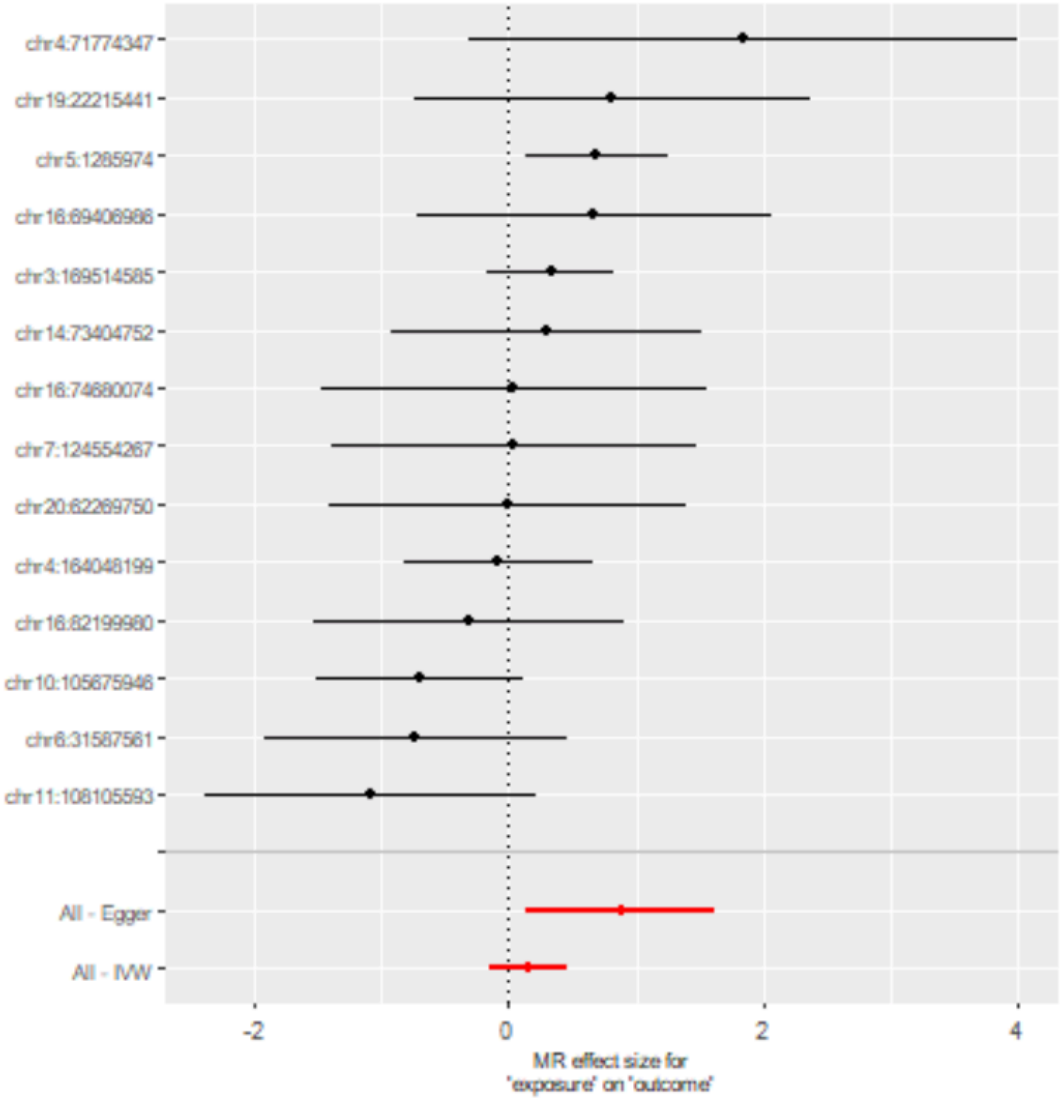

Figure 5.9: Forest plot of the confirmatory MR analysis using the updated IV instrument

Wald ratios generated from SNPs associated with leucocyte telomere length (LTL) and risk for PD: Wald ratios including 95% CIs are listed per allele according to effect size in the instrumental variable analysis. Pooled effects using inverse-variance weighted (IVW) & MR-Egger regression are plotted below. Dots represent the point estimate, bars represent the 95% confidence interval. The wald ratios of each IV are displayed over an x-axis showing the non-significant effect size for Parkinson´s disease per 1 standard deviation increase in telomere length.

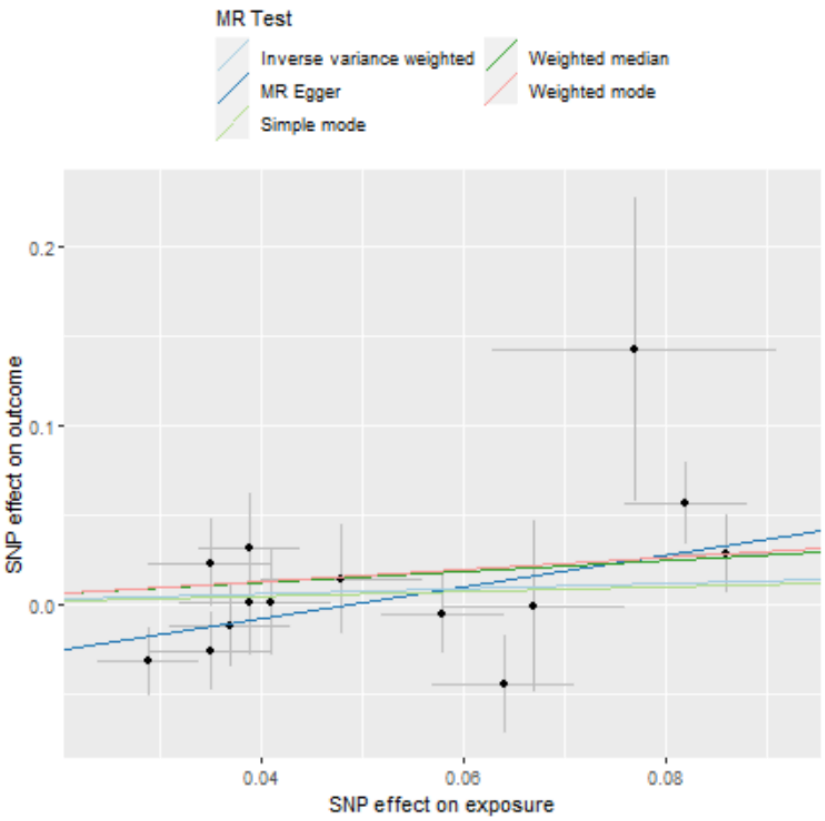

Figure 5.10: Scatter plot displaying the regression analysis of the confirmatory MR analysis using the updated IV instrument

Whilst inverse-variance weighted and penalized weighted median regression work very similarly by forcing the regression line through the origin, MR-Egger does allow for the intercept on the y-axis to deviate from zero, giving additional information whether an observed effect might be over- or underestimated. Dots represent the point estimate, bars represent the 95% confidence interval.

Similarly, the pooled OR of PD per standard deviation telomere length increase across all IVs based on 12,576 cases and 9,565 controls from the independent COURAGE-PD dataset was 0.97 (95% CI: 0.76 – 1.25; P=0.81) for IVW and 1.17 (95% CI: 0.55 – 2.47; P=0.67) for MR Egger regression, inferring no significant association between TL and PD risk.

5.5.7 Gene expression analysis

To further explore the molecular mechanism leading to region-specific TL, I utilized detailed human brain gene expression data. In a first step, I compared the regional-expression levels of genes regulating TL between central and peripheral nervous tissue and blood from the accessible GTex database (sample size between min. n=114 (SN) to max. n=209 (CRBL); Figure 5.11).

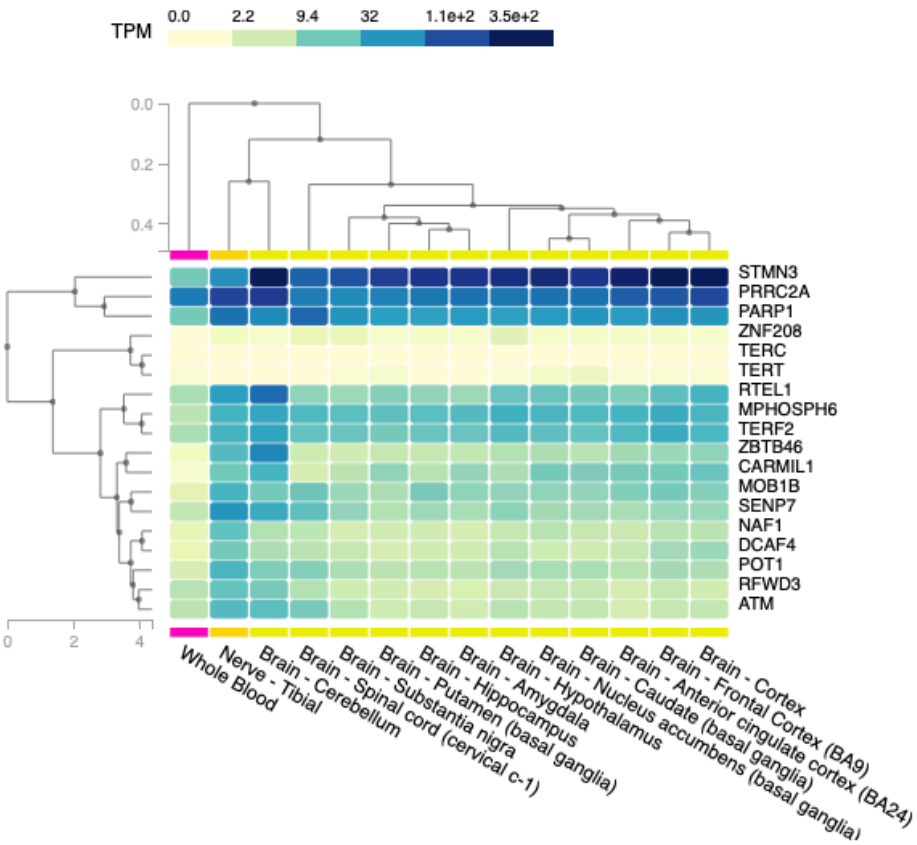

Figure 5.11: Gene regulation pattern of TL-regulating genes in human central and peripheral nervous tissue in comparison to blood.

Cluster plot depicting the relative gene expression values by tissue. Interestingly, cerebellar TL regulation is more similar to peripheral nervous tissue than to other brain regions. Given unit: transcript per kilobase million (TPM); Data obtained from the GTex portal on July 5th 2020.

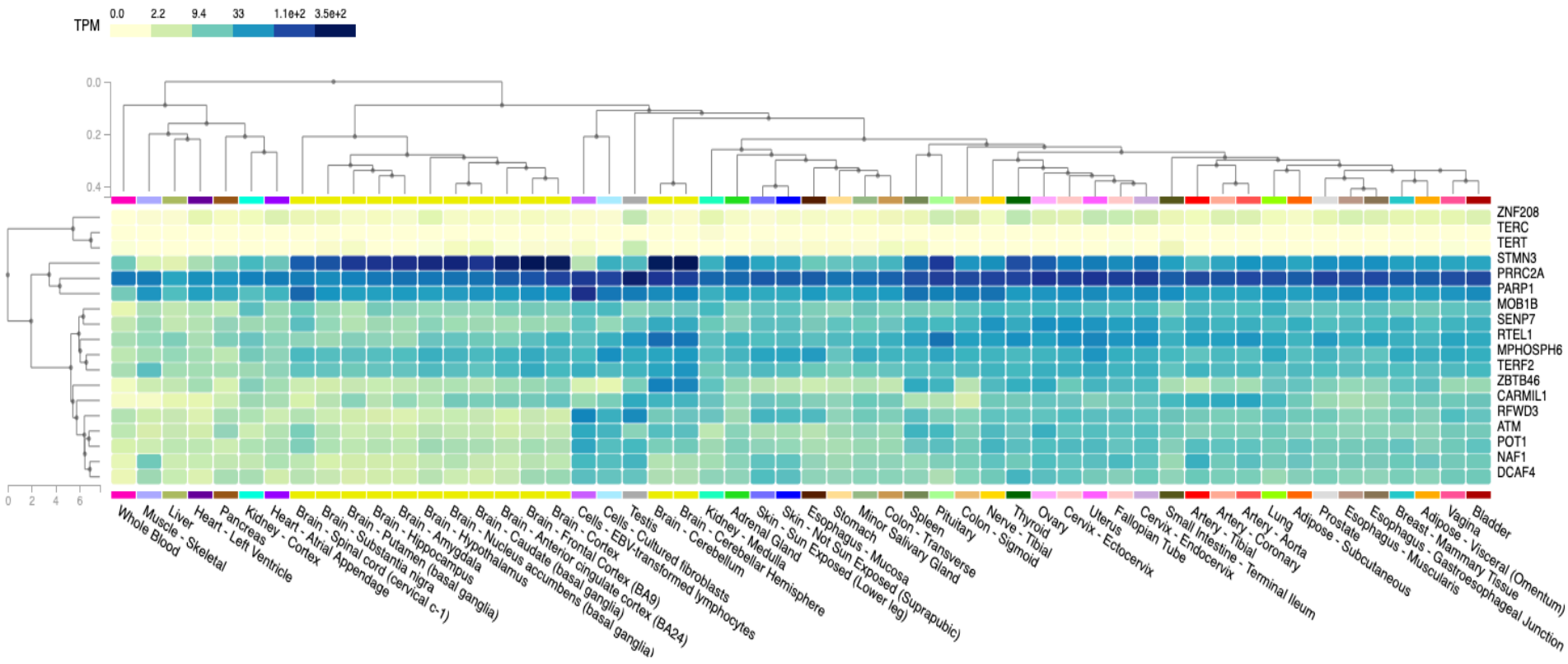

Figure 5.12: Gene regulation pattern of TL-regulating genes across human tissue types.

The expression pattern in brain clearly differs from blood and other organs. Given unit: transcript per kilobase million (TPM); Data obtained from the GTex portal on July 5th 2020.

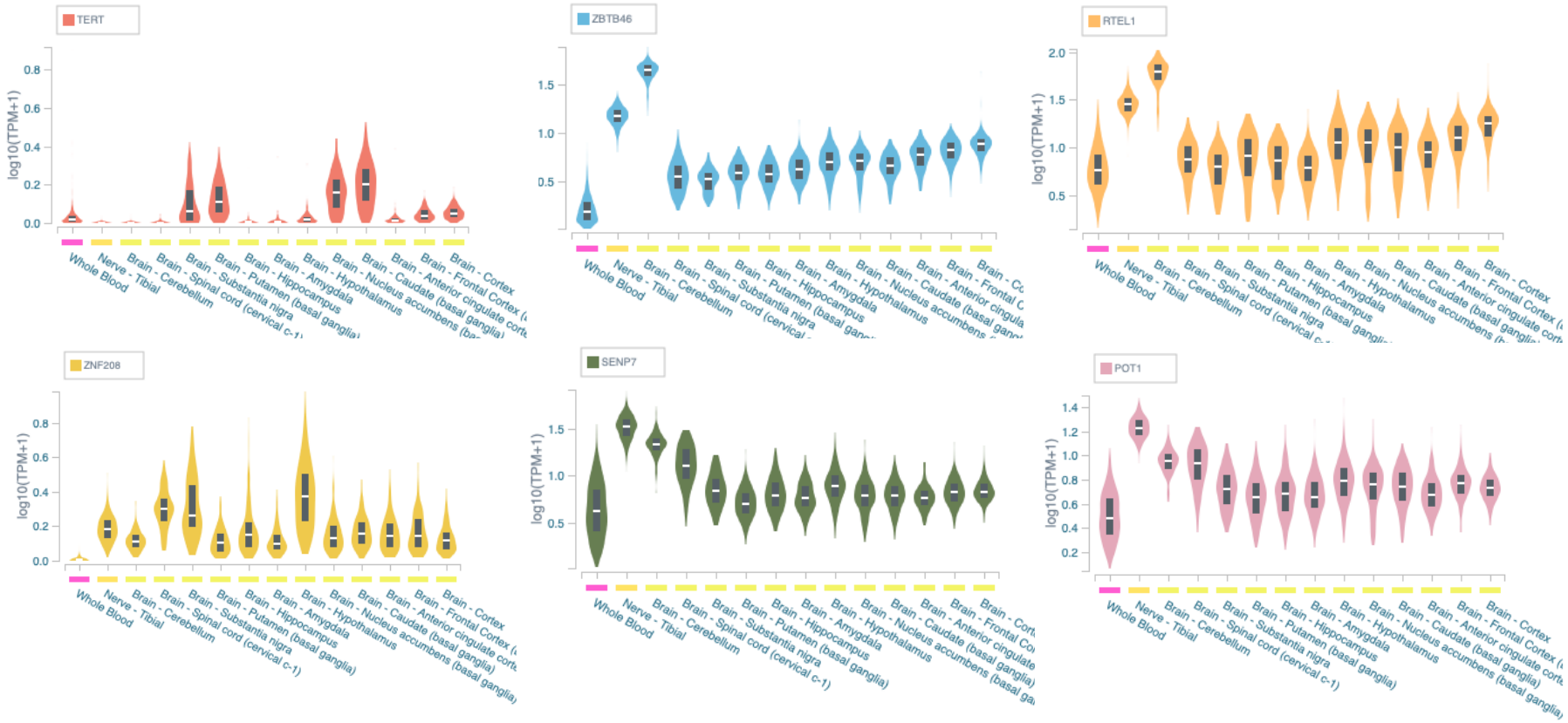

Figure 5.13: Example gene expression plots:

Gene- and region-specific expression pattern for TL regulating genes from blood, peripheral and central nervous system tissue, which can differ between regions by up to an order of magnitude. Given unit: transcript per kilobase million (TPM); Data obtained from the GTex portal on July 5th 2020.

This revealed a highly gene- and region-specific gene expression pattern. On clustering analysis, and in direct comparison to other tissue types, brain regions displayed a similar pattern of TL regulating gene expression. An important exception was the cerebellum (Figure 5.11 & Figure 5.12), which appeared more similar to peripheral nervous tissue, or even pituitary and spleen tissue, than other brain regions.

Per-gene analysis however showed that the gene expression pattern differs substantially between brain regions: for example, TERT is predominantly expressed in the nigro-striatal system (SN, caudate + PUTM) and nucleus accumbens, while the highest regional expression of RTEL1, RTEL1/ZBTB46, SENP7 and to a lesser degree also POT1 etc. are to be found in the cerebellum (Figure 5.13).

5.6 Discussion

5.6.1 Genetically determined Telomere length does not affect overall Parkinson´s disease risk

The availability of large datasets from GWA studies and the development of dedicated statistical methods to explore these allows to overcome some of the shortcomings of classic observational epidemiology. Mendelian Randomization (MR) explores estimates of causal effects by using gene variants associated with intermediate phenotypes or exposures as instrumental variables (IV) to estimate the exposure effect on disease risk. It thereby circumvents the limitations of observational epidemiology (Burgess *et al.*, 2013). MR has been used in PD to confirm (Noyce *et al.*, 2017; Pichler *et al.*, 2013; Simon *et al.*, 2014) or refute (Larsson *et al.*, 2017) previous epidemiological evidence on the influence of environmental factors on disease risk.

The initial exploration of a causal relationship between genetically determined TL and PD risk in early 2017 yielded a significant and highly interesting result. Based on the largest, available PD case-control dataset at the time (Nalls *et al.*, 2014), MR analyses indicated that genetically determined *longer* leucocyte telomeres are causally related to an increased risk to develop PD (OR 1.29; 95% CI: 1.05-1.58). A meta-analysis of studies elucidating this relationship via observational epidemiology so far had been inconclusive on a background of substantial heterogeneity (I^2=97%) (Forero *et al.*, 2016). As PD is an age-related condition, the result was however surprising and counterintuitive, since so far ageing (Müezzinler *et al.*, 2013), cognitive decline (Hägg *et al.*, 2017), brain atrophy patterns (Jacobs *et al.*, 2014; King *et al.*, 2014) and neurodegeneration had been associated with *shorter*

TL. For AD, similarly closely associated with advancing age, an association with shorter TL had been shown both by actual TL measurements and MR (Thomas *et al.*, 2008; Zhan *et al.*, 2015).

Nevertheless, the consistency between the significant IVW and MR Egger estimates, together with the signal for directional horizontal pleiotropy indicating a possible underestimation of the effect size, argued for a true, albeit unexpected association.

This prompted further experiments into the underlying biological mechanism. In addition to the need for replication in an independent, large PD case-control GWAS dataset, several conceptional barriers remained: a) it was unknown if peripheral (blood) and brain TL correlate in healthy human controls, i.e. if a blood based genetic analysis relates to changes in central nervous tissue; b) the knowledge on region-specific TL in human brain was scarce (Mamdani *et al.*, 2015), and it was unclear in how far region-specific TL differences relate to PD pathophysiology; c) the temporal dynamics of TL had been studied in human cerebral cortex but not basal ganglia structures, crucially involved in PD pathophysiology.

During the attempts to replicate the peculiar MR results in larger/independent datasets, TL quantification experiments were performed. Importantly, these experiments establish a strong correlation between peripheral blood and brain TL, for which so far there had been only circumstantial evidence from a small number of patients with AD (n=29) (Lukens *et al.*, 2009). This result confirmed that changes in the leucocyte based IV instrument actually reflect brain TL.

There is an apparent link supporting our initial MR results through cancer epidemiology in PD: An MR study on GWAS summary data of 1.5 Mio samples from participants of European ancestry had reported longer TL to significantly increase risk for glioma > ovarian cancer > lung adenocarcinoma > neuroblastoma > bladder

cancer > melanoma > testicular cancer > kidney cancer, whereas risk for other cancers was not significantly associated with TL (Telomeres Mendelian Randomization Collaboration *et al.*, 2017). This is particularly interesting in the context of epidemiological data on cancer risk and PD (Catalá-López *et al.*, 2014; P.-Y. Lin *et al.*, 2015; Ong *et al.*, 2014): Overall, cancer incidence in PD patients is lower than in healthy controls (OR 0.92; 95% CI: 0.91-0.93) (Ong *et al.*, 2014). Nevertheless, a health record-based study from England including 220`000 PD patients and 9Mio. controls suggests that certain types of cancer are more frequent among PD patients, such as brain (RR 1.5, 95% CI: 1.34-1.68), melanoma (RR 1.19, 95% CI: 1.04-1.36) and kidney cancer (RR 1.11, 95% CI: 1.02-1.21) (Ong *et al.*, 2014).

A methodologically robust Taiwanese cohort study, based on 24.7million individuals, used age- and sex-matched systematic random sampling with multivariate regression analysis to show an increased hazard ratio (HR) in PD patients, among others, for malignant brain tumours (HR 3.42, 95% CI: 1.84 – 6.38) > melanoma (HR 2.75, 95% CI: 1.35 – 5.59) > kidney (HR 1.99, 95% CI: 1.54 – 2.57) (P.-Y. Lin *et al.*, 2015). Interestingly, this is the only study that sub-specified the type of lung cancer and showed an actually increased risk for lung-adenocarninoma among PD patients (HR 1.61, 95% CI: 1.35-1.92), which is not smoking-related (P.-Y. Lin *et al.*, 2015).

The similarities in cancers associated with longer TL and the cancers associated with PD (in particular melanoma, brain and kidney cancer and adenocarcinoma of the lung) lend indirect epidemiological support to the preliminary result of *longer* telomeres apparently causing higher PD risk.

In early 2020, finally, replication data sets from both IPDGC and COURAGE-PD became accessible and were assessed to replicate a causal association between TL and PD risk. Using the original and an updated IV instrument based on the latest TL GWAS (Li *et al.*, 2020), IVW as well as MR Egger regression analyses of both datasets provided insignificant results, failing to reproduce the surprising association of longer TL with increased PD risk, even after accounting for considerable heterogeneity. Although the initial, promising result were generated on a considerable number of patients and controls, they ultimately failed to replicate in an even larger dataset. Hence, from the current evidence the genetic predisposition for telomere length is not associated with PD risk.

5.6.2 Age-related Telomere length attrition is unique to the putamen

Telomere length is closely regulated by shortening and elongating processes: in mitotic cells TL decreases with each cell cycle in all somatic cells (Aubert and Lansdorp, 2008). Together with telomerase, a ribonucleoprotein enzyme able to elongate the telomeric sequence (Schmidt and Cech, 2015), telomer maintenance mechanisms tightly regulate TL. The annual LTL attrition from this has been estimated as 20-40 base pairs (bp)/year in human peripheral blood as confirmed by a large meta-analysis (Müezzinler *et al.*, 2013).

The results presented in this work are based on unique, matching human healthy control spleen and brain tissue samples and indicate a physiological attrition of TL in human putamen with advancing age during normal adult life between 20-79 years of age. To support this notion, the results of Southern blot and MMQ-PCR analysis are concordant, based on a robust sample size and of excellent consistency

(overall MMQ-PCR CoV 1.62%). The fact that a negative correlation of TL with advancing age in PUTM did not reach significance in females (male: F=27.97, p<0.0001; female: F=3.09, p=0.09; not shown) is most likely due to a limited number of female samples in this cohort - future studies will have to establish if this effect is an artefact or a true biological effect.

By combining measurements from matching brain and SPL, which were used as a proxy for circulating leucocytes (Takubo *et al.*, 2002), this establishes a positive correlation between blood and putaminal TL in humans. As leucocytes are the only longitudinally proven source for age-related TL attrition in humans (Müezzinler *et al.*, 2013), and given the impossibility to collect longitudinal brain samples in humans, this correlation is a strong indication for actual age-related TL attrition in the human striatum.

This is in contrast to previous reports that did not document age-related changes in TL during adult life from pooled cerebral (Allsopp *et al.*, 1995), occipital cortical samples (Nakamura *et al.*, 2007; Takubo *et al.*, 2002; Tomita et al., 2018) and subcortical samples (supplement in (Mamdani *et al.*, 2015)).

There are at least two possible explanations for this: Previous studies pooled donor samples from infancy and very late adulthood (50-100yrs of age) into the same analyses, extrapolating results for much of the normal adult life span (Allsopp *et al.*, 1995; Nakamura *et al.*, 2007; Takubo *et al.*, 2002). Given that the foetal and infant period is a time of rapid neural growth and development (Paredes *et al.*, 2016), including drastic changes in the degree of myelination (Deoni *et al.*, 2011), known to effect glial TL (Tomita *et al.*, 2018), they should be investigated separately from adult life. Whereas previous studies excel in covering extreme ends of the ageing spectrum (Nakamura *et al.*, 2007; Takubo *et al.*, 2002), the present study provides

an even sample across the normal adult life span, allowing for analyses without the need for extrapolation.

Further, this study is the first to examine TL in a sub-cortical nucleus over age (Allsopp *et al.*, 1995; Nakamura *et al.*, 2007; Takubo *et al.*, 2002; Tomita *et al.*, 2018). A previous study pooled samples from patients with bipolar disorder, major depression and schizophrenia together with healthy controls. Based on qPCR measurements from control samples of variable age (48 ± 13 years SD) and sex (f/m=3/7), this study reported that TL from human midbrain was 24x longer than from prefrontal cortex (Mamdani *et al.*, 2015). This substantially differs from the results presented in this work (Figure 5.6 & Figure 5.7), in which tissue donors were all male and closely matched for age (Table 5.5), and measurements based on both relative (MMQ-PCR) and absolute (Southern blot) quantifications (Figure 5.6 & Figure 5.7). The inclusion of MB samples (relating to red nucleus/medial lemniscus) taken directly from adjacent to the SN, further strengthens the observation that TL does not substantially differ between SN and cortex. Given the closer sample matching, additional absolute quantification, and additional midbrain samples, showing concordant results, a 24x difference as claimed before (Mamdani *et al.*, 2015) appears to be likely erroneous.

At the same time PUTM samples showed the shortest TL in comparison to other brain regions, and the correlation in TL between PUTM and other cortical regions was much weaker than between all other examined brain regions (Figure 5.7).

Taken together, the dynamics of TL in the PUTM fundamentally differ from the other, studied brain regions.

5.6.3 Region-specific Telomere length in human brain follows region-specific Telomere length regulating gene expression

Due to tissue availability, the TL comparison between brain regions was based on two independent cohorts of all male donors of similar age and from the same set of samples and institution. Importantly, the PMI was significantly higher among "infratentorial" samples. Nevertheless, sample characteristics and uniform sample treatment allow a qualitative comparison between "infratentorial" and "CRBL+supratentorial" cohorts. In both set of samples, samples from CRBL showed the longest TL in comparison to SN/MB, respectively PUTM samples. Among "CRBL+supratentorial" samples, OCTX showed significantly longer TL than PUTM, confirming a region-specific pattern of TL across the human brain, but not its absolute differences as reported previously: in particular it refutes the SN to have the longest TL across different CNS tissues (Mamdani *et al.*, 2015).

Exploring detailed gene expression data based on n=114-209 (depending on tissue type) samples from the GTex consortium, the expression of TL regulating genes similarly follows a region- and gene-specific pattern (Figure 5.11 & Figure 5.13). Together with the variable effect size of the respective gene variants on TL (Codd *et al.*, 2013; Li *et al.*, 2020), this region-specific expression appears in concordance with the longest TL identified in the cerebellum.

The reason for a region-specific regulation of TL in the human brain remains speculative, and possible underlying differences in stress response or mitotic activity should be examined by future studies.

5.6.4 Age-related telomere length attrition in the nigro-striatal system – linking age and PD risk?

A previous study that evaluated TL over age in SN showed a clear trend for age-related attrition in a relatively small (n=17) number of healthy controls (Spearman`s r=-0.20, P=0.06; Hudson et al., 2011). Together with the findings from this work, TL dynamics in the nigro-striatal system hence seem to differ substantially from other brain regions (Allsopp *et al.*, 1995; Nakamura *et al.*, 2007; Takubo *et al.*, 2002; Tomita *et al.*, 2018).

As the nigro-striatal system is intricately connected with PD pathophysiology (1.1.4), the discovery of a physiological, age-related TL attrition in the nigro-striatal system, apparently unique among human brain regions, is a potential explanation for the close association between advancing age and PD risk.

There are several possible reasons behind this effect apparently confined to the nigro-striatal system: The putamen is crucially involved in motor control, sensori-motor integration and cognition (Alexander *et al.*, 1990; Lehéricy *et al.*, 2004; Middleton and Strick, 2000), and together with the pallidum and caudate nucleus forms the striatum. It contains the highest neuronal density with a mean glia:neuron ratio of 3.7:1 (Schröder *et al.*, 1975). Medium spiny neurons constitute 95% of striatal neurons with a known selective vulnerability to metabolic stress due to their excessive baseline energy expenditure to maintain cell membrane ion gradients (Calabresi *et al.*, 2000; Mitchell *et al.*, 1999).

Similarly, their extensive arborization and synaptic abundance (Bolam and Pissadaki, 2012) places midbrain dopaminergic neurons under constant metabolic demand (Surmeier, 2007). Oxidative stress has been shown to lead to TL attrition *in vitro* (Zglinicki, 2002) and *in vivo* (Pineda-Pampliega *et al.*, 2020) and chronic

metabolic stress, causing reactive oxygen species, might be one possible explanation for the age-related TL attrition in the nigro-striatal system.

Alternatively, TL attrition in the putamen might be an indicator of on-going mitotic activity in a sub-population of cells in the human striatum. Mitotically active glial cells are a possible source for this and the measurement approaches used in this work indeed cannot differentiate between neuronal and glial cells. It is however unlikely that the TL shortening observed is driven by glial cells, as a quantitative fluorescence in situ hybridization (Q-FISH) study previously did not find age-related attrition in human glial TL across the adult age range (Tomita *et al.*, 2018). It is similarly unlikely that this effect is due to a change in cell numbers, respectively neuron/glia ratio with advancing age, as decreasing numbers with age have only been found for oligodendrocytes, but neither neurons in the human neocortex (Fabricius *et al.*, 2013; Pelvig *et al.*, 2008), nor putamen (Santos-Lobato *et al.*, 2015; Selden *et al.*, 1994).

Even more so, the observation of adult neurogenesis in the human striatum (Ernst *et al.*, 2014) offers a tantalizing, but speculative, possible explanation. Although our observation cannot serve as evidence for (Eriksson *et al.*, 1998; Ernst *et al.*, 2014; Spalding *et al.*, 2013) nor against (Cipriani *et al.*, 2018; Sorrells *et al.*, 2018) human adult striatal neurogenesis, age-related TL attrition is in principle compatible with low level neuronal turnover during adulthood in the striatum (Ernst *et al.*, 2014).

5.6.5 Limitations and Conclusion

It is of course tempting to understand the reason why the seemingly clear signal from the 2014 IPDGC dataset eventually vanished. The data structure between the

2014 vs. 2019 IPDGC summary statistics datasets does differ, as the latter consists of 13 additional cohorts collected since 2014 and a cohort of PD proxy cases, i.e. cases with a definitive positive family history of PD: importantly, the two by far largest sub-cohorts (23andMe: 2448 cases, 571.411 controls; UK BioBank: 18.618 cases, 436.419 controls) were based on self-reported diagnosis (23andMe) and the mentioned proxy cases defined by family history (UK BioBank), and not - like all other cohorts - on clinician assessment based on UK Brain Bank criteria (Table S9). This holds the risk of ascertainment bias, although extensive quality control measures were applied to exclude genetic bias (such as sample duplicates by identity-by-descent filtering, European ancestry through principal-component analysis and overt/cryptical relatedness through proportional sharing) (see supplement (Nalls *et al.*, 2019)). To address this criticism, 23andMe previously had conducted a telemedicine study, in which a neurologist confirmed the diagnosis of PD in 50 out of 50 affected individuals in this cohort (personal communication with Karl Heilbron, 23andMe). Although this was intended to validate the correct attribution of case/control status in this large dataset, scepticism remains, not only as this study remains unpublished.

Of note, several other traits, explored for causal association with PD by colleagues within the IPDGC framework, similarly did not replicate in the IPDGC 2019 dataset after showing promising results in the explorative 2014 IPDGC dataset. A per-cohort analysis, examining telomere length MR signals for each cohort separately, done by Sara Bandres-Ciga at NIH, Bethesda, who had access to individual cohort data, did not provide evidence that the failure to replicate originates from a particular cohort (results not shown). Several additional attempts within the IPDGC framework to identify the reason for this remained unsuccessful.

Ultimately, the reason for the inability to replicate our initial results for the time being remains unsatisfactorily unknown. It nevertheless proves that genetic results, even if based on apparently vast and sound data and adequate methods rely on replication and independent validation.

Regarding the wet lab experiments, quantification using Southern blot or qPCR cannot differentiate between TL attrition in neuronal vs. glial cells. In principal this could influence results, as oligodendroglia are mitotically active and can show TL attrition with human disease (Szebeni *et al.*, 2014). However, as there has been no age-related attrition in human glial TL across the adult age range in a study explicitly differentiating between these cell types and in this age-range using Q-FISH (Tomita *et al.*, 2018), this possibility appears highly unlikely.

Technically, it is unfortunate, that the post-mortem brain samples could not be soured from the same donors, but instead had to be matched in two different groups "CRBL+supratentorial" and "infratentorial", which was due to tissue availability. Comparison between SN, MB and cortical samples (FCTX, OCTX, etc.) hence are only indirectly possible by referencing to CRBL, which is present in both groups.

Given other brain functions are similarly influenced by age, such as memory, it would be interesting to explore if there is an age-related effect on TL in other sub-cortical structures, such as e.g. the hippocampus.

Nevertheless, based on post-mortem corresponding brain and spleen samples and two different quantification techniques, this report provides solid experimental data documenting an age-related attrition of TL in the human putamen, which appears unique for post-mitotic brain tissue. It further shows region-specific TL

dynamics due to the specific expression pattern of TL-regulating genes, offering an explanation for apparent region-specific telomere vulnerability. Although MR experiments failed to show a consistent causal relationship between genetically determined TL with PD risk, this physiological TL attrition in the striatum potentially offers an explantion for the close association between increasing age and risk for PD and other conditions pathophysiologically linked to the striatum.

Conclusion and Future Directions

In this work I report results of experiments aimed at probing the pathophysiological basis of dystonia and its overlap with PD.

This work presents first preliminary evidence for decreased lysosomal activity as a novel disease mechanism across the phenotypic spectrum in dystonia. The applied comprehensive approach of enzyme activity quantification in wbc and brain tissue, as well as full sequencing of the *GBA* gene in a retrospective and a prospective cohort of dystonia patients, implies lysosomal dysfunction in a significant minority of dystonia cases. This is a significant step in unravelling the underlying cause in a condition with a still large proportion of cases of idiopathic, i.e. unknown origin.

In this study I used an approach starting from a common phenotype, applying detailed evaluation leading to a target-gene approach in order to explore the underlying aetiology.

However, a number of questions remain to be answered and necessitate independent replication before lysosomal dysfunction can confidently be added as a confirmed cause of dystonia. Future studies should explore the partial discordance between enzymology and genetic findings in the above results. Based on the results presented in this work, mutations in *GBA* seem to act as a modifier and risk factor for dystonia and not in a mendelian fashion. Further work will therefore need to explore the role of molecular modifiers of GCase activity, such as SCARB2 and TFEB, respectively GCase activators, such as Saposin C (Siebert *et al.*, 2014) in patients with abdnormal enzyme activity but without *GBA* mutation.

From a genetics perspective, replicating an increased OR for *GBA* mutations in an independent dystonia cohort will be key to establish a definitive link. Given the difficult structure of the *GBA* gene, and in particular its proximity to the highly homologous *GBAP* pseudogene, unambiguous identification of GBA will be crucial. In this context it remains to be seen in how far NGS-based technology, such as WES or WGS will yield reliable *GBA* sequencing results. Although this would allow data-mining of large amounts of existing NGS data, the technical problem of adequate differentiation between real and pseudogene seems unsurmountable. Along Sanger sequencing - still the gold sequencing standard - long-read NGS technology such as the Oxford Nanopore MinION might help to facilitate reliable variant identification in larger samples in the future (Leija-Salazar *et al.*, 2019).

Obviously, the post-mortem enzyme activity measurements in patients with and without dystonia should be supplemented with the donor genotype (respective experiments had been planned but had to be cancelled due to the Covid19 pandemic situation and lockdown) to allow better interpretation.

Ultimately, much larger numbers of cases are needed to ascertain the distribution of genetic variants across cohorts of dystonia patients and genetic backgrounds, and ultimately genotype-phenotype correlation.

If lysosomal dysfunction due to GCase deficiency indeed proves to be a cause of dystonia, this opens the future possibility of causal treatment options, such as Ambroxol, an inhibitory chaperone mediating the transport of GCase to the lysosome. A recent non-randomized, non-controlled trial of oral Ambroxol therapy in GBA+ PD patients proved cerebrospinal fluid (CSF) penetration and

engagement with the GCase target (Mullin *et al.*, 2020), a prerequisite for the use of this medication in a potential future dystonia trial.

Furthermore, I used a cross-sectional study of movement disorders in a considerably sized cohort of patients with genetically confirmed mitochondrial disease to explore a common anatomical target of disease pathology. Using detailed phenotyping in conjunction with genetic and volumetric brain imaging data, as well as sporadic brain post-mortem and functional PET imaging data, this report found evidence for cerebellar dysfunction and structural atrophy of the cerebellum, in particular of cerebellar lobule VI and VIIa, as the correlate of movement disorders in patients with mitochondrial disease.

In this part of the work, I used a different approach, starting from a defined molecular aetiology, and explored the common anatomical basis for movement disorders phenotype.

Concurring with the literature, dystonia was the most frequent phenotype in this series of patients. Surprisingly, mitochondrial disease was found to present as isolated dystonia in three cases of writer`s cramp and one further task-specific dystonia in this series. This raises in turn the question how high is the prevalence of mitochondrial disease in focal dystonia? Future studies will have to elucidate this further. A step-wise combination of blood-based routine markers and genetic screening for mitochondrial mutations appears to be the best possible screening tool for large-cohort analyses. Further structural and functional imaging analyses in such a more phenotypically compact series of patients would allow more detailed mechanistic insight into the pathophysiology of focal dystonia.

Finally, I explored the underlying mechanisms behind age-related increased risk for PD using a combination of population genetics and molecular biology methods.

In this chapter I applied a post-GWAS population genetic method on existing, substantial case-control data and supplemented this with wet lab experiments based on post-mortem tissue samples.

Although fascinating initial results based on the largest available GWAS data set at the time indicated a causal role of genetically determined TL on PD risk, we found insufficient evidence for this during replication attempts on two independent even larger data sets. The inability to replicate the initially strong association signal, as for other traits using the same methodology within the IPDGC network, came as a surprise to all of us involved in the process. Although the reason behind this remains unfortunately nebulous, it confirms two fundamental scientific principles that should always be obeyed: "only an independently confirmed association is true" and "try to disprove your hypothesis as thoroughly as possible". In this respect, although unfortunate in terms of publication outcome, this study had been most instructive.

Nevertheless, the wet lab experiments, examining age- and brain region-specific TL and its regulation, offered fascinating novel insights into the dynamics of this age-related physiological process. While I found an explanation for region-specific TL in the expression pattern of TL regulating genes, the reason for the TL attrition with age in the human putamen remains to be explored further.

The finding of an age-related vulnerability of the striatum via telomere biology is a potential explanation for similar age-dependent presentation patterns in conditions anatomically linked to the striatum, such as dystonia.

There have been attempts at studying human age-related changes in gene expression in peripheral blood (Peters *et al.*, 2015) and brain (Ramasamy *et al.*, 2014; Soreq *et al.*, 2017) and the exploration and comparison of gene expression relating to oxidative stress response, telomere maintenance, adult neurogenesis or other mechanisms might yield additional insight into why the regulation of TL within the nigro-striatal system differs from other brain regions. Given the wealth of already existing data from GWAS studies (e.g. within the IPDGC consortium), gene expression databases (GTex, UKBEC, etc.) and other sources, future attempts should aim at connecting the available sources. Alternative post-GWAS computational approaches might yield further insights into a possible genetic explanation behind the strong age-associationg in PD. For example, the Pathway scoring algorithm (PASCAL) extracts gene scores from case-control GWAS summary statistics and corrects for linkage disequilibrium structure (Lamparter *et al.*, 2016). Based on externally defined gene pathways, it then calculates pathway enrichment scores, which could be applied, for example, to genes most consistently regulated with age (Peters *et al.*, 2015). Nevertheless, a definitive answer to the conundrum of age-related incidence of PD still remains to be found.

Abbreviations

α-synuclein (SNCA)

apolipoprotein-E (APOE)

base pairs (bp)

beta-Galactosidase (b-GAL)

Bicinchoninic acid (BCA)

Bovine Serum Albumin (BSA)

Chitotriosidase (CHIT)

chronic progressive external ophthalmoparesis (CPEO)

Cerebellar dentate nucleus (CDN)

cerebellar cortex (CRB)

coefficient of variation (CoV)

control (ctrl)

dopamine-transporter (DaT)

Diffeomorphic Anatomical Registration using Exponentiated Lie algebra (DARTEL)

deoxyribonucleotides (dNTPs)

dideoxynucleotides (ddNTPs)

dopamine-transporter (DaT)

Ethylenediaminetetraacetic acid (EDTA)

Essential Tremor (ET)

Fragile-X tremor ataxia syndrome (FXTAS)

Gaucher`s disease (GD)

Glucocerebrosidase (GCase)

glucosidase acid beta (GBA)

glucosidase acid beta pseudo-gene (GBAP)

Genome-wide association studies (GWAS)

International Parkinson´s Disease Genetics Consortium (IPDGC)

instrumental variables (IV)

inverse-variant weighted (IVW)

Locus coeruleus (LC)

lysosomal storage disorder (LSD)

lysosomal membrane protein 2 (LIMP2)

Mendelian Randomization (MR)

minor allele frequency (MAF)

Mitochondrial disease (MiD)

Mitochondrial encephalomyopathy, lactic acidosis and stroke-like episodes (MELAS)

mitochondrial (mtDNA)

Monochrome multiplex q-PCR (MMQ-PCR)

Montreal Neurological Institute (MNI)

myoclonus epilepsy, ataxia and myopathy with ragged-red fibers (MERFF)

Neuromelanin (NM)

Next generation sequencing (NGS)

nuclear DNA (nDNA)

Pallidum (PALL)

polymerase gamma (POLG)

Polymerase Chain Reaction (PCR)

post-mortem interval (PMI)

Queen Square Brain Bank (QSBB)

Quantitative PCR (qPCR)

Quantitative fluorescence in-situ hybridization (Q-FISH)

reactive oxygen species (ROS)

restriction fragment length polymorphism (RFLP)

Single Telomere Length Analysis (STELA) – single molecule PCR

single nucleotide polymorphisms (SNPs)

Scans Without evidence of Dopaminergic Deficit, SWEDDs

single strand confirmation polymorphism (SSCP)

Statistical parametric mapping (SPM)

Strength independent of the direct effect (InSIDE)

Substantia nigra (SN)

succinate dehydrogenase (SDH)

superior colliculus (SCol)

Telomere repeat fragment (TRF)

tris(hydroxymethyl)amino-methane (TRIS)

Real time PCR (rtPCR)

Telomere restriction fragment (TRF)

United Kingdom Accreditation service (UKAS)

Voxel-based morphometry (VBM)

white blood cell (wbc)

whole exome sequencing (WES)

whole genome sequencing (WGS)

young-onset Parkinson´s disease (YOPD)

References:

Angot E, Steiner JA, Hansen C, Li J-Y, Brundin P. Are synucleinopathies prion-like disorders? The Lancet Neurology 2010; 9: 1128–1138.

Aarsland D, Bronnick K, Williams-Gray C, Weintraub D, Marder K, Kulisevsky J, et al. Mild cognitive impairment in Parkinson disease: a multicenter pooled analysis. Neurology 2010; 75: 1062–1069.

Acosta-Cabronero J, Betts MJ, Cardenas-Blanco A, Yang S, Nestor PJ. In Vivo MRI Mapping of Brain Iron Deposition across the Adult Lifespan. J. Neurosci. 2016; 36: 364–374.

Adler CH. Nonmotor complications in Parkinson's disease. Mov. Disord. 2005; 20 Suppl 11: S23–9.

Aharon-Peretz J, Rosenbaum H, Gershoni-Baruch R. Mutations in the glucocerebrosidase gene and Parkinson's disease in Ashkenazi Jews. N Engl J Med 2004; 351: 1972–1977.

Ahmed Z, Josephs KA, Gonzalez J, DelleDonne A, Dickson DW. Clinical and neuropathologic features of progressive supranuclear palsy with severe pallido-nigro-luysial degeneration and axonal dystrophy. Brain 2008; 131: 460–472.

Albanese A, Bentivoglio AR, Fenici R, Melillo G, Colosimo C, Tonali P. Multiple system atrophy presenting as parkinsonism: clinical features and diagnostic criteria. Journal of Neurology, Neurosurgery & Psychiatry 1995; 59: 144–151.

Albanese A, Bhatia K, Bressman SB, Delong MR, Fahn S, Fung VSC, et al. Phenomenology and classification of dystonia: a consensus update. Mov. Disord. 2013; 28: 863–873.

Alcalay RN, Levy OA, Waters CC, Fahn S, Ford B, Kuo S-H, et al. Glucocerebrosidase activity in Parkinson's disease with and without GBA mutations. Brain 2015; 138: 2648–2658.

Alcalay RN, Wolf P, Levy OA, Kang UJ, Waters C, Fahn S, et al. Alpha galactosidase A activity in Parkinson's disease. Neurobiol. Dis. 2018; 112: 85–90.

Alexander GE, Crutcher MD, DeLong MR. Basal ganglia-thalamocortical circuits: parallel substrates for motor, oculomotor, "prefrontal" and ‘limbic’ functions. Prog. Brain Res. 1990; 85: 119–146.

Alexander SK, Rittman T, Xuereb JH, Bak TH, Hodges JR, Rowe JB. Validation of the new consensus criteria for the diagnosis of corticobasal degeneration. J. Neurol. Neurosurg. Psychiatr. 2014; 85: 925–929.

Alfonso P, Aznarez S, Giralt M, Pocovi M, Giraldo P, Spanish Gaucher's Disease Registry. Mutation analysis and genotype/phenotype relationships of Gaucher disease patients in Spain. J. Hum. Genet. 2007; 52: 391–396.

Allsopp RC, Chang E, Kashefi-Aazam M, Rogaev EI, Piatyszek MA, Shay JW, et al. Telomere shortening is associated with cell division in vitro and in vivo. Exp. Cell Res. 1995; 220: 194–200.

Alston CL, Rocha MC, Lax NZ, Turnbull DM, Taylor RW. The genetics and pathology of mitochondrial disease. J. Pathol. 2017; 241: 236–250.

Appelqvist H, Wäster P, Kågedal K, Öllinger K. The lysosome: from waste bag to potential therapeutic target. J Mol Cell Biol 2013; 5: 214–226.

Arash-Kaps L, Komlosi K, Seegräber M, Diederich S, Paschke E, Amraoui Y, et al. The Clinical and Molecular Spectrum of GM1 Gangliosidosis. J. Pediatr. 2019; 215: 152–157.e3.

Armstrong MJ, Litvan I, Lang AE, Bak TH, Bhatia KP, Borroni B, et al. Criteria for the diagnosis of corticobasal degeneration. Neurology 2013; 80: 496–503.

Asgeirsson H, Jakobsson F, Hjaltason H, Jonsdottir H, Sveinbjörnsdóttir S. Prevalence study of primary dystonia in Iceland. Mov. Disord. 2006; 21: 293–298.

Ashburner J, Friston KJ. Voxel-based morphometry--the methods. Neuroimage 2000; 11: 805–821.

Atashrazm F, Hammond D, Perera G, Dobson-Stone C, Mueller N, Pickford R, et al. Reduced glucocerebrosidase activity in monocytes from patients with Parkinson's disease. Sci Rep 2018; 8: 15446–12.

Aubert G, Lansdorp PM. Telomeres and aging. Physiol. Rev. 2008; 88: 557–579.

Aviv A, Hunt SC, Lin J, Cao X, Kimura M, Blackburn E. Impartial comparative analysis of measurement of leukocyte telomere length/DNA content by Southern blots and qPCR. Nucleic Acids Res. 2011; 39: e134.

Bain HDC, Davidson YS, Robinson AC, Ryan S, Rollinson S, Richardson A, et al. The role of lysosomes and autophagosomes in frontotemporal lobar degeneration. Neuropathol Appl Neurobiol 2019; 45: 244–261.

Balint B, Bhatia KP. Dystonia: an update on phenomenology, classification, pathogenesis and treatment. Curr. Opin. Neurol. 2014; 27: 468–476.

Ballard PA, Tetrud JW, Langston JW. Permanent human parkinsonism due to 1-methyl-4-phenyl-1,2,3,6-tetrahydropyridine (MPTP): seven cases. Neurology 1985; 35: 949–956.

Baloh RH, Salavaggione E, Milbrandt J, Pestronk A. Familial parkinsonism and ophthalmoplegia from a mutation in the mitochondrial DNA helicase twinkle. Arch. Neurol. 2007; 64: 998–1000.

Bargiela D, Shanmugarajah P, Lo C, Blakely EL, Taylor RW, Horvath R, et al. Mitochondrial pathology in progressive cerebellar ataxia. Cerebellum Ataxias 2015; 2: 16.

Barragán-Campos HM, Vallée J-N, Lô D, Barrera-Ramírez CF, Argote-Greene M, Sánchez-Guerrero J, et al. Brain magnetic resonance imaging findings in patients with mitochondrial cytopathies. Arch. Neurol. 2005; 62: 737–742.

Bartzokis G, Tishler TA, Lu PH, Villablanca P, Altshuler LL, Carter M, et al. Brain ferritin iron may influence age- and gender-related risks of neurodegeneration. Neurobiology of Aging 2007; 28: 414–423.

Batla A, Erro R, Stamelou M, Schneider SA, Schwingenschuh P, Ganos C, et al. Patients with scans without evidence of dopaminergic deficit: A long-term follow-up study. Mov. Disord. 2014; 29: 1820–1825.

Bauer E, Toepper M, Gebhardt H, Gallhofer B, Sammer G. The significance of caudate volume for age-related associative memory decline. Brain Res. 2015; 1622: 137–148.

Baumann CR, Held U, Valko PO, Wienecke M, Waldvogel D. Body side and predominant motor features at the onset of Parkinson's disease are linked to motor and nonmotor progression. Mov. Disord. 2014; 29: 207–213.

Bellou V, Belbasis L, Tzoulaki I, Evangelou E, Ioannidis JPA. Environmental risk factors and Parkinson's disease: An umbrella review of meta-analyses. Parkinsonism Relat. Disord. 2016; 23: 1–9.

Bembi B, Zambito Marsala S, Sidransky E, Ciana G, Carrozzi M, Zorzon M, et al. Gaucher‘s disease with Parkinson’s disease: Clinical and pathological aspects. Neurology 2003; 61: 99–101.

Benito-León J, Bermejo-Pareja F, Morales-González JM, Porta-Etessam J, Trincado R, Vega S, et al. Incidence of Parkinson disease and parkinsonism in three elderly populations of central Spain. Neurology 2004; 62: 734–741.

Bennett LL, Mohan D. Gaucher disease and its treatment options. Ann Pharmacother 2013; 47: 1182–1193.

Berg D, Postuma RB, Adler CH, Bloem BR, Chan P, Dubois B, et al. MDS research criteria for prodromal Parkinson's disease. Mov. Disord. 2015; 30: 1600–1611.

Berg D, Postuma RB, Bloem B, Chan P, Dubois B, Gasser T, et al. Time to redefine PD? Introductory statement of the MDS Task Force on the definition of Parkinson's disease. Mov. Disord. 2014; 29: 454–462.

Bernier FP, Boneh A, Dennett X, Chow CW, Cleary MA, Thorburn DR. Diagnostic criteria for respiratory chain disorders in adults and children. Neurology 2002; 59: 1406–1411.

Betarbet R, Sherer TB, MacKenzie G, Garcia-Osuna M, Panov AV, Greenamyre JT. Chronic systemic pesticide exposure reproduces features of Parkinson's disease. Nat Neurosci 2000; 3: 1301–1306.

Beutler E, Gelbart T, Scott CR. Hematologically important mutations: Gaucher disease. Blood Cells, Molecules, and Diseases 2005; 35: 355–364.

Bhatia KP, Marsden CD. The behavioural and motor consequences of focal lesions of the basal ganglia in man. Brain 1994; 117 (Pt 4): 859–876.

Blanchard A, Ea V, Roubertie A, Martin M, Coquart C, Claustres M, et al. DYT6 dystonia: review of the literature and creation of the UMD Locus-Specific Database (LSDB) for mutations in the THAP1 gene. Human Mutation 2011; 32: 1213–1224.

Bolam JP, Pissadaki EK. Living on the edge with too many mouths to feed: why dopamine neurons die. Mov. Disord. 2012; 27: 1478–1483.

Bostan AC, Dum RP, Strick PL. The basal ganglia communicate with the cerebellum. Proc. Natl. Acad. Sci. U.S.A. 2010; 107: 8452–8456.

Bowden J, Davey Smith G, Burgess S. Mendelian randomization with invalid instruments: effect estimation and bias detection through Egger regression. Int J Epidemiol 2015; 44: 512–525.

Bower JH, Maraganore DM, McDonnell SK, Rocca WA. Incidence and distribution of parkinsonism in Olmsted County, Minnesota, 1976-1990. Neurology 1999; 52: 1214–1220.

Bower JH, Maraganore DM, McDonnell SK, Rocca WA. Influence of strict, intermediate, and broad diagnostic criteria on the age- and sex-specific incidence of Parkinson's disease. Mov. Disord. 2000; 15: 819–825.

Braak H, Del Tredici K, Rüb U, de Vos RA, Jansen Steur E, Braak E. Staging of brain pathology related to sporadic Parkinson's disease. Neurobiology of Aging 2003; 24: 197–211.

Braak H, Ghebremedhin E, Rüb U, Bratzke H, Del Tredici K. Stages in the development of Parkinson's disease-related pathology. Cell Tissue Res 2004; 318: 121–134.

Braak H, Del Tredici K. Assessing fetal nerve cell grafts in Parkinson's disease. Nat Med 2008

Brandon BR, Diederich NJ, Soni M, Witte K, Weinhold M, Krause M, et al. Autosomal dominant mutations in POLG and C10orf2: association with late onset chronic progressive external ophthalmoplegia and Parkinsonism in two patients. J Neurol 2013; 260: 1931–1933.

Bras J, Guerreiro R, Hardy J. SnapShot: Genetics of Parkinson’s Disease. CELL 2015; 160: 570–570.e1.

Bras J, Paisan-Ruiz C, Guerreiro R, Ribeiro MH, Morgadinho A, Januario C, et al. Complete screening for glucocerebrosidase mutations in Parkinson disease patients from Portugal. Neurobiology of Aging 2009; 30: 1515–1517.

Brockmann K, Berg D. The significance of GBA for Parkinson's disease. J. Inherit. Metab. Dis. 2014; 37: 643–648.

Brockmann K, Srulijes K, Hauser AK, Schulte C, Csoti I, Gasser T, et al. GBA-associated PD presents with nonmotor characteristics. Neurology 2011; 77: 276–280.

Broer L, Codd V, Nyholt DR, Deelen J, Mangino M, Willemsen G, et al. Meta-analysis of telomere length in 19,713 subjects reveals high heritability, stronger maternal inheritance and a paternal age effect. Eur. J. Hum. Genet. 2013; 21: 1163–1168.

Brun L, Ngu LH, Keng WT, Ch'ng GS, Choy YS, Hwu WL, et al. Clinical and biochemical features of aromatic L-amino acid decarboxylase deficiency. Neurology 2010; 75: 64–71.

Brundin P, Li J-Y, Holton JL, Lindvall O, Revesz T. Research in motion: the enigma of Parkinson's disease pathology spread. Nat. Rev. Neurosci. 2008; 9: 741–745.

Brundin P, Ma J, Kordower JH. How strong is the evidence that Parkinson's disease is a prion disorder? Curr. Opin. Neurol. 2016; 29: 459–466.

Buchman AS, Shulman JM, Nag S, Leurgans SE, Arnold SE, Morris MC, et al. Nigral pathology and parkinsonian signs in elders without Parkinson disease. Ann Neurol. 2012; 71: 258–266.

Bugiani O, Murrell JR, Giaccone G, Hasegawa M, Ghigo G, Tabaton M, et al. Frontotemporal dementia and corticobasal degeneration in a family with a P301S mutation in tau. J. Neuropathol. Exp. Neurol. 1999; 58: 667–677.

Burgess S, Butterworth A, Thompson SG. Mendelian randomization analysis with multiple genetic variants using summarized data. Genet. Epidemiol. 2013; 37: 658–665.

Burke DG, Rahim AA, Waddington SN, Karlsson S, Enquist I, Bhatia K, et al. Increased glucocerebrosidase (GBA) 2 activity in GBA1 deficient mice brains and in Gaucher leucocytes. J. Inherit. Metab. Dis. 2013; 36: 869–872.

Caer M, Viala K, Levy R, Maisonobe T, Chochon F, Lomb s AS, et al. Adult-onset chorea and mitochondrial cytopathy. Mov. Disord. 2005; 20: 490–492.

Cai X, Chen X, Wu S, Liu W, Zhang X, Zhang D, et al. Homozygous mutation of VPS16 gene is responsible for an autosomal recessive adolescent-onset primary dystonia. Sci Rep 2016; 6: 25834.

Calabresi P, Centonze D, Bernardi G. Cellular factors controlling neuronal vulnerability in the brain: a lesson from the striatum. Neurology 2000; 55: 1249–1255.

Camargos S, Scholz S, Simón-Sánchez J, Paisan-Ruiz C, Lewis P, Hernandez D, et al. DYT16, a novel young-onset dystonia-parkinsonism disorder: identification of a segregating mutation in the stress-response protein PRKRA. The Lancet Neurology 2008; 7: 207–215.

Calne DB, Snow BJ, Lee C. Criteria for diagnosing Parkinson's disease. Ann Neurol. 1992; 32 Suppl: S125–7.

Casali C, Bonifati V, Santorelli FM, Casari G, Fortini D, Patrignani A, et al. Mitochondrial myopathy, parkinsonism, and multiple mtDNA deletions in a Sephardic Jewish family. Neurology 2001; 56: 802–805.

Catalá-López F, Suárez-Pinilla M, Suárez-Pinilla P, Valderas JM, Gómez-Beneyto M, Martinez S, et al. Inverse and direct cancer comorbidity in people with central nervous system disorders: a meta-analysis of cancer incidence in 577,013 participants of 50 observational studies. Psychother Psychosom 2014; 83: 89–105.

Cawthon RM. Telomere measurement by quantitative PCR. Nucleic Acids Res. 2002; 30: e47.

Cawthon RM. Telomere length measurement by a novel monochrome multiplex quantitative PCR method. Nucleic Acids Res. 2009; 37: e21–e21.

Cáceres-Redondo MT, Carrillo F, Palomar FJ, Mir P. DYT-1 gene dystonic tremor presenting as a "scan without evidence of dopaminergic deficit". Mov. Disord. 2012; 27: 1469–1469.

Chahine LM, Qiang J, Ashbridge E, Minger J, Yearout D, Horn S, et al. Clinical and Biochemical Differences in Patients Having Parkinson Disease With vs Without GBAMutations. JAMA Neurol 2013; 70: 852–7.

Chan CS, Guzman JN, Ilijic E, Mercer JN, Rick C, Tkatch T, et al. 'Rejuvenation“ protects neurons in mouse models of Parkinson”s disease. Nature 2007; 447: 1081–1086.

Charlesworth G, Bhatia KP, Wood NW. The genetics of dystonia: new twists in an old tale. Brain 2013; 136: 2017–2037.

Charlesworth G, Plagnol V, Holmström KM, Bras J, Sheerin U-M, Preza E, et al. Mutations in ANO3 cause dominant craniocervical dystonia: ion channel implicated in pathogenesis. Am. J. Hum. Genet. 2012; 91: 1041–1050.

Chérin P, Rose C, de Roux-Serratrice C, Tardy D, Dobbelaere D, Grosbois B, et al. The neurological manifestations of Gaucher disease type 1: the French Observatoire on Gaucher disease (FROG). J. Inherit. Metab. Dis. 2010; 33: 331–338.

Chiasserini D, Paciotti S, Eusebi P, Persichetti E, Tasegian A, Kurzawa-Akanbi M, et al. Selective loss of glucocerebrosidase activity in sporadic Parkinson's disease and dementia with Lewy bodies. Mol Neurodegener 2015; 10: 15.

Chinnery PF, Hudson G. Mitochondrial genetics. Br. Med. Bull. 2013; 106: 135–159.

Cilia R, Reale C, Castagna A, Nasca A, Muzi-Falconi M, Barzaghi C, et al. Novel DYT11 gene mutation in patients without dopaminergic deficit (SWEDD) screened for dystonia. Neurology 2014; 83: 1155–1162.

Cipriani S, Ferrer I, Aronica E, Kovacs GG, Verney C, Nardelli J, et al. Hippocampal Radial Glial Subtypes and Their Neurogenic Potential in Human Fetuses and Healthy and Alzheimer's Disease Adults. Cereb. Cortex 2018; 28: 2458–2478.

Clark LN, Kartsaklis LA, Wolf Gilbert R, Dorado B, Ross BM, Kisselev S, et al. Association of glucocerebrosidase mutations with dementia with lewy bodies. Arch. Neurol. 2009; 66: 578–583.

Clark LN, Ross BM, Wang Y, Mejia-Santana H, Harris J, Louis ED, et al. Mutations in the glucocerebrosidase gene are associated with early-onset Parkinson disease. Neurology 2007; 69: 1270–1277.

Codd V, Nelson CP, Albrecht E, Mangino M, Deelen J, Buxton JL, et al. Identification of seven loci affecting mean telomere length and their association with disease. Nat. Genet. 2013; 45: 422–7– 427e1–2.

Collins SJ, Ahlskog JE, Parisi JE, Maraganore DM. Progressive supranuclear palsy: neuropathologically based diagnostic clinical criteria. Journal of Neurology, Neurosurgery & Psychiatry 1995; 58: 167–173.

Collier TJ, Kanaan NM, Kordower JH. Aging and Parkinson's disease: Different sides of the same coin? Mov. Disord. 2017; 32: 983–990.

Constantinescu R, Richard I, Kurlan R. Levodopa responsiveness in disorders with parkinsonism: A review of the literature. Mov. Disord. 2007; 22: 2141–2148.

Corral-Debrinski M, Horton T, Lott MT, Shoffner JM, Beal MF, Wallace DC. Mitochondrial DNA deletions in human brain: regional variability and increase with advanced age. Nat. Genet. 1992; 2: 324–329.

Coutinho MF, Alves S. From rare to common and back again: 60years of lysosomal dysfunction. Molecular Genetics and Metabolism 2015; 0

Davidzon G, Greene P, Mancuso M, Klos KJ, Ahlskog JE, Hirano M, et al. Early-onset familial parkinsonism due to POLGmutations. Ann Neurol. 2006; 59: 859–862.

Dash D, Pandey S. Movement disorders associated with neuronal antibodies. Acta Neurologica Scandinavica 2019; 139: 106–117.

De Duve C, Pressman BC, Gianetto R, Wattiaux R, Appelmans F. Tissue fractionation studies. 6. Intracellular distribution patterns of enzymes in rat-liver tissue. Biochem. J. 1955; 60: 604–617.

de Lau LM, Breteler MM. Epidemiology of Parkinson's disease. The Lancet Neurology 2006; 5: 525–535.

de Lau LML, Giesbergen PCLM, de Rijk MC, Hofman A, Koudstaal PJ, Breteler MMB. Incidence of parkinsonism and Parkinson disease in a general population: the Rotterdam Study. Neurology 2004; 63: 1240–1244.

Debray F-G, Lambert M, Lortie A, Vanasse M, Mitchell GA. Long-term outcome of Leigh syndrome caused by the NARP-T8993C mtDNA mutation. Am. J. Med. Genet. A 2007; 143A: 2046–2051.

Del Tredici K, Braak H. Review: Sporadic Parkinson's disease: development and distribution of α-synuclein pathology. Neuropathol Appl Neurobiol 2016; 42: 33–50.

Deoni SCL, Mercure E, Blasi A, Gasston D, Thomson A, Johnson M, et al. Mapping infant brain myelination with magnetic resonance imaging. Journal of Neuroscience 2011; 31: 784–791.

de Carvalho Aguiar P, Sweadner KJ, Penniston JT, Zaremba J, Liu L, Caton M, et al. Mutations in the Na+/K+ -ATPase alpha3 gene ATP1A3 are associated with rapid-onset dystonia parkinsonism. Neuron 2004; 43: 169–175.

Dick FD, De Palma G, Ahmadi A, Scott NW, Prescott GJ, Bennett J, et al. Environmental risk factors for Parkinson's disease and parkinsonism: the Geoparkinson study. Occup Environ Med 2007; 64: 666–672.

DiMauro S, Schon EA, Carelli V, Hirano M. The clinical maze of mitochondrial neurology. Nat Rev Neurol 2013; 9: 429–444.

Dolhun R, Presant EM, Hedera P. Novel polymerase gamma (POLG1) gene mutation in the linker domain associated with parkinsonism. BMC Neurol 2013; 13: 92.

Dupuis JP, Bioulac BH, Baufreton J. Long-term depression at distinct glutamatergic synapses in the basal ganglia. Rev Neurosci 2014; 25: 741–754.

Eblan MJ, Walker JM, Sidransky E. The glucocerebrosidase gene and Parkinson's disease in Ashkenazi Jews. N Engl J Med 2005; 352: 728–31– author reply 728–31.

Ebrahimi-Fakhari D, Hildebrandt C, Davis PE, Rodan LH, Anselm I, Bodamer O. The Spectrum of Movement Disorders in Childhood-Onset Lysosomal Storage Diseases. Mov Disord Clin Pract 2018; 5: 149–155.

Eickhoff SB, Stephan KE, Mohlberg H, Grefkes C, Fink GR, Amunts K, et al. A new SPM toolbox for combining probabilistic cytoarchitectonic maps and functional imaging data. Neuroimage 2005; 25: 1325–1335.

Elbers CC, Garcia ME, Kimura M, Cummings SR, Nalls MA, Newman AB, et al. Comparison between southern blots and qPCR analysis of leukocyte telomere length in the health ABC study. GERONA 2014; 69: 527–531.

Ellard S, Charlton R, Yau S, Gokhale D, Taylor GR, Wllace A, et al. Practice guidelines for Sanger Sequencing Analysis and Interpretation. 2016.

Eriksson PS, Perfilieva E, Björk-Eriksson T, Alborn AM, Nordborg C, Peterson DA, et al. Neurogenesis in the adult human hippocampus. Nat Med 1998; 4: 1313–1317.

Erro R, Schneider SA, Stamelou M, Quinn NP, Bhatia KP. What do patients with scans without evidence of dopaminergic deficit (SWEDD) have? New evidence and continuing controversies. Journal of Neurology, Neurosurgery & Psychiatry 2016; 87: 319–323.

Ernst A, Alkass K, Bernard S, Salehpour M, Perl S, Tisdale J, et al. Neurogenesis in the Striatum of the Adult Human Brain. CELL 2014; 156: 1072–1083.

Eskow Jaunarajs KL, Bonsi P, Chesselet MF, Standaert DG, Pisani A. Striatal cholinergic dysfunction as a unifying theme in the pathophysiology of dystonia. Prog. Neurobiol. 2015; 127-128: 91–107.

Evatt ML, Freeman A, Factor S. Adult-onset dystonia. Handb Clin Neurol 2011; 100: 481–511.

Ewing B, Green P. Base-calling of automated sequencer traces using phred. II. Error probabilities. Genome Res. 1998; 8: 186–194.

Fabricius K, Jacobsen JS, Pakkenberg B. Effect of age on neocortical brain cells in 90+ year old human females--a cell counting study. Neurobiology of Aging 2013; 34: 91–99.

Fabry J. Ein Beitrag zur Kenntniss der Purpura haemorrhagica nodularis (Purpura papulosa haemorrhagica Hebrae). Arch. Dermatol. Res. 1898: 178–200.

Fanciulli A, Wenning GK. Multiple-System Atrophy. N Engl J Med 2015; 372: 249–263.

Fearnley JM, Lees AJ. Ageing and Parkinson's disease: substantia nigra regional selectivity. Brain 1991; 114 (Pt 5): 2283–2301.

Feigin A, Tang C, Ma Y, Mattis P, Zgaljardic D, Guttman M, et al. Thalamic metabolism and symptom onset in preclinical Huntington's disease. Brain 2007; 130: 2858–2867.

Fernandes HJR, Hartfield EM, Christian HC, Emmanoulidou E, Zheng Y, Booth H, et al. ER Stress and Autophagic Perturbations Lead to Elevated Extracellular α-Synuclein in GBA-N370S Parkinson's iPSC-Derived Dopamine Neurons. Stem Cell Reports 2016; 6: 342–356.

Ferreira M, Massano J. An updated review of Parkinson's disease genetics and clinicopathological correlations. Acta Neurologica Scandinavica 2016: 1–12.

Filip P, Gallea C, Lehéricy S, Bertasi E, Popa T, Mareček R, et al. Disruption in cerebellar and basal ganglia networks during a visuospatial task in cervical dystonia. Mov. Disord. 2017; 32: 757–768.

Filip P, Lungu OV, Bareš M. Dystonia and the cerebellum: a new field of interest in movement disorders? Clin Neurophysiol 2013; 124: 1269–1276.

Finsterer J. Leigh and Leigh-like syndrome in children and adults. Pediatric Neurology 2008; 39: 223–235.

Finsterer J, Harbo HF, Baets J, Van Broeckhoven C, Di Donato S, Fontaine B, et al. EFNS guidelines on the molecular diagnosis of mitochondrial disorders. Eur. J. Neurol. 2009; 16: 1255–1264.

Flønes IH, Fernandez-Vizarra E, Lykouri M, Brakedal B, Skeie GO, Miletic H, et al. Neuronal complex I deficiency occurs throughout the Parkinson's disease brain, but is not associated with neurodegeneration or mitochondrial DNA damage. Acta Neuropathol 2018; 135: 409–425.

Forero DA, González-Giraldo Y, López-Quintero C, Castro-Vega LJ, Barreto GE, Perry G. Telomere length in Parkinson's disease: A meta-analysis. EXG 2016; 75: 53–55.

Frei K, Truong DD, Fahn S, Jankovic J, Hauser RA. The nosology of tardive syndromes. J. Neurol. Sci. 2018; 389: 10–16.

Frucht S, Fahn S, Chin S, Dhawan V, Eidelberg D. Levodopa-induced dyskinesias in autopsy-proven cortical-basal ganglionic degeneration. Mov. Disord. 2000; 15: 340–343.

Fuchs T, Saunders-Pullman R, Masuho I, Luciano MS, Raymond D, Factor S, et al. Mutations in GNAL cause primary torsion dystonia. Nat. Genet. 2013; 45: 88–92.

Fung VSC, Jinnah HA, Bhatia K, Vidailhet M. Assessment of patients with isolated or combined dystonia: an update on dystonia syndromes. Mov. Disord. 2013; 28: 889–898.

Gallagher DA, Lees AJ, Schrag A. What are the most important nonmotor symptoms in patients with Parkinson's disease and are we missing them? Mov. Disord. 2010; 25: 2493–2500.

Gan-Or Z, Amshalom I, Kilarski LL, Bar-Shira A, Gana-Weisz M, Mirelman A, et al. Differential effects of severe vs mild GBA mutations on Parkinson disease. Neurology 2015; 84: 880–887.

Gan-Or Z, Giladi N, Orr-Urtreger A. Differential phenotype in Parkinson's disease patients with severe versus mild GBA mutations. Brain 2009; 132: e125.

Gan-Or Z, Giladi N, Rozovski U, Shifrin C, Rosner S, Gurevich T, et al. Genotype-phenotype correlations between GBA mutations and Parkinson disease risk and onset. Neurology 2008; 70: 2277–2283.

Ganos C, Kassavetis P, Erro R, Edwards MJ, Rothwell J, Bhatia KP. The role of the cerebellum in the pathogenesis of cortical myoclonus. Mov. Disord. 2014; 29: 437–443.

Gardner M, Bann D, Wiley L, Cooper R, Hardy R, Nitsch D, et al. Gender and telomere length: systematic review and meta-analysis. Exp. Gerontol. 2014; 51: 15–27.

Gaucher P. De l'epithelioma primitif de la rate (MD thesis). 1882

Gegg ME, Burke D, Heales SJR, Cooper JM, Hardy J, Wood NW, et al. Glucocerebrosidase deficiency in substantia nigra of parkinson disease brains. Ann Neurol. 2012; 72: 455–463.

Gelb DJ, Oliver E, Gilman S. Diagnostic criteria for Parkinson disease. Arch. Neurol. 1999; 56: 33–39.

Gibb WR, Lees AJ. The significance of the Lewy body in the diagnosis of idiopathic Parkinson's disease. Neuropathol Appl Neurobiol 1989; 15: 27–44.

Gibb WR, Lees AJ. Anatomy, pigmentation, ventral and dorsal subpopulations of the substantia nigra, and differential cell death in Parkinson's disease. Journal of Neurology, Neurosurgery & Psychiatry 1991; 54: 388–396.

Gilman S, Wenning GK, Low PA, Brooks DJ, Mathias CJ, Trojanowski JQ, et al. Second consensus statement on the diagnosis of multiple system atrophy. Neurology 2008; 71: 670–676.

Goker-Alpan O, Lopez G, Vithayathil J, Davis J, Hallett M, Sidransky E. The spectrum of parkinsonian manifestations associated with glucocerebrosidase mutations. Arch. Neurol. 2008; 65: 1353–1357.

Goker-Alpan O, Stubblefield BK, Giasson BI, Sidransky E. Glucocerebrosidase is present in α-synuclein inclusions in Lewy body disorders. Acta Neuropathol 2010; 120: 641–649.

Goodwin S, McPherson JD, McCombie WR. Coming of age: ten years of next-generation sequencing technologies. Nature Publishing Group 2016; 17: 333–351.

Goto S, Kawarai T, Morigaki R, Okita S, Koizumi H, Nagahiro S, et al. Defects in the striatal neuropeptide Y system in X-linked dystonia-parkinsonism. Brain 2013; 136: 1555–1567.

Goto S, Lee LV, Munoz EL, Tooyama I, Tamiya G, Makino S, et al. Functional anatomy of the basal ganglia in X-linked recessive dystonia-parkinsonism. Ann Neurol. 2005; 58: 7–17.

Grabowski GA. Phenotype, diagnosis, and treatment of Gaucher's disease. Lancet 2008; 372: 1263–1271.

Grijalvo-Perez A, Litvan I. Corticobasal Degeneration. Semin Neurol 2014; 34: 160–173.

Groen J, van Rootselaar A-F, van der Salm SMA, Bloem BR, Tijssen M. A new familial syndrome with dystonia and lower limb action myoclonus. Mov. Disord. 2011; 26: 896–900.

Guerreiro R, Ross OA, Kun-Rodrigues C, Hernandez DG, Orme T, Eicher JD, et al. Investigating the genetic architecture of dementia with Lewy bodies: a two-stage genome-wide association study. The Lancet Neurology 2018; 17: 64–74.

Guo Y, He W, Boer AM, Wevers RA, de Bruijn AM, Groener JE, et al. Elevated plasma chitotriosidase activity in various lysosomal storage disorders. J. Inherit. Metab. Dis. 1995; 18: 717–722.

Hägg S, Zhan Y, Karlsson R, Gerritsen L, Ploner A, van der Lee SJ, et al. Short telomere length is associated with impaired cognitive performance in European ancestry cohorts. Transl Psychiatry 2017; 7: e1100.

Hallett M. Neurophysiology of dystonia: The role of inhibition. Neurobiol. Dis. 2011; 42: 177–184.

Hanna MG, Bhatia KP. Movement disorders and mitochondrial dysfunction. Current Opinion in Neurology 1997; 10: 351–356.

Hanssen H, Heldmann M, Prasuhn J, Tronnier V, Rasche D, Diesta CC, et al. Basal ganglia and cerebellar pathology in X-linked dystonia-parkinsonism. Brain 2018; 141: 2995–3008.

Hers HG. Alpha-glucosidase deficiency in generalized glycogen storage disease (Pompe's disease). Biochem. J. 1963: 11–16.

Herskind AM, McGue M, Holm NV, Sørensen TI, Harvald B, Vaupel JW. The heritability of human longevity: a population-based study of 2872 Danish twin pairs born 1870-1900. Hum. Genet. 1996; 97: 319–323.

Hervé D. Identification of a specific assembly of the g protein golf as a critical and regulated module of dopamine and adenosine-activated cAMP pathways in the striatum. Front Neuroanat 2011; 5: 48.

Holmes AL, Forcelli PA, DesJardin JT, Decker AL, Teferra M, West EA, et al. Superior colliculus mediates cervical dystonia evoked by inhibition of the substantia nigra pars reticulata. Journal of Neuroscience 2012; 32: 13326–13332.

Honig LS, Kang MS, Schupf N, Lee JH, Mayeux R. Association of shorter leukocyte telomere repeat length with dementia and mortality. Arch. Neurol. 2012; 69: 1332–1339.

Horowitz M, Pasmanik-Chor M, Ron I, Kolodny EH. The enigma of the E326K mutation in acid β-glucocerebrosidase. Molecular Genetics and Metabolism 2011; 104: 35–38.

Horowitz M, Wilder S, Horowitz Z, Reiner O, Gelbart T, Beutler E. The human glucocerebrosidase gene and pseudogene: structure and evolution. Genomics 1989; 4: 87–96.

Horvath R, Kley RA, Lochmuller H, Vorgerd M. Parkinson syndrome, neuropathy, and myopathy caused by the mutation A8344G (MERRF) in tRNALys. Neurology 2007; 68: 56–58.

Hruska KS, LaMarca ME, Scott CR, Sidransky E. Gaucher disease: mutation and polymorphism spectrum in the glucocerebrosidase gene (GBA). Human Mutation 2008; 29: 567–583.

Hudson G, Faini D, Stutt A, Eccles M, Robinson L, Burn DJ, et al. No evidence of substantia nigra telomere shortening in Parkinson's disease. Neurobiology of Aging 2011; 32: 2107.e3–5.

Hudson G, Schaefer AM, Taylor RW, Tiangyou W, Gibson A, Venables G, et al. Mutation of the linker region of the polymerase gamma-1 (POLG1) gene associated with progressive external ophthalmoplegia and Parkinsonism. Arch. Neurol. 2007; 64: 553–557.

Hughes AJ, Daniel SE, Ben-Shlomo Y, Lees AJ. The accuracy of diagnosis of parkinsonian syndromes in a specialist movement disorder service. Brain 2002; 125: 861–870.

Husárová I, Lungu OV, Mareček R, Mikl M, Gescheidt T, Krupa P, et al. Functional imaging of the cerebellum and basal ganglia during predictive motor timing in early Parkinson's disease. J Neuroimaging 2014; 24: 45–53.

Im SY, Kim YE, Kim YJ. Genetics of Progressive Supranuclear Palsy. J Mov Disord 2015; 8: 122–129.

International Parkinson Disease Genomics Consortium, Nalls MA, Plagnol V, Hernandez DG, Sharma M, Sheerin U-M, et al. Imputation of sequence variants for identification of genetic risks for Parkinson's disease: a meta-analysis of genome-wide association studies. Lancet 2011; 377: 641–649.

Invernizzi F, Varanese S, Thomas A, Carrara F, Onofrj M, Zeviani M. Two novel POLG1 mutations in a patient with progressive external ophthalmoplegia, levodopa-responsive pseudo-orthostatic tremor and parkinsonism. Neuromuscul. Disord. 2008; 18: 460–464.

Irani SR, Michell AW, Lang B, Pettingill P, Waters P, Johnson MR, et al. Faciobrachial dystonic seizures precede Lgi1 antibody limbic encephalitis. Ann Neurol. 2011; 69: 892–900.

Jacobs EG, Epel ES, Lin J, Blackburn EH, Rasgon NL. Relationship between leukocyte telomere length, telomerase activity, and hippocampal volume in early aging. JAMA Neurol 2014; 71: 921–923.

Jackson MJ, Schaefer JA, Johnson MA, Morris AA, Turnbull DM, Bindoff LA. Presentation and clinical investigation of mitochondrial respiratory chain disease. A study of 51 patients. Brain 1995; 118 (Pt 2): 339–357.

Jacobs EG, Epel ES, Lin J, Blackburn EH, Rasgon NL. Relationship between leukocyte telomere length, telomerase activity, and hippocampal volume in early aging. JAMA Neurol 2014; 71: 921–923.

Jain IH, Zazzeron L, Goli R, Alexa K, Schatzman-Bone S, Dhillon H, et al. Hypoxia as a therapy for mitochondrial disease. Science 2016; 352: 54–61.

Janavs JL, Aminoff MJ. Dystonia and chorea in acquired systemic disorders. Journal of Neurology, Neurosurgery & Psychiatry 1998; 65: 436–445.

Jeanclos E, Schork NJ, Kyvik KO, Kimura M, Skurnick JH, Aviv A. Telomere length inversely correlates with pulse pressure and is highly familial. Hypertension 2000; 36: 195–200.

Jia X, Liang P, Li Y, Shi L, Wang D, Li K. Longitudinal Study of Gray Matter Changes in Parkinson Disease. AJNR Am J Neuroradiol 2015; 36: 2219–2226.

Jinnah HA, Neychev V, Hess EJ. The Anatomical Basis for Dystonia: The Motor Network Model. Tremor Other Hyperkinet Mov (N Y) 2017; 7: 506.

Josephs KA, Katsuse O, Beccano-Kelly DA, Lin W-L, Uitti RJ, Fujino Y, et al. Atypical progressive supranuclear palsy with corticospinal tract degeneration. J. Neuropathol. Exp. Neurol. 2006; 65: 396–405.

Jung HH, Danek A, Walker RH. Neuroacanthocytosis syndromes. Orphanet J Rare Dis 2011; 6: 68.

Kaji R, Bhatia K, Graybiel AM. Pathogenesis of dystonia: is it of cerebellar or basal ganglia origin? J. Neurol. Neurosurg. Psychiatr. 2018; 89: 488–492.

Kanazawa M, Shimohata T, Toyoshima Y, Tada M, Kakita A, Morita T, et al. Cerebellar involvement in progressive supranuclear palsy: A clinicopathological study. Mov. Disord. 2009; 24: 1312–1318.

Karimi M, Perlmutter JS. The role of dopamine and dopaminergic pathways in dystonia: insights from neuroimaging. Tremor Other Hyperkinet Mov (N Y) 2015; 5: 280.

Kägi G, Klein C, Wood NW, Schneider SA, Pramstaller PP, Tadic V, et al. Nonmotor symptoms in Parkin gene-related parkinsonism. Mov. Disord. 2010; 25: 1279–1284.

Kaushik S, Cuervo AM. Proteostasis and aging. Nature Medicine 2015; 21: 1406–1415.

King KS, Kozlitina J, Rosenberg RN, Peshock RM, McColl RW, Garcia CK. Effect of leukocyte telomere length on total and regional brain volumes in a large population-based cohort. JAMA Neurol 2014; 71: 1247–1254.

Kume K, Kikukawa M, Hanyu H, Takata Y, Umahara T, Sakurai H, et al. Telomere length shortening in patients with dementia with Lewy bodies. Eur. J. Neurol. 2012; 19: 905–910.

Klapper W, Parwaresch R, Krupp G. Telomere biology in human aging and aging syndromes. Mech. Ageing Dev. 2001; 122: 695–712.

Koga S, Aoki N, Uitti RJ, van Gerpen JA, Cheshire WP, Josephs KA, et al. When DLB, PD, and PSP masquerade as MSA: an autopsy study of 134 patients. Neurology 2015; 85: 404–412.

Kompoliti K, Goetz CG, Boeve BF, Maraganore DM, Ahlskog JE, Marsden CD, et al. Clinical presentation and pharmacological therapy in corticobasal degeneration. Arch. Neurol. 1998; 55: 957–961.

Koprivica V, Stone DL, Park JK, Callahan M, Frisch A, Cohen IJ, et al. Analysis and Classification of 304 Mutant Alleles in Patients with Type 1 and Type 3 Gaucher Disease. The American Journal of Human Genetics 2000; 66: 1777–1786.

Korczyn AD. Vascular parkinsonism--characteristics, pathogenesis and treatment. Nat Rev Neurol 2015; 11: 319–326.

Kordower JH, Chu Y, Hauser RA, Freeman TB, Olanow CW. Lewy body-like pathology in long-term embryonic nigral transplants in Parkinson's disease. Nature Medicine 2008; 14: 504–506.

Köroğlu Ç, Baysal L, Cetinkaya M, Karasoy H, Tolun A. DNAJC6 is responsible for juvenile parkinsonism with phenotypic variability. Parkinsonism Relat. Disord. 2013; 19: 320–324.

Kramer ML, Schulz-Schaeffer WJ. Presynaptic alpha-synuclein aggregates, not Lewy bodies, cause neurodegeneration in dementia with Lewy bodies. J. Neurosci. 2007; 27: 1405–1410.

Kurian MA, Zhen J, Cheng S-Y, Li Y, Mordekar SR, Jardine P, et al. Homozygous loss-of-function mutations in the gene encoding the dopamine transporter are associated with infantile parkinsonism-dystonia. J. Clin. Invest. 2009; 119: 1595–1603.

Lacerda L, Amaral O, Pinto R, Oliveira P, Aerts J, Sá Miranda MC. Gaucher disease: N370S glucocerebrosidase gene frequency in the Portuguese population. Clin. Genet. 1994; 45: 298–300.

Lamparter D, Marbach D, Rueedi R, Kutalik Z, Bergmann S. Fast and Rigorous Computation of Gene and Pathway Scores from SNP-Based Summary Statistics. PLoS Comput. Biol. 2016; 12: e1004714.

Langston JW, Ballard PA. Parkinson's disease in a chemist working with 1-methyl-4-phenyl-1,2,5,6-tetrahydropyridine. N Engl J Med 1983; 309: 310.

Lang AE, Lozano AM. Parkinson's disease. First of two parts. N Engl J Med 1998; 339: 1044–1053.

Langston JW, Ballard PA. Parkinson's disease in a chemist working with 1-methyl-4-phenyl-1,2,5,6-tetrahydropyridine. N Engl J Med 1983; 309: 310.

Larsson SC, Singleton AB, Nalls MA, Richards JB, International Parkinson's Disease Genomics Consortium (IPDGC). No clear support for a role for vitamin D in Parkinson's disease: A Mendelian randomization study. Mov. Disord. 2017; 32: 1249–1252.

Leehey MA, Hagerman PJ. Fragile X-associated tremor/ataxia syndrome. Handb Clin Neurol 2012; 103: 373–386.

Lees AJ, Hardy J, Revesz T. Parkinson's disease. Lancet 2009; 373: 2055–2066.

Lehéricy S, Ducros M, Van de Moortele P-F, Francois C, Thivard L, Poupon C, et al. Diffusion tensor fiber tracking shows distinct corticostriatal circuits in humans. Ann Neurol. 2004; 55: 522–529.

Leija-Salazar M, Sedlazeck FJ, Toffoli M, Mullin S, Mokretar K, Athanasopoulou M, et al. Evaluation of the detection of GBA missense mutations and other variants using the Oxford Nanopore MinION. Mol Genet Genomic Med 2019; 7: e564.

Lesage S, Anheim M, Condroyer C, Pollak P, Durif F, Dupuits C, et al. Large-scale screening of the Gaucher‘s disease-related glucocerebrosidase gene in Europeans with Parkinson’s disease. Human Molecular Genetics 2010; 20: 202–210.

Lesage S, Drouet V, Majounie E, Deramecourt V, Jacoupy M, Nicolas A, et al. Loss of VPS13C Function in Autosomal-Recessive Parkinsonism Causes Mitochondrial Dysfunction and Increases PINK1/Parkin-Dependent Mitophagy. Am. J. Hum. Genet. 2016; 98: 500–513.

Leuzzi V, Carducci C, Carducci C, Cardona F, Artiola C, Antonozzi I. Autosomal dominant GTP-CH deficiency presenting as a dopa-responsive myoclonus-dystonia syndrome. Neurology 2002; 59: 1241–1243.

Levy D, Neuhausen SL, Hunt SC, Kimura M, Hwang S-J, Chen W, et al. Genome-wide association identifies OBFC1 as a locus involved in human leukocyte telomere biology. Proc. Natl. Acad. Sci. U.S.A. 2010; 107: 9293–9298.

Lewy FH. Paralysis agitans I. Pathologische Anatomie. In: Lewandowsky M, editor(s). Handbuch der Neurologie. Berlin: 1920. p. 920.

Li J-Y, Englund E, Holton JL, Soulet D, Hagell P, Lees AJ, et al. Lewy bodies in grafted neurons in subjects with Parkinson's disease suggest host-to-graft disease propagation. Nat Med 2008; 14: 501–503.

Li Y, Li P, Liang H, Zhao Z, Hashimoto M, Wei J. Gaucher-Associated Parkinsonism. Cell Mol Neurobiol 2015; 35: 755–761.

Li C, Stoma S, Lotta LA, Warner S, Albrecht E, Allione A, et al. Genome-wide Association Analysis in Humans Links Nucleotide Metabolism to Leukocyte Telomere Length. Am. J. Hum. Genet. 2020; 106: 389–404.

Liang C, Ahmad K, Sue CM. The broadening spectrum of mitochondrial disease: shifts in the diagnostic paradigm. Biochim. Biophys. Acta 2014; 1840: 1360–1367.

Lindsey J, McGill NI, Lindsey LA, Green DK, Cooke HJ. In vivo loss of telomeric repeats with age in humans. Mutation Research - Fundamental and Molecular Mechanisms of Mutagenesis 1991; 256: 45–48.

Lin MT, Beal MF. Mitochondrial dysfunction and oxidative stress in neurodegenerative diseases. Nature 2006; 443: 787–795.

Lin P-Y, Chang S-N, Hsiao T-H, Huang B-T, Lin C-H, Yang P-C. Association Between Parkinson Disease and Risk of Cancer in Taiwan. JAMA Oncol 2015; 1: 633–640.

Litvan I, Agid Y, Calne D, Campbell G, Dubois B, Duvoisin RC, et al. Clinical research criteria for the diagnosis of progressive supranuclear palsy (Steele-Richardson-Olszewski syndrome): report of the NINDS-SPSP international workshop. Neurology 1996; 47: 1–9.

Litvan I, Bhatia KP, Burn DJ, Goetz CG, Lang AE, McKeith I, et al. Movement Disorders Society Scientific Issues Committee report: SIC Task Force appraisal of clinical diagnostic criteria for Parkinsonian disorders. 2003. p. 467–486.

Liu S-Y, Wu J-J, Zhao J, Huang S-F, Wang Y-X, Ge J-J, et al. Onset-related subtypes of Parkinson's disease differ in the patterns of striatal dopaminergic dysfunction: A positron emission tomography study. Parkinsonism Relat. Disord. 2015; 21: 1448–1453.

Lohr KM, Masoud ST, Salahpour A, Miller GW. Membrane transporters as mediators of synaptic dopamine dynamics: implications for disease. Eur J Neurosci 2016: 1–14.

Lopez G, Bayulkem K, Hallett M. Progressive supranuclear palsy (PSP): Richardson syndrome and other PSP variants. Acta Neurologica Scandinavica 2016; 134: 242–249.

Lukens JN, Van Deerlin V, Clark CM, Xie SX, Johnson FB. Comparisons of telomere lengths in peripheral blood and cerebellum in Alzheimer's disease. Alzheimers Dement 2009; 5: 463–469.

Luoma P, Melberg A, Rinne JO, Kaukonen JA, Nupponen NN, Chalmers RM, et al. Parkinsonism, premature menopause, and mitochondrial DNA polymerase γ mutations: clinical and molecular genetic study. The Lancet 2004; 364: 875–882.

Macaya A, Munell F, Burke RE, De Vivo DC. Disorders of movement in Leigh syndrome. Neuropediatrics 1993; 24: 60–67.

Machaczka M, Paucar M, Björkvall CK, Smith NJC, Cox TM, Forsgren L, et al. Novel hyperkinetic dystonia-like manifestation and neurological disease course of Swedish Gaucher patients. Blood Cells, Molecules, and Diseases 2018; 68: 86–92.

Maciejowski J, de Lange T. Telomeres in cancer: tumour suppression and genome instability. Nature Publishing Group 2017; 18: 175–186.

Madureira M, Connor-Robson N, Wade-Martins R. "LRRK2: Autophagy and Lysosomal Activity". Front. Neurosci. 2020; 14: 498.

Mahlknecht P, Seppi K, Poewe W. The Concept of Prodromal Parkinson's Disease. JPD 2015; 5: 681–697.

Mallett V, Ross JP, Alcalay RN, Ambalavanan A, Sidransky E, Dion PA, et al. GBA p.T369M substitution in Parkinson disease: Polymorphism or association? A meta-analysis. Neurol Genet 2016; 2: e104.

Mamdani F, Rollins B, Morgan L, Myers RM, Barchas JD, Schatzberg AF, et al. Variable telomere length across post-mortem human brain regions and specific reduction in the hippocampus of major depressive disorder. Transl Psychiatry 2015; 5: e636.

Mancuso M, Nesti C, Petrozzi L, Orsucci D, Frosini D, Kiferle L, et al. The mtDNA A8344G 'MERRF' mutation is not a common cause of sporadic Parkinson disease in Italian population. Parkinsonism & Related Disorders 2008; 14: 381–382.

Mangino M, Hwang S-J, Spector TD, Hunt SC, Kimura M, Fitzpatrick AL, et al. Genome-wide meta-analysis points to CTC1 and ZNF676 as genes regulating telomere homeostasis in humans. Hum. Mol. Genet. 2012; 21: 5385–5394.

Mann VM, Cooper JM, Krige D, Daniel SE, Schapira AH, Marsden CD. Brain, skeletal muscle and platelet homogenate mitochondrial function in Parkinson's disease. Brain 1992; 115 (Pt 2): 333–342.

Martin-Ruiz C, Dickinson HO, Keys B, Rowan E, Kenny RA, Zglinicki von T. Telomere length predicts poststroke mortality, dementia, and cognitive decline. Ann Neurol. 2006; 60: 174–180.

Marecos C, Ng J, Kurian MA. What is new for monoamine neurotransmitter disorders? J. Inherit. Metab. Dis. 2014; 37: 619–626.

Marek M, Linnepe S, Klein C, Hummel T, Paus S. High prevalence of olfactory dysfunction in cervical dystonia. Parkinsonism Relat. Disord. 2018; 53: 33–36.

Marshall VL, Patterson J, Hadley DM, Grosset KA, Grosset DG. Two-year follow-up in 150 consecutive cases with normal dopamine transporter imaging. Nucl Med Commun 2006; 27: 933–937.

Martikainen MH, Ng YS, Gorman GS, Alston CL, Blakely EL, Schaefer AM, et al. Clinical, Genetic, and Radiological Features of Extrapyramidal Movement Disorders in Mitochondrial Disease. JAMA Neurol 2016

Martin-Bastida A, Pietracupa S, Piccini P. Neuromelanin in parkinsonian disorders: an update. Int J Neurosci 2017; 127: 1116–1123.

Masellis M, Momeni P, Meschino W, Heffner R, Elder J, Sato C, et al. Novel splicing mutation in the progranulin gene causing familial corticobasal syndrome. Brain 2006; 129: 3115–3123.

Massano J, Bhatia KP. Clinical approach to Parkinson's disease: features, diagnosis, and principles of management. Cold Spring Harb Perspect Med 2012; 2: a008870–a008870.

Mayer S, Brüderlein S, Perner S, Waibel I, Holdenried A, Ciloglu N, et al. Sex-specific telomere length profiles and age-dependent erosion dynamics of individual chromosome arms in humans. Cytogenet. Genome Res. 2006; 112: 194–201.

Mc Govern EM, Killian O, Narasimham S, Quinlivan B, Butler JB, Beck R, et al. Disrupted superior collicular activity may reveal cervical dystonia disease pathomechanisms. Sci Rep 2017; 7: 16753–11.

McNaught KSP, Kapustin A, Jackson T, Jengelley T-A, JnoBaptiste R, Shashidharan P, et al. Brainstem pathology in DYT1 primary torsion dystonia. Ann Neurol. 2004; 56: 540–547.

McNaught KSP, Shashidharan P, Perl DP, Jenner P, Olanow CW. Aggresome-related biogenesis of Lewy bodies. Eur J Neurosci 2002; 16: 2136–2148.

McNeill A, Duran R, Hughes DA, Mehta A, Schapira AHV. A clinical and family history study of Parkinson's disease in heterozygous glucocerebrosidase mutation carriers. J. Neurol. Neurosurg. Psychiatr. 2012; 83: 853–854.

Meek D, Wolfe LS, Andermann E, Andermann F. Juvenile progressive dystonia: a new phenotype of GM2 gangliosidosis. Ann Neurol. 1984; 15: 348–352.

Meikle PJ, Hopwood JJ, Clague AE, Carey WF. Prevalence of lysosomal storage disorders. JAMA 1999; 281: 249–254.

Mencacci NE, Isaias IU, Reich MM, Ganos C, Plagnol V, Polke JM, et al. Parkinson's disease in GTP cyclohydrolase 1 mutation carriers. Brain 2014; 137: 2480–2492.

Mencacci NE, Rubio-Agusti I, Zdebik A, Asmus F, Ludtmann MHR, Ryten M, et al. A missense mutation in KCTD17 causes autosomal dominant myoclonus-dystonia. Am. J. Hum. Genet. 2015; 96: 938–947.

Meyer E, Carss KJ, Rankin J, Nichols JME, Grozeva D, Joseph AP, et al. Mutations in the histone methyltransferase gene KMT2B cause complex early-onset dystonia. Nat. Genet. 2016: 1–18.

Middleton FA, Strick PL. Basal ganglia output and cognition: evidence from anatomical, behavioral, and clinical studies. Brain Cogn 2000; 42: 183–200.

Migdalska-Richards A, Schapira AHV. The relationship between glucocerebrosidase mutations and Parkinson disease. J Neurochem 2016; 139 Suppl 1: 77–90.

Millar T, Walker R, Arango J-C, Ironside JW, Harrison DJ, MacIntyre DJ, et al. Tissue and organ donation for research in forensic pathology: the MRC Sudden Death Brain and Tissue Bank. J. Pathol. 2007; 213: 369–375.

Milone M, Wong L-J. Diagnosis of mitochondrial myopathies. Molecular Genetics and Metabolism 2013; 110: 35–41.

Mirabello L, Huang W-Y, Wong JYY, Chatterjee N, Reding D, Crawford ED, et al. The association between leukocyte telomere length and cigarette smoking, dietary and physical variables, and risk of prostate cancer. Aging Cell 2009; 8: 405–413.

Mitchell IJ, Cooper AJ, Griffiths MR. The selective vulnerability of striatopallidal neurons. Prog. Neurobiol. 1999; 59: 691–719.

Mitsui J, Mizuta I, Toyoda A, Ashida R, Takahashi Y, Goto J, et al. Mutations for Gaucher disease confer high susceptibility to Parkinson disease. Arch. Neurol. 2009; 66: 571–576.

Mizuno Y, Ohta S, Tanaka M, Takamiya S, Suzuki K, Sato T, et al. Deficiencies in complex I subunits of the respiratory chain in Parkinson's disease. Biochem. Biophys. Res. Commun. 1989; 163: 1450–1455.

Mok KY, Sheerin U, Simón-Sánchez J, Salaka A, Chester L, Escott-Price V, et al. Deletions at 22q11.2 in idiopathic Parkinson's disease: a combined analysis of genome-wide association data. The Lancet Neurology 2016; 15: 585–596.

Mollenhauer B, Trautmann E, Sixel-Doring F, Wicke T, Ebentheuer J, Schaumburg M, et al. Nonmotor and diagnostic findings in subjects with de novo Parkinson disease of the DeNoPa cohort. Neurology 2013; 81: 1226–1234.

Montpetit AJ, Alhareeri AA, Montpetit M, Starkweather AR, Elmore LW, Filler K, et al. Telomere length: a review of methods for measurement. Nurs Res 2014; 63: 289–299.

Moors TE, Paciotti S, Ingrassia A, Quadri M, Breedveld G, Tasegian A, et al. Characterization of Brain Lysosomal Activities in GBA-Related and Sporadic Parkinson's Disease and Dementia with Lewy Bodies. Mol Neurobiol 2019; 56: 1344–1355.

Morais VA, Haddad D, Craessaerts K, De Bock P-J, Swerts J, Vilain S, et al. PINK1 loss-of-function mutations affect mitochondrial complex I activity via NdufA10 ubiquinone uncoupling. Science 2014; 344: 203–207.

Moyzis RK, Buckingham JM, Cram LS, Dani M, Deaven LL, Jones MD, et al. A highly conserved repetitive DNA sequence, (TTAGGG)n, present at the telomeres of human chromosomes. Proc. Natl. Acad. Sci. U.S.A. 1988; 85: 6622–6626.

Mottolese C, Richard N, Harquel S, Szathmari A, Sirigu A, Desmurget M. Mapping motor representations in the human cerebellum. Brain 2013; 136: 330–342.

Mukai M, Sugaya K, Yabe I, Goto Y-I, Yokochi F, Miyamoto K, et al. Neuromelanin MRI in a family with mitochondrial parkinsonism harboring a Y955C mutation in POLG1. Parkinsonism Relat. Disord. 2013; 19: 821–824.

Mullin S, Hughes D, Mehta A, Schapira AHV. Neurological effects of glucocerebrosidase gene mutations. Eur. J. Neurol. 2019; 26: 388–e29.

Mullin S, Smith L, Lee K, D'Souza G, Woodgate P, Elflein J, et al. Ambroxol for the Treatment of Patients With Parkinson Disease With and Without Glucocerebrosidase Gene Mutations: A Nonrandomized, Noncontrolled Trial. JAMA Neurol 2020; 77: 427–434.

Muraresku CC, McCormick EM, Falk MJ. Mitochondrial Disease: Advances in clinical diagnosis, management, therapeutic development, and preventative strategies. Curr Genet Med Rep 2018; 6: 62–72.

Murphy KE, Gysbers AM, Abbott SK, Tayebi N, Kim WS, Sidransky E, et al. Reduced glucocerebrosidase is associated with increased α-synuclein in sporadic Parkinson’s disease. Brain 2014; 137: 834–848.

Muthane UB, Swamy HS, Satishchandra P, Subhash MN, Rao S, Subbakrishna D. Early onset Parkinson's disease: are juvenile- and young-onset different? Mov. Disord. 1994; 9: 539–544.

Müezzinler A, Zaineddin AK, Brenner H. A systematic review of leukocyte telomere length and age in adults. Ageing Res. Rev. 2013; 12: 509–519.

Müller J, Kiechl S, Wenning GK, Seppi K, Willeit J, Gasperi A, et al. The prevalence of primary dystonia in the general community. Neurology 2002; 59: 941–943.

Muñoz Y, Carrasco CM, Campos JD, Aguirre P, Núñez MT. Parkinson's Disease: The Mitochondria-Iron Link. Parkinsons Dis 2016; 2016: 7049108–21.

Nakagaki H, Furuya J-I, Santa Y, Nagano S, Araki E, Yamada T. [A case of MELAS presenting juvenile-onset hyperglycemic chorea-ballism]. Rinsho Shinkeigaku 2005; 45: 502–505.

Nakamura K-I, Takubo K, Izumiyama-Shimomura N, Sawabe M, Arai T, Kishimoto H, et al. Telomeric DNA length in cerebral gray and white matter is associated with longevity in individuals aged 70 years or older. EXG 2007; 42: 944–950.

Nalls MA, Blauwendraat C, Vallerga CL, Heilbron K, Bandres-Ciga S, Chang D, et al. Identification of novel risk loci, causal insights, and heritable risk for Parkinson's disease: a meta-analysis of genome-wide association studies. The Lancet Neurology 2019; 18: 1091–1102.

Nalls MA, Pankratz N, Lill CM, Do CB, Hernandez DG, Saad M, et al. Large-scale meta-analysis of genome-wide association data identifies six new risk loci for Parkinson's disease. Nat. Genet. 2014; 46: 989–993.

Nalls Michael A, Duran R, Lopez G, Kurzawa-Akanbi M, McKeith IG, Chinnery PF, et al. A multicenter study of glucocerebrosidase mutations in dementia with Lewy bodies. JAMA Neurol 2013; 70: 727–735.

Napolitano F, Pasqualetti M, Usiello A, Santini E, Pacini G, Sciamanna G, et al. Dopamine D2 receptor dysfunction is rescued by adenosine A2A receptor antagonism in a model of DYT1 dystonia. Neurobiol. Dis. 2010; 38: 434–445.

Neil JF, Glew RH, Peters SP. Familial psychosis and diverse neurologic abnormalities in adult-onset Gaucher's disease. Arch. Neurol. 1979; 36: 95–99.

Nelson I, Hanna MG, Alsanjari N, Scaravilli F, Morgan-Hughes JA, Harding AE. A new mitochondrial DNA mutation associated with progressive dementia and chorea: a clinical, pathological, and molecular genetic study. Ann Neurol. 1995; 37: 400–403.

Nelson AJ, Blake DT, Chen R. Digit-specific aberrations in the primary somatosensory cortex in Writer's cramp. Ann Neurol. 2009; 66: 146–154.

Neudorfer O, Giladi N, Elstein D, Abrahamov A, Turezkite T, Aghai E, et al. Occurrence of Parkinson's syndrome in type I Gaucher disease. QJM 1996; 89: 691–694.

Neumann J, Bras J, Deas E, O'Sullivan SS, Parkkinen L, Lachmann RH, et al. Glucocerebrosidase mutations in clinical and pathologically proven Parkinson's disease. Brain 2009; 132: 1783–1794.

Neychev VK, Gross RE, Lehéricy S, Hess EJ, Jinnah HA. The functional neuroanatomy of dystonia. Neurobiol. Dis. 2011; 42: 185–201.

Niemann A. Ein unbekanntes Krankheitsbild. Jahrb. Kinderheilkd. 1914: 1–10.

Nightingale H, Pfeffer G, Bargiela D, Horvath R, Chinnery PF. Emerging therapies for mitochondrial disorders. Brain 2016; 139: 1633–1648.

Njajou OT, Cawthon RM, Damcott CM, Wu S-H, Ott S, Garant MJ, et al. Telomere length is paternally inherited and is associated with parental lifespan. Proc. Natl. Acad. Sci. U.S.A. 2007; 104: 12135–12139.

Niyazov DM, Kahler SG, Frye RE. Primary Mitochondrial Disease and Secondary Mitochondrial Dysfunction: Importance of Distinction for Diagnosis and Treatment. Mol Syndromol 2016; 7: 122–137.

Njajou OT, Cawthon RM, Damcott CM, Wu S-H, Ott S, Garant MJ, et al. Telomere length is paternally inherited and is associated with parental lifespan. Proc. Natl. Acad. Sci. U.S.A. 2007; 104: 12135–12139.

Noyce AJ, Kia DA, Hemani G, Nicolas A, Price TR, De Pablo-Fernandez E, et al. Estimating the causal influence of body mass index on risk of Parkinson disease: A Mendelian randomisation study. PLoS Med. 2017; 14: e1002314.

Oeda T, Umemura A, Mori Y, Tomita S, Kohsaka M, Park K, et al. Impact of glucocerebrosidase mutations on motor and nonmotor complications in Parkinson's disease. Neurobiology of Aging 2015: 1–8.

Olgiati S, Quadri M, Fang M, Rood JPMA, Saute JA, Chien HF, et al. DNAJC6 Mutations Associated With Early-Onset Parkinson's Disease. Ann Neurol. 2016; 79: 244–256.

Ong ELH, Goldacre R, Goldacre M. Differential risks of cancer types in people with Parkinson's disease: a national record-linkage study. Eur. J. Cancer 2014; 50: 2456–2462.

Osaki Y, Morita Y, Kuwahara T, Miyano I, Doi Y. Prevalence of Parkinson's disease and atypical parkinsonian syndromes in a rural Japanese district. Acta Neurologica Scandinavica 2011; 124: 182–187.

Outeiro TF, Putcha P, Tetzlaff JE, Spoelgen R, Koker M, Carvalho F, et al. Formation of toxic oligomeric alpha-synuclein species in living cells. PLoS ONE 2008; 3: e1867.

Ozaki K, Ohnishi Y, Iida A, Sekine A, Yamada R, Tsunoda T, et al. Functional SNPs in the lymphotoxin-alpha gene that are associated with susceptibility to myocardial infarction. Nat. Genet. 2002; 32: 650–654.

Ozelius LJ, Hewett JW, Page CE, Bressman SB, Kramer PL, Shalish C, et al. The early-onset torsion dystonia gene (DYT1) encodes an ATP-binding protein. Nat. Genet. 1997; 17: 40–48.

Pakkenberg B, Gundersen HJ. Neocortical neuron number in humans: effect of sex and age. J. Comp. Neurol. 1997; 384: 312–320.

Palm W, de Lange T. How shelterin protects mammalian telomeres. Annu. Rev. Genet. 2008; 42: 301–334.

Pankratz N, Beecham GW, DeStefano AL, Dawson TM, Doheny KF, Factor SA, et al. Meta-analysis of Parkinson's disease: identification of a novel locus, RIT2. Ann Neurol. 2012; 71: 370–384.

Papadimitriou D, Antonelou R, Miligkos M, Maniati M, Papagiannakis N, Bostantjopoulou S, et al. Motor and Nonmotor Features of Carriers of the p.A53T Alpha-Synuclein Mutation: A Longitudinal Study. Mov. Disord. 2016; 31: 1226–1230.

Paredes MF, James D, Gil-Perotin S, Kim H, Cotter JA, Ng C, et al. Extensive migration of young neurons into the infant human frontal lobe. Science 2016; 354: aaf7073–aaf7073.

Parikh S, Goldstein A, Koenig MK, Scaglia F, Enns GM, Saneto R, et al. Diagnosis and management of mitochondrial disease: a consensus statement from the Mitochondrial Medicine Society. Genet. Med. 2015; 17: 689–701.

Park J-S, Davis RL, Sue CM. Mitochondrial Dysfunction in Parkinson's Disease: New Mechanistic Insights and Therapeutic Perspectives. Curr Neurol Neurosci Rep 2018; 18: 21.

Park J-S, Davis RL, Sue CM. Mitochondrial Dysfunction in Parkinson's Disease: New Mechanistic Insights and Therapeutic Perspectives. Curr Neurol Neurosci Rep 2018; 18: 21.

Parkinson J. An essay on the shaking palsy. 1817. J Neuropsychiatry Clin Neurosci 2002; 14: 223–36– discussion 222.

Paudel R, Kiely A, Li A, Lashley T, Bandopadhyay R, Hardy J, et al. Neuropathological features of genetically confirmed DYT1 dystonia: investigating disease-specific inclusions. Acta Neuropathol Commun 2014; 2: 159.

Peall KJ, Kurian MA. Benign Hereditary Chorea: An Update. Tremor Other Hyperkinet Mov (N Y) 2015; 5: 314.

Pelvig DP, Pakkenberg H, Stark AK, Pakkenberg B. Neocortical glial cell numbers in human brains. Neurobiology of Aging 2008; 29: 1754–1762.

Peters MJ, Joehanes R, Pilling LC, Schurmann C, Conneely KN, Powell J, et al. The transcriptional landscape of age in human peripheral blood. Nat Commun 2015; 6: 1–14.

Peterson DA, Sejnowski TJ, Poizner H. Convergent evidence for abnormal striatal synaptic plasticity in dystonia. Neurobiol. Dis. 2010; 37: 558–573.

Pichler I, Del Greco M F, Gögele M, Lill CM, Bertram L, Do CB, et al. Serum iron levels and the risk of Parkinson disease: a Mendelian randomization study. PLoS Med. 2013; 10: e1001462.

Pick L. Der Morbus Gaucher und die ihm ähnlichen Krankheiten (die lipoidzellige Splenohepatomegalie Typus Niemann und die diabetische Lipoidzellenhypoplasie der Milz). Ergeb. Inn. Med. Kinderheilkd. 1926: 519–627.

Pickrell AM, Pinto M, Hida A, Moraes CT. Striatal dysfunctions associated with mitochondrial DNA damage in dopaminergic neurons in a mouse model of Parkinson's disease. Journal of Neuroscience 2011; 31: 17649–17658.

Pickrell AM, Youle RJ. The roles of PINK1, parkin, and mitochondrial fidelity in Parkinson's disease. Neuron 2015; 85: 257–273.

Pineda-Pampliega J, Herrera-Dueñas A, Mulder E, Aguirre JI, Höfle U, Verhulst S. Antioxidant supplementation slows telomere shortening in free-living white stork chicks. Proc. Biol. Sci. 2020; 287: 20191917.

Planetta PJ, Kurani AS, Shukla P, Prodoehl J, Corcos DM, Comella CL, et al. Distinct functional and macrostructural brain changes in Parkinson's disease and multiple system atrophy. Hum Brain Mapp 2014; 36: 1165–1179.

Poewe W, Seppi K, Tanner CM, Halliday GM, Brundin P, Volkmann J, et al. Parkinson disease. Nat Rev Dis Primers 2017; 3: 17013.

Poisson A, Krack P, Thobois S, Loiraud C, Serra G, Vial C, et al. History of the 'geste antagoniste' sign in cervical dystonia. J Neurol 2012; 259: 1580–1584.

Polymeropoulos MH, Lavedan C, Leroy E, Ide SE, Dehejia A, Dutra A, et al. Mutation in the alpha-synuclein gene identified in families with Parkinson's disease. Science 1997; 276: 2045–2047.

Pompe JC. Over idiopatische hypertropie van het hart. Ned. Tijdschr. Geneeskd. 1932: 304.

Pooley KA, Bojesen SE, Weischer M, Nielsen SF, Thompson D, Amin Al Olama A, et al. A genome-wide association scan (GWAS) for mean telomere length within the COGS project: identified loci show little association with hormone-related cancer risk. Hum. Mol. Genet. 2013; 22: 5056–5064.

Postuma RB, Berg D, Stern M, Poewe W, Olanow CW, Oertel W, et al. Abolishing the 1-year rule: How much evidence will be enough? Mov. Disord. 2016; 31: 1623–1627.

Pringsheim T, Jette N, Frolkis A, Steeves TDL. The prevalence of Parkinson's disease: A systematic review and meta-analysis. Mov. Disord. 2014; 29: 1583–1590.

Prodoehl J, Planetta PJ, Kurani AS, Comella CL, Corcos DM, Vaillancourt DE. Differences in brain activation between tremor- and nontremor-dominant Parkinson disease. JAMA Neurol 2013; 70: 100–106.

Prudente CN, Pardo CA, Xiao J, Hanfelt J, Hess EJ, LeDoux MS, et al. Neuropathology of cervical dystonia. Experimental Neurology 2013; 241: 95–104.

Quadri M, Fang M, Picillo M, Olgiati S, Breedveld GJ, Graafland J, et al. Mutation in the SYNJ1Gene Associated with Autosomal Recessive, Early-Onset Parkinsonism. Human Mutation 2013; 34: 1208–1215.

Quartarone A, Hallett M. Emerging concepts in the physiological basis of dystonia. Mov. Disord. 2013; 28: 958–967.

Ramanathan R, Kohli A, Ingaramo MC, Jain A, Leng SX, Punjabi NM, et al. Serum chitotriosidase, a putative marker of chronically activated macrophages, increases with normal aging. GERONA 2013; 68: 1303–1309.

Ramasamy A, Trabzuni D, Guelfi S, Varghese V, Smith C, Walker R, et al. Genetic variability in the regulation of gene expression in ten regions of the human brain. Nat Neurosci 2014; 17: 1418–1428.

Rana AQ, Siddiqui I, Yousuf MS. Challenges in diagnosis of young onset Parkinson's disease. J. Neurol. Sci. 2012; 323: 113–116.

Rebeiz JJ, Kolodny EH, Richardson EP. Corticodentatonigral degeneration with neuronal achromasia: a progressive disorder of late adult life. Trans Am Neurol Assoc 1967; 92: 23–26.

Rees EM, Farmer R, Cole JH, Haider S, Durr A, Landwehrmeyer B, et al. Cerebellar abnormalities in Huntington's disease: a role in motor and psychiatric impairment? Mov. Disord. 2014; 29: 1648–1654.

Reetz K, Gaser C, Klein C, Hagenah J, Büchel C, Gottschalk S, et al. Structural findings in the basal ganglia in genetically determined and idiopathic Parkinson's disease. Mov. Disord. 2009; 24: 99–103.

Reeve A, Simcox E, Turnbull D. Ageing and Parkinson's disease: Why is advancing age the biggest risk factor? Ageing Res. Rev. 2014; 14: 19–30.

Rizzo G, Copetti M, Arcuti S, Martino D, Fontana A, Logroscino G. Accuracy of clinical diagnosis of Parkinson disease: A systematic review and meta-analysis. Neurology 2016; 86: 566–576.

Robak LA, Jansen IE, van Rooij J, Uitterlinden AG, Kraaij R, Jankovic J, et al. Excessive burden of lysosomal storage disorder gene variants in Parkinson's disease. Brain 2017; 140: 3191–3203.

Rocha EM, Smith GA, Park E, Cao H, Brown E, Hallett P, et al. Progressive decline of glucocerebrosidase in aging and Parkinson's disease. Ann Clin Transl Neurol 2015; 2: 433–438.

Rodenburg RJT, Schoonderwoerd GC, Tiranti V, Taylor RW, Rötig A, Valente L, et al. A multi-center comparison of diagnostic methods for the biochemical evaluation of suspected mitochondrial disorders. Mitochondrion 2013; 13: 36–43.

Rodríguez M, Rodriguez-Sabate C, Morales I, Sanchez A, Sabate M. Parkinson's disease as a result of aging. Aging Cell 2015; 14: 293–308.

Rogaeva E, Hardy J. Gaucher and Parkinson diseases: unexpectedly related. Neurology 2008; 70: 2272–2273.

Rosales RL. X-linked dystonia parkinsonism: clinical phenotype, genetics and therapeutics. J Mov Disord 2010; 3: 32–38.

Rosenberg-Katz K, Herman T, Jacob Y, Giladi N, Hendler T, Hausdorff JM. Gray matter atrophy distinguishes between Parkinson disease motor subtypes. Neurology 2013; 80: 1476–1484.

Ryan BJ, Hoek S, Fon EA, Wade-Martins R. Mitochondrial dysfunction and mitophagy in Parkinson's: from familial to sporadic disease. Trends Biochem. Sci. 2015; 40: 200–210.

Sachs B. On arrested cerebral development with special reference to cortical pathology. J. Nerv. Ment. Dis. 1887: 541–553.

Sadnicka A, Hoffland BS, Bhatia KP, van de Warrenburg BP, Edwards MJ. The cerebellum in dystonia - help or hindrance? Clin Neurophysiol 2012; 123: 65–70.

Sanders JL, Newman AB. Telomere length in epidemiology: a biomarker of aging, age-related disease, both, or neither? Epidemiol Rev 2013; 35: 112–131.

Santos-Lobato BLD, Del-Bel EA, Pittella JEH, Tumas V. Effects of aging on nitrergic neurons in human striatum and subthalamic nucleus. Arq Neuropsiquiatr 2015; 73: 779–783.

Sato Kazunori, Yabe I, Yaguchi H, Nakano F, Kunieda Y, Saitoh S, et al. Genetic analysis of two Japanese families with progressive external ophthalmoplegia and parkinsonism. J Neurol 2011; 258: 1327–1332.

Sato Kenta, Sumi-Ichinose C, Kaji R, Ikemoto K, Nomura T, Nagatsu I, et al. Differential involvement of striosome and matrix dopamine systems in a transgenic model of dopa-responsive dystonia. Proc. Natl. Acad. Sci. U.S.A. 2008; 105: 12551–12556.

Sauerbier A, Jenner P, Todorova A, Chaudhuri KR. Non motor subtypes and Parkinson's disease. Parkinsonism & Related Disorders 2016; 22: S41–S46.

Scaglia F, Wong L-JC, Vladutiu GD, Hunter JV. Predominant cerebellar volume loss as a neuroradiologic feature of pediatric respiratory chain defects. AJNR Am J Neuroradiol 2005; 26: 1675–1680.

Schaefer AM, McFarland R, Blakely EL, He L, Whittaker RG, Taylor RW, et al. Prevalence of mitochondrial DNA disease in adults. Ann Neurol. 2008; 63: 35–39.

Schapira AH, Cooper JM, Dexter D, Jenner P, Clark JB, Marsden CD. Mitochondrial complex I deficiency in Parkinson's disease. The Lancet 1989; 1: 1269.

Schapira AHV. Mitochondria in the aetiology and pathogenesis of Parkinson's disease. The Lancet Neurology 2008; 7: 97–109.

Schmidt JC, Cech TR. Human telomerase: biogenesis, trafficking, recruitment, and activation. Genes Dev. 2015; 29: 1095–1105.

Schneider SA, Dusek P, Hardy J, Westenberger A, Jankovic J, Bhatia KP. Genetics and Pathophysiology of Neurodegeneration with Brain Iron Accumulation (NBIA). Curr Neuropharmacol 2013; 11: 59–79.

Schneider SA, Paisan-Ruiz C, Quinn NP, Lees AJ, Houlden H, Hardy J, et al. ATP13A2 mutations (PARK9) cause neurodegeneration with brain iron accumulation. Mov. Disord. 2010; 25: 979–984.

Schneider SA, Walker RH, Bhatia KP. The Huntington‘s disease-like syndromes: what to consider in patients with a negative Huntington’s disease gene test. Nat Clin Pract Neurol 2007; 3: 517–525.

Schönecker M. Ein eigentümliches Syndrom im oralen Bereich bei Megaphenapplikation. Nervenarzt 1956; 27: 178–180.

Schöndorf DC, Aureli M, McAllister FE, Hindley CJ, Mayer F, Schmid B, et al. iPSC-derived neurons from GBA1-associated Parkinson's disease patients show autophagic defects and impaired calcium homeostasis. Nat Commun 2014; 5: 4028–17.

Schrag A, Schott JM. Epidemiological, clinical, and genetic characteristics of early-onset parkinsonism. The Lancet Neurology 2006; 5: 355–363.

Schröder KF, Hopf A, Lange H, Thörner G. [Morphometrical-statistical structure analysis of human striatum, pallidum and subthalamic nucleus]. J Hirnforsch 1975; 16: 333–350.

Schwingenschuh P, Ruge D, Edwards MJ, Terranova C, Katschnig P, Carrillo F, et al. Distinguishing SWEDDs patients with asymmetric resting tremor from Parkinson's disease: A clinical and electrophysiological study. Mov. Disord. 2010; 25: 560–569.

Sedel F, Saudubray J-M, Roze E, Agid Y, Vidailhet M. Movement disorders and inborn errors of metabolism in adults: a diagnostic approach. J. Inherit. Metab. Dis. 2008; 31: 308–318.

Segawa M, Hosaka A, Miyagawa F, Nomura Y, Imai H. Hereditary progressive dystonia with marked diurnal fluctuation. Adv Neurol 1976; 14: 215–233.

Segawa M, Nomura Y, Nishiyama N. Autosomal dominant guanosine triphosphate cyclohydrolase I deficiency (Segawa disease). Ann Neurol. 2003; 54 Suppl 6: S32–45.

Selden N, Geula C, Hersh L, Mesulam MM. Human striatum: chemoarchitecture of the caudate nucleus, putamen and ventral striatum in health and Alzheimer's disease. NSC 1994; 60: 621–636.

Selikhova M, Kempster PA, Revesz T, Holton JL, Lees AJ. Neuropathological findings in benign tremulous parkinsonism. Mov. Disord. 2013; 28: 145–152.

Setó-Salvia N, Pagonabarraga J, Houlden H, Pascual-Sedano B, Dols-Icardo O, Tucci A, et al. Glucocerebrosidase mutations confer a greater risk of dementia during Parkinson's disease course. Mov. Disord. 2012; 27: 393–399.

Shakkottai VG, Batla A, Bhatia K, Dauer WT, Dresel C, Niethammer M, et al. Current Opinions and Areas of Consensus on the Role of the Cerebellum in Dystonia. Cerebellum 2016: 1–18.

Sharma M, Ioannidis JPA, Aasly JO, Annesi G, Brice A, Bertram L, et al. A multi-centre clinico-genetic analysis of the VPS35 gene in Parkinson disease indicates reduced penetrance for disease-associated variants. J. Med. Genet. 2012; 49: 721–726.

Shay JW, Wright WE. Telomeres and telomerase: three decades of progress. Nature Publishing Group 2019; 20: 299–309.

Siderowf A, Stern MB. Premotor Parkinson's disease: clinical features, detection, and prospects for treatment. Ann Neurol. 2008; 64 Suppl 2: S139–47.

Sidransky E, Lopez G. The link between the GBA gene and parkinsonism. The Lancet Neurology 2012; 11: 986–998.

Sidransky E, Nalls MA, Aasly JO, Aharon-Peretz J, Annesi G, Barbosa ER, et al. Multicenter analysis of glucocerebrosidase mutations in Parkinson's disease. N Engl J Med 2009; 361: 1651–1661.

Siebert M, Westbroek W, Chen Y-C, Moaven N, Li Y, Velayati A, et al. Identification of miRNAs that modulate glucocerebrosidase activity in Gaucher disease cells. RNA Biol 2014; 11: 1291–1300.

Siebert M, Sidransky E, Westbroek W. Glucocerebrosidase is shaking up the synucleinopathies. Brain 2014; 137: 1304–1322.

Simić G, Kostović I, Winblad B, Bogdanović N. Volume and number of neurons of the human hippocampal formation in normal aging and Alzheimer's disease. J. Comp. Neurol. 1997; 379: 482–494.

Simon KC, Eberly S, Gao X, Oakes D, Tanner CM, Shoulson I, et al. Mendelian randomization of serum urate and parkinson disease progression. Ann Neurol. 2014; 76: 862–868.

Simonyan K, Cho H, Hamzehei Sichani A, Rubien-Thomas E, Hallett M. The direct basal ganglia pathway is hyperfunctional in focal dystonia. Brain 2017; 140: 3179–3190.

Singleton A, Hardy J. The Evolution of Genetics: Alzheimer‘s and Parkinson’s Diseases. Neuron 2016; 90: 1154–1163.

Singleton AB, Farrer M, Johnson JD, Singleton A, hague S, Kachergus J, et al. alpha-Synuclein locus triplication causes Parkinson's disease. Science 2003; 302: 841–841.

Smith PK, Krohn RI, Hermanson GT, Mallia AK, Gartner FH, Provenzano MD, et al. Measurement of protein using bicinchoninic acid. Analytical Biochemistry 1985; 150: 76–85.

Smith SM, Jenkinson M, Woolrich MW, Beckmann CF, Behrens TEJ, Johansen-Berg H, et al. Advances in functional and structural MR image analysis and implementation as FSL. Neuroimage 2004; 23 Suppl 1: S208–19.

Soreq L, UK Brain Expression Consortium, North American Brain Expression Consortium, Rose J, Soreq E, Hardy J, et al. Major Shifts in Glial Regional Identity Are a Transcriptional Hallmark of Human Brain Aging. CellReports 2017; 18: 557–570.

Soong NW, Hinton DR, Cortopassi G, Arnheim N. Mosaicism for a specific somatic mitochondrial DNA mutation in adult human brain. Nat. Genet. 1992; 2: 318–323.

Sorrells SF, Paredes MF, Cebrian-Silla A, Sandoval K, Qi D, Kelley KW, et al. Human hippocampal neurogenesis drops sharply in children to undetectable levels in adults. Nature 2018; 555: 377–381.

Spalding KL, Bergmann O, Alkass K, Bernard S, Salehpour M, Huttner HB, et al. Dynamics of hippocampal neurogenesis in adult humans. CELL 2013; 153: 1219–1227.

Spillantini MG, Schmidt ML, Lee VM, Trojanowski JQ, Jakes R, Goedert M. Alpha-synuclein in Lewy bodies. Nature 1997; 388: 839–840.

Spillantini MG, Yoshida H, Rizzini C, Lantos PL, Khan N, Rossor MN, et al. A novel tau mutation (N296N) in familial dementia with swollen achromatic neurons and corticobasal inclusion bodies. Ann Neurol. 2000; 48: 939–943.

Spina S, Murrell JR, Huey ED, Wassermann EM, Pietrini P, Grafman J, et al. Corticobasal syndrome associated with the A9D Progranulin mutation. J. Neuropathol. Exp. Neurol. 2007; 66: 892–900.

Stamelou M, Bhatia KP. Atypical parkinsonism – new advances. Current Opinion in Neurology 2016; 29: 480–485.

Stamelou M, Charlesworth G, Cordivari C, Schneider SA, Kägi G, Sheerin U-M, et al. The phenotypic spectrum of DYT24 due to ANO3 mutations. Mov. Disord. 2014; 29: 928–934.

Stamelou M, Mencacci NE, Cordivari C, Batla A, Wood NW, Houlden H, et al. Myoclonus-dystonia syndrome due to tyrosine hydroxylase deficiency. Neurology 2012; 79: 435–441.

Stamelou M, Edwards MJ, Bhatia KP. Late onset rest-tremor in DYT1 dystonia. Parkinsonism Relat. Disord. 2013; 19: 136–137.

Stark AK, Pakkenberg B. Histological changes of the dopaminergic nigrostriatal system in aging. Cell Tissue Res 2004; 318: 81–92.

Steeves TD, Day L, Dykeman J, Jette N, Pringsheim T. The prevalence of primary dystonia: A systematic review and meta-analysis. Mov. Disord. 2012; 27: 1789–1796.

Stebbins GT, Goetz CG, Burn DJ, Jankovic J, Khoo TK, Tilley BC. How to identify tremor dominant and postural instability/gait difficulty groups with the movement disorder society unified Parkinson‘s disease rating scale: comparison with the unified Parkinson’s disease rating scale. Mov. Disord. 2013; 28: 668–670.

Steele JC, Richardson JC, Olszewski J. Progressive supranuclear Palsy. A heterogeneous degeneration involving the brain stem, basal ganglia and cerebellum with vertical gaze and pseudobulbar palsy, nuchal dystonia and dementia. Arch. Neurol. 1964; 10: 333–359.

Steeves TD, Day L, Dykeman J, Jette N, Pringsheim T. The prevalence of primary dystonia: A systematic review and meta-analysis. Mov. Disord. 2012; 27: 1789–1796.

Stoodley CJ, Schmahmann JD. Functional topography in the human cerebellum: a meta-analysis of neuroimaging studies. Neuroimage 2009; 44: 489–501.

Stone DL, Tayebi N, Orvisky E, Stubblefield B, Madike V, Sidransky E. Glucocerebrosidase gene mutations in patients with type 2 Gaucher disease. Human Mutation 2000; 15: 181–188.

Strader S, Rodnitzky RL, Gonzalez-Alegre P. Secondary dystonia in a botulinum toxin clinic: clinical characteristics, neuroanatomical substrate and comparison with idiopathic dystonia. Parkinsonism Relat. Disord. 2011; 17: 749–752.

Sudarsky L, Plotkin GM, Logigian EL, Johns DR. Dystonia as a presenting feature of the 3243 mitochondrial DNA mutation. Mov. Disord. 1999; 14: 488–491.

Sulzer D. Multiple hit hypotheses for dopamine neuron loss in Parkinson's disease. Trends Neurosci. 2007; 30: 244–250.

Suomalainen A, Elo JM, Pietiläinen KH, Hakonen AH, Sevastianova K, Korpela M, et al. FGF-21 as a biomarker for muscle-manifesting mitochondrial respiratory chain deficiencies: a diagnostic study. The Lancet Neurology 2011; 10: 806–818.

Surmeier DJ. Calcium, ageing, and neuronal vulnerability in Parkinson's disease. The Lancet Neurology 2007; 6: 933–938.

Suzuki K. Neuropathology of late onset gangliosidoses. A review. Dev. Neurosci. 1991; 13: 205–210.

Szebeni A, Szebeni K, DiPeri T, Chandley MJ, Crawford JD, Stockmeier CA, et al. Shortened telomere length in white matter oligodendrocytes in major depression: potential role of oxidative stress. Int. J. Neuropsychopharmacol. 2014; 17: 1579–1589.

Tadic V, Kasten M, Brüggemann N, Stiller S, Hagenah J, Klein C. Dopa-responsive dystonia revisited: diagnostic delay, residual signs, and nonmotor signs. Arch. Neurol. 2012; 69: 1558–1562.

Takubo K, Izumiyama-Shimomura N, Honma N, Sawabe M, Arai T, Kato M, et al. Telomere lengths are characteristic in each human individual. EXG 2002; 37: 523–531.

Tang F-L, Zhao L, Zhao Y, Sun D, Zhu X-J, Mei L, et al. Coupling of terminal differentiation deficit with neurodegenerative pathology in Vps35-deficient pyramidal neurons. Cell Death Differ. 2020; 10: 1055–18.

Tay W. Symmetrical changes in the region of the yellow spot in each eye of an infant. Trans. Ophthalmol. Soc. U. K. 1881: 55–57.

Tayebi N, Stubblefield BK, Park JK, Orvisky E, Walker JM, LaMarca ME, et al. Reciprocal and nonreciprocal recombination at the glucocerebrosidase gene region: implications for complexity in Gaucher disease. The American Journal of Human Genetics 2003; 72: 519–534.

Taylor AE, Saint-Cyr JA, Lang AE. Frontal lobe dysfunction in Parkinson's disease. The cortical focus of neostriatal outflow. Brain 1986; 109 (Pt 5): 845–883.

Taylor RW, Pyle A, Griffin H, Blakely EL, Duff J, He L, et al. Use of whole-exome sequencing to determine the genetic basis of multiple mitochondrial respiratory chain complex deficiencies. JAMA 2014; 312: 68–77.

Taylor RW, Turnbull DM. Mitochondrial DNA mutations in human disease. Nat. Rev. Genet. 2005; 6: 389–402.

Telomeres Mendelian Randomization Collaboration, Haycock PC, Burgess S, Nounu A, Zheng J, Okoli GN, et al. Association Between Telomere Length and Risk of Cancer and Non-Neoplastic Diseases: A Mendelian Randomization Study. JAMA Oncol 2017

Thomas P, O' Callaghan NJ, Fenech M. Telomere length in white blood cells, buccal cells and brain tissue and its variation with ageing and Alzheimer's disease. Mech. Ageing Dev. 2008; 129: 183–190.

Tomita K-I, Aida J, Izumiyama-Shimomura N, Nakamura K-I, Ishikawa N, Matsuda Y, et al. Changes in telomere length with aging in human neurons and glial cells revealed by quantitative fluorescence in situ hybridization analysis. Geriatr Gerontol Int 2018; 18: 1507–1512.

Tranchant C, Anheim M. Movement disorders in mitochondrial diseases. Rev. Neurol. (Paris) 2016; 172: 524–529.

Tremblay C, Achim AM, Macoir J, Monetta L. The heterogeneity of cognitive symptoms in Parkinson's disease: a meta-analysis. J. Neurol. Neurosurg. Psychiatr. 2013; 84: 1265–1272.

Truong DD, Harding AE, Scaravilli F, Smith SJ, Morgan-Hughes JA, Marsden CD. Movement disorders in mitochondrial myopathies. A study of nine cases with two autopsy studies. Mov. Disord. 1990; 5: 109–117.

Tsuang D, Leverenz JB, Lopez OL, Hamilton RL, Bennett DA, Schneider JA, et al. GBA mutations increase risk for Lewy body disease with and without Alzheimer disease pathology. Neurology 2012; 79: 1944–1950.

Valanne L, Ketonen L, Majander A, Suomalainen A, Pihko H. Neuroradiologic findings in children with mitochondrial disorders. AJNR Am J Neuroradiol 1998; 19: 369–377.

Van Den Eeden SK, Tanner CM, Bernstein AL, Fross RD, Leimpeter A, Bloch DA, et al. Incidence of Parkinson's disease: variation by age, gender, and race/ethnicity. Am. J. Epidemiol. 2003; 157: 1015–1022.

van Veen S, Martin S, Van den Haute C, Benoy V, Lyons J, Vanhoutte R, et al. ATP13A2 deficiency disrupts lysosomal polyamine export. Nature 2020; 578: 419–424.

vB Hjelmborg J, Iachine I, Skytthe A, Vaupel JW, McGue M, Koskenvuo M, et al. Genetic influence on human lifespan and longevity. Hum. Genet. 2006; 119: 312–321.

Vekrellis K, Xilouri M, Emmanouilidou E, Rideout HJ, Stefanis L. Pathological roles of α-synuclein in neurological disorders. The Lancet Neurology 2011; 10: 1015–1025.

Vidailhet M, Jutras M-F, Grabli D, Roze E. Deep brain stimulation for dystonia. J. Neurol. Neurosurg. Psychiatr. 2013; 84: 1029–1042.

Vu TC, Nutt JG, Holford NHG. Progression of motor and nonmotor features of Parkinson's disease and their response to treatment. Br J Clin Pharmacol 2012; 74: 267–283.

Wakabayashi K, Tanji K, Mori F, Takahashi H. The Lewy body in Parkinson's disease: Molecules implicated in the formation and degradation of α-synuclein aggregates. Neuropathology 2007; 27: 494–506.

Walker UA, Collins S, Byrne E. Respiratory chain encephalomyopathies: a diagnostic classification. Eur. Neurol. 1996; 36: 260–267.

Walkley SU, Suzuki K. Consequences of NPC1 and NPC2 loss of function in mammalian neurons. Biochim. Biophys. Acta 2004; 1685: 48–62.

Watson JD. Origin of concatemeric T7 DNA. Nature New Biol. 1972; 239: 197–201.

Weinreb NJ, Charrow J, Andersson HC, Kaplan P, Kolodny EH, Mistry P, et al. Effectiveness of enzyme replacement therapy in 1028 patients with type 1 Gaucher disease after 2 to 5 years of treatment: a report from the Gaucher Registry. Am. J. Med. 2002; 113: 112–119.

Wenger DA, Clark C, Sattler M, Wharton C. Synthetic substrate beta-glucosidase activity in leukocytes: a reproducible method for the identification of patients and carriers of Gaucher's disease. Clin. Genet. 1978; 13: 145–153.

Wenning GK, Ben-Shlomo Y, Hughes A, Daniel SE, Lees A, Quinn NP. What clinical features are most useful to distinguish definite multiple system atrophy from Parkinson's disease? Journal of Neurology, Neurosurgery & Psychiatry 2000; 68: 434–440.

Wenning GK, Colosimo C, Geser F, Poewe W. Multiple system atrophy. The Lancet Neurology 2004; 3: 93–103.

Wenning GK, Litvan I, Jankovic J, Granata R, Mangone CA, McKee A, et al. Natural history and survival of 14 patients with corticobasal degeneration confirmed at postmortem examination. Journal of Neurology, Neurosurgery & Psychiatry 1998; 64: 184–189.

Wenning GK, Litvan I, Tolosa E. Milestones in atypical and secondary Parkinsonisms. Mov. Disord. 2011; 26: 1083–1095.

Wickremaratchi MM, Ben-Shlomo Y, Morris HR. The effect of onset age on the clinical features of Parkinson's disease. Eur. J. Neurol. 2009; 16: 450–456.

Wickremaratchi MM, Knipe MDW, Sastry BSD, Morgan E, Jones A, Salmon R, et al. The motor phenotype of Parkinson's disease in relation to age at onset. Mov. Disord. 2011; 26: 457–463.

Wider C, Dickson DW, Wszolek ZK. Leucine-rich repeat kinase 2 gene-associated disease: redefining genotype-phenotype correlation. Neurodegener Dis 2010; 7: 175–179.

Wider C, Wszolek ZK. Rapidly progressive familial parkinsonism with central hypoventilation, depression and weight loss (Perry syndrome) - A literature review. Parkinsonism & Related Disorders 2008; 14: 1–7.

Wijemanne S, Jankovic J. Dopa-responsive dystonia--clinical and genetic heterogeneity. Nat Rev Neurol 2015; 11: 414–424.

Willemsen MA, Verbeek MM, Kamsteeg EJ, de Rijk-van Andel JF, Aeby A, Blau N, et al. Tyrosine hydroxylase deficiency: a treatable disorder of brain catecholamine biosynthesis. Brain 2010; 133: 1810–1822.

Williams DR, de Silva R, Paviour DC, Pittman A, Watt HC, Kilford L, et al. Characteristics of two distinct clinical phenotypes in pathologically proven progressive supranuclear palsy: Richardson's syndrome and PSP-parkinsonism. Brain 2005; 128: 1247–1258.

Williams DR, Lees AJ. Progressive supranuclear palsy: clinicopathological concepts and diagnostic challenges. The Lancet Neurology 2009; 8: 270–279.

Winfield SL, Tayebi N, Martin BM, Ginns EI, Sidransky E. Identification of three additional genes contiguous to the glucocerebrosidase locus on chromosome 1q21: implications for Gaucher disease. Genome Res. 1997; 7: 1020–1026.

Winter Y, Bezdolnyy Y, Katunina E, Avakjan G, Reese JP, Klotsche J, et al. Incidence of Parkinson's disease and atypical parkinsonism: Russian population-based study. Mov. Disord. 2010; 25: 349–356.

Wise JL, Crout RJ, McNeil DW, Weyant RJ, Marazita ML, Wenger SL. Human telomere length correlates to the size of the associated chromosome arm. PLoS ONE 2009; 4: e6013.

Wolf RC, Thomann PA, Sambataro F, Wolf ND, Vasic N, Landwehrmeyer GB, et al. Abnormal cerebellar volume and corticocerebellar dysfunction in early manifest Huntington's disease. J Neurol 2015; 262: 859–869.

Wong K, Sidransky E, Verma A, Mixon T, Sandberg GD, Wakefield LK, et al. Neuropathology provides clues to the pathophysiology of Gaucher disease. Molecular Genetics and Metabolism 2004; 82: 192–207.

Wong L-JC, Scaglia F, Graham BH, Craigen WJ. Current molecular diagnostic algorithm for mitochondrial disorders. Molecular Genetics and Metabolism 2010; 100: 111–117.

Wu T, Hallett M. The cerebellum in Parkinson's disease. Brain 2013; 136: 696–709.

Xiao J, Uitti RJ, Zhao Y, Vemula SR, Perlmutter JS, Wszolek ZK, et al. Mutations in CIZ1 cause adult onset primary cervical dystonia. Ann Neurol. 2012; 71: 458–469.

Ysselstein D, Nguyen M, Young TJ, Severino A, Schwake M, Merchant K, et al. LRRK2 kinase activity regulates lysosomal glucocerebrosidase in neurons derived from Parkinson's disease patients. Nat Commun 2019; 10: 5570–9.

Zarranz JJ, Alegre J, Gómez-Esteban JC, Lezcano E, Ros R, Ampuero I, et al. The new mutation, E46K, of alpha-synuclein causes Parkinson and Lewy body dementia. Ann Neurol. 2004; 55: 164–173.

Zeviani M, Simonati A, Bindoff LA. Ataxia in mitochondrial disorders. Handb Clin Neurol 2012; 103: 359–372.

Zglinicki von T. Oxidative stress shortens telomeres. Trends Biochem. Sci. 2002; 27: 339–344.

Zimprich A, Grabowski M, Asmus F, Naumann M, Berg D, Bertram M, et al. Mutations in the gene encoding epsilon-sarcoglycan cause myoclonus-dystonia syndrome. Nat. Genet. 2001; 29: 66–69.

Zhan Y, Song C, Karlsson R, Tillander A, Reynolds CA, Pedersen NL, et al. Telomere Length Shortening and Alzheimer Disease--A Mendelian Randomization Study. JAMA Neurol 2015; 72: 1202–1203.

Zhang Y, Shu L, Sun Q, Zhou X, Pan H, Guo J, et al. Integrated Genetic Analysis of Racial Differences of Common GBA Variants in Parkinson's Disease: A Meta-Analysis. Front. Mol. Neurosci. 2018; 11: 1972–9.

Zucca FA, Segura-Aguilar J, Ferrari E, Muñoz P, Paris I, Sulzer D, et al. Interactions of iron, dopamine and neuromelanin pathways in brain aging and Parkinson's disease. Prog. Neurobiol. 2015

Supplement

Table S1: Atypical parkinsonian disorders

Disease name	Mean age at onset	Characteristic clinical features	*Post-mortem* pathology	Additional findings
Atypical parkinsonian disorders				
Multiple System Atrophy-Parkinsonism (MSA-P, 60% of MSA cases worldwide, 30% in Japan)	53 years	Parkinsonism > cerebellar (gait or limb ataxia ataxic dysarthria, cerebellar oculomotor signs) autonomic (orthostatic hypotension, urinary incontinence, erectile dysfunction), pyramidal features, nocturnal stridor, REM-sleep behaviour disorder	Oligodendroglial cytoplasmic alpha-synuclein accumulation	Brain MRI: pontine "hot cross bun" sign, atrophy of middle cerebellar peduncle, putamen, pons, cerebellum
Multiple System Atrophy-Cerebellar (MSA-C, 30% of MSA cases worldwide, 60% in Japan)	53 years	Cerebellar > parkinsonism, autonomic, pyramidal features, nocturnal stridor, REM-sleep behaviour disorder		Brain MRI: hyperintense "putaminal rim" (MSA-P), atrophy of middle cerebellar peduncle, putamen, pons
Progressive Supranuclear Palsy (PSP)	63 years	Combination of supranuclear gaze palsy, gait abnormalities with falls within first three years	4-repeat tau aggregates in astrocytes (tufts), oligodendrocytes (coiled bodies) and neurons (neurofibrillary tangles)	Brain MRI: midbrain atrophy – mickey mouse / penguin sign
PSP phenotypes				

PSP-Richardson´s Syndrome (PSP-RS, 40% of all PSP cases)	66 yrs.	Symmetric, axial, akinetic-rigid, levodopa-resistant parkinsonism, early postural instability and vertical supranuclear gaze palsy	PSP pathology predominantly in globus pallidus, substantia nigra, subthalamic nucleus, red nucleus, pontine tegmentum, oculomotor nucleus, dentate nucleus	Brain MRI: midbrain atrophy – mickey mouse / penguin sign
PSP-Parkinsonism (PSP-P, 20% of all PSP cases)	64 yrs.	Initially levodopa-responsive, asymmetric, limb-predominant parkinsonism, and later onset postural instability, falls and supranuclear gaze palsy	Less severe tau pathology in midbrain (substantia nigra and ventral tegmentum)	-
Pure akinesia with gait freezing (PAGF; <5% of all PSP cases)	6th decade	Gait freezing without rigidity & late-onset supranuclear gaze palsy	Severe atrophy and neuronal loss in globus pallidus, substantia nigra and subthalamic nucleus only	-
PSP- Behavioural variant frontotemporal dementia phenotype (bvFTD; 15% of all PSP cases)	6th decade	Apathy, social disinhibition, loss of empathy and impaired executive functions, parkinsonism within 3-7 yrs. of onset, late supranuclear gaze palsy	n.k.	-
PSP-Progressive non-fluent Aphasia phenotype (PNFA; 5% of PSP cases)	6th decade	Non-fluent speech production & agrammatism	Additional severe temporal cortex and superior frontal gyrus cortical tau pathology	-
PSP-Corticobasal syndrome Phenotype (PSP-CBS; <5% of cases)	66 yrs.	Combination of cortical and extrapyramidal symptoms, aphasia, araxia, asymmetric	Additional severe midfrontal and inferior parietal cortical tau pathology	-

PSP-Cerebellar phenotype (PSP-C; rare)	69 yrs.	Prominent gait and limb ataxia up to 7 years before onset of parkinsonian features, sometimes before onset of supranuclear gaze palsy	Additional tau-positive inclusion bodies in Purkinje cells	-
PSP-primary lateral sclerosis Phenotype (PSP-PML)	71 yrs.	Mixture of prominent parkinsonian and pyramidal signs	Additional PSP-pathology in precentral gyrus and pyramidal tract	-
PSP-pallido-nigro-luysian-Atrophy phenotype (PSP-PNLA, rare)	57 yrs.	Similar presentation to PSP-RS but earlier gait abnormalities, hand-writing difficulties and freezing, falls late feature	Severe degeneration and axonal dystrophy in pallido-nigro-luysial distribution	-
Corticobasal Degeneration (CBD)	64 yrs.	Variable; At least one cortical (apraxia, loss of cortical sensitivity, alien limb) and one extrapyramidal (akinesia, rigidity, myoclonus, dystonia) symptom	CBD describes pathological entity: Astrocytic, oligodendrocytic and neuronal 4-repeat tau protein aggregation in basal ganglia and neocortex	-
CBD phenotypes				
Corticobasal syndrome (CBS)		Markedly asymmetric combination of symptoms of cortical (apraxia, astereognosis, myoclonus, alien limb) and basal ganglia dysfunction (rigidity, akinesia, dystonia, myoclonus), levodopa-unresponsive	CBS describes clinical entity – pathology unchanged form CBD	-
CBD-Frontal behavioural-spatial syndrome (fBS); ca 10% of all CBD cases)	?	Executive dysfunction, behavioural/personality changes, visuospatial defecits	CBD pathology more in the frontal cortex	-

CBD-Richardson´s syndrome (RS) **ca 40% of all CBD cases)**	?	Symmetric axial, akinetic-ridig, levodopa-resistant parkinsonism with early-onset postural instability and vertical supranuclear gaze palsy	CBD pathology prominent in the brainstem	-
CBD-Progressive nonfluent aphasia **(PNFA; <5% of all CBS cases)**	?	Additional non-fluent speech production with agrammatism	CBD pathology	-

Table S2: Monogenic familial PD

Gene symbol (disease name)	Gene name	Mean age at onset	Characteristic clinical features	*Post-mortem* pathology	Pathophysiology
Autosomal-dominant					
SNCA **p.A30P** **p.H50Q** **p.E46K**	Alpha-synuclein p.A30P, p.H50Q, p.E46K mutations	6th – 7th decade	Depending on genotype	Alpha-synuclein	Synaptic/mitochondrial function, autophagy
SNCA **p.A53E** **p.A53T**	Alpha-synuclein p.A53E, p.A53T mutations	3rd – 6th decade	PD + cognitive involvement	-	-
SNCA **p.G51D**	Alpha-synuclein p.G51D	2nd -4th decade	Aggressive PD + spasticity, cognitive involvement + seizures	-	-
SNCA **multiplications**	Alpha-synuclein	Depending on gene number	Similar to PD but more cognitive involvement with increasing gene copy number	-	-
LRRK2	Leucine-rich repeat kinase 2	Mostly 6th decade, variable	Majority indistinguishable from sporadic PD, single CBS, PSP cases described	Majority neuronal degeneration with Lewy bodies, minority without Lewy bodies, individual cases with PSP, MSA and FTD pathology	Synaptic function, inflammation, autophagy

***VPS35* pD620N**	Vacuolar protein sorting 35 homolog	53 yrs.	Similar to sporadic PD with slow progression	n.k.	Autophagy, endocytosis
Autosomal-recessive					
***GBA* p.N370S**	Glucocerebrosidase	4th decade	Similar to sporadic PD + hepatosplenomegaly, anaemia, thrombocytopenia	Alpha-synuclein pathology in brainstem, hippocampus and cortex	Inflammation, autophagy, metabolic
parkin	Parkin RBR E3 ubiquitin protein ligase	~35 yrs.	Similar to sporadic PD but frequent (foot) dystonia, slower disease progression and early levodopa-induced dyskinesia	Severe Substantia nigra cell loss, often wihout Lewy body pathology, occasional cortical and brainstem neurofibrillary tangles	Mitochondrial/synaptic function, ubiquitination
PINK1	PTEN-induced putative kinase 1	~35 yrs.	Slowly-progressive, levodopa-responsive PD, often prominent dystonia	Substantia nigra cell loss, brainstem Lewy body pathology	Mitophagy
DJ-1	Daisuke-Junko 1 gene	~35 yrs.	Similar to sporadic PD with slow disease progression, frequent focal dystonia	n.k.	Inflammation, mitochondrial function
PLA2G6	Phospholipase A2, group VI	2nd – 3rd decade	Subacute onset dystonia-parkinsonism, pyramidal signs, eye movement abnormalities, cognitive	Prominent basal ganglia and cortical Alpha-synuclein +/- tau, axonal spheroids	Mitochondrial function

			decline, initially levodopa-responsive		
FBX07	F-box protein 7	Childhood onset equinovarus, parkinsonism in 2nd - 3rd decade	Equinovarus deformity, lower limb spasticity, pyramidal signs + parkinsonism	+	Ubiquitination, mitochondrial function
***ATP13A2* (Kufor-Rakeb)**	ATPase type 13A2	12-16 yrs.	Rapid progressive Parkinsonism + pyramidal signs, cognitive decline, (incomplete) supranuclear gaze palsy, usually levodopa-responsive	n.k.	Mitochondrial function, autophagy
DNAJC6	DnaJ (Hsp40) homolog, subfamily C, member 6	Some families <11 yrs., others 3rd – 5th decade	Dependent on age at onset: juvenile onset: rapid progression, levodopa-non-responsive, dominant dystonia, pyramidal features, seizures and mental retardation; late adulthood onset: slow progression, levodopa-responsive	n.k.	Synaptic vesicle function, endocytosis
SYNJ1	Synaptojanin 11	22-28 yrs.	Rapidly progressive bradykinesia, fatigue, leg rigidity, cognitive	n.k.	Synaptic vesicle function, endocytosis

			decline and dysarthria, supranuclear gaze palsy, levodopa-induced severe oromandibular and limb dystonia		
VPS13C	Vacuolar protein sorting 13C	25-46 yrs.	Rapid and severe progression with early cognitive decline, dysarthria, dysautonomia	Diffuse alpha-synuclein throughout + brainstem, hippocampus and motor cortex tau-positive neurofibrillary tangles	PINK1/Parkin-dependent mitophagy
X-linked					
RAB39B	RAB39B, member RAS oncogene family	Childhood-onset intellectual disability; parkinsonism <45 yrs	Variable degree of intellectual disability and parkinsonism	Wide-spread classic alpha-synuclein, iron accumulation, tau immuno-reactivity, axonal spheroids	Alpha-synuclein homeostasis, synapse formation / maintenance
X-linked dystonia-parkinsonism (Lubag)	Xq13.1	4th – 5th decade	Starts with focal dystonia progressing into generalized dystonia, action/rest tremor, only minority show parkinsonism	n.k.	n.k.
High-risk variants (odds ratio 5-8)					

GBA	Glucocerebrosidase	1-6 yrs. younger than sporadic PD	Similar to sporadic PD but higher incidence of cognitive impairment, anxiety, depression; more rapid disease progression	Alpha-synuclein pathology in brainstem, hippocampus and cortex	Inflammation, autophagy, metabolic
Additionally, established genetic associations with prominent parkinsonism					
***GCH-1* (dopa-responsive dystonia)**	GTP-cyclohydroxylase 1	~46 yrs.	Similar to sporadic PD	n.k.	Dopamine-synthesis
22q11.2 deletion	n.a.	~37 yrs.	Childhood cognitive impairment, psychotic features, early drug-related dyskinesia, +/- orofacial dysmorphia	n.k.	n.k.

Table S3: Neurodegeneration with brain iron accumulation (NBIA)

Disease name / Gene symbol	Gene name (inheritance)	Mean age at onset	Characteristic clinical features	Postmortem pathology	Classical findings
Panthothenate-kinase associated neurodegeneration (PKAN)	PANK2 (AR)	< 6yrs, (classic, rapid-progressive)	Lower limb dystonia - opisthotonus, mild cognitive impairment, pyramidal tract signs, pigmentary retinopathy, progressive	Perivascular Globus pallidus iron accumulation, neuroaxonal spheroids, alpha-synuclein negative	Eye of the tiger sign on T2-weighed MRI; +/- acanthocytes
-	-	Adolescence (atypical, slowly progressive)	Change in speech pattern, eating dystonia, progressive tics, neuropsychiatric symptoms, mixed degree of dystonia, parkinsonism, spasticity	-	-
Phospholipase A2-associated neurodegeneration (PLAN)	PLA2G6 (AR)	6m – 3yrs (INAD)	Slowing and cessation of development, regression in all domains, pronounced cerebellar features, death before 10yrs.	Dystrophic axonal spheroids in peripheral and central nervous tissue	cerebellar atrophy, thinning of corpus callosum and optic chiasma; iron deposition often only on SWI-weighed MRI
-	-	Adolescence (adult form)	Dystonia-parkinsonism, cognitive & psychiatric features	+ prominent basal ganglia and cortical alpha-Synuclein +/- Tau	Globus pallidus iron accumulation
Mitochondrial membrane protein-associated	C19orf12 (AR)	0-10 yrs	Spastic gait, optic atrophy, cognitive impairment, distal dystonia	Prominent generalized alpha-Synuclein in basal	Imaging: T2-weighed hypointense signal (iron deposition) in Globus

neurodegeneration (MPAN)				ganglia and neocortex (protein load 40x more than sporadic PD), Globus pallidus iron	pallidus and Substantia nigra
		Early adulthood	Parkinsonism, cognitive & behavioural changes	-	-
Beta-propeller protein-associated neurodegeneration (BPAN; previously called "static encephalopathy with neurodegeneration in childhood", SENDA)	WDR45 (X-linked dominant)	Biphasic course with childhood onset and decline in adolescence	Global developmental delay, pyramidal signs, disordered sleep in childhood; parkinsonism, dystonia, dementia in adolescence	Axonal spheroids, Tau-positive neurofibrillary tangles	Imaging: T2-weighed hypointensities in Globus pallidus, cerebral peduncles and particularly Substantia nigra; T1-weighed hyperintense "halo" in Substantia nigra
Fatty acid hydroxylase-associated neurodegeneration (FAHN)	FA2H (AR)	0-10 yrs	Progressive spasticity, dystonia, cerebellar dysfunction, dysarthria, dysphagia, cognitive decline, optic atrophy	n.k.	Imaging: T2-weighed hypointensity in Globus pallidus, white matter lesions, thinning of corpus callosum, atrophy of cerebellum, pons, medulla & chord
Coenzyme A synthase protein-associated neurodegeneration (CoPAN)	COASY (AR)	0-10 yrs	Gait difficulties, cognitive impairment, dysarthria, spasticity, axonal neuropathy, parkinsonism	n.k.	n.k.
Kufor-Rakeb	ATP13A2 (AR)	11-22 yrs	Slowly progressive, fatigue, gait difficulties, parkinsonism, facial-faucial finger minim-	n.k.	Generalized brain atrophy, hypointensities in lentiform nucleus

			myoclonus, supranuclear gaze palsy, visual hallucinations		
Woodhouse-Sakati syndrome	DCAF17 (AR)	10-20 yrs	Progressive alopecia, hypogonadism, choreoathetosis, dystonia, dysarthria, dysphagia, diabetes mellitus, sensorineural deafness	n.k.	Basal ganglia hypointensities, extensive whiter matter hypertintensities on T2-weighed MRI
Neuroferritinopathy	FTL (AR)	mid-life	Asymmetric chorea, predominant orofacial dystonia, parkinsonism, cognitive decline, low serum ferritin	n.k.	T2-weighed hypointensities in putamen, caudate, thalamus, globus pallidus, substantia nigra and red nucleus
Aceruloplasminemia	CP (AR)	adulthood	Microcytic anaemia, diabetes, retinal disease, facial dystonia, chorea, tremor, parkinsonism, ataxia, cognitive decline; Low or absent serum coeruloplasmin, elevated ferritin, low iron, low serum copper but normal urinary copper;	n.k.	Basal ganglia T2-weighed hypointensities

Table S4: Other heredo-degenerative causes of parkinsonism; n.k. not known

Syndrome (gene)	onset	Clinical features	pathology	Suggestive features
Fragile-X tremor ataxia syndrome (*FMR1* CGG 55-200 repeat expansions)	60 yrs. (men), unknown in women	Action>intention>rest tremor, cerebellar gait and eye movement abnormalities, parkinsonism, neuropathy	Spherical, eosinophilic, ubiquitin-positive neuronal & astrocytic inclusions throughout the brain, Purkinje cell loss	Ovarian failure, family history of cognitive impairment, MCP-sign on T2-weighed MRI
Perry syndrome (*DCTN1*)	46 yrs.	Rapid-progressive, levodopa-non-responsive parkinsonism, apathy, depression, weight loss, nocturnal central apnoea	Massive cell loss in Substantia nigra, locus coeruleus, dorsal raphe nucleus, caudate, pallidum, putamen and pre-Bötzinger complex (medullar respiratory pacemaker) with few or no Lewy bodies	-
X-linked dystonia parkinsonism (DYT3, Lubag)	39-40 yrs.	Male : Female 100:1; starting predominantly as progressive, generalizing dystonia, over time more parkinsonian features, after 15 yrs. predominantly akinetic-rigid, often + tremor, myoclonus, chorea and myorhythmia	Atrophy in striatum, caudate nucleus, changing pattern of involvement of striosome and matrix over time;	Depression, high suicide rate; MRI: hyperintense putaminal ring (dystonic & parkinsonian phase), atrophy in caudate and putamen in parkinsonian phase
Dopa-responsive dystonia (*GCH1*, DYT5a)	4.5 yrs.	Slowly progressive lower limb onset dystonia, generalizing, late-onset parkinsonism;	Reduction in nigral melanin and dopamine content without cell loss or degeneration	Diurnal fluctuations, excellent and sustained effect of low doses of levodopa on motor features

Rapid-onset dystonia parkinsonism (*ATP1A3*, DYT12)	75% <25 yrs.	Abrupt onset of dystonia-parkinsonism, cranial-caudal severity gradient, triggered by acute illness or event	Possible channelopathy located at cortical interneurons	-
Autosomal recessive, early-onset dystonia-parkinsonism (*PRKRA*, DYT16)	childhood	Variable parkinsonism + dystonia, generalization	n.k.	-
Dopamine transporter deficiency syndrome (*SLC6A3*)	infancy	Complex disorder with progressive parkinsonism-dystonia	n.k.	-
Huntington`s disease (CAG repeat expansion in *HTT*)	1st decade 2nd decade	Westphal variant: developmental delay, cognitive dysfunction, behavioural difficulties, followed by parkinsonism	Predominant striatal medium spiny neuron pathology	-
Huntington-disease like type 3 (chr. 4p15.3)	3-4 yrs.	Parkinsonism, dystonia, chorea, pyramidal signs	n.k.	-
Chorea-Acanthocytosis (*VPS13A*)	2nd -3rd decade	Chorea, "feeding" dystonia with tongue protrusion, tics, subcortical dementia, eye movement abnormalities, self-mutilation, parkinsonism in minority	n.k.	Acanthocytes on blood film, elevated creatine kinase, hepatomegaly
MacLeod (*XK*)	25-60 yr.	Chorea, facial dyskinesia >>tongue biting, dysphagia, dystonia or parkinsonism	n.k.	Acanthocytes on blood film, elevated creatine kinase; Cardiac: atrial fibrillations, dilatative cardiomyopathy
SCA 2, 3, 6, 13, 17	Variable, 3rd - 5th decade	Adult onset gait and limb ataxia, slowed saccades, lower	variable	-

		limb spasticity +/- parkinsonism		
Dentato-rubro-pallido-luysian atrophy (CAG repeat expansion in *ATN1*)	20-30 yrs.	Chorea, ataxia, myoclonus, parkinsonism	n.k.	-
Hereditary spastic paraparesis type 11 (*KIAA1840*, SPG11)	Early infancy - adulthood	Progressive lower limb weakness and spasticity + ataxia, early-onset levodopa-responsive parkinsonism in singular patients	n.k.	Thin corpus callosum on MRI
Hereditary spastic paraparesis type 11 (*ZFYVE26*, SPG15)	1st – 2nd decade	Progressive lower limb weakness and spasticity + intellectual disability, dysarthria, parkinsonism, axonal neuropathy	n.k.	Thin corpus callosum on MRI
Frontotemporal dementia with parkinsonism (*MAPT*, FTDP-17)	variable	Behaviour / personality change, cognitive dysfunction, atypical parkinsonism	Cortical and subcortical neuronal & glial hyper-phosphorylated tau-inclusions	-
Creutzfeld-Jakob/Prion disease	Sporadic / familial / infectious	Subacute, rapidly progressive, cognitive decline, cerebellar symptoms, visual changes +/- parkinsonism, alien limb, supranuclear gaze palsy, dystonia, myoclonus	Generalized atrophy, cell loss, vacuolation	CSF protein 14-3-3, EEG: periodic sharp waves, cortical ribboning on DWI-MRI
Gerstmann-Sträussler-Scheinker (*PRNP*) / familial prion disease	4th – 6th decade	Slightly slower progressive course with subacute progressive ataxia or parkinsonism	Generalized atrophy, cell loss, vacuolation	CSF protein 14-3-3, EEG: periodic sharp waves, limbic DWI-hyperintensities

Parkinsonism-dementia-ALS-complex of Guam	52 yrs.	Parkinsonism, upper motor neuron signs, dementia, apathy, supranuclear gaze palsy	Substantia nigra degeneration, severe tau neurofibrillary tangles, beta-amyloid pathology inconsistent	-
Fahr`s disease	3nd – 5th decade	Parkinsonism, chorea, tremor, cognitive, neuropsychiatric symptoms	Basal ganglia calcifications	-

Table S5: Other causes of metabolic, toxic and structural causes of parkinsonism

Metabolic
Wilson´s disease, Maple syrup urine disease, Neuronal ceroid lipofuscinosis, Mitochondrial (e.g. POLG), Niemann-Pick type C, GM1 gangliosidosis, Phenylketonuria, Cerebrotendinous xanthomatosis, Hemiparkinsonism-hemiatrophy syndrom
Structural
Vascular parkinsonism, Post-traumatic, Post-encephalitic, Post-anoxic
Toxic
MPTP, Ephedrone, Manganese, Cyanide, Carbon monoxide
Drug-induced
Typical antipsychotics (Haloperidol, Chlorpromazine), atypical antipsychotics (Risperidone, Olanzapine), Metoclopramide, Valproate, Tetrabenazine, Reserpine, Anti-histamines (Flunarizine, Cinnirizine), Lithium

Table S6: Monogenic Isolated and Combined dystonia; * the use of the DYT-based classification has been abandoned

Syndrome		Inheritance	Gene / designation *	Distribution	Suggestive clinical features
Isolated Dystonia	Adolescence-onset cranio-cervical dystonia	AD	*ANO3* / DYT24	Focal, segmental	Tremulous cervical dystonia, can present as arm tremor
		AD	*GNAL* / DYT25	Focal, segmental, generalized (in 10% of cases)	Cervical dystonia, often tremulous +/- laryngeal dystonia
		AD	*TUBB4A* / DYT4	Focal, segmental	Prominent laryngeal & oromandibular involvement, “whispering dystonia”, sometimes as more complex hypomyelination with atrophy of the basal ganglia (H-ABC) syndrome
		AD	*CIZ1*	Focal	(Tremulous) cervical dystonia
		AR	*HPCA*	Segmental, generalized	Upper limb, cranio-cervical region
		AR	*VPS16*	Segmental	
		AR	*COL6A3*	Segmental	Upper limb onset, cranio-cervical involvement
	Early-onset generalized dystonia	AD	*TOR1A* / DYT1	Generalized, leg-onset	sparing of larynx/neck
		AD	*THAP1* / DYT6	Generalized > segmental	Prominent laryngeal involvement, rostro-caudal gradient
		AD	*KMT2B* / DYT28	Generalized	Intellectual disability, dysmorphia, short stature, hypointense lateral streak of external globus pallidus

Combined dystonia	Early-onset Myoclonus-Dystonia	AD	*KCTD17* / DYT26	Generalized	motor developmental delay
		AD	*SGCE* / DYT11	Generalized	Most frequent form of myoclonus-dystonia, psychiatric co-morbidities (anxiety, depression)
		AD	*CACNA1B*	Focal, segmental, generalized	Action myoclonus of legs
	Early-onset dystonia-chorea-myoclonus	AD and AR	*ADCY5*	Generalized	Benign hereditary chorea, episodic hyperkinesia triggered by sleep
		AD	*TITF1*	Generalized	Benign hereditary chorea, "brain-thyroid-lung disease" onset in infancy with chorea developing into myoclonus-dystonia phenotype; association with thyroid and respiratory disorders
		X-linked	*SLC16A2*	Generalized	Allan-Herndon-Dudley Syndrome, onset in infancy with axial hypotonia, initially limb chorea, later dystonia, sometimes thyroid disease
	Early-onset Dystonia-Parkinsonism	AR	*PPKRA* / DYT16	Generalized, limb-onset	Marked axial & laryngeal involvement, striking retrocollis/opisthotonus possible, sardonic smile, no response to L-dopa
		AR	*SLC6A3*	Focal, segmental, generalized	Axial hypotonia, irritability, delayed motor milestones, poor L-dopa response

		X-linked	*TAF1* / DYT3	Focal, segmental, multi-focal, generalised	Filipino males from Panay, oromandibular involvement possible
		AR	*GCDH*	Generalized	Glutaric Acidaemia Type 1: infancy onset with intermittent metabolic decompensation, encephalopathy
		AR	*GLB1 / HEXa, HEXB, GM2A*	Generalized	GM1 / GM2 gangliosidosis: infantile onset, dystonia-parkinsonism, ataxia, pyramidal signs, cognitive decline
	Adult-onset Dystonia-Parkinsonism	AR	*ATP7B*	Generalized	Hepatolenticular degeneration / Wilson disease: psychiatric (depression) or congnitive symptoms followed by dystonia +/- parkinsonism, tremor, cerebellar
			SLC30A10	Generalized	Manganese transportopathy: childhood-onset dystonia-parkinsonism
			SLC39A14	Generalized	Manganese transportopathy: childhood-onset dystonia-parkinsonism
	Rapid-onset Dystonia Parkinsonism	AD	*ATP1A3* / DYT12	Focal, segmental, generalized	Abrupt onset after triggers, prominent speech and swallowing; can also present as: Alternating hemiplegia of childhood; paroxysmal limb dystonia; cerebellar ataxia- pes cavus, optic atrophy-sensorineural hearing loss (CAPOS) syndrome
	Dopa-Responsive Dystonia	AD and AR	*GCH1* / DYT5a	Segmental, generalized	Childhood onset, diurnal fluctuations +/- pyramidal signs

		AR	*TH* / DYT5b	Segmental, generalized	Infancy onset, oculogyric crisis (paroxysmal, conjugate, tonic upward deviation), truncal hypotonia, autonomic disturbance, tremor and myoclonus
		AR	*SPR*	Segmental, generalized	Infancy onset, axial hypotonia, motor and language delay, oculogyric crisis, diurnal fluctuation, behavioural abnormalities
		AR	*AADC*	Segmental, generalized	Infancy onset, axial hypotonia (95%), oculogyric crisis (86%), developmental retardation, hypokinesia, bulbar dysfunction, sleep disturbance, autonomic dysfunction, labile temperature regulation
	Dopamine transporter deficiency syndrome	AR	*SLC6A3*	Segmental, generalized	Infancy onset, axial hypotonia, irritability, oculogyric crisis, eye flutter, global developmental delay, bulbar dysfunction, initially hyperkinetic dystonia developing into hypokinetic parkinsonism, hypersalivation, sweating, sleeping difficulties
	Vesicular monoamine transporter disease	AR	*SLC18A2*	Segmental, generalized	Infancy onset, axial hypotonia, severe dystonia-parkinsonism, oculogyric crisis, temperature instability, sweating, ptosis, depression, sleep disturbance
		AR	*DHPR*	Segmental, generalized	axial hypotonia, oculogyric crisis, seizures, hyperphenylalanaemia

		AR	*PTS*	Segmental, generalized	axial hypotonia, oculogyric crisis, seizures, hyperphenylalanaemia
		AR	*DNAJC12*	Segmental, generalized	Intellectual disability, hyperphenylalanaemia
Paroxysmal dystonia	Kinesiogenic	AD	*PRRT2* / DYT10	Generalized	Familial infantile epilepsy, hemiplegic migraine
		AD	*SCN8A*	Generalized	Familial infantile epilepsy
		AD	*KCNA1*	Generalized	Paroxysmal ataxia with interictal myokymia
	Non-Kinesiogenic	AD	*PNKD*	Generalized	Paroxysmal attacks, typically painful, duration minutes - hours
		AD	*CACNA1A*	Generalized	Paroxysmal torticollis of infancy, paroxysmal ataxia with interictal dystonia, hemiplegic migraine, spinocerebellar ataxia 6, early infantile epileptic encephalopathy
		AD	*KCNMA1*	Generalized	Epilepsy, cerebellar ataxia
	Exercise-induced	AD	*SLC2A1* / DYT9	Generalized	GLUT1-deficiency, spasticiy, microcephaly, ataxia, epilepsy

Table S7: Clinical and demographic details of brain tissue donors for lysosomal enzyme activity measurement

Dystonia	sex	AAO	disease duration	Age at death	post mortem delay	cause of death	phenotype
dystonia	m	16	63	79	28	aspiration pneumonia	initially writer`s cramp, then generalizing: cervical, spasmodic dysphonia, dystonic gait, bilateral thalamotomy aged 35, spinal rhizotomy aged 46, generalized dystonia & anarthria from age 52
dystonia	m	15	54	69	72	unknown	torsion dystonia; onset cervical, by 21 segmental cervical, arm, face + swallowing, by 30 nearly anarthric, dysphagia
dystonia	f	18	57	75	20	unknown	segmental neck & arm dystonia; started Cervical, spread to face, symptoms improved during pregnancy, developed cervical myelopathy, right hand tremor, spasmodic dysphonia,
dystonia	f	64	25	89	72	COPD, pneumonia	cervical dystonia; received Botox until death
dystonia	f	35	23	58	72	respiratory arrest	cerviacl dystonia, previous surgeries to neck muscles, then Botox
dystonia	m	68	24	92	96	carcinomatosis	blepharospasm ->oromandibular
dystonia	f	53	31	84	54	hypoadrenalism	blepharospasm for 9 years, treated with botox, then subsided age 62, earlier pituiutary adenoma = radiotherapy
dystonia	f	44	40	84	96	unknown	blepharospasm, tremulous cervical dystonia (fhx: stammer and tremor in mother), facial nerve avulsion
dystonia	f	18	56	74	unknown	unknown	bleharospasm from 18, writer`s cramp from age 39, father and paternal granddad ptosis without blepharospasm
dystonia	f	56	14	70	27	unknown	blepharospasm

ctrl	f	n.a.	n.a.	82	96	renal failure, UTI	no neurological symptoms
ctrl	m	n.a.	n.a.	89	41	bronchopneumonia	peirpheral neuropathy of unknown aetiology
ctrl	m	n.a.	n.a.	88	96	lung metastases of unknown primary	no neurological symptoms
ctrl	f	n.a.	n.a.	87	41	unknown	no neurological symptoms
ctrl	m	n.a.	n.a.	84	72	prostate cancer	no neurological symptoms
ctrl	f	n.a.	n.a.	88	34	metastatic colon carcinoma	Meniere"s disease
ctrl	m	n.a.	n.a.	76	72	multiple organ failure	no neurological symptoms
ctrl	f	n.a.	n.a.	71	72	metastatic lung cancer	no neurological symptoms
ctrl	f	54	42	96	61	unknown, in nursing home	no neurological symptoms
ctrl	f	n.a.		90	42	pneumonia	no neurological symptoms

Table S8: Details of spleen and putaminal samples used to assess a correlation between blood and brain TL with respective demographic details. Further demographic details, as far as supplied by the collecting tissue brain bank, are summarized in table S11.

Spleen (SPL)	**Putamen (PUTM)**	**SEX**	**AGE**	**Spleen (SPL)**	**Putamen (PUTM)**	**SEX**	**AGE**
018/05	018/05	M	45	**033/09**	033/09	M	56
025/05	025/05	M	28	**034/09**	034/09	M	49
004/06	004/06	F	52	**035/09**	035/09	M	32
007/06	007/06	M	41	**036/09**	036/09	F	44
022/06	022/06	M	53	**038/09**	038/09	M	60
030/06	030/06	M	53	**001/10**	001/10	M	62
034/06	034/06	M	53	**002/10**	002/10	M	38
035/06	035/06	M	54	**003/10**	003/10	M	65
043/06	043/06	F	53	**004/10**	004/10	M	50
009/07	009/07	M	45	**006/10**	006/10	F	32
015/07	015/07	M	60	**007/10**	007/10	M	70
020/07	020/07	F	22	**008/10**	008/10	M	61
026/07	026/07	M	57	**010/10**	010/10	M	39
002/08	002/08	F	45	**011/10**	011/10	M	60
003/08	003/08	M	50	**012/10**	012/10	M	40
004/08	004/08	M	45	**013/10**	013/10	M	60
006/08	006/08	M	41	**014/10**	014/10	M	61
007/08	007/08	M	55	**015/10**	015/10	M	52
012/08	012/08	M	62	**016/10**	016/10	F	63
014/08	014/08	M	67	**018/10**	018/10	M	69
017/08	017/08	F	51	**019/10**	019/10	M	47
018/08	018/08	M	61	**020/10**	020/10	M	36
019/08	019/08	M	58	**021/10**	021/10	M	27

020/08	020/08	M	51	**023/10**	023/10	M	74
021/08	021/08	M	44	**025/10**	025/10	M	75
022/08	022/08	F	57	**028/10**	028/10	M	43
023/08	023/08	F	24	**032/10**	032/10	M	34
025/08	025/08	M	37	**033/10**	033/10	M	51
026/08	026/08	M	45	**036/10**	036/10	M	52
033/08	033/08	M	22	**039/10**	039/10	M	48
034/08	034/08	M	70	**040/10**	040/10	M	43
036/08	036/08	F	20	**041/10**	041/10	M	57
038/08	038/08	M	46	**011/11**	011/11	M	63
040/08	040/08	M	48	**012/11**	012/11	M	53
005/09	empty	M	76	**013/11**	013/11	M	58
006/09	006/09	M	25	**014/11**	014/11	M	62
013/09	013/09	F	79	**016/11**	016/11	M	74
014/09	014/09	M	26	**018/11**	018/11	F	50
015/09	015/09	M	67	**019/11**	019/11	M	66
018/09	018/09	M	57	**020/11**	020/11	M	66
021/09	021/09	M	65	**025/11**	025/11	M	66
022/09	022/09	F	60	**026/11**	026/11	M	62
023/09	023/09	F	64	**029/11**	029/11	F	43
024/09	024/09	M	48	**030/11**	030/11	M	30
025/09	025/09	M	59	**032/11**	032/11	M	58
026/09	026/09	M	73	**033/11**	033/11	F	72
028/09	028/09	M	50	**036/11**	036/11	M	48
030/09	030/09	F	61	**037/11**	037/11	M	48
031/09	031/09	M	51	**041/11**	041/11	M	42
032/09	032/09	F	60				

Table S9.: Structure of 2019 IPDGC PD GWAS data set, used the MR replication attempt (adopted from supplement {Nalls:2019ew})

Study	Cases (N)	Controls (N)	Total (N)	fem cases (%)	fem ctrl (%)	Case age at onset (mean, SD; yrs)	Ctrl age at last exam (mean, SD; yrs)	Case ascertainment criteria	Status
23andMe, post-Chang et al. 2017 enrollment	2.448	571.411	573.859	39,1	54,9	symptoms: 58.04 (11.64); diagnosis: 61.78 (10.94)	51.47 (16.8)	Unrelated individuals with >97% genetically inferred European ancestry who self-reported having been diagnosed with PD. Exclusion: 1) a change in diagnosis, 2) uncertainty about their diagnosis, and 3) a history of stroke, deep vein thrombosis, or pulmonary embolism. In a previous telemedicine study, a neurologist confirmed a diagnosis of PD in 50 out of 50 individuals tested in this cohort.	New dataset
Baylor College of Medicine / University of Maryland	769	195	964	33,8	69,7	64.83 (10.1)	65.48 (8.3)	Clinic visit; standard UK Brain Bank criteria with a modification to allow the inclusion of cases that had a family history of PD	New dataset

Finnish Parkinson's	386	493	879	45,9	78,9	55.27 (5.6)	92.35 (3.9)	Clinic visit; standard UK Brain Bank criteria with a modification to allow the inclusion of cases that had a family history of PD	New dataset
Harvard Biomarker Study (HBS)	527	472	999	34,4	61,6	66.31 (10.1)	69.9 (9.0)	Clinic visit; standard UK Brain Bank criteria with a modification to allow the inclusion of cases that had a family history of PD	New dataset
McGill Parkinson's	582	905	1.487	34,5	48,4	65.71 (9.8)	55.79 (10.7)	Clinic visit; standard UK Brain Bank criteria with a modification to allow the inclusion of cases that had a family history of PD	New dataset
Oslo Parkinson's Disease Study	476	462	938	35,7	42,2	65.32 (9.3)	61.85 (11.1)	Clinic visit; standard UK Brain Bank criteria with a modification to allow the inclusion of cases that had a family history of PD	New dataset
Parkinson's Disease Biomarker's Program (PDBP)	512	282	794	38,7	51,1	64.46 (9.4)	62.19 (10.7)	Clinic visit; standard UK Brain Bank criteria with a modification to allow the inclusion of cases that had a family history of PD	New dataset
Parkinson's Progression Markers Initiative (PPMI)	363	165	528	33,1	33,3	64.24 (9.7)	63.79 (10.6)	Clinic visit; standard UK Brain Bank criteria with a modification to allow the inclusion of cases that had a family history of PD	New dataset

System Genomics of Parkinson's Disease (SGPD)	1.169	968	2.137	35,2	53,9	59.88 (10.9)*	66.64 (9.7)*	Clinic visit; standard UK Brain Bank criteria with a modification to allow the inclusion of cases that had a family history of PD	New dataset
Spanish Parkinson's (IPDGC)	2.110	1.333	3.443	43,1	54,4	63.92 (12.5)	64.03 (12.6)	Clinic visit; standard UK Brain Bank criteria with a modification to allow the inclusion of cases that had a family history of PD	New dataset
Tubingen Parkinson's Disease cohort (CouragePD)	666	542	1.208	36,0	57,9	59.89 (11.3)	67.48 (8.4)	Clinic visit; standard UK Brain Bank criteria with a modification to allow the inclusion of cases that had a family history of PD	New dataset
Vance (dbGap phs000394)	620	299	919	27,7	50,8	77.47 (8.4)	81.98 (12.8)	Clinic visit; standard UK Brain Bank criteria with a modification to allow the inclusion of cases that had a family history of PD	New dataset
UK PDMED (CouragePD)	1.025	655	1.680	32,8	72,7	NA	NA	Clinic visit; standard UK Brain Bank criteria with a modification to allow the inclusion of cases that had a family history of PD	New dataset
UK BioBank	18.618	436.419	455.037	57,6	54,10	58.45 (7.2)	56.69 (8.1)	Proxy cases defined by family history	New dataset
IPDGC (Nalls et al. 2014 discovery phase)	13.708	95.282	108.990	See PMID: 25064009 for details.				Clinic visit; standard UK Brain Bank criteria with a modification to allow the	Previously published

					inclusion of cases that had a family history of PD; Unrelated individuals with >97% genetically inferred European ancestry who self-reported having been diagnosed with PD.	meta-analysis
NeuroX - dbGaP phs000918.v1.p1	5.851	5.866	11.717	See PMID: 25064009 for details.	Clinic visit; standard UK Brain Bank criteria with a modification to allow the inclusion of cases that had a family history of PD	Previously published dataset
Parkinson's Disease Web-based Study (PDWBS)	6.476	302.042	308.518	See PMID: 28892059 for details.	Unrelated individuals with >97% genetically inferred European ancestry who self-reported having been diagnosed with PD. Excluded individuals with: 1) a change in diagnosis, 2) uncertainty about their diagnosis, and 3) a history of stroke, deep vein thrombosis, or pulmonary embolism (to reduce the probability of including individuals with vascular parkinsonism). In a previous telemedicine study, a neurologist confirmed a diagnosis of PD in 50 out of 50	Previously published dataset

						individuals tested in this cohort.	
Nalls et al. 2019	56.306	1.417.791	1.474.097	See above.		Clinic visit; standard UK Brain Bank criteria with a modification to allow the inclusion of cases that had a family history of PD; Unrelated individuals with >97% genetically inferred European ancestry who self-reported having been diagnosed with PD. Excluded individuals with: 1) a change in diagnosis, 2) uncertainty about their diagnosis, and 3) a history of stroke, deep vein thrombosis, or pulmonary embolism (to reduce the probability of including individuals with vascular parkinsonism). In a previous telemedicine study, a neurologist confirmed a diagnosis of PD in 50 out of 50 individuals tested in this cohort; Proxy cases defined by family history.	Current meta-analysis

Table S10: Summary of available brain region samples and their demographic details.

Spleen (SPL)	**Putamen (PUTM)**	**Cerebellum (CRBL)**	**Occipital Cortex (OCTX)**	**Frontal Cortex (FCTX)**	**White Matter (wm, BA39 & BA40)**	**SEX**	**AGE**	**pH**
030/06	030/06	030/06	030/06	030/06	030/06	M	53	6,4
034/06	034/06	034/06	034/06	034/06	034/06	M	53	6,4
035/06	035/06	035/06	035/06	035/06	035/06	M	54	6,3
026/07	026/07	026/07	026/07	026/07	026/07	M	57	6,4
007/08	007/08	007/08	007/08	007/08	007/08	M	55	6,5
018/09	018/09	018/09	018/09	018/09	018/09	M	57	6,2
033/09	033/09	033/09	033/09	033/09	033/09	M	56	6,2
041/10	041/10	041/10	041/10	041/10	041/10	M	57	6,5
012/11	012/11	012/11	012/11	012/11	012/11	M	53	6,3
032/11	032/11	032/11	032/11	032/11	032/11	M	58	6,4
							55.3 ± 1.95	6.36 ± 0.11

Table S11: Demographic and clinical details of human control spleen-brain tissue donors arranged by age at death as collected by the MRC Sudden Death Brain and tissue bank, Edinburgh. Cause of death has been ranked by the tissue donor bank by most immediate cause of death in numerical-alphabetical order. Abbreviations: post-mortem interval (PMI)

Donor	Sex	Age	pH	PMI (hours)	Cause of Death	Neuropathology report	Known medical records
036/08	F	20	6,5	40	1a - Suspension by ligature	No significant abnormality.	Depression, Alcohol abuse Amlodipine 5mg daily, Bendrofluazide 2.5mg daily, Aspirin EC 300mg daily. Perindopril 2mg daily, Simvastatin 40mg nocte
020/07	F	22	6,36	44	1a - Butane inhalation	No significant abnormality.	Alcohol & solvent abuse, Drug misuse , Depression, smoker
033/08	M	22	6,6	95	1a - Bilateral pulmonary embolism,1b - Deep vein thrombosis, 2 - Combined effects of	No significant abnormality.	smoker, on no prescribed medication at time of death, Asthma

					hypertensive heart disease and ischaemic heart disease,2 - Obesity		
023/08	F	24	6,4	47	1a - Suspension by ligature	No significant abnormalities	Depression - recurrent
006/09	M	25	6,4	81	1a - Multiple Injuries, 1b - Road traffic collision (passenger)	No significant abnormalities	on no prescribed medication at time of death
014/09	M	26	6,3	44	1a - Methadone and diazepam toxicity	No significant abnormality.	No Medical History
021/10	M	27	6,2	67	1a – MDMA (ecstasy) toxicity, 2 - Ischaemic heart disease, coronary artery atherosclerosis and Type 1 Diabetes	No significant abnormality.	Type 1 Diabetes
025/05	M	28	6,6	38	1a - Suspension	No significant	occasionally used

					by ligature	abnormalities	cannabis
030/11	M	30	6,4	71	1a - Unascertained	No significant abnormalities	On no prescribed medication at time of death.
035/09	M	32	6,2	99	1a - Suspension by ligature	No significant abnormalities	Chlorpromazine 50mg, Fluoxetine 20mg daily, Venlafaxine 150mg dailt, Trazodone 200 - 300mg daily
006/10	F	32	6,3	63	1a - Acute decompensation of mitral valve disease and cardiomyopathy, 1b - Marfan's Syndrome	No significant abnormalities	Marfan Syndrome, Ramipril at time of death, Bisoprolol at time of death
032/10	M	34	6,4	57	1a - Sudden adult cardiac death	Old microscopic cerebellar infarct	On no prescribed medication at time of death
020/10	M	36	6,4	41	1a - Cardiomegaly, 1b - Ischaemic heart disease	No significant abnormalities	smoker, on no prescribed medication at time of death

025/08	M	37	6,4	63	1a - Ischaemic heart disease,1b - Coronary artery atherosclerosis	Hyaline arteriosclerosis	On no prescribed medication at time of death
002/10	M	38	6,3	49	1a - Right ventricular hypertrophy	No significant abnormalities	On no prescribed medication at time of death.
010/10	M	39	6,3	81	1a - Sudden Adult Death	No significant abnormalities	Depression - Venafaxine
012/10	M	40	6,2	48	1a - Pulmonary thromboembolism 1b - Deep vein thrombosis 2 - Rupture of Achilles tendon	No significant abnormalities	NO MEDICAL RECORDS AS UNTRACEABLE
007/06	M	41	6,4	49	1a - Dilated cardiomyopathy	No significant abnormalities	On no prescribed medication at time of death
006/08	M	41	6,26	50	1a - Ischaemic heart disease 1b - Coronary artery thrombosis 1c -	No significant abnormalities	On no prescribed medication at time of death.

					Coronary artery atheroma 2 - Hypertensive heart disease		
041/11	M	42	6,4	61	1a - Ischaemic heart disease,1b - Coronary artery atherosclerosis	No significant abnormalities	Depression.Prescribed medication at time of death: Dihydrocodeine 120mg tds,Terbinafin 250mg,Gabapentin 900mg bd
028/10	M	43	6,1	44	1a - Ischaemic heart disease,1b - Coronary artery atherosclerosis	No significant abnormalities	On no prescribed medication at time of death
040/10	M	43	6,3	53	1a - Sudden cardiac death	No significant abnormalities	On no prescribed medication at time of death
029/11	F	43	6,0 0	86	1a - Bronchial asthma , 2 - Pulmonary congestion	No significant abnormalities	Asthma, Depression, Hypertension . Medication prescribed at time of death: Amlodipine 5mg, Enalapril 10mg, Symbicort inhaler,Salbutamol

							inhaler
021/08	M	44	6,3	83	1a - Suspension by ligature	No significant abnormalities	Amitriptyline, Diazepam for stress
036/09	F	44	6,3	49	1a - Combined methadone, temazepam and codeine toxicity	No significant abnormalities	Depression, migraine Propanolol 40mg tds, Paroxetine 30mg daily
018/05	M	45	6,4	75	1a - Ischaemic heart disease,1b - Coronary artery atheroma, 1c - Atherosclerosis , 2 - Chronic renal failure	No significant abnormalities	On no medication at time of death.
009/07	M	45	6,2	67	1a - Myocardial infarction,1b - Coronary artery thrombosis,1c - Coronary artery atheroma	No significant abnormalities	Epigastric reflux , lansoprazole 15mg
002/08	F	45	6,4	28	1a - Ischaemic heart disease,	No significant	Non-smoker, Citalopram 10mg at time of death for

					1b - Severe coronary artery atheroma	abnormalities	depression
004/08	M	45	6,46	43	1a - Combined effects of hypertensive heart disease and ischaemic heart disease, 2-Diabetes (Type 1)	Early ischaemic neuronal injury	Hypertension, Type 1 Diabetes Simvastatin, Lantus insulin, Loratidine, Lisinopril
026/08	M	45	6,4	39	1a - Ischaemic heart disease, 1b - Coronary artery thrombosis and atherosclerosis	No significant abnormalities	On no prescribed medication at time of death
038/08	M	46	5,9	91	1a - Ischaemic heart disease, 1b - Coronary artery atherosclerosis, 2 - Diabetes Mellitus	Small vessel disease, No other significant abnormality.	Type 1 Diabetes, Atorvastatin 10mg for Hypercholesterolaemia
019/10	M	47	6	93	1a - Acute Myocardial	Atherosclerosis small vessel	On no prescribed medication at time of

					Reinfarction, 1b - Previous Small Infarctions, 1c - Focally Advanced Atherosclerosis	disease	death
040/08	M	48	6,5	59	1a - Ischaemic heart disease, 1b - Coronary artery atherosclerosis, 2 - Hypertensive heart disease	Small vessel disease in the form of hyaline arteriosclerosis, No other significant abnormality	Hypercholesterolaemia, Hypertension. Ramipril 5mg at time of death prescribed for Hyptension
024/09	M	48	5,4	67	1a - Myocardial infarction,1b - Coronary artery atherosclerosis (Angioplasty 12/05/09)	Small vessel disease. Cerebellar ischaemia.	Smoker. Pizotifen 3mg at time of death for migraine, Omeprazole 20mg at time of death for Dyspepsia
039/10	M	48	6,2	95	1a - Myocardial re-infarction,1b - Previous myocardial infarcts, 1c -	No significant abnormality	On no prescribed medication at time of death. Smoker, 28-30 units of alcohol weekly

					Coronary atherosclerosis, 2 - Hypertensive heart disease		
036/11	M	48	6,4	72	1a - Coronary artery atherosclerosis	No significant abnormalities	Depression. On no prescribed medication at time of death.
037/11	M	48	6,2	46	1a - Coronary artery atherosclerosis	No significant abnormalities	diagnosed with Crohn's Disease, Prescribed Mesalamine 400mg qds for Crohn's at time of death
034/09	M	49	6,23	79	1a - Ischaemic and hypertensive heart disease	Neuropathological examination has demonstrated small vessel disease with evidence of microhaemorrhages. No significant acute pathology is identified.	Asthma. On no prescribed medication at time of death.
003/08	M	50	6,5	44	1a - Myocardial	No significant	smoker.On no prescribed

			9		infarction, 1b - Severe coronary artery disease	abnormalities	medication at time of death
028/09	M	50	6,5	46	1a - Ischaemic heart disease, 1b - Coronary artery atherosclerosis	No significant abnormalities	smoker. On no prescribed medication at time of death.
004/10	M	50	6,2	63	1a - Ischaemic heart disease	No significant abnormalities	Hypertension,Ischaemic heart disease Atenolol 100mg, GTN spray, Amlodipine 10mg, Atorvastatin 40mg, Aspirin 75mg, Isosorbide Mononitrate 20mg
018/11	F	50	6,2	51	1a - Peritonitis, 1b - Bowel infarction	Small vessel disease. No other significant abnormality	smoker. On no prescribed medication at time of death.
017/08	F	51	6,3	41	1a - Unascertained	No significant abnormalities	On no prescribed medication at time of death
020/08	M	51	6,5	47	1a - Ischaemic heart disease, 1b - Coronary	Small vessel disease. No significant	On no prescribed medication at time of

					arteriosclerosis	abnormality.	death. Non smoker
031/09	M	51	6,3	84	1a - Ischaemic heart disease, 1b - Coronary artery atherosclerosis	small vessel disease-	Hypercholesterolaemia Bezafibrate 400mg nocte, Simvastatin 80mg daily
033/10	M	51	6,3	52	1a - Ischaemic and hypertensive heart disease	No significant abnormalities	Hypertension Carbimazole 15mg tds, Felodipine 5mg daily
004/06	F	52	5,7	63	1a - Acute myocardial infarct, 2 - Dilated cardiomyopathy	No significant abnormalities	On no prescribed medication at time of death.
015/10	M	52	6,2	47	1a - Coronary thrombosis, 1b - Ischaemic heart disease,1c - Advanced coronary atherosclerosis	No significant abnormalities	On no prescribed medication at time of death
036/10	M	52	6,4	52	1a - Ischaemic and	No significant	Hypertension,Hypercholesterolaemia , Alcohol

					hypertensive heart disease	abnormalities	abuse. Lisinopril 10mg daily, Simvastatin 20mg daily
022/06	M	53	6,3	51	1a - Acute myocardial infarct, 2 - Dilated cardiomyopathy 1b - Severe coronary artery atheroma 2 - Hypertensive heart disease	Hypoxic brain damage.Global cerebral ischaemia. Mineralisation of hippocampal and basal ganglia vessels.	moderate smoker and drinker who took regular exercise. On no medication at time of death
030/06	M	53	6,4	43	1a - Combined effects of ischaemic heart disease and hypertensive heart disease	Small vessel disease consistent with chronic hypertension. No other significant abnormalities	Hypercholesterolaemia On no prescribed medication at time of death.
034/06	M	53	6,4	36	1a - Suspension by ligature	No significant abnormalities	Hypercholesterolaemia,Hypertension Atorvastatin 80mg at time of death, Atendol 25mg at time of death, Asprin 75mg at time of death

043/06	F	53	6,38	42	1a - Ischaemic heart disease,1b - Coronary artery atheroma, 1c - Atherosclerosis, 2 - Chronic obstructive pulmonary disease	No significant abnormalities	On no prescribed medication at time of death.
012/11	M	53	6,3	42	1a - Ischaemic heart disease, 1a - Coronary artery atherosclerosis	No significant abnormalities	On no prescribed medication at time of death. Untraceable on NHS system, therefore no medical records.
035/06	M	54	6,3	69	1a -Ischaemic heart disease, 1b- Severe coronary artery atheroma, 2- Chronic obstructive pulmonary disease	No significant abnormalities	No medication at time of death.
007/08	M	55	6,5	51	1a - Combined effects of	No significant	On no prescribed medication at time of

					hypertensive heart disease and ischaemic heart disease 2 - Chronic obstructive pulmonary disease	abnormalities	death
033/09	M	56	6,2	61	1a - Acute myocardial infarction,1b - Coronary thrombosis,1c - Coronary artery disease 2 - Hodgkin's disease on therapy	No significant abnormalities	Hypercholesterolaemia Simvastatin 40mg daily, Omeprazole, Dihydrocodeine
026/07	M	57	6,4	53	1a - Ischaemic heart disease,1b - Coronary artery atheroma,1c - Atherosclerosis ,2 - Hypertensive	Lipohyalinosis (chronic hypertension)	On no prescribed medication at time of death

					heart disease		
022/08	F	57	6,5	95	1a - Pulmonary thromboembolism	Small vessel disease.	Depression, Alcohol abuse Venlafaxine 75mg daily, Antabuse
018/09	M	57	6,2	49	1a - Ruptured abdominal aortic aneurysm	No significant abnormalities	non smoker, Simvastin 40ng at time of death, Candesartan 8mg at time of death
041/10	M	57	6,5	66	1a - Ischaemic heart disease, 1b - Coronary artery atherosclerosis	No significant abnormalities	On no prescribed medication at time of death
019/08	M	58	5,5	69	1a - Myocardial infarction,1b - Small previous infarctions,1c - Coronary arteriosclerosis ,2 - General arteriosclerosis	Hyaline arteriosclerosis (small vessel disease).No significant abnormality.	No GP Notes available (possibly destroyed).
013/11	M	58	6,2	137	1a - Ischaemic heart disease , 1b - Coronary artery atherosclerosis,	No significant abnormalities	Smoker ,Hypertension On Bendrofluazide, Atenolol and Simvastatin at time of death.

					2 - Pulmonary congestion and oedema		
032/11	M	58	6,4	43	1a - Acute myocardial infarction,1b - Coronary thrombosis,1c - Coronary artery atherosclerosis	Cerebrovascular disease	On no prescribed medication at time of death.
025/09	M	59	6,3	51	1a - Cardiac tamponade, 1b - Myocardial re-infarction, 1c - Coronary artery thrombosis, 1d - Ischaemic heart disease, 2 - Chronic hypertension	No significant abnormalities	Smoker; Asthma, Hypertension Lansoprazole daily at time of death
015/07	M	60	6,5 4	66	1a - Ischaemic heart disease, 1b - Coronary artery	No significant abnormalities	Smoker,Hypertension ,Alcohol abuse Ramipril at time of death

					atheroma		
022/09	F	60	6,3	36	1a - Hypertensive heart disease, 2 - Morbid obesity	Cerebrovascular disease. Small vessel disease, atheroscleroisi, lacunar infarcts	smoker, Temazepam, Doxepin, Sulbutamol inhaler all at time of death
032/09	F	60	5,4	38	1a - Haemopericardium, 1b - Ruptured myocardial infarction, 1c - Coronary artery atherosclerosis, 2 - Hypertensive heart disease	No significant abnormalities Enalapril 20mg daily, Serivastatin	Smoker,Hypertension ,Hypercholesterolaemia Enalapril 20mg daily, Xipamide 20mg daily, Atenolol 100mg daily, Serivastatin
038/09	M	60	6,4	41	1a - Ischaemic heart disease,1b - Coronary artery atherosclerosis	Cerebrovascular disease.Atherosclerosis.Small vessel disease,Subacute infarction	EX smoker On no prescribed medication at time of death
011/10	M	60	6,3	40	1a - Coronary artery	Small vessel disease	EX smoker. Aspirin 75mg daily,

					thrombosis 1b - Ischaemic heart disease		Atenolol 25mg daily, GTN spray
013/10	M	60	6,3	68	1a - Coronary artery thrombosis, 1b - Coronary artery atherosclerosis, 2 - Hypertensive heart disease	No significant abnormalities	Hypercholesterolaemia ,Hypertension . Simvastatin 20mg, Atenolol 100mg
018/08	M	61	6,5	43	1a - Ruptured coronary artery atherosclerotic plaque,1b - Coronary artery atherosclerosis	No significant abnormalities	On no prescribed medication at time of death
030/09	F	61	6,1	70	1a - Coronary artery atherosclerosis (coronary angiography and angioplasty	No significant abnormalities	Hypercholesterolaemia, Hypertension , Ischaemic heart disease. Atenolol 50mg, Asprin 75mg, Simvastatin 40mg, Isosorbide Mononitrate 20mg

008/10	M	61	6,2	47	1a - Ischaemic heart disease, 1b - Coronary artery atherosclerosis	Small vessel disease	On no prescribed medication at time of death
014/10	M	61	6,2	47	1a - Ischaemic heart disease, 1b - Coronary artery atherosclerosis	No significant abnormalities	Smoker ,Hypertension Bendrofluazide 2.5mg at time of death
012/08	M	62	6,5	67	1a - Ischaemic heart disease, 1b - Previous myocardial infarctions,1c - Advanced coronary arteriosclerosis	No significant abnormalities	Hypercholesterolaemia Simvastatin , Asprin
001/10	M	62	6,1	35	1a - Haemopericardium, 1b - Ruptured myocardial infarction, 1c - Coronary artery thrombosis, 1d-	Old infarct (Hypothalamus). No other significant abnormality	Not on any prescribed medication at time of death

					Coronary artery atherosclerosis		
014/11	M	62	6,3	135	1a - Ruptured abdominal aortic aneurysm, 2 - Hypertensive heart disease, 2 - Chronic obstructive pulmonary disease	Cerebrovascular disease. Atherosclerosis. Lipohyalinosis. Old microscopic frontal infarct	Asthma, hypertension, hypercholesterolaemia, stopped smoking 2006. Symbicort inhaler at time of death, Salbutamol inhaler at time of death, Diclofenac at time of death, Atorvastin at time of death.
026/11	M	62	6,2	46	1a - Pontine haemorrhage, 1b - Hypertensive heart disease	Pontine hypertensive haemorrhage. Small vessel disease.	Smoker. On no prescribed medication at time of death
016/10	F	63	6,3	35	1a - Ischaemic heart disease, 1b - Advanced Coronary Atherosclerosis	No significant abnormality.	diagnosed with coeliac disease was smoking 10 - 20 icgarettes daily, drinking 6 units alcohol 28/02/2000: diagnosed with osteoporosis. 04/07/2008: Hypertensive at 194/111 and lipids

							high02/04/2009: had been diagnosed with a liver lesion that was initially thought to be metastic disease from an unknown primary. However, liver lesion was now confirmed as a haemangioma. Commenced on Amlodipine and a statin. Alendfronate 10mg daily, Amlodipine ??, Simvastatin ??
011/11	M	63	6,3	67	1a - Hypertensive and ischaemic heart disease, 1b - Coronary artery atherosclerosis	Small vessel disease	Hypertension, Bendrofluazide 2.5mg at time of death, Coracten XI M/R 30 mg daily at time of death.
023/09	F	64	6,6	48	1a - Ischaemic heart disease, 1b - Coronary artery atherosclerosis, 2 - Hypertensive	No significant abnormalities	Hypertension. Lisinopril 40mg at time of death, Bendrofluazide 2.5mg at time of death

					heart disease		
021/09	M	65	6,4	40	1a - Ischaemic heart disease, 1b - Coronary artery atherosclerosis	No significant abnormalities	Smoker. On no prescribed medication at time of death
003/10	M	65	5,6	34	1a - Diabetic Keto-acidosis and Morphine Toxicity,2 - Ischaemic heart disease	Small vessel disease.	Type 1 Diabetes, Hypertension, Smoker Amytriptyline 150mg daily, Enalapril 5mg daily.
019/11	M	66	6,4 0	144	1a - Haemopericardium, 1b - Ruptured atherosclerotic aortic root aneurysm, 2 - Hypertensive heart disease	No significant abnormalities	1991 - osteoarthritis, 1993 - duodenal ulcer Not on any prescribed medication.
020/11	M	66	6,3	81	1a - Cardiac tamponade,1b - Ruptured myocardial infarct, 1c -	Small vessel disease., Subacute lacunar infarct.Large vessel	Non-smoker On no prescribed medication at time of death.

					Coronary artery atherosclerosis	atherosclerosis	
025/11	M	66	6,4	69	1a - Cardiac tamponade,1b - Ruptured myocardial infarct, 1c - Coronary artery atherosclerosis	No significant abnormalities	On no prescribed medication.
014/08	M	67	6,6	50	1a - Ruptured abdominal aortic aneurysm and coronary thrombosis, 1b - Atherosclerosis, 2 - Ischaemic heart disease, 2 - Chronic obstructive pulmonary disease	No significant abnormalities	Smoker Lisinopril 2.5mg daily, Atorvastatin, Digoxin, Warfarin,
015/09	M	67	6,4	47	1a - Ischaemic heart disease,	No significant	Stopped smoking in 2005. Minimal alcohol On no

					1b - Coronary artery thrombosis, 1c - Coronary artery atherosclerosis	abnormalities	prescribed medication at time of death
018/10	M	69	6,00	35	1a - Ischaemic & Hypertensive Heart Disease, 2 - Diabetes mellitus Type 1	Cerebrovascular disease	Type 2 Diabetes, Hypertension , Smoker Metformin 850mg bd, Gliclazide 160mg am, 80mg pm, Adalat Retard 10mg bd
034/08	M	70	6,2	50	1a - Pulmonary embolism, 1b - Deep vein thrombosis, 2 - Previous pulmonary embolism, 2 - Hypertension	No significant abnormalities	Depression,Hypercholesterolaemia , Hypertension Lisinopril 5mg daily, Simvastatin 20mg daily
007/10	M	70	6,3	96	1a - Coronary thrombosis, 1b - Ischaemic heart disease,2 - Chronic pulmonary	Small vessel disease. Lacunar infarcts	On no prescribed medication at time of death

					emphysema		
033/11	F	72	6,3	30	1a - Haemopericardium, 1c - Coronary artery thrombosis, 1d - Coronary artery atherosclerosis, 1b - Ruptured myocardial infarct	No significant abnormalities Vascular disease	No Medical History. Nil of relevance in GP notes
026/09	M	73	6,2	51	1a - Ischaemic heart disease, 1b - Coronary artery atherosclerosis	Small vessel disease, Old lacunar infarct.	Ischaemic heart disease,Smoker Simvastatin 10mg daily, Nifedipine 10mg daily, Aspirin 75mg daily, GTN spray
023/10	M	74	6,4	44	1a - Ischaemic heart disease, 1b - Coronary artery atherosclerosis	No significant abnormalities	On no prescribed medication at time of death
016/11	M	74	6,3	66	1a - Ischaemic heart disease,	Cerebrovascular disease,Large	Hypertension, Arendol 100mg daily, Asprin 75mg

					1c - Coronary artery atherosclerosis, 1b - Coronary artery occlusion	vessel atherosclerosis, Small vessel disease	daily
025/10	M	75	5,4	47	1a - Ischaemic heart disease, 1b - Coronary atherosclerosis	Small vessel disease. No other significant abnormality	On no prescribed medication at time of death
005/09	M	76	6,3	50	1a - Ruptured abdominal aortic aneurysm, 2 - Hypertensive heart disease,	Small vessel cerebrovascular disease. Amyloid angiopathy. Alzheimer's pathology	Hypertension Non-smoker Lisinopril 2.5mg at time of death. Etodolac 200mg nocte at time of death, Nifedipine 30mg at time of death, Lansoprazole 15mf at time of death, Atenolol 50 mg at time of death
013/09	F	79	6,3	45	1a - Ischaemic heart disease, 1b - Coronary artery atherosclerosis	Small vessel disease.	Hypertension. rheumatoid arthritis. letter in notes detailing that she suffered from hypertension and hypothyroidism but no actual record of when she was diagnosed. left ankle replacement. Thyroxine ??

	Dosage, Tenoret 50 ??, Pulsatilla 6 2-3 daily